A Holistic Approach to Study Carbon Cycling in the Plant-Soil System Based on Stable Isotope Labelling

---

Dissertation

zur

Erlangung der naturwissenschaftlichen Doktorwürde

(Dr. sc. nat.)

vorgelegt der

Mathematisch-naturwissenschaftlichen Fakultät

der

Universität Zürich

von

Mirjam Susanne Studer

von

Vilters-Wangs, Wangs SG

Promotionskomitee

Prof. Dr. Michael W. I. Schmidt (Vorsitz)

Dr. Samuel Abiven (Leitung der Dissertation)

Dr. Rolf T. W. Siegwolf

Zürich, 2015

"If an organism is nothing but a set of atoms and molecules, what then is the difference between a living organism and a dead one?" (Looijen, 1998)

Zusammenfassung

Die Erforschung des terrestrischen Kohlenstoff-(C)-Kreislaufs trägt zur Erstellung zuverlässiger Klimaprognosen und den darauf basierenden Anpassungs- und Verminderungsstrategien bei. Im terrestrischen C-Kreislauf wird das Treibhausgas Kohlendioxid (CO_2) nach der pflanzlichen Assimilation über eine Reihe von Prozessen in Pflanzen und im Boden transformiert und schliesslich wieder an die Atmosphäre abgegeben. Physische, chemische und biologische Interaktionen zwischen der Atmosphäre, den Lebewesen und den abiotischen Bodenbestandteilen beeinflussen diese C-Transformationsprozesse massgeblich und damit auch die Emission von CO_2 (und anderen Treibhausgasen) aus terrestrischen Ökosystemen. Somit sind Interaktionen von grosser Bedeutung für Rückkoppelungseffekte zwischen dem terrestrischen C-Kreislauf und dem Klima.

Im ersten Teil dieser Arbeit zeige ich anhand von Literaturbeispielen, dass das mechanistische Verständnis von Rückkoppelungseffekten, welches die Grundlage für Klimamodelle ist, gering ist. Das mechanistische Verständnis kann durch Grundlagenforschung unter kontrollierten und vereinfachten Bedingungen und der Erforschung der so identifizierten Mechanismen in komplexen natürlichen Systemen erweitert werden. Hierbei ist es wichtig, den C-Kreislauf mit einem holistischen Ansatz im Gesamtsystem Pflanze-Boden zu untersuchen, welches sowohl die ober- als auch die unterirdischen Pflanzenteile sowie biotische und abiotische Bodenbestandteile und dessen Interaktionen umfasst. In diesem Doktoratsprojekt wurde eine neue Forschungseinrichtung und Methodik, basierend auf stabilen Isotopen, entwickelt um die grundlegenden Mechanismen des C-Kreislaufs im System Pflanze-Boden unter verschiedenen Klimabedingungen zu untersuchen.

Im zweiten Teil dieser Arbeit stelle ich den Aufbau der Forschungseinrichtung sowie die Ergebnisse und Schlussfolgerungen vor. Die MICE ("Multi-Isotope labelling in a Controlled Environment") Einrichtung besteht aus zwei Klimakammern, welche Platz für insgesamt 30 Pflanzen-Boden Systeme in individuellen Töpfen bieten. In den Kammern sind die ober- und unterirdischen Teile (Spross bzw. Wurzeln und Boden) hermetisch getrennt. Durch diesen einzigartigen Aufbau können ober- und unterirische C-Prozesse separat aber gleichzeitig gemessen werden. Die Regulierung der atmosphärischen Bedingungen (Licht, Temperatur, Luftfeuchtigkeit und CO_2 Konzentration) erfolgt automatisch und unabhängig für die zwei Kammern. Die Markierung mit stabilen Isotopen kann ober- oder unterirdisch erfolgen und Proben können jederzeit genommen werden

um die Verlagerung der markierten Elemente in den C-Flüssen und Vorräten zu verfolgen. Dies macht die MICE Einrichtung sehr vielseitig in ihrer Anwendung bezüglich der Simulation von Umweltbedingungen, Markierungsmethoden und Beprobungszeitpunkten.

Drei Experimente wurden parallel zur Entwicklung der Forschungseinrichtung durchgeführt. (i) Vergleich der zwei häufigsten Markierungsmethoden welche stabile C Isotope einsetzen, Pulsmarkierung (kurzzeitig) und kontinuierliche Markierung mit ^{13}C-CO_2, und Prüfung ihrer Anwendbarkeit für einen holistischen Ansatz. (ii) Test einer neuen Markierungsmethode mit der gleichzeitigen Anwendung mehrerer Isotope (^{13}C, ^{18}O, ^{2}H). (iii) Beobachtung der ober- und unterirdischen C-Flüsse (Photosynthese, Dunkelatmung, pflanzenbürtige- und Gesamtbodenatmung) während der Entwicklung der Rhizosphäre von Pflanzen, die wachstumslimitiert waren.

Die Ergebnisse des ersten Experimentes haben gezeigt, dass die Verlagerung der Assimilate von den Blättern in den Boden mit der ^{13}C-CO_2 Pulsmarkierung aufgrund der stärkeren Markierung der (ersten) Assimilate schneller in der Bodenluft detektiert wird als mit der kontinuierlichen Markierungsmethode (nach 5 bwz. 9 Stunden). Andererseits markiert die kontinuierliche Markierung eine grössere Menge an Assimilaten über eine längere Zeit, wodurch diese Methode besser geeignet ist um grosse Kohlenstoffvorräte, wie z.B. die organische Bodensubstanz zu markieren und die mittlere Verlagerungsdauer (inklusive Kurzzeitspeicherung) zu ermitteln. Beide Markierungsmethoden erzielten bei kurzzeitiger Anwendung die gleichen Ergebnisse für die Kohlenstoffverteilung, sofern der Beprobungszeitpunkt nach der mittleren Verlagerungsdauer erfolgte, welche 6 - 8 Tage von der Assimilation im Blatt bis zur CO_2 Emission aus dem Boden betrug. Das erste Experiment hat zudem klar aufgezeigt, dass die oft angewandten, aber stark vereinfachten Modelle zur Ermittlung der mittleren Kohlenstoffverweildauer in Vorräten nicht gültig sind für Pflanzen-Bodensysteme im Wachstum.

Im zweiten Experiment markierten wir Assimilate mit ^{13}C, ^{18}O und ^{2}H durch gasförmige Zugabe (^{13}C-CO_2, $^{2}H/^{18}O$-H_2O) der drei stabilen Isotopen. Dabei hat sich gezeigt, dass bei hoher Luftfeuchtigkeit 58 - 69 % des Blattwassers über die Diffusion von Wasserdampf aus der Atmosphäre in das Blatt gelangt. Die Verteilung der drei Isotopen im organischen Material nach dessen Aufnahme bestätigte, dass Sauerstoff und Wasserstoff während des Transportes und der Synthese von Molekülen ausgetauscht werden.

Im dritten Experiment beobachteten wir wie Pflanzen ihren Kohlenstoffhaushalt aktiv verändern können um auf einschränkende Bedingungen zu reagieren. Wachstumslimitierte Pappeln erhöhten den Anteil des assimilierten Kohlenstoffs, welcher über die

Wurzeln abgegeben wird, von regulär 18 ± 3 % auf 29 - 90 %, aller Wahrscheinlichkeit nach um die Nährstoffaufnahme zu verbessern. Dies führte zu einer massiven Erhöhung der Bodenatmung (um 5 - 59 mg C Tag^{-1}), obwohl die Änderung des wurzelbürtigen Kohlenstoffeintrages quantitativ gering war (1 - 2 mg C Tag^{-1}). Dies weist darauf hin, dass die Pflanze spezifische Stoffe absonderte um die mikrobielle Aktivität zu erhöhen und ist damit ein klarer Beweis für die Interaktion zwischen Pflanzen und Boden im Kohlenstoffkreislauf.

Die Experimente haben gezeigt, dass beide ^{13}C-CO_2 Markierungsmethoden die Verlagerungsgeschwindigkeit, die Verteilung und die Verweildauer von Kohlenstoff im System Pflanze-Boden erfassen können, wobei sich die kontinuierliche Markierung für einen holistischen Ansatz als besser geeignet erwies, als die Pulsmarkierung. Des Weiteren haben wir erwiesen, dass organisches Material während der Photosynthese mit ^{13}C, ^{18}O und ^{2}H markiert werden kann. Diese neue Markierungsmethode könnte nützlich sein um Prozesse zu untersuchen, bei denen die chemische Zusammensetzung des organischen Materials eine wichtige Rolle spielt (z.B. Abbau von organischem Material im Boden). Im dritten Experiment stellte sich der direkte Vergleich der ober- und unterirdischen C Flüsse als ein wichtiges Instrument heraus um funktionelle Zusammenhänge im C-Kreislauf zu erfassen. Die wachstumslimitierten Pflanzen erhöhten den Anteil an assimiliertem C, der über die Wurzeln abgegeben wird, und verstärkten dadurch den mikrobiellen Abbau von organischer Bodensubstanz ("priming"). Dieser Mechanismus könnte zu positiven Rückkoppelungseffekten mit dem Klima führen.

Die Forschungseinrichtung MICE und die Methodenentwicklung dieses Doktoratsprojektes sind wichtige Instrumente für die zukünftige Erforschung der Prozesse und Interaktionen im C-Kreislauf. Sie können eingesetzt werden um unser Wissen schrittweise zu erweitern, insbesondere in Bezug auf grundlegende Mechanismen der Kurzzeit- und Langzeiteffekte der Klimaänderung auf den C-Kreislauf verschiedener Pflanzen-Boden Systeme. Die Ergebnisse aus der MICE Forschungseinrichtung werden zum mechanistischen Verständnis der Rückkopplungseffekte zwischen dem C-Kreislauf und dem Klima und damit zur Weiterentwicklung von Klimamodellen beitragen.

Summary

Terrestrial carbon (C) cycling research is essential to improve future climate projections and provide reliable information for mitigation and adaptation strategies. Carbon dioxide (CO_2), one of the most important greenhouse gases, is assimilated by plants and transformed in a cascade of processes within the plant-soil system until it is emitted back to the atmosphere. Physical, chemical and biological interactions between the atmosphere, biota and soil are important drivers of these C cycle processes and their feedback to climate change. Therefore it is essential to study plant-soil C cycling with a holistic approach, i.e. studying C cycling including interactions within and between plants, soil biota and soil.

In the introduction part of this thesis I illustrate with examples from literature that our mechanistic understanding of terrestrial C cycle feedbacks to climate change, which is needed for global climate models, is still limited. To improve our knowledge of feedback mechanisms we first need to explore the complex interactions of plant-soil C cycling in controlled and simplified environments to formulate hypothesis about potential feedback mechanisms in a second step, which can then be tested in more complex natural environments. In this PhD project we developed and applied a new facility and methodology to study the responses of plant-soil systems to environmental changes based on stable isotope labelling techniques.

The developed MICE ("Multi-Isotope labelling in a Controlled Environment") facility consists of two labelling chambers containing 30 plant-soil systems in individual pots. The above- and belowground system is hermetically separated. The unique setup allows simultaneous measurement of above- and belowground C dynamics with a holistic approach. The atmospheric conditions (temperature, humidity, CO_2 concentration, light) are automatically regulated and can simulate different climatic conditions in the two chambers with high precision. The isotope labels are added to the above- or belowground system and can be traced at any time during an experiment. The isotopes are used to separate C and other elemental stocks and fluxes. Thus the MICE facility is very versatile providing diverse treatment, labelling and sampling options.

Together with the development of the facility we conducted three experiments in which we i) compared the commonly applied pulse and continuous stable C isotope (^{13}C) labelling techniques and assessed their suitability to study plant-soil C cycling with a holistic approach, ii) tested a new multi-labelling technique to label organic matter with C, O and H stable isotopes and iii) studied the dynamics in the plant and soil CO_2

exchange (photosynthesis, dark respiration, plant-derived and total soil respiration) during initial development of plants with and without growth limitation.

In the first experiment we demonstrated that the transfer of assimilates from the leaves to the soil CO_2 efflux is detected faster with ^{13}C-CO_2 pulse labelling (after 5 h) than with the continuous labelling (after 9 h) technique, due to the higher label strength. However, the larger amount of C atoms labelled in the continuous labelling make this technique more suitable to study the mean transfer time (including short-term storage stocks) and the C dynamics in large C stocks, such as the soil organic matter. The experiment revealed that both techniques, when applied short-term (2 weeks), yield the same results for C partitioning, but that the lag time in the homogeneous tracer distribution within the plant-soil system (6-8 days) has to be taken into account if the belowground C partitioning is of interest. Furthermore the ^{13}C distribution dynamics detected in this experiment clearly showed that the commonly applied exponential decay model and the analogue proposed logistic model are not valid to estimate the mean residence time in plant-soil systems at growth (non-steady state).

With the second experiment we successfully labelled fresh assimilates with three stable isotopes (^{13}C, ^{18}O and ^{2}H) by its gaseous application (^{13}C-CO_2, $^{2}H/^{18}O$-H_2O). The results indicated that a considerable amount of the leaf water (58 - 69 %) entered the leaf by back-diffusion of atmospheric vapour into the leaves. The label distribution dynamics measured in the bulk organic matter confirmed that O and H exchange during the transport of assimilates within the plant or during biosynthesis of new compounds.

The third experiment we observed, that plants actively respond to limiting conditions in their environment by changing their C allocation. Poplar plants that were strongly limited in their growth increased temporarily their belowground C release from 18 ± 3 % to 29 - 90 % of net assimilated C, presumably to increase the nutrient acquisition. Even though this change in plant C release was quantitatively small (total of 1 - 2 mg C day^{-1}) it induced a massive change in the soil organic matter respiration (5 - 59 mg C day^{-1}). This indicates that the plants released specific compounds that stimulated the microbial activity and is a direct proof of the close interactions between plant and soil in C cycling.

The results of the three experiments highlight that i) both labelling techniques can be used to asses C transfer, partitioning and residence time and that the continuous labelling is more suitable to study plant-soil C cycling with a holistic approach than the pulse labelling technique, ii) organic matter can be labelled with ^{13}C, ^{18}O and ^{2}H added through the gaseous phase (CO_2, water vapour) and that this new technique has the

potential to trace dynamics related to the form of organic matter (e.g. during degradation), and that iii) the direct comparison of above- and belowground C fluxes is an efficient approach to detect functional changes in the plant-soil C cycling, as for example the increase in the relative amount of assimilated C released belowground in growth limited plants that induces a rhizosphere priming (increase in the soil organic matter mineralisation). This mechanism might lead to positive feedbacks with climate through the increase in CO_2 emissions from the soil.

The facility and the methodology developed and tested in this PhD project is the foundation for future research to elucidate the mechanisms behind the response of terrestrial C cycling to climate change. It will be applied to improve our knowledge of the basic mechanisms of short-term responses of plant-soil C cycle processes and interactions to multi-factorial climate changes, to explore their relevance compared to the lagged effects induced in the long-term and in different plant-soil systems. Thus it will contribute to the improvement of models to predict future climate.

Content

Abbreviations (Part A)

MB	Microbial biomass
MICE	Multi-Isotope labelling in a Controlled Environment
OM	Organic matter
SOM	Soil organic matter

Figures (Part A)

Tables (Part A)

Part A: Synopsis

1 Introduction

1.1 The C cycle in a changing world

Human activity (e.g. land use change, fossil fuel burning) has been leading to an increase in atmospheric greenhouse gas concentrations of carbon dioxide (CO_2, + 40 %), methane (CH_4, +150 %) and nitrous oxide (N_2O, + 20 %) since pre-industrial times (IPCC, 2013a). As a consequence, the global temperature are rising and precipitation patterns are changing with large impacts on human and ecological systems (Walther et al., 2002; Lenton et al., 2008). To reduce negative impacts, such as drought-induced crop shortfalls, we need to develop new technologies and strategies to adapt to, and mitigate climate change. Efficient adaptation and mitigation requires reliable projections of future climate and its impacts (based on modelling approaches) and profound understanding of greenhouse gas sources and sinks. In this, the knowledge of the carbon (C) cycle is of major importance, since the C cycle involves two of the most important greenhouse gases (CO_2 and CH_4) and is affected by climate change (IPCC, 2013b).

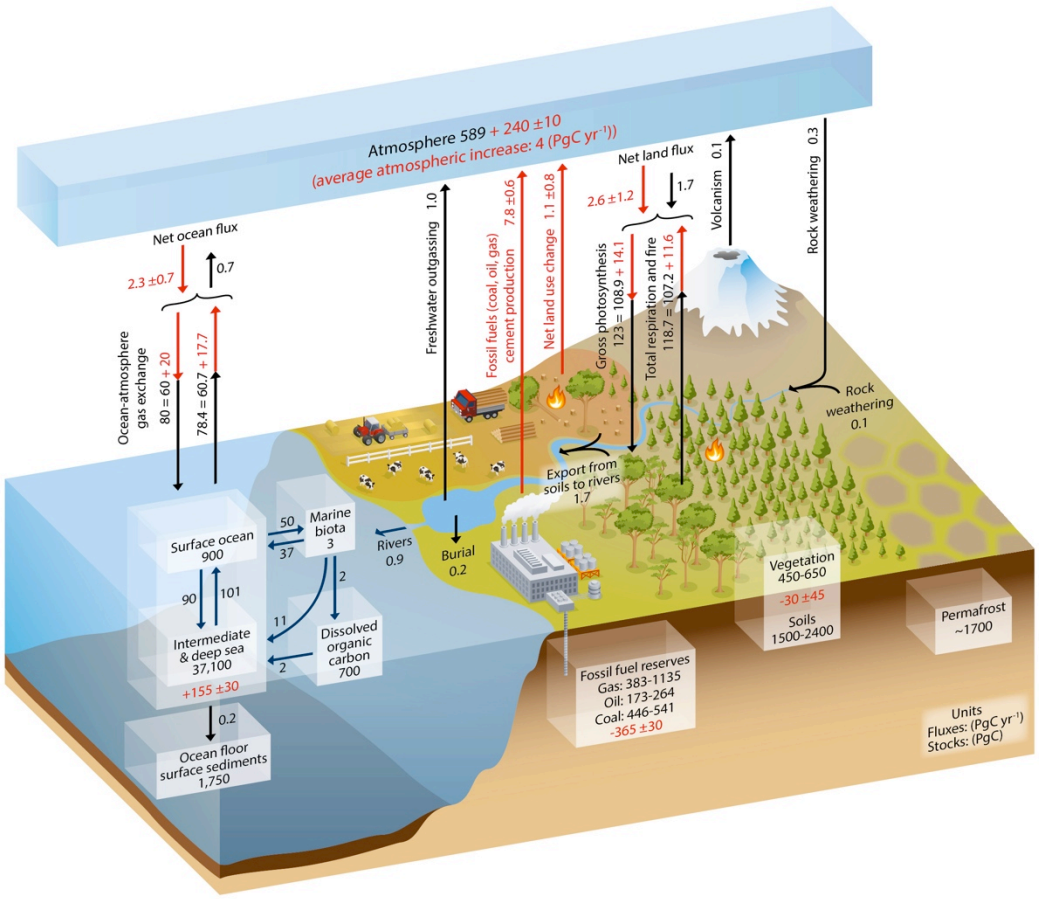

Figure 1 The global carbon cycle. Magnitude of the major C stocks (boxes) and fluxes (arrows) in the global carbon cycle in Pg (10^{15} g) and Pg per year. The red arrows and numbers indicate the anthropogenic contribution to the stocks and fluxes relative to preindustrial values (IPCC, 2013b).

The C exchanges between four major global C stocks, the atmosphere, ocean, land and the lithosphere (**Figure 1**). Most C is stored in the lithosphere and deep ocean, but these stocks are relatively static, i.e. the C exchange with other stocks is small compared to their reservoir size. On the contrary, the Earth's surface layers, the atmosphere, ocean surface and terrestrial systems, are very dynamic C stocks. The C exchange between the atmosphere and the ocean and land is mainly driven by biological processes (Schulze, 2006; Chapin III et al., 2012a). Currently both, ocean and land are net sinks of atmospheric C (**Figure 1**). Future projections indicate that the ocean sink will persist, while the response of terrestrial C cycling to climate change is uncertain (Houghton, 2007). Positive feedbacks of terrestrial ecosystems are expected to accelerate climate change, but its magnitudes are uncertain (Meir et al., 2006; Heimann & Reichstein, 2008; Friedlingstein & Prentice, 2010). For example the predicted change in the atmospheric CO_2 concentration for the year 2100 due to the increased CO_2 emission from terrestrial ecosystems varies by 200 ppm (µmol mol^{-1}) and thus contributes to an uncertainty in the global temperature projections of 1.5 °C (Meir et al., 2006).

Terrestrial C cycling research is essential to improve future climate projections and to assess the capacity of C sinks. Based on this knowledge we can develop adaptation and mitigation strategies to cope with the predicted negative impacts of climate change.

1.2 Terrestrial C cycling

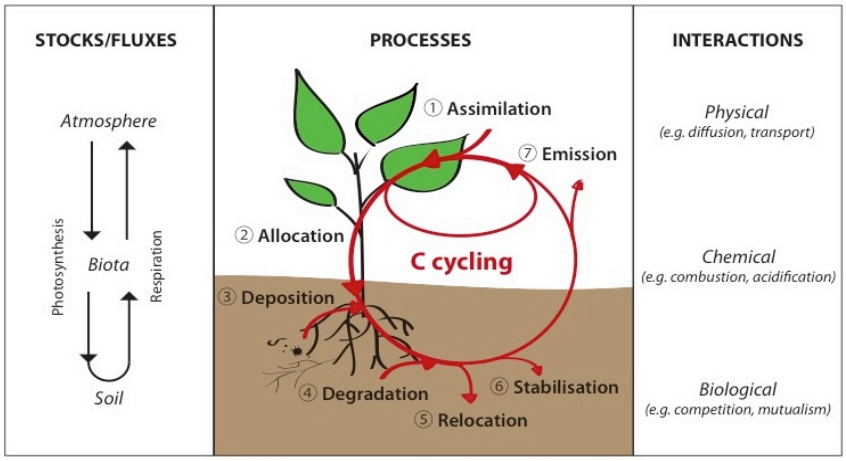

Figure 2 Terrestrial carbon cycling. Scheme of the main stocks and fluxes in the terrestrial C cycle (left), the processes that transform and relocate the assimilated CO_2 within the plant-soil system until it is emitted back to the atmosphere (middle), and the interactions between atmosphere, biota and soil (right).

In the terrestrial C cycle three main stocks are present (**Figure 2**), the atmosphere, biota (flora, fauna) and the soil. More than 99 % of atmospheric C is present as CO_2, which is also the most common C form exchanged with terrestrial ecosystems via photosynthesis

and respiration (IPCC, 2013b). C assimilated by photosynthesis is the main source for organic matter (OM) formed in biota (biomolecules) and residing in soil C stocks (soil organic matter, SOM). In this thesis I focus on the description of the C cycle processes, interactions and feedbacks related to the exchange of CO_2.

1.2.1 C cycle processes

Overview on the main C cycle processes

C cycle processes describe the transformation of OM (resource) into a new condition (product) and take place within plant-soil compartments (e.g. leaves, roots, soil microbial biomass) or at their interfaces (**Table 1**). The product of a process is the resource for subsequent processes, linking seven main C processes to a cycle (**Figure 2**): C is (1) assimilated by autotrophic organisms, (2) allocated within the living biomass, (3) deposited at the soil surface or belowground after cell death or by living organisms, where it is (4) degraded by heterotrophic organisms, (5) relocated within and out of the soil profile and/or (6) temporarily stabilized before C is (7) mineralized and emitted back to the atmosphere. The main steps are the result of sub-processes summarized in **Table 1**. However, the C cycle is not unidirectional and assimilated C does not always undergo all the seven process steps. For example, fresh assimilates are used for leaf maintenance respiration before they are allocated elsewhere, C released by roots can be directly mineralized or recaptured by the roots (Jones et al., 2009), or OM protected in aggregates can get destabilized by aggregate breakdown (Kim et al., 2012).

Table 1 Main processes in the terrestrial carbon cycle. Description of the process inputs (resources), agents (compartments), outputs (products) and the sub-processes involved in the transformation of organic matter during C cycling in the plant-soil system (SOM = soil organic matter).

Resource	Process / Compartment	Product	Sub-processes
CO_2, H_2O, nutrients, light	Assimilation / Plant	Assimilates, (O_2)	Water and nutrient acquisition Photosynthesis
Assimilates, stored compounds, (H_2O)	Allocation / Plant (Reallocation)	Biomass, protective and stored compounds	Phloem uploading, transport and unloading Biosynthesis (growth, maintenance, storage and defence)
Assimilates, protective and stored compounds, plant and edaphic necromass	Deposition / Plant, soil biota	Rhizodeposits, detritus (fresh SOM)	Rhizodeposition Necromass deposition (edaphic and plant-derived)
Fresh SOM, (H_2O, O_2)	Degradation / Soil biota, soil	Degradation products (degraded SOM)	Abiotic degradation (oxidation, hydrolysis) Biotic degradation (fragmentation, depolymerisation)
Fresh and degraded SOM (topsoil)	Relocation / Soil biota, soil	Fresh and degraded SOM (subsoil, groundwater, surface runoff, atmosphere)	Transport within the soil (bioturbation, eluviation) Transport out of the system (leaching, erosion)
Fresh and degraded SOM (labile SOM)	(De-)Stabilisation / Soil	Protected SOM (stable SOM)	Chemical protection (recalcitrance) Physico-chemical protection (organo-mineral interactions) Physical protection (physical disconnection)
Assimilates, stored compounds, fresh and degraded SOM, (O_2)	Emission / Soil, plant, soil biota	CO_2, CH_4, VOC, H_2O	Biotic respiration (autotroph/heterotroph; aerobic/anaerobic) Acidification (abiotic CO_2) Emission of CH_4 and volatile organic compounds (VOC)

Bias towards aboveground processes and CO_2 fluxes

The basic mechanisms of C cycle processes are well understood and were recently summarized by (Chapin III et al., 2012). However, their magnitude and their response to climate change are less well known and there is a bias towards aboveground processes. Leuzinger & Hättenschwiler (2013) demonstrated, based on publication numbers, that there is a very strong bias in global change research towards photosynthesis, compared to dark respiration, litter decomposition and soil respiration, while other important fluxes like rhizodeposition are poorly quantified. There are mainly methodological reasons for this bias. Leaf CO_2 gas exchange is technically easier to measure than C fluxes within the plant (Körner, 2011). The same applies for belowground processes related to the degradation and stabilisation of SOM that are more difficult to assess than soil CO_2 emission. The plant-soil interface was identified already twenty years ago as the "hidden" but not less important "half" of ecosystems, and nowadays it is recognized that belowground processes are crucial for our understanding of ecosystem responses to climate change (Norby & Jackson, 2000; Bardgett, 2011; Matamala & Stover, 2013). Thus there is a strong need to study belowground C cycling and overcome methodological constraints related to them, also in respect to the large soil C stocks that might be vulnerable to climate change.

1.2.2 Interactions as drivers of C cycling processes

Biological, chemical and physical interactions between the atmosphere, biota and soil limit or promote C cycle processes (section 1.2.1), either by changing the resource supply and product abundance or by affecting the agent or the conditions in the plant-soil compartment where the process takes place (described in **Table 1**). While it is generally accepted that interactions are crucial for the understanding of terrestrial C cycling and their responses to climate change, our knowledge about them is still limited (Ostle et al., 2009; Singh et al., 2010; Bardgett, 2011; van der Putten et al., 2013). Some examples of interactions are given below to illustrate their importance for C cycling.

Biological interactions - mediators of community structure and ecosystem functioning

Biological interactions highly important for C cycling are the competition for above- and belowground resources, mutualistic symbiosis between plants and soil biota and antagonistic interactions across trophic levels (e.g. herbivory, grazing) and with pathogens (e.g. Matyssek et al. 2005). For example (i) the competition for nutrients in the rhizosphere might be a key factor for the response of microbial degradation and respiration to C deposition ("priming effect", Dijkstra et al., 2013; Chen et al., 2014), (ii) mutualistic interactions between roots and mycorrhizal fungi, rhizobia and other plant

growth promoting rhizobacteria increases the C deposition (Jones et al., 2004) and improves the C assimilation (Richardson et al., 2009; Behie & Bidochka, 2014).

Many biological interactions are species specific and thus plants shape (at least partly) belowground communities (Hartmann et al., 2008; Berg & Smalla, 2009; Churchland & Grayston, 2014). There is also strong evidence that belowground biological interactions feed back to the aboveground community structure (Wardle et al., 2004; Kulmatiski et al., 2008; van der Putten et al., 2013; Hodge & Fitter, 2013). Thus, changes in biological interactions might change ecosystem structures and induce massive changes in C cycling (Bardgett et al., 2013). How interactions affect the species responses to global change is still a fundamental question in ecology (Sutherland et al., 2013).

Physical interactions - from climate conditions to soil structure

The atmosphere, biota and soil interact physically by the movement of material (e.g. diffusion) or the change in the physical properties of compartments (e.g. soil structure).

The (physical) climate conditions in the atmosphere determine terrestrial biomes and its C cycle characteristics (Prentice et al., 1992; De Deyn et al., 2008; Carvalhais et al., 2014). Weather events, diffusion of gases and the reflection or absorption of radiation by the land cover are further physical atmosphere-ecosystem interactions that affect C cycling. For example, (i) precipitation mediates processes related to the transport or abundance of water, such as C relocation, assimilation, degradation and emission, and extreme weather events (e.g. heavy storms, drought) massively disturb ecosystem C cycling (Reichstein et al., 2013), (ii) gas concentration gradients drive the diffusion of CO_2 and H_2O from the atmosphere through the stomata into the leaves (Parkhurst, 1994), which affects C assimilation or allocation either directly via resource availability or indirectly via changes in transpiration (Farquhar & Sharkey, 1982; McDowell et al., 2008) and (iii) the surface reflection of radiation (albedo) is a crucial factor for the land temperature (Chapin III et al., 2005; Meir et al., 2006) affecting the process rates of the biochemical reactions, such as C assimilation, allocation, degradation and emission.

Physical interactions between biota and soil occur at the soil surface (e.g. reduction of soil temperature by vegetation shading), at the root-soil interface (e.g. water uptake) or along the soil profile (e.g. bioturbation). One of the most important effects of physical biota-soil interactions on C cycling is the change in soil structure (Oades, 1993; Bronick, 2005). Enhanced soil aggregation in the rhizosphere by root mediated wet-dry cycles, compaction and biological binding agents improves the oxygen and water availability and thus stimulates microbial activity and plant growth (C assimilation, degradation), countervails soil erosion (relocation) and protects SOM inside aggregates (stabilisation, Six et al., 2004; Blanco-Canqui & Lal, 2004; Gregory, 2006; Hinsinger et al., 2009).

Further root growth and faunal activity generates biopores along the soil profile that provide a pathway for SOM transport to lower soil horizons (C relocation, stabilisation) and improves the oxygen availability for microbial C degradation (Dungait et al., 2012).

Chemical interactions - the milieu for processes and the link to other biogeochemical cycles

Chemical interactions include the exchange of compounds (e.g. acids) and chemical reactions (e.g. oxidation) that alter the chemical conditions within compartments.

A prominent example for a chemical reaction that strongly affects C cycling is the combustion of OM in wildfires, which can be understood as the chemical interaction between the atmosphere (O_2) and ecosystems (biomass). Fire has a large and immediate impact on vegetation C stocks and on the emission of soot and CO_2 (Chapin III et al., 2009; Reichstein et al., 2013). Furthermore, lagged effects of combustion occur by the change in quantity and quality of C deposition that impedes C degradation and potentially promotes C stabilisation (Preston & Schmidt, 2006; Singh et al., 2012; Maestrini et al., 2014). Another example for atmosphere-ecosystem interactions is the deposition of nitrogen (N) with precipitation that changes the nutrient availability in the soil with large impacts on C cycle processes (Liu & Greaver, 2009, 2010; Lu et al., 2011), for example by improved plant productivity (C assimilation), higher relative above- vs. belowground growth (C allocation), increased litter quality and quantity (C deposition), reduced microbial activity (C degradation), enlarged C leaching (C relocation) or increased net CH_4 exchange (C emissions). However, there are still large knowledge gaps in how the N and C cycle interact (Luo & Weng, 2011; Gärdenäs et al., 2011).

The most important chemical interactions between biota and soil occur in the rhizosphere. The root and microbial activity (absorption, respiration, exudation) alters the chemical conditions in the soil, such as the pH and redox potential (O_2 availability) and the abundance of nutrients, toxic elements, complexing/chelating compounds and enzymes (Hinsinger et al., 2005). These changes in the chemical conditions affect C cycling (Gregory, 2006; Hinsinger et al., 2009; Lambers et al., 2009) for example through increased nutrient acquisition due to enhanced nutrient mobility (C assimilation), increased SOM hydrolysis by extracellular enzymes (C degradation), accelerated inorganic CO_2 release from rock weathering (C emission) or the formation of biogenic carbonates due to precipitation of accumulated calcium as calcite (C stabilisation).

The assimilated C is transformed in a cascade of processes until it is emitted back to the atmosphere. Physical, chemical and biological interactions in the atmosphere-biota-soil system are important drivers of C cycle processes. However, there are large knowledge gaps in the belowground C cycling.

1.3 Climate feedbacks of terrestrial ecosystems

Terrestrial climate feedbacks involve biophysical and biochemical mechanisms (Meir et al., 2006; Field et al., 2007; Chapin III et al., 2008). Biophysical effects are related to the albedo (reflection of solar radiation), evapotranspiration (surface cooling, moisture for cloud formation), aerosols (light absorption and scattering) and surface roughness (water and energy exchange). Biochemical feedbacks occur through climate-induced changes in the greenhouse gas exchange. The magnitude of biochemical feedbacks is still highly uncertain, but it is assumed to be similar to the biophysical feedbacks (Arneth et al., 2010).

1.3.1 Understanding of C cycle feedbacks - a short history

The research on C cycle feedbacks on climate was guided by the fundamental assumption, that the aboveground assimilation, driven by plant photosynthesis, and the belowground emission, driven by heterotrophic respiration, can be conceptually isolated and analysed separately (Heimann & Reichstein, 2008). It was hypothesised that the main feedbacks would be induced by elevated CO_2, stimulating photosynthesis and thus the CO_2 assimilation (negative feedback, CO_2 fertilization of plant productivity), and by increased temperature, accelerating microbial degradation of SOM and thus CO_2 emissions (positive feedback, temperature driven soil respiration), while the research communities of plant and soil scientist were largely disconnected. However, this simplistic view was challenged by (contradicting) results from field experiments (Körner, 2006; Wang et al., 2014), and lead to recent changes in paradigm unifying the research disciplines (Högberg & Read, 2006; Körner, 2011; Schmidt et al., 2011). Below I illustrate on these two examples how plant and soil science became connected through the rising awareness that interactions drive C cycling processes and climate feedback.

1.3.2 Does elevated CO_2 fertilize plant productivity?

More CO_2 -> higher photosynthesis -> higher plant productivity = higher C sequestration?

The immediate response of plants to elevated CO_2 concentrations in the atmosphere is an increase in photosynthesis and adjustment of the stomatal conductance reducing transpiration (Franks et al., 2013). The increase in the photosynthetic rate was presumed to stimulate plant growth and thus lead to increased productivity (Körner, 2011). However, field observations often revealed a diminishing CO_2 fertilization effect in the long-term (Körner, 2006; Norby & Zak, 2011). The awareness rose that plant growth is rather sink (biosynthesis) than source (photosynthesis) driven (Fatichi et al., 2013) and that thus primary productivity is more often nutrient, water or temperature

than C limited (LeBauer & Reseder, 2008; Smith & Dukes, 2013). This implies on the one hand, that the primary productivity might not be predominantly CO_2 fertilized, but strongly influenced by the indirect effect of elevated CO_2 via the reduction of transpiration that increases the soil moisture (Holtum & Winter, 2010), as for example observed in shallow rooting grasslands (Morgan et al., 2004; Körner, 2006). On the other hand, the CO_2 fertilization effect is limited by soil fertility, especially in nutrient limited ecosystem like mature forests (Luo et al., 2004; Oren et al., 2006; Körner, 2006). Nevertheless, it is generally expected that the biomass production will rise in response to elevated CO_2. But whether the overall effect of elevated CO_2 results in an increase in net ecosystem productivity and thus enhanced C sequestration (negative feedback) is not clear, since the CO_2 efflux and thus ecosystem C loss was often observed to be enlarged as well (Zak et al., 2000; Pendall et al., 2004).

Higher assimilation = higher C emissions?

The increase of the net C efflux at elevated CO_2 concentrations is considered to be the result of several mechanisms: i) Reduced C residence times in the vegetation C stocks by decreased tree longevity (Bugmann & Bigler, 2011). ii) Enhanced plant-derived CO_2 emissions (autotrophic and rhizomicrobial respiration) due to higher C allocation into unproductive CO_2 respiring biomass relative to assimilating tissues, changes in phenology (e.g. delay in bud burst) or increased belowground C allocation (Drigo et al., 2008; Fransson, 2012; Leuzinger & Hättenschwiler, 2013). iii) Enhanced microbial respiration due to increased C deposition (rhizodeposition and litter), that stimulates the microbial SOM degradation and induces positive priming effects (Bardgett et al., 2008; Blagodatskaya & Kuzyakov, 2008; Kuzyakov, 2011). iv) Increased destabilisation of former protected SOM in deep soil layers due to deeper rooting under elevated CO_2 (Fontaine et al., 2007; Heimann & Reichstein, 2008; Iversen, 2010).

Feedbacks induced by elevated CO_2 depend on plant-soil interactions

Measurements of the CO_2 efflux in field experiments did not always detect the expected increase in C emissions under elevated CO_2, whereby these results of reduced CO_2 efflux probably often remained unpublished (Dieleman & Janssens, 2011). The reduced C emissions could be the result of negative priming, i.e. a reduction of microbial respiration of SOM due to changes in microbial community and higher microbial C use efficiency (Carrillo et al., 2014) or due to increased nutrient limitation of the microbial communities, since plants are the better competitors for nutrients in the long-term (Bardgett et al., 2008; Kuzyakov & Xu, 2013; Dijkstra et al., 2013). On the other hand the C loss could be reduced by enhanced SOM stability. Either through better aggregation

(physical protection of SOM) due to increased root and mycorrhizal activity (Treseder, 2004; Iversen, 2010) or due to increased deposition of root-derived C and low quality litter with high C:N ratios, which are thought to persist longer in the soil (Rasse et al., 2005; Luo et al., 2006; De Deyn et al., 2008; Kuzyakov, 2011).

To conclude, higher C assimilation (and lower transpiration) affects further C cycle processes that might increase the ecosystem C losses (Phillips, 2007; Drigo et al., 2008). The overall response of an ecosystem to elevated CO_2 is dependent on its environmental resources (e.g. nutrient and water availability) and physical and biological constraints (Reich et al., 2006; McCarthy et al., 2010; Norby & Zak, 2011), i.e. is the result of biological, physical and chemical interactions between plants and the soil.

1.3.3 Does decomposition temperature sensitivity drive soil C loss?

Higher temperature = higher decomposition rate = diminishing soil C stocks?

It is known for centuries that biochemical reactions are stimulated by temperature. Q10, the factor by which the rate increases with a temperature increase of 10 °C, has been widely used to describe the temperature sensitivity of reaction rates, hence also the soil respiration rate (recently reviewed by Wang et al., 2014). Consequently the molecular structure of SOM, i.e. its recalcitrance, was thought to make C persist in the soil and the C stocks were expected to decrease along with warming. However, such a clear correlation between temperature and C stocks or soil CO_2 efflux could hardly be observed, while precipitation and ecosystem productivity turned out to be important co-variants (Post et al., 1982; Raich & Schlesinger, 1992).

It became evident that decomposition is an enzyme-catalyzed process that can be limited by substrate availability at the active site of the enzyme (described by Michaelis-Menten kinetics). This eventually led to the concept of the "apparent" temperature sensitivity of decomposition, which is the result of the "intrinsic" temperature sensitivity related to the molecular structure and environmental constraints (sorption to minerals, aggregation, anaerobic conditions, water limitation, freezing) that reduce the substrate availability (Davidson & Janssens, 2006). This new concept along with findings that recalcitrant compounds (e.g. lignin) turn over faster than the bulk SOM (Amelung et al., 2008) were the basis for a change in paradigm in soil science (described in Schmidt et al., 2011). Nowadays the persistence of SOM is perceived to be not solely the result of its molecular structure (recalcitrance), but rather to be the consequence of environmental constraints on decomposition (e.g. soil moisture, oxygen availability) and its inaccessibility to decomposer organisms and catalytic enzymes (e.g. protected in soil aggregates or by organo-mineral interactions; Schmidt et al., 2011; Dungait et al., 2012).

Temperature feedbacks depend on interactions of the biota with its abiotic environment

The (intrinsic) temperature sensitivity of degradation is still a matter of debate, whereby most of the studies agree with the Arrhenius and enzyme kinetic theory (Kirschbaum, 2006; Sierra, 2011). However, it is doubtful that the increase in the process rate is highly relevant for climate feedbacks, since it does not per se lead to a decrease in C stocks (e.g. as demonstrated by Giardina et al., 2014), or to higher soil CO_2 emissions (e.g. as demonstrated by Billings & Ballantyne, 2013) and the decomposer community might adapt to warming (Bradford, 2013). More important for the feedback of C cycling to temperature might be the (indirect) effects on the substrate availability through changes in C deposition and stabilisation and on the environment affecting microbial physiology (Davidson & Janssens, 2006; von Lützow & Kögel-Knabner, 2009; Subke & Bahn, 2010; Conant et al., 2011).

For example, temperature is closely coupled to soil moisture by evapotranspiration (Seneviratne et al., 2010). Thus warming-induced drying reduces the soil CO_2 efflux in dryer areas due to lower substrate diffusion and root activity (Wang et al., 2014), while it increases the C effluxes from wetlands by improved aerobic decomposition and higher fire frequency (Davidson & Janssens, 2006; Wang et al., 2014). Further examples for the change of substrate availability is the temperature induced thawing of permafrost that will render large soil organic C stocks accessible to microbial decomposition (Davidson & Janssens, 2006; Field et al., 2007; Heimann & Reichstein, 2008; Arneth et al., 2010) and the change in the quantity and quality of plant C input (litter, rhizodeposition) due to accelerated assimilation, prolonged growing seasons or altered species composition (Luo, 2007; Metcalfe et al., 2011). A recent meta-analysis indicated that warming might not significantly decrease the net ecosystem C exchange, since the stimulation of plant-derived C influx counterbalances the increased efflux (Lu et al., 2013). However, there are still large knowledge gaps in the response of C cycling processes and interactions to warming and their relevance in different ecosystems (Luo & Weng, 2011).

The mechanistic understanding of terrestrial C cycle feedbacks to climate change is still limited. In the past the hypothesis on feedbacks were driven by the research on direct effects on photosynthetic and respiratory process rates. Today the physical, chemical and biological interactions between biota and soil are expected to be of higher relevance for the response of the ecosystem C exchange.

1.4 Towards a holistic approach to study C cycling

1.4.1 The challenge of scale - handling complexity

The main challenge in the research of C cycle feedbacks of terrestrial ecosystems to climate change is, that we cannot experimentally explore the spatial (global) and temporal scales (decades to centuries) the feedbacks occur on. Thus we can only formulate hypothesis about "potential feedback mechanisms" and incorporate them into complex climate models to predict future changes in climate and C cycling (Moorcroft, 2006). These models are based on our mechanistic understanding of C cycle processes and interactions (Moorcroft, 2006; Ostle et al., 2009; Friedlingstein & Prentice, 2010).

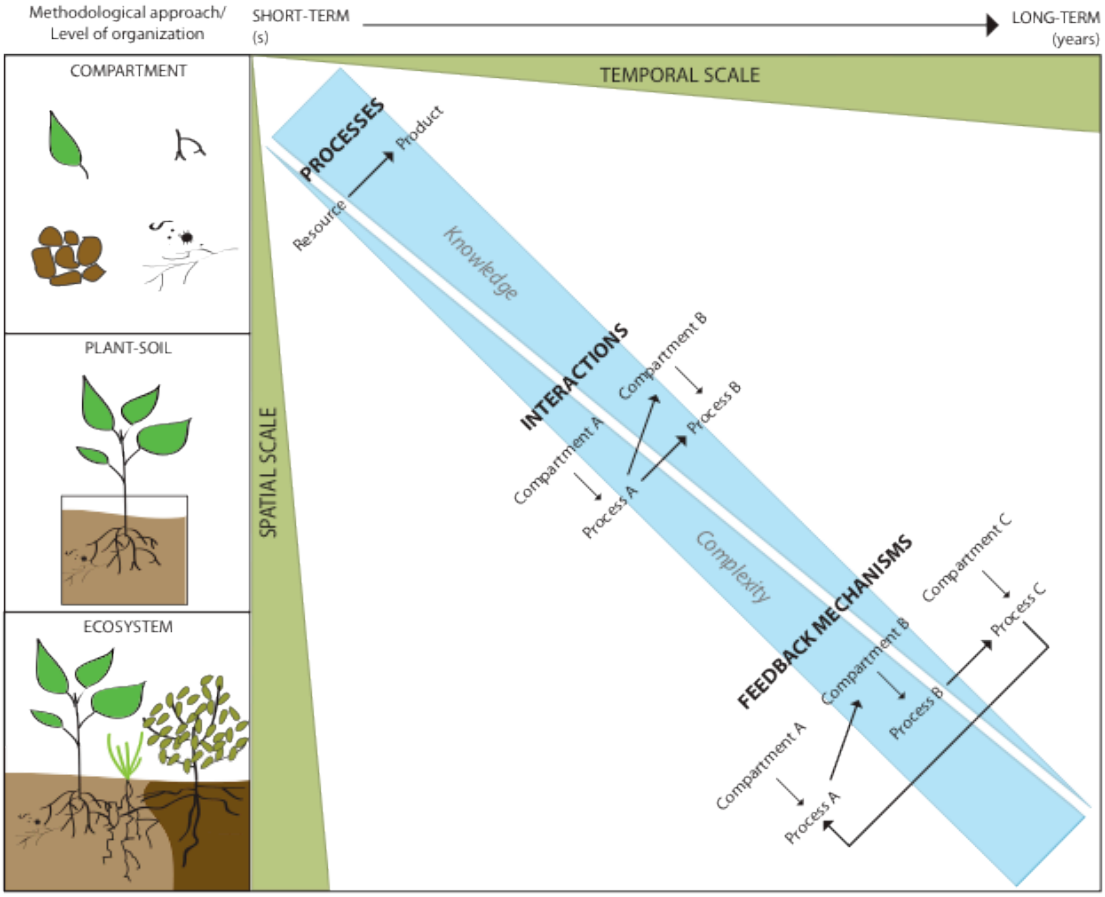

Figure 3 Terrestrial carbon cycling across scales. Three levels of organization can be identified in the terrestrial C cycle research, which are coupled to increasing spatial scale: compartments (leaves/roots, soil, soil biota), plant-soil and ecosystems. Single processes and their immediate responses to environmental change can be studied on compartment level, while the response including the direct and indirect interactions between (above- and belowground) processes and compartments can only be captured by approaches based on intact plant-soil systems. Climate feedback mechanisms are the result of a cascade of processes and physical, chemical and biological interactions between the atmosphere and terrestrial ecosystems that accelerate or retard climate change. Thus they occur at large spatial and temporal scales. With increasing temporal and spatial scale the level of complexity increases and the knowledge decreases.

The difficulty in formulating "potential feedback mechanisms" is, that feedback mechanisms are the result of a cascade of processes and interactions (**Figure 3**). Thus the level of complexity increases with scale and impairs the mechanistic understanding of observations at large scales (Leuzinger et al., 2011). Therefore empirical observations at large scales (e.g. by remote sensing or paleoecology) often lack a mechanistic explanation and cannot serve as a base to (re)define global models (nonetheless, they are crucial to test their performance). Thus we need to break down the complexity to a level that allows a mechanistic explanation of the observations.

Today, we have advanced knowledge about processes occurring at small scales, while our understanding declines as the scale increases from molecular to global (Gärdenäs et al., 2011). The study of single processes of the plant-soil C cycle bears also risks. On the one hand, the study of a single process essentially requires only the medium where the process occurs (e.g. the leaf, soil matrix). This directed scientist from different disciplines (e.g. plant physiology, microbiology, soil science) towards component-level studies of single processes, neglecting the interactions between them that are crucial for the C cycling in ecosystems (section 1.2.2). On the other hand, it is challenging to scale up measurements at compartment level to the large spatial scales at which feedback mechanisms occur. Processes and drivers relevant at one level of organization are not necessarily relevant or scale to higher levels of organization (Körner, 2011; Smith & Dukes, 2013; Gornish & Tylianakis, 2013). For example, an increase in leaf-level transpiration under elevated CO_2 does not necessarily indicate an overall increase in transpiration of the ecosystem, since the latter is dependent on other factors such as the overall leaf area (Leuzinger & Hättenschwiler, 2013). Thus process-level research led to misconceptions in plant and soil science as described above (section 1.3).

Hence we are confronted with the dilemma of allowing not too much (mechanistic explanatory power) vs. not too less complexity (scaling limits) in our research on terrestrial C cycling. Our task is to advance our knowledge by continuously shift the levels of "too much" and "too less" towards higher levels of complexity. For this we need to further explore and formulate hypothesis under controlled environments (small scales) and test their applicability at larger scales with field-scale and long-term experiments (Luo et al., 2011; Kreyling et al., 2014). Though, I think we should shift our focus from process-based to interaction-based research, i.e. acknowledge the importance of physical, chemical and biological interactions for C cycle processes and feedbacks and integrate them in the development of interdisciplinary research hypothesis and methodologies.

1.4.2 A holistic understanding of C cycling

I advocate for a more holistic understanding of C cycling. Holistic in the sense that everything has a physical, chemical and biological component, but that biology can not be purely explained by chemistry and physics (Looijen, 1998). Thus feedback mechanisms are not solely an addition of processes that are causally related (e.g. by static quantitative relations), but are the result of biological driven processes and interactions that are functionally related. Biota (flora, fauna) can be understood as the interface between the atmosphere and the soil, regulating the fluxes between these two C stocks. The particular characteristic of the biota is that it consists of living organisms, which have the ability to actively respond to and thus also change their environment. This holistic view has three major implications for terrestrial C cycle studies on climate feedbacks:

i) Biota (living organisms) and soil interact: Soil organic matter dynamics (e.g. degradation, stabilisation and respiration) should always be studied in combination with changes in plant activity (e.g. assimilation, allocation and deposition), and vice versa.
ii) Living conditions of biota drive the response of plant-soil systems to climate change: the response of individuals and communities depends on the most limiting factor of the environment as a whole (above- and belowground physical, chemical and biological conditions).
iii) Living organisms can adapt to changes: responses are dynamic and should thus be observed over time.

Processes and interactions of C cycling should therefore be studied at least at the spatial level of the plant-soil system and at mid-term temporal scale (**Figure 3**). Furthermore, the responses to climate change should be investigated by multi-factorial approaches to allow interactions that determine the environmental conditions for the biota. To gain a mechanistic understanding of whole plant-soil C cycling we need innovative methods that are able to separate different C fluxes and stocks and detect the dynamic changes at time scales of weeks to months.

1.4.3 Measure C dynamics in a C environment

The biggest challenge in studying C cycling in plant-soil system is to separate C fluxes and stocks in a C dominated system. For example, a net increase in the atmospheric CO_2 can derive from a decrease in CO_2 assimilation or an increase in CO_2 effluxes. Thus it could be the result of decreased photosynthesis or increased autotrophic respiration, heterotrophic respiration of SOM or plant-derived OM or acidification of inorganic soil C.

A powerful tool to study C cycling in the plant-soil system is stable isotope tracing (Amelung et al., 2008; Werner et al., 2012). Stable isotopes differ in their mass (e.g. ^{12}C and ^{13}C), but behave chemically very similar in the environment. 99 % of terrestrial C atoms are abundant as ^{12}C (Dawson et al., 2002). We can artificially change the abundance of ^{13}C in the plant-soil system, for example by adding ^{13}C via plant assimilation or deposition to the soil, and trace it at a later stage. This technique has the great advantage that C can be traced with minor disturbance. Thus the ^{13}C marked C can be differentiated from other C stocks and fluxes without affecting the processes and interactions between atmosphere, biota and soil.

Two ^{13}C-CO_2 labelling approaches are commonly applied: the pulse and continuous labelling technique (reviewed in Meharg, 1994; Kuzyakov & Domanski, 2000). The pulse labelling technique exposes plants for a short time (min to hours) only, but to highly labelled CO_2. The assimilated ^{13}C can be traced in the plant-soil compartments for a few days. The continuous labelling technique exposes plant continuously to less strongly labelled CO_2 than in pulse labelling experiments, or even to depleted CO_2 (from fossil sources) as for example in Free Air CO_2 Enrichment (FACE) experiments. There are no limits in the time of labelling and tracing, except for the maximum detectable label strength that has to be taken into account. However, there is no generally accepted approach to extract the information (e.g. about C residence time) in continuous labelling experiments, and there is only one systematic comparisons with pulse labelling (Warembourg & Estelrich, 2000). Furthermore, it is not clear if the results (e.g. of C partitioning) depend on the time of sampling. These two issues are crucial for the validity of data comparisons between techniques or sampling dates (e.g. to assess the dynamics after changes in environmental conditions).

To improve our mechanistic understanding of the complex interactions in plant-soil C cycling that lead to climate feedbacks we need to improve our knowledge of interactions in controlled and simplified environments, formulate hypothesis about potential feedback mechanisms and test them in long-term settings on ecosystem level. This requires advanced methods to separately measure C fluxes and stocks without disturbance of the plant-soil system, such as stable isotope techniques.

2 Objectives

Objective 1: Develop a facility to measure processes and interactions of C cycling in the plant-soil system and its dynamics over time (e.g. after an environmental change).

The first aim of the project was the development of a facility than can be to study responses of plant-soil C cycling under controlled environmental conditions with a holistic approach. The requirement were:

1. Entire plant-soil systems to study different C cycling processes simultaneously and to investigate plant-soil interactions.
2. Controlled environmental conditions with the possibility to simulate multi-factorial climate changes (CO_2, temperature, moisture).
3. Setup to study dynamics, i.e. to measure C fluxes and stock changes over time, at time scales relevant to the investigated processes and interactions (weeks-months).

Objective 2: Compare the pulse and continuous ^{13}C-CO_2 labelling techniques and assess their suitability to estimate plant-soil C cycling (C transfer, partitioning and residence time) with a holistic approach.

The second aim of this PhD project was to test if continuous labelling is more suitable than pulse labelling to study plant-soil C cycling with a holistic approach (labelling of all stocks, independent on sampling date) and to find a comparable way of data extraction. The hypothesis were:

1. The continuous labelling leads to a stronger labelling of the soil compartments (microbial biomass, SOM) than the pulse labelling (and is thus more suitable for a holistic approach to study plant-soil C cycling).
2. The continuous labelling technique can be used to estimate the C transfer, partitioning and residence time based on ^{13}C tracing in different plant-soil C compartments (as the pulse labelling technique).
3. The pulse and (short-term) continuous labelling yield the same results for C transfer, partitioning and residence time.
4. The time of sampling does not affect the result of C partitioning and thus ^{13}C tracing is a suitable technique to study C dynamics over time (holistic approach).

Objective 3: Explore the potential of a multi-isotope (^{13}C, ^{18}O, ^{2}H) labelling approach to label assimilates and trace organic matter within the plant-soil system.

The third aim of the PhD thesis was to develop a new multi-isotope labelling technique to label and trace OM as a whole, since the chemical form of OM is of importance for many processes and interactions in terrestrial C cycling (e.g. allocation, degradation,

stabilisation). Organic compounds consist of C and different amounts of oxygen (O) and hydrogen (H). The atomic ratios of these elements (O/C and H/C) can be used to differentiate major groups of organic compounds graphically in a van Krevelen diagram (Kim et al., 2003; Ohno et al., 2010). Therefore we tested if fresh assimilates can be labelled with ^{13}C, ^{18}O and ^{2}H at their place of formation (leaf photosynthesis) and if the OM dynamics can be traced in the plant-soil system based on the isotopic ratios ($^{18}O/^{13}C$, $^{2}H/^{13}C$) of bulk OM. The hypothesis were:

1. The atmospheric ^{18}O and ^{2}H label equilibrates with the leaf water (as it is known for the ^{13}C label), whereby the label strength does not vary between leaves at different positions on the shoot.
2. The leaf OM can be labelled simultaneously with three stable isotopes by the addition of ^{13}C-CO_2 and ^{2}H and ^{18}O labelled water vapour to the plant atmosphere.
3. The ^{13}C, ^{2}H and ^{18}O label assimilated in the leaves is transferred to other plant-soil compartments (stems, roots, microbial biomass, SOM).
4. The isotopic ratios of the label recovered in the plant compartments (leaves, stems, roots) can be used to determine the characteristics of the OM formed, analogues to a van Krevelen diagram.

Objective 4: Study the dynamics of belowground plant C release relative to the aboveground assimilation at plant growth limiting conditions and assess its effect on the soil respiratory fluxes.

The forth aim of this project was to improve our mechanistic understanding of rhizosphere priming, a key mechanisms for terrestrial feedbacks to climate change. However, the relations between the amounts of C assimilated, deposited and primed are unknown. We traced the dynamics in aboveground C assimilation and belowground plant C deposition and respiration during the initial development of rhizospheres. The hypothesis were:

1. The plant-derived soil CO_2 efflux is a constant proportion of the C assimilated aboveground .
2. The amount of C released belowground increases with plant growth and gradually enhances the SOM-derived respiration (positive rhizosphere priming).

The work done related to these four objectives resulted in four manuscripts for scientific publication presented in Part B of this thesis. In the following sections, some highlights out of these manuscripts are presented.

3 Methodology

3.1 Experimental approach

3.1.1 Plant-soil systems in controlled environments

Labelling chambers

The experiments were conducted in two automatically operated labelling chambers, which contain 15 plant-soil systems each. The plants share a common atmosphere (upper chamber system), but root in individual soil pots (lower chamber system). The development of this laboratory facility called MICE ("Multi-Isotope labelling in a Controlled Environment") was a crucial part of this PhD project (objective 1) and it is thus described in detail in the result section 4.1.1.

The first version of the facility (MICE 1.0) was limited in the control of the environmental conditions in the upper system and in the monitoring of the lower system. The experiments of this PhD project were conducted in MICE 1.0 and supported the development of MICE 2.0. In the second version of the facility (MICE 2.0, Manuscript I 'The MICE facility') we improved the light intensity (plasma light engines), established the temperature control (air conditioning system) and the adapted the humidity control (ultrasonic vaporizers). Further the soil respiration monitoring was extended from nine to twenty pots to increase the number of replicate measurements.

Environmental conditions

We used steady environmental conditions optimized for plant growth: humid air (71 ± 6 % relative air humidity), moist soil (watered to field capacity every 3rd day) and CO_2 levels close to saturation (520 ± 20 ppm). Only the temperature (31 ± 2 °C) and the light intensity (80 µmol m^{-2} s^{-1}) were not optimal in MICE 1.0. The temperature was at the upper limit for active plant growth and the light quantity was 3.5 mol photons day^{-1} (12 hours day/night cycles) correspondent to a shady place in nature (Poorter et al., 2012).

Plant and soil

As model plant we used poplar (*Populus deltoides x nigra*, Dorskamp clone) grown from stem cuttings. Poplar was the ideal species, because it is fast growing and its physiology has been intensively studied and because it allows a clear separation of above- and belowground plant compartments in the labelling chambers.

The soil was collected in a deciduous forest (8°33'E, 47°23'N, 500 m elevation) from the uppermost 15 cm of a cambisol. The soil had a clay loam texture (21 % sand, 43 % silt, 36 % clay). We left the soil structure as intact as possible and sieved the soil only with a large sieve (3.5 cm mesh size) to remove gravel and large pieces of OM.

3.1.2 Stable isotope labelling and tracing

We used stable isotopes to label and trace OM within the plant-soil systems. The labels were added in the gaseous phase to the shoots by ^{13}C enriched CO_2 and ^{2}H and ^{18}O depleted water vapour and we traced them in the bulk material of plant-soil compartments. We conducted three experiments with different labelling approaches. With the first two experiments we addressed objective 2 and 3 and the details on the methods applied are described in Manuscript II '^{13}C labelling techniques' and Manuscript III 'Multi-isotope labelling' (Part B). The third experiment was designed to answer the hypothesis of objective 3 and is described in detail in Manuscript IV 'Rhizosphere priming'.

Experiment 1 - Pulse labelling with ^{13}C

We labelled six weeks old poplars with 99 atom% ^{13}C-CO_2 (Cambridge Isotope Laboratories, Inc.) for 2.5 hours. The CO_2 concentration within the chamber was lowered to 250 ppm before the addition of the label to minimize its dilution with the ^{12}C present. After the pulse labelling the plants were fed with CO_2 from mineral sources with isotopic signatures close to ambient air.

We destructively harvested three plant-soil systems at five sampling dates: before labelling (unlabelled reference) and after 0.1, 1, 2 and 8 days. We analysed leaves, petioles, stems, cuttings, roots, microbial biomass and bulk SOM. The isotopic signature of the soil respiration was analysed in the three pots of the last destructive harvest. Gas samples were taken before labelling and then frequently traced during the first day (2, 4, 6, 8, 21 after labelling) and after 1, 2, 3, 4, 5 and 8 days.

Experiment 2 - Continuous labelling with ^{13}C, ^{18}O and ^{2}H

As in the first experiment we labelled six weeks old poplars, but now with 10 atom% ^{13}C-CO_2 (Cambridge Isotope Laboratories, Inc.) and continuously for 14 days. In addition we used water depleted in ^{18}O and ^{2}H to humidify the atmosphere around the shoots. The labelled gases added during the experiment were thus enriched by 8.9 atom% ^{13}C and depleted by 0.07 and 0.01 atom% ^{18}O and ^{2}H, respectively, compared to the atmosphere.

The harvests were performed as in the previous pulse labelling experiment, but one was done at the end of the experiment (14 days) instead of directly after the labelling (0.1 days). The soil respiration was additionally sampled at day 11 and 14. To trace the water label, we extracted the water vapour from the chamber atmosphere and the tissue water from the leaves, stems, roots and the soil.

Experiment 3 - Continuous labelling with ^{13}C from first emergence of leaves

We grew poplars from first emergence of leaves, either in a standard atmosphere (control) or in an atmosphere enriched in ^{13}C-CO_2 for 70 days. We applied 6 atom% ^{13}C-CO_2 during initial plant development to label all freshly produced plant biomass. The isotopic signal of the chamber atmosphere and the soil respiration (in six pots) was measured every 3-4 days during the first 24 days and every 7th day thereafter.

After 70 days the plant-soil systems were destructively harvested. Five pots were harvested above- and belowground and ten aboveground only. We used their belowground parts for a decomposition study (not presented here). The harvested plant-soil systems were separated into leaves, stems (including petioles), cuttings, roots and the microbial biomass and SOM of rhizosphere and root-free soil.

3.2 Measurement of C stocks

3.2.1 Atmosphere

CO_2 concentration

The CO_2 concentration of the shoot atmosphere (in µmol mol^{-1}) was monitored every 5 s with an infrared gas analyzer (IRGA, LI-840, Licor Inc.) in the upper chamber system. Manual gas samples of the chamber atmosphere were taken with a syringe through a septum inserted in the main gas circuit of the facility. The samples were transferred into evacuated glass vials for $\delta^{13}C$ later isotopic analysis (section 3.4).

The atmosphere above the soil (lower chamber system) was measured less frequently, since one IRGA is used to measure several pots. Details are described in section 3.3.2.

H_2O concentration

The H_2O concentration in the chamber atmosphere (in mmol mol^{-1}) was monitored with the IRGA along with the CO_2 concentration. The relative humidity (in %) was calculated based on the room atmospheric pressure (measured by the IRGA) and the chamber temperature (measured by a Pt-100) as described in Manuscript I 'The MICE facility' (Part B). The water vapour was collected by a peltier cooled water condenser, which used to be in line of the gas circuit in MICE 1.0. The water samples were frozen in glass vials before $\delta^{18}O$ and $\delta^{2}H$ analysis (section 3.4).

3.2.2 Plant

Tissue separation

The destructive harvests were done in two steps. First the leaves were detached and its leaf area measured by a handheld leaf area meter (CID-203 Laser, CID Inc.). Then

petioles were clipped from the leaves and the stems were cut from the cutting. The aboveground compartments (leaves, petioles, stems) were then either directly dried in the oven or stored frozen in glass vials for later tissue extraction.

In a second step the belowground compartments were sampled. We cut off the roots from the cutting and collected them out of the soil by tweezers. Then we washed the roots with deionised water and dried them gently with paper tissues. The cuttings and roots were then either oven dried or frozen, analogue to the aboveground compartments.

Tissue water extraction

The water was extracted from leaves, stems, roots (and soil) by cryogenic vacuum extraction. The frozen samples were attached to an evacuation line and warmed up in a water bath. The evaporating water was collected in U-vials submersed in liquid nitrogen cold traps. The extracted tissue water was transferred in glass vials and stored frozen for later $\delta^{18}O$ and $\delta^{2}H$ analysis (section 3.4).

3.2.3 Soil

Rhizosphere vs. root-free soil

A mesh cylinder in the soil pots was used to separate the soil into rhizosphere (inside) and root-free soil (outside the cylinder). The mesh cylinder was made of a stainless steal grid and was coated with a fine mesh (30 µm PETEX, Sefar AG) to prevent the roots to grow through.

At a destructive harvest 3-4 soil subsamples were taken. One sample was dried in the oven and used for later isotopic analysis of $\delta^{13}C$ (section 3.4), two samples were kept fresh in the fridge for the extraction of the microbial biomass and one sample was kept in the freezer for water extraction (section 3.2.2).

Extraction of microbial biomass

The soil microbial biomass was extracted by chloroform fumigation (Murage & Voroney, 2007). The two soil samples stored in the fridge were sieved to 5 mm. One sample was first fumigated for 24 h with chloroform to break up microbial cell walls, while the other was directly extracted with KCl solution. Half of the extracts were frozen for elemental analysis and half were lyophilised for $\delta^{13}C$ analysis (section 3.4). The microbial biomass was assessed by the difference between the fumigated and non-fumigated sample and applying a factor of 0.45 for the extractable fraction of microbial C (Joergensen, 1996).

3.3 Measurement of C fluxes

3.3.1 Photosynthesis and shoot respiration

The net photosynthetic and the dark respiratory fluxes were estimated by the change in atmospheric CO_2 concentrations in the daytime and at night-time, respectively, and the total leaf area of the shoots in the upper chamber system. The CO_2 concentration changes were monitored during 5 min every half an hour, whilst the automatic regulation of the CO_2 concentration by the labelling chambers (CO_2 scrubbing and injection) was switched off. The linear regression line yielded the concentration change (in µmol CO_2 mol^{-1} s^{-1}), which was used to calculate the flux rates.

The shoot C fluxes were expressed either as average rate (µmol CO_2 m^{-2} s^{-1}) of net photosynthesis and dark respiration per leaf area or as daily amount of net assimilated C per plant individual (mg C day^{-1}). The latter was calculated by the sum of C net assimilated during the light hours and the C respired during the dark hours. Details on the calculation pathways are given in Manuscript I 'The MICE facility' (Part B).

3.3.2 Soil respiration

The soil respiration was measured in the lower chamber system. Each pot was aerated with outdoor air. The CO_2 concentration of the air in- and efflux was frequently scanned in three (Experiment 1 and 2) or six pots (Experiment 3) with an IRGA (LI-840 Licor Inc.). The monitored pots were manually switched to a loop to circulate the air between the pot and the IRGA and to sample the evolving CO_2 with a syringe through a septum.

Soil CO_2 efflux rate

The soil CO_2 efflux rate was assessed by two different approaches, either as single point measurements (Experiment 1 and 2) or by continuous monitoring (Experiment 3).

In the first two experiments the CO_2 efflux was estimated by the speed of CO_2 concentration increase during the septum loop sampling by the slope of the linear regression line. The efflux rate (in µmol m^{-2} s^{-1}) was then calculated based on the concentration change rate, the pot air volume and its ground area (details in Manuscript II '^{13}C labelling techniques').

In the third experiment the CO_2 concentration was measured hourly, whereby the pot in- and outlet air was recorded for five minutes each. The CO_2 efflux rate was calculated based on the CO_2 concentration difference between in- and outlet, the aeration rate and the pot ground. The daily amount of C respired belowground by a plant-soil system (in mg C day^{-1}) was estimated by the sum of the 24 hourly respiration rates area (details in Manuscript IV 'Rhizosphere priming').

Isotopic signature of CO_2 efflux

The isotopic composition of the soil CO_2 efflux was estimated by the Keeling plot approach (Keeling, 1958; Pataki, 2003), which is based on a two end-members isotopic mixing model (with preservation of mass). The air sampled within the septum loop represents a mixture between the background air (pot air inlet) and the CO_2 emitted from the soil. We sampled the inlet air and took two samples with an offset of 100 µmol CO_2 mol^{-1} in the septum loop and analysed it for its isotopic composition (section 3.4). The isotopic signature of the air has a linear relationship to the inverse of its CO_2 concentration. Thus the isotopic signature of the second end-member (CO_2 efflux) can be estimated by the intercept of the linear regression line.

Plant- vs. SOM-derived respiration

The isotope label added to the shoots was used in the third experiment to partition the plant-derived (root and rhizomicrobial respiration) from the total soil CO_2 efflux. We applied another two end-members mixing model, whereby the isotopic signature of the total CO_2 efflux represents a mixture between SOM-derived and plant-derived CO_2.

The signature of the SOM-derived efflux was estimated in the unlabelled control experiment. The signature of the second source, the plant-derived C, had to be estimated, since we did not sample the plants during the experiment. Thus the isotopic composition was assessed by cumulating the daily amounts of ^{12}C and ^{13}C assimilated, based on the signature measured in the chamber atmosphere (section 3.2.1) and the assimilation rate (section 3.3.1). We fitted a logarithmic function to the chamber air signatures to receive continuous data and assumed that the signature of fresh assimilated C bears the isotopic signature of the chamber air minus the isotopic discrimination of 27 ‰ (Farquhar et al., 1989). Details on the calculations are given in Manuscript IV 'Rhizosphere priming' in Part B.

3.4 Elemental and isotopic analysis

The solid samples were milled to a fine powder with a steel ball mill prior to analysis and were weighed into tin (C analysis) or silver (O and H analysis) capsules. The liquid and gaseous samples were not pre-treated and directly injected into the analyzers.

Elemental analysis

The elemental C, H, N and O analysis of solid samples were done at the 'Micro-Laboratory' at the ETH Zurich (CHN-900 and RO-478, Leco Corp.). The elemental C analyses of the liquid microbial biomass extracts were measured with a TOC-500

analyzer (Shimadzu Corp.) in the laboratory of 'Forest soil and Biogeochemistry' at the Swiss Federal Institute for Forest, Snow and Landscape Research (WSL Birmensdorf).

Isotopic analysis

The isotopic composition was measured by isotope ratio mass spectrometry. We measured $\delta^{13}C$ and $\delta^{18}O$ of the solid samples, $\delta^{18}O$ and $\delta^{2}H$ of the liquid samples and $\delta^{13}C$ of the gaseous samples in the 'Laboratory for Atmospheric Chemistry' at the Paul Scherrer Institute (Villigen, Switzerland). The $\delta^{2}H$ of the solid samples were measured on the non-exchangeable fraction of hydrogen after equilibration with vapour in the laboratory for 'Climate and Environmental Physics' at the University of Bern. Technical details on the mass spectrometry analysis are given in the Manuscripts (Part B).

The stable isotope composition of materials was measured and is usually expressed in the delta (δ) notation in permill (‰) relative to the international standards (Werner & Brand, 2001). However, the δ-notation is not linear, and the use of the atom fraction expression is suggested when working with isotopic ratios largely different from natural abundances (Brand & Coplen, 2012). Thus we expressed the label strength as excess atom fraction compared to unlabelled material according to Coplen (2011) and multiplied it with the C stock or flux present in order to estimate mass balances.

4 Results and Discussion

4.1 Multi-Isotope labelling in a Controlled Environment (MICE)

4.1.1 Special features of the MICE facility

General overview

The MICE facility was built to maintain plant-soil systems in controlled environments and to study the response of C cycling to environmental changes with isotope labelling techniques. The facility can hold up to 30 individual plant-soil systems in two labelling chambers that can be operated independently. Each chamber consists of three units (**Figure 4**): i) the light system that controls the day/night cycles, ii) the upper chamber system, a polycarbonate cuboid (1.2 m^3) that encloses the shoots of 15 plants and various sensors and instruments to monitor and regulate the atmospheric conditions (CO_2, H_2O, temperature) and iii) the lower system, a valve system that aerates 15 individual pots and monitors the soil respiration selectively. The concept and the configuration of the facility is described in detail in Manuscript I 'The MICE facility'.

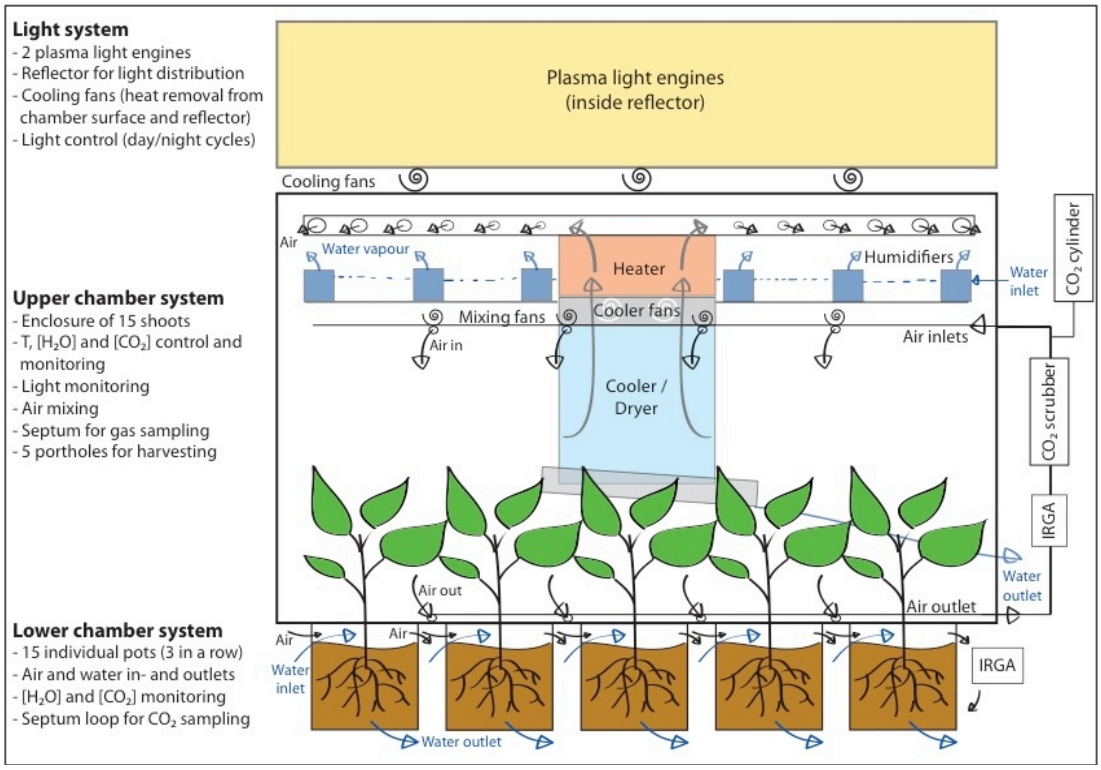

Figure 4 The MICE 2.0 facility. Scheme represents one out of two labelling chambers of the MICE facility. The labelling chamber is separated into the light system (control of day/night cycles), the upper chamber system (control of atmospheric conditions, monitoring of aboveground C fluxes) and the lower chamber system (control of soil conditions, monitoring of belowground C fluxes).

Hermetical separation of above- and belowground system

The most important feature of the MICE facility is the hermetical separation of the aboveground plant-soil compartments (atmosphere, shoots) from the lower compartments (roots, soil; **Figure 5**). The front plate of the polycarbonate cuboid of the upper system can be removed to insert the plant-soil systems, whereby the stems are fed through slots in the bottom plate. The pots are wound up until their edge, a foamed rubber in a notch, presses against the bottom plate. The slots are closed with polycarbonate pieces, sealed with tape and a malleable sealant around the stems.

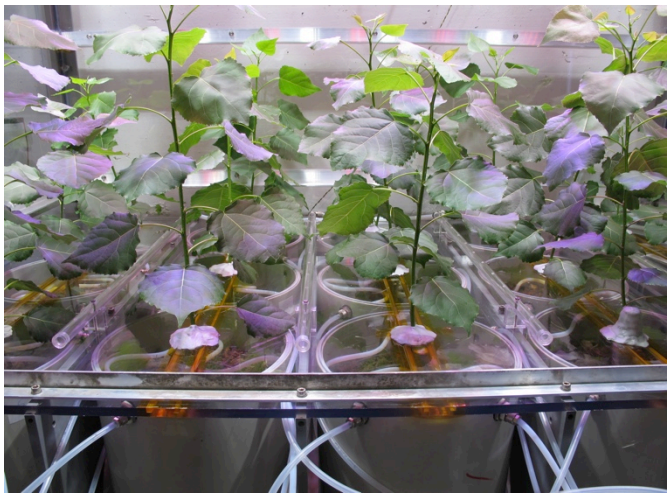

Figure 5 Separation of above- and belowground compartments in the MICE facility. The upper system containing the plant shoots is hermetically separated from the lower system (individual soil pots). The picture was taken before closing the chamber for the pulse labelling experiment (Experiment 1).

This setup allows the separation of above- and belowground C fluxes and stocks. The net C gas exchange is measured separately for net photosynthesis, dark respiration and soil respiration and the stocks can be partitioned by addition of an isotope label to either of the systems. For example the addition of ^{13}C-CO_2 to the shoots allows the partitioning of plant-derived and SOM-derived soil C stocks and fluxes, since all ^{13}C recovered belowground had to be transferred through the plant. Furthermore, the setup prevents artefacts in the soil respiration measurements that are otherwise created by the diffusion of ^{13}C-CO_2 into the soil pores during the labelling and efflux thereafter (e.g. as in Högberg et al., 2008; Bahn et al., 2009). This unique setup with the simultaneous measurement of above- and belowground C dynamics will improve the mechanistic understanding of C cycling processes and their interactions.

The setup of plant-soil systems sharing a common atmosphere, but rooting in individual pots enables manipulation experiments in which the plants experience the same environmental conditions aboveground (e.g. warming, elevated CO_2), but separate conditions belowground (e.g. soil moisture, nutrient availability). Such experiments will

help us to further explore the importance and specificity of plant-soil interactions in regulating the response of C cycling to climate change.

The upper chamber system can be completely sealed as alternative to the setup with above- and belowground separation. Thus the chambers can be used to label a larger amount of plant-soil systems, for example in meso- or microcosms, for follow up studies (e.g. field incubation studies) designed to estimate long term effects.

Independent and automatic control of environmental conditions in two climate chambers

The main software of the MICE facility (developed by DMP GmbH) controls different instruments (**Figure 4**) that regulate the atmospheric temperature (heater, cooler), air humidity (humidifiers, dryer) and CO_2 concentration (scrubber, gas injection) in the upper system based on infrared gas analysis (IRGA) and temperature measurements. Another software regulates the light engines (developed by Lumartix SA). For each chamber day/night cycles, CO_2 concentration thresholds and day-/night-time temperatures and air humidity levels can be chosen, which are automatically regulated with high precision (described in Manuscript I 'The MICE facility'). Thus the two chambers can be used in parallel with different environmental conditions (e.g. to simulate climate scenarios) and for long-term experiments with steady conditions.

Continuous monitoring and sampling of fluxes and stocks

The MICE facility is constructed to study the dynamics in C cycling over time. On the one hand the changes in above- and belowground CO_2 fluxes are monitored by continuous IRGA measurements and frequent gas samplings. Further the dissolved organic carbon can be collected at the water outlets of the individual pots. On the other hand subsamples or whole plant-soil systems can be harvested during a labelling experiment with minor disturbance to the atmosphere through five portholes inserted in the front plate of the polycarbonate cuboid. Thus with the MICE facility we can study dynamics in C processes and interactions, such as adaptation or acclimatisation that are crucial in the response of C cycling to climate change.

4.1.2 Pulse vs. continuous (^{13}C-CO_2) labelling to trace C dynamics

General overview

The MICE facility can be used to apply both ^{13}C-CO_2 labelling techniques, the pulse (PL) and continuous labelling (CL). Our first set of experiments confirmed that both techniques are suitable to assess C transfer, partitioning and residence time, even though their ^{13}C distribution dynamics in plant-soil compartments are fundamentally different (**Figure 6**). In PL a peak in ^{13}C abundance is observed, while in CL the label strength increases over time due to sustained ^{13}C label addition. The ^{13}C dynamics after

PL are commonly described by an exponential decay function (Epron et al., 2012). For CL no common method of data extraction exists. We suggest using a logistic function to describe the initial ^{13}C dynamics during CL. In Manuscript II '^{13}C labelling techniques' we compare the results achieved by the two techniques and discuss the information about C cycling we gain out of the ^{13}C distribution in the plant-soil compartments.

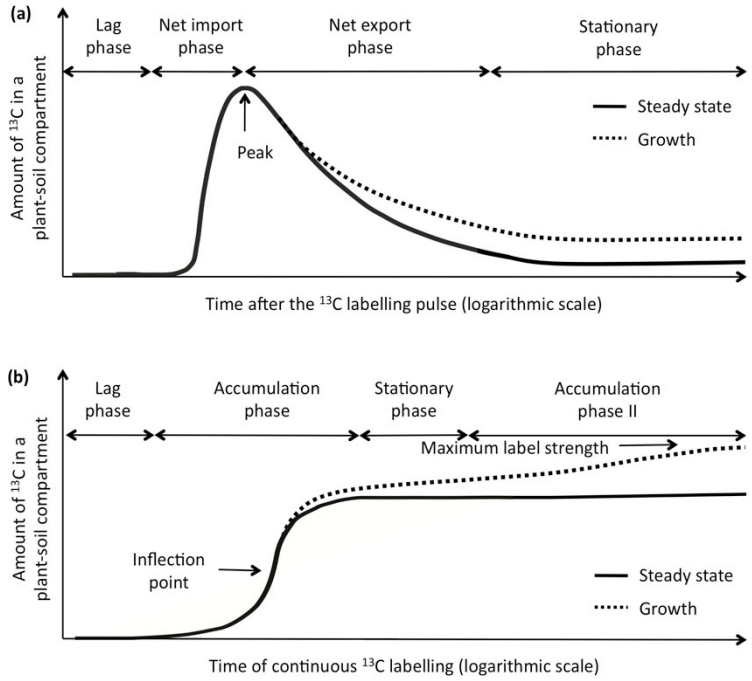

Figure 6 Pulse vs. continuous labelling technique. Visualisation of the ^{13}C dynamics detected in plant-soil compartments after pulse labelling (a) or during continuous labelling (b) given for a system at steady state or at growth (change in stock size). The short-term dynamics can be described by three phases: (1) lag phase (time needed for C transfer), (2) phase dominated by ^{13}C import or net accumulation and (3) phase dominated by ^{13}C export or stationary phase (equilibrium between ^{13}C import and export). On the long-term a forth phase can be identified, which is characterized by stationary (pulse labelling) or increasing (continuous labelling) ^{13}C contents (Manuscript II '^{13}C labelling techniques', Figure 1).

Do the two labelling techniques achieve the same results?

The C transfer and residence time estimates differ (**Table 2**), while the C partitioning estimates, assessed by the ^{13}C recovery at specific sampling dates, are comparable for the pulse and continuous labelling technique (**Figure 10**).

The C transfer, measured by the first ^{13}C signal detection, differed only for a few hours. However, pulse labelling is generally more suitable to estimate the speed of C transport than continuous labelling due to the strong labelling of the fresh assimilates that facilitates a fast signal detection (at least in smaller C stocks).

The mean residence time estimated by the rate constants of the exponential (PL) and logistic (CL) model (**Table 2**) were not comparable. One explanation might be that the

models assume steady state conditions (no change in stock size and proportional fluxes). These conditions are, as in this study, often not given for plant-soil systems, i.e. due to plant growth. Therefore the application of the models in this setting is not valid and we suggest using the length of the accumulation phase in the CL as an indicator for the residence time instead.

The C partitioning estimates were comparable for the two techniques, except for the microbial biomass, which contained more of the label in the CL. This was expected since short-term CL mainly labels non-structural C pools (as PL). However, in long-term CL the C partitioning estimates might differ compared to PL, since structural C pools would be labelled as well. This is of special importance for the belowground C cycling processes such as rhizodeposition, which not only consist of labile C release (e.g. root exudation), but also include the input of other compounds (e.g. border cells).

Table 2 Parameters of models describing the ^{13}C distribution after labelling. Parameters (a, b, k) of the exponential and the logistic model used to describe the ^{13}C dynamics in the plant-soil compartments (MB= microbial biomass, SOM = soil organic matter) in the pulse (PL) and continuous (CL) labelling, respectively. Parameter a is the total amount of ^{13}C (in mg) at the signal peak (PL) or at the stationary level (CL), parameter b marks the time of the signal peak (PL) or the time of inflection (CL) and parameter k is the rate constant describing the decrease (PL) and increase (CL) of the ^{13}C abundance in a compartment, which is the basis for the mean residence time (MRT) calculation (Manuscript II '^{13}C labelling techniques', Table 2).

	Pulse labelling, exponential model				Continuous labelling, logistic model				
Plant-soil compartment	Peak, amount (mg ^{13}C (fraction of total)) (a)	Peak, time (days) (b)	Rate constant (k)	MRT (days) (1/k)	Stationary level, amount (mg ^{13}C (fraction of total)) (a)	Inflection, time (days) (b)	Rate constant (k)	MRT (days) (1/k)	Stationary level, time (days)
Leaves	13.70 (73 %)	0.1	0.286	3.5	19.85 (62 %)	3.6	0.83	1.2	7.2
Petioles	0.68 (4 %)	1	0.047	21.1	2.14 (7 %)	3.3	1.08	0.9	6.5
Stems	3.17 (17 %)	1	0.077	13.0	7.76 (24 %)	3.8	0.89	1.1	7.6
Cuttings	0.85 (5 %)	1	0.118	8.5	1.44 (4 %)	3.1	0.78	1.3	6.2
Roots	0.35 (2 %)	2	0.029	34.0	0.92 (3 %)	3.8	1.33	0.8	7.6
MB	0.02 (0 %)	1	0.179	5.6	0.06 (0 %)	2.9	1.10	0.9	5.9
SOM					0.44	2.1	1.29	0.8	4.2
Soil respiration	0.39	1	0.520	1.9	0.31	2.9	0.73	1.4	5.9

The information we gain out of the ^{13}C distribution by the two techniques

The ^{13}C dynamics in a compartment after PL (**Figure 6a**) provides us three pieces of information (detailed discussion in Epron et al., 2012): i) how fast fresh assimilated C is transported (lag phase), ii) how much the fresh assimilated C was mixed with other C compounds before arriving (broadness of the peak) and iii) the turnover time of the (labile) C (rate of exponential decay). Further the comparison of the peak heights or the amounts of ^{13}C detected at a specific sampling date can be used to estimate the C partitioning between different compartments. However, the ^{13}C dynamics after PL mainly reflect the (short-term) C cycling of fresh assimilates and its allocation to active growing tissues (Kuzyakov & Domanski, 2000; Paterson et al., 2009).

The ^{13}C dynamics during CL (**Figure 6b**) generally provide the same information, but with slight differences. CL labels assimilates less strongly, but continuously, and thus labels C stocks more homogeneously than PL (Meharg, 1994; Paterson et al., 2009). This causes i) a delay in signal detection (lag time) due to lower label strength (longer duration till minimum detection limit is reached compared to PL), ii) a relatively fast labelling of transient storage pools that is detected by the time of inflection and iii) a realistic estimation of the C residence times at non-steady state conditions (based on the length of accumulation phase). Thus the ^{13}C dynamic during initial CL reflects the C cycling of OM including re-allocation from transient storage pools. The long-term ^{13}C dynamics (stationary level, accumulation phase II) can be used to assess C dynamics in larger C stocks with slower turnover (discussed in section 4.2.1) and the continuous labelling with ^{13}C from first emergence of leaves is suitable to trace the total amount of plant-derived C input to the soil (Kuzyakov & Domanski, 2000).

4.1.3 Multi-isotope (^{13}C, ^{18}O, ^{2}H) labelling to trace OM dynamics

With the first set of experiments in the MICE facility we could proof that OM can be labelled at its place of formation, i.e. during leaf photosynthesis, with its three major components ^{13}C, ^{18}O and ^{2}H by applying the labels to the plant's atmosphere. However, the multi-labelling was only successful at continuous exposure to the labelled water vapour (pulse labelling did not label the OM with ^{18}O and ^{2}H). The new labelling technique and its potential, also for other fields of research as for example paleoclimatology, is discussed in the Manuscript III 'Multi-isotope labelling'.

Label incorporation from the atmosphere into the leaves

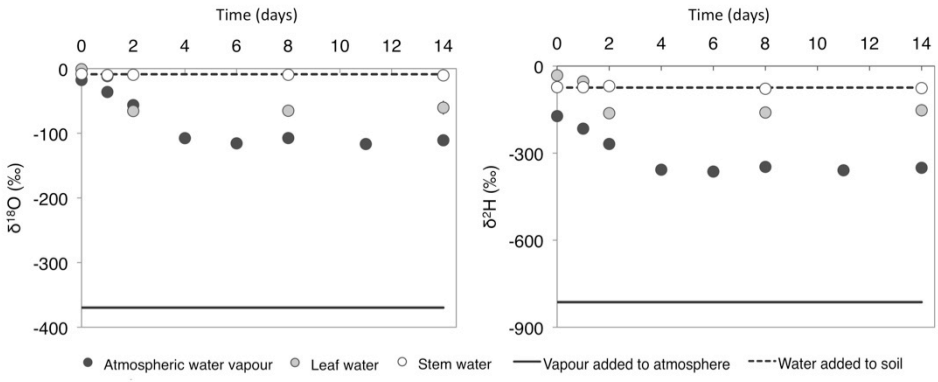

Figure 7 Diffusion of ^{18}O and ^{2}H labelled vapour into the leaf water. Dynamics detected in the water isotopic signatures of the plant-soil-atmosphere system during continuous $^{2}H_2{}^{18}O$ labelling. $\delta^{18}O$ (left) and $\delta^{2}H$ (right) signature (in ‰) of the depleted water label added as water vapour to the atmosphere, of the water added to the soil, of the resulting water vapour in the chamber atmosphere and of the extracted leaf and stem water. Error bars on the leaf water indicate ± one standard deviation of three plant replicates (based on Figure 1, Manuscript III 'Multi-isotope labelling').

The ^{18}O and ^{2}H label added to the plant's atmosphere via water vapour diffused into the leaves (**Figure 7**). With a sophisticated isotope-mixing model we demonstrated that a large fraction of the leaf water originated from the labelled atmosphere (58-69 %) at the humid air conditions present. The label within the leaf water did not spread further to the stem water (in opposite direction to the xylem stream), but it was incorporated into the leaf OM and could be traced in other plant compartments.

Does the technique improve our understanding of OM dynamics in the plant-soil system?
Our aim was to trace the OM dynamics by the isotope ratios of the label added ($^{18}O/^{13}C$, $^{2}H/^{13}C$). The ratios did differ in the leaf, stem and root bulk OM (**Figure 8a**). This indicates that the OM synthesised in the leaves was transformed during transport and allocation to the other compartments, whereby a part of the ^{18}O and ^{2}H was lost. However, with this first experiment we could not dedicate it to a specific process. The distinct isotopic ratios of the compartments could be the result of more condensed compounds synthesised in roots and stems (e.g. lignin) or of O and H exchange and fractionation processes during transport and biosynthesis.

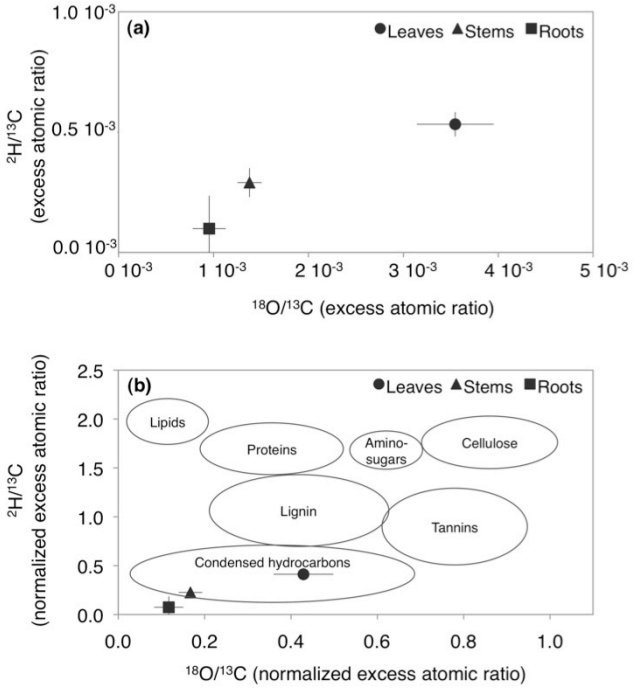

Figure 8 Multi-isotope labelling of organic matter. Isotopic ratios of the oxygen and hydrogen to carbon label recovered within the leaves, stems and roots. Figure **(a)** illustrates the isotopic ratios of the ^{13}C, ^{18}O and ^{2}H excess atom fraction (relative to the unlabelled tissues) measured after equilibrium in the labelling was reached (t = 8 and 14 days, six replicates ± one standard deviation) and in Figure **(b)** the isotopic ratios after normalization with the maximum label strength are shown. The circles overlain on plot (b) indicate the atomic ratios characteristic for different compound classes (van Krevelen diagram, adapted from Sleighter & Hatcher, 2007). The Figures are adapted from Fig. 2 Manuscript III 'Multi-isotope labelling'.

The attempt to plot the isotopic ratios of the label detected in the compartments analogous to the van Krevelen diagram (**Figure 8b**) made it obvious that we first need to improve our understanding of the exchange and fractionation processes during plant OM cycling, before we can use the multi-isotope labelling technique to identify the labelling of different compound groups. Nevertheless, the technique could be used to reveal the mechanisms behind these exchange and fractionation processes and the multi-labelled plant OM could be used to further explore OM dynamics during soil C cycling processes such as degradation, relocation or stabilisation (**Figure 2**).

4.2 Plant-soil C stocks

4.2.1 Challenges in plant-soil C stock analysis

Signal dilution in large C stocks

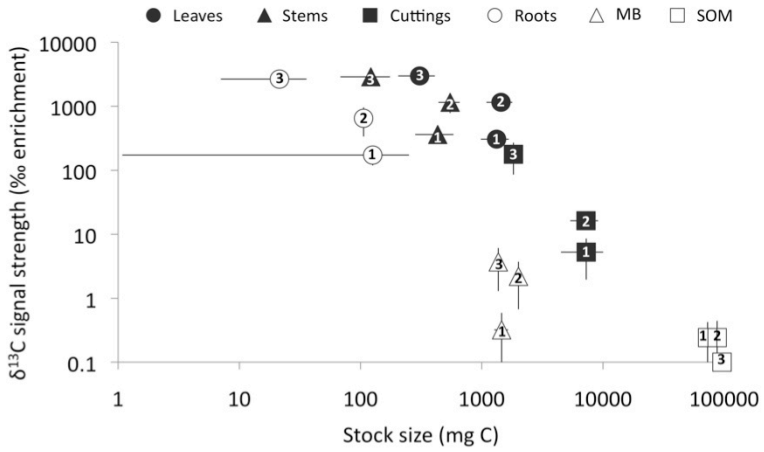

Figure 9 Stock size vs. signal strength. Comparison of C stock size (in mg C) and the $\delta^{13}C$ signal strength (in ‰ enrichment compared to unlabelled isotopic compositions) measured in plant-soil compartments at the end of the Experiment 1 (pulse labelling of six weeks old plants, sampling after 8 days), 2 (continuous labelling of six weeks old plant, sampling after 14 days) and 3 (continuous labelling from first emergence of leaves, sampling after 70 days). Aboveground compartments are illustrated with black and belowground compartments with white symbols (MB = microbial biomass, SOM = soil organic matter). Represented are average values of three (Experiment 1 and 2) and five (Experiment 3) replicates (± one standard deviation).

A major challenge in the holistic observation of plant-soil systems based on stable isotope techniques is, that large C stocks are involved in C cycling (SOM, microbial biomass). The isotopic signature is measured based on the ratio of the heavier to the lighter isotope. Therefore a higher amount of labelled substrate needs to be added to detect a significant change in the isotopic signal in larger C stocks (Kuzyakov & Domanski, 2000). Our results confirm the $\delta^{13}C$ signal strength decreased with stock size (**Figure 9**). Further the signal strength decreased with the distance to the leaf and was lower in the roots and the microbial biomass than expected based on their stock size.

During C cycling other non-labelled sources enter the cycle and thus dilute the signal derived from fresh assimilates.

Continuous labelling overcomes this dilution effect with time. In our data, this can be seen by the proportionally strong increase in the signal strengths in the roots, cuttings or microbial biomass from pulse (Experiment 1) towards long-term continuous labelling (Experiment 3). Nevertheless, the labelling duration and/or strength were not sufficient to detect significant signal strengths in the bulk SOM.

Signal variability in C stock subsamples

A possibility to overcome the problem of signal dilution is the specific sampling of (defined) C pools within the main stocks, as for example the rhizosphere soil stuck to roots during sampling. Sub-sampling, for example of single leaves, is also an approach to measure the C dynamics over time without sacrificing one of the limited plant-soil systems by a destructive harvest. However, taking subsamples does also bear risks.

In the first set of experiments we took leaf subsamples at different shoot positions. The leaves sampled at the upper half were 670 ‰ $\delta^{13}C$ more enriched after 14 days of continuous labelling than leaves sampled just below (Figure 2 in Manuscript III 'Multi-isotope labelling'). The difference was most likely caused by higher photosynthetic and growth activity of younger upper leaves than older and more shadowed lower leaves. The analysis of the mixture of the remaining material (bottom- and topmost newly formed leaves) revealed once more a higher enrichment by 690 ‰. Thus the subsamples had isotopic signatures in the range of 270-1630 ‰ $\delta^{13}C$ and were not representative for the whole leaf C stock (1060 ‰ $\delta^{13}C$).

4.2.2 C transfer and residence time affect C partitioning estimates

The C partitioning based on stable isotopes is important to assess the changes in plant C allocation, especially for large C stocks, where changes based on mass measurements are either quantitatively too small to be detected (e.g. C storage in cuttings) or the stock itself is too large to be sampled (e.g. SOM). However, the assessment of changes in C allocation based on ^{13}C dynamics is only valid if the C partitioning estimates (at constant conditions) are not affected by the time of sampling.

The results of the first two experiments indicate that this is generally the case for the plant C stocks (**Figure 10a**). Most of the assimilated C was invested into aboveground and especially into leaf biomass at the given environmental conditions (low light and optimal soil water availability). This allocation pattern is in line with the functional equilibrium theory, which implies that plants invest into the growth of the tissues that help reducing the most limiting factor (Poorter et al., 2012).

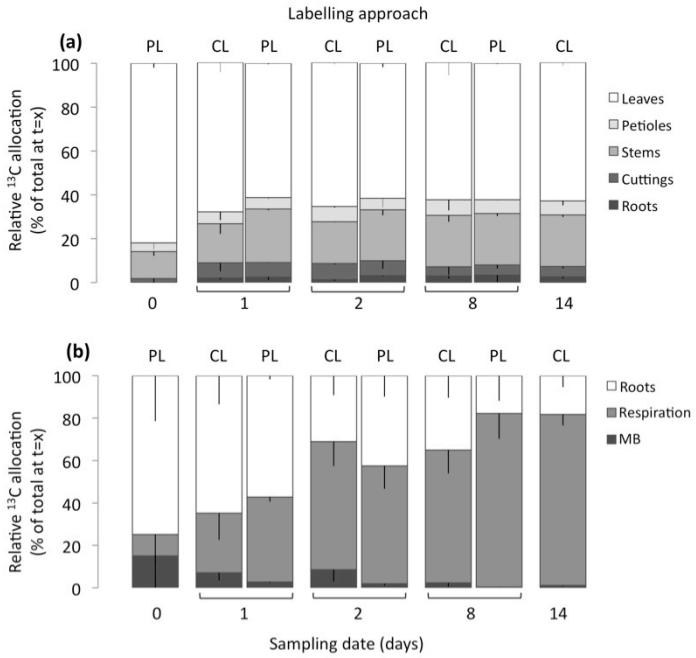

Figure 10 C partitioning at different sampling dates. C partitioning (in % of total ^{13}C recovered at a specific sampling date) after the pulse (PL) and during the continuous labelling (CL) assessed **(a)** for the plant compartments and **(b)** for the belowground compartments (including the cumulative soil respiration, MB = microbial biomass). The data represented are average values minus one standard deviation (data overview in Table 3 and 4, Manuscript II '^{13}C labelling techniques').

On the contrary, the belowground C partitioning was significantly different between sampling dates (**Figure 10b**). The proportion of belowground C allocated to root or microbial biomass was overestimated compared to the proportion released as CO_2 during the first week. This was most likely caused by a time lag in the tracer distribution at the plant-soil interface (Warembourg & Estelrich, 2000; Thornton et al., 2004), which was estimated to be 6-8 days in our experiments (**Table 2**, time until stationary level was reached). The mean transfer and residence time of C stocks can be assessed by the lag time and the length of the accumulation phase during continuous labelling (**Figure 6**) and has to be awaited before the allocation dynamics can be estimated based on the ^{13}C distribution.

4.3 Plant-soil C fluxes

4.3.1 Aboveground C assimilation vs. plant-derived respiration

The MICE facility is a unique tool to study the relation between above- and belowground C fluxes. It is generally assumed that plants release a constant fraction of the aboveground assimilated C into the soil environment through rhizodeposition (Kuzyakov & Domanski, 2000) and in C cycle models the belowground C dynamics (if respected at all) are treated as a passive continuation of the aboveground dynamics

(Matamala & Stover, 2013). Our results of the third experiment with continuous labelling of all assimilated C indicate that this is not necessarily the case.

The destructive harvests after ten weeks of growth confirmed that the belowground C release was quantitatively related to the aboveground C assimilation. The amount of ^{13}C detected in the cumulative ^{13}C efflux and the root and microbial C stocks of the individual plant-soil systems was the higher the larger the leaf area, i.e. the larger the overall C assimilation aboveground (Figure 2 in Manuscript IV 'Rhizosphere priming'). But the monitoring of the net photosynthetic and plant-derived respiratory fluxes during the ten weeks of labelling revealed opposite dynamics (**Figure 11**).

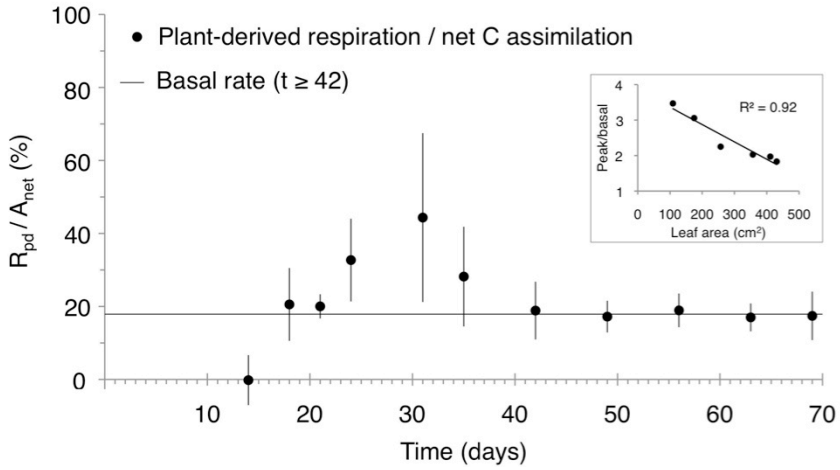

Figure 11 Belowground vs. aboveground plant-C fluxes. Dynamics in the proportion of the daily amount (mg C pot^{-1} day^{-1}) of plant-derived C respired belowground (root and rhizomicrobial respiration, R_{pd}) on the amount of net C assimilated aboveground (A_{net}). The basal rate of belowground C release relative to the assimilation is indicated with a black line and was calculated as the average of the last five data points (t ≥ 42). The small Figure shows the correlation between the leaf area and the magnitude of the increase (peak maximum of R_{pd}/A_{net}) relative to the basal rate of belowground C release. The error bars indicate +/- one standard deviation of six plant-soil systems (Manuscript IV 'Rhizosphere priming', Figure 3c).

The plant individuals released a constant fraction of 18 ± 3 % of net assimilated C belowground towards the end of the experiment, but at the beginning of plant development this belowground C release was massively increased by 6-63 %. The increase above the basal rate was the largest in the smallest plants (small figure in **Figure 11**), which were restricted in their growth. The growth limitation was induced by diminished cutting reserves after long storage (7 months). Thus the plants seem to be able to actively change the rhizodeposition in response to an environmental constraint, in this case to nutrient limitation and do not only release passively a certain fraction of the net assimilated C belowground. Thus rhizodeposition cannot solely be explained by a causal relationship to photosynthesis, because there is also a functional component related to it (e.g. increase in soil nutrient availability) that is biologically driven.

4.3.2 Belowground plant C release vs. soil respiration

One of the big unknowns in the feedback mechanisms of C cycle to climate change is the priming effect, i.e. the change in SOM mineralisation due to fresh OM inputs (Kuzyakov, 2010; Cheng et al., 2014). On the one hand elevated atmospheric CO_2 concentrations might lead to a higher plant C deposition (Heimann & Reichstein, 2008) and on the other hand the rhizodeposition might be actively altered by the plants in response to environmental constraints, as shown in the previous section (4.3.1) and induce a rhizosphere priming effect. It is generally presumed that there is a causal relation to the amount of C deposited in the sense of "the more C deposited, the higher the priming effect" (e.g. as observed in Paterson & Sim, 2013 or Zhu et al., 2014) and the direction and the intensity of the priming effect is thought to depend on the nutrition availability in the soil (Dijkstra et al., 2013; Chen et al., 2014).

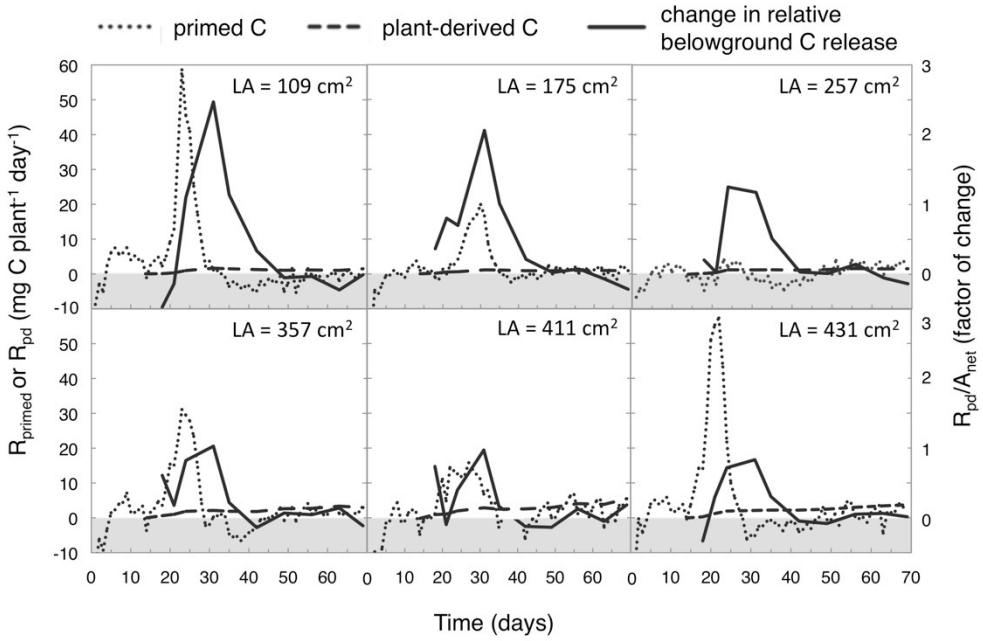

Figure 12 Plant-C release vs. SOM priming. Dynamics in the daily amount of primed C (R_{primed}) and plant-derived C respiration (R_{pd}) and the change in the relative belowground C release expressed as factor of increase/decrease relative to the basal rate of assimilated C released belowground (R_{pd}/A_{net}, see **Figure 11**) of six individual plant-soil systems characterized by different leaf areas (LA). The plant-derived C respiration is an indicator for the quantity of rhizodeposition, the increase in the relative belowground C release is considered to be associated with the release of compounds with a specific function for the plant nutrient acquisition and the leaf area is a proxy for the development stage of the plant individual (measured after 70 days of growth), which is most probably related to the nutrient deficiency in the individuals. Negative values are marked with a grey bar (Manuscript IV 'Rhizosphere priming', Figure 4).

In our study we did not find a clear quantitative relation between the belowground C release and the primed C (details in Manuscript IV 'Rhizosphere priming'). The amount of plant-derived C respired by the roots and the rhizomicrobial community did rise

continuously with the development of the plant-soil systems, but the amount of primed C did not. Conversely, we detected a large positive priming effect during the first weeks of growth (**Figure 12**), in parallel to the peak in the relative belowground C release (section 4.3.1). These results suggest that the decomposition of SOM was accelerated by the active release of plant-derived compounds, which most probably held the specific function to increase the plant nutrient acquisition (e.g. exudation of exoenzymes, C transfer to symbionts). However, there was no correlation between the relative increase in belowground C release and the amount of primed C in the individual plant-soil systems. Thus, we could neither find a quantitative (causal) relation between the amount of C deposited and primed nor a clear functional relation between the type of C deposited and the amount of C primed. Other factors in the soil (e.g. spatial distribution of plant C inputs, microbial community and available SOM) might determine the magnitude of the rhizosphere priming effect.

5 Conclusions

To mitigate negative impacts of climate change, there is a need to improve our mechanistic understanding of terrestrial C cycle feedbacks to climate (section 1.3). To test hypothesis about potential feedback mechanisms we need the possibility to consolidate them by experiments in controlled environments with manageable complexity before we test them with costly and complex experimental setups in natural ecosystems (section 1.4.1). This PhD project developed and applied a new facility and methodology to study individual responses of plant-soil systems to environmental change with a holistic approach (section 1.4.2) based on stable isotope techniques (section 1.4.3).

5.1 The MICE facility is a new tool for holistic approaches

The MICE facility (section 4.1.1) developed in this PhD project allows separate, but simultaneous measurements of above- and belowground C stocks and fluxes. C dynamics can be studied in up to 30 plant-soil systems under controlled environmental conditions at time scales relevant for plant-soil interactions. The setup of the facility is very versatile in respect to

- treatment options: The two independently controlled chambers can be used to compare the C cycling under two different climate conditions (e.g. current and future scenario), whereby multifactor climate changes can be simulated by the simultaneous regulation of light, air temperature, CO_2 and H_2O concentrations. The individual pots of the lower system can be filled with different soils and supplied by different amounts of water and amendments (e.g. nutrients) to manipulate the soil conditions.
- labelling options: The above- and belowground compartments of the plant-soil systems can be labelled separately due to its hermetical separation in the facility. Pulse or continuous labelling with single (e.g. ^{13}C-CO_2) or multiple isotopes (e.g. ^{13}C, ^{18}O, ^{2}H) can be applied to study short- to mid-term (days-months) responses of C cycling or to produce labelled material for long-term (months-years) studies.
- sampling options: The automatic monitoring provides flux measurements with high temporal resolution (min-hours) aboveground and in up to 20 pots belowground. The plant-soil systems are arranged in five rows that can be either sub-sampled or completely harvested during labelling experiments through portholes in the chamber.

5.2 Choosing the appropriate experimental approach

In this project we applied different labelling techniques. The comparison of the pulse and continuous ^{13}C-CO_2 labelling techniques revealed that i) they differ in the induced signal strength and potential tracing duration (section 4.1.2 and 4.2.1) due to different amount and length of label application, ii) their results regarding C dynamics are not directly comparable (section 4.1.2) due to labelling of different compounds and iii) the results on C partitioning depend on sampling date (section 4.2.2) due to different time lags and residence times of fluxes and in stocks. Therefore the experimental approach (labelling technique, sampling scheme) should be chosen in respect to the C cycle process of interest and the C transfer and residence times (**Table 3**).

Table 3 Experimental approaches to study carbon cycling processes. Listed are for each C cycle sub-process the compounds to be traced (OM = organic matter, SOM = soil organic matter), the technique to label them (PL = pulse labelling, CL = continuous labelling, first emerg. = complete labelling from first emergence of leaves) and the experimental setting to trace them (MICE = tracing within the MICE facility, incubation = tracing of compounds labelled in MICE in laboratory or field incubation studies), the stocks and fluxes to be sampled (MB = microbial biomass, DOC = dissolved organic carbon, VOC = volatile organic compounds) and their sampling frequency .

Process	Traced compound	Technique / setting	Sampled stock / flux	Sampling frequency
Assimilation				
Photosynthesis	Fresh assimilates	PL (or CL) / MICE	Shoot C fluxes, shoot OM	Days-weeks
Resource acquisition	Soil resources (nutrients, water)	PL (or CL) / MICE	Tissue water, plant OM	Days-weeks
Allocation				
Phloem transport	Fresh assimilates	PL / MICE	Tissue water, soil C efflux	MInutes-days
Biosynthesis	OM (quantity, quality)	CL / MICE	Plant OM	Days-months
Deposition				
Rhizodeposition	Rhizodeposits	CL (first emerg.) / MICE	DOC, soil C efflux, SOM	Days-months
Necromass deposition	Dead OM (quantity, quality)	CL (first emerg.) / MICE	Plant OM, MB	Weeks-months
Degradation				
Abiotic degradation	OM input (quantity, quality)	CL (first emerg.) / incubation	SOM, DOC, soil C efflux	Days-months
Biotic degradation	OM input (quantity, quality)	CL (first emerg.) / incubation	SOM, MB, DOC, soil C efflux	Days-months
Relocation				
Bioturbation, eluviation	SOM (particulate, dissolved)	CL (first emerg.) / incubation	SOM (soil horizons), biota	Weeks-years
Erosion, leaching	SOM (particulate, dissolved)	CL (first emerg.) / incubation, MICE	OM (wind, water), DOC	Days-years
Stabilisation				
Chemical protection	SOM (detritus)	CL (first emerg.) / incubation	SOM (free light fraction)	Weeks-years
Physico-chemical protection	SOM (mineral- & oxide-complexes)	CL (first emerg.) / incubation	SOM (heavy fraction)	Months-years
Physical protection	SOM (in aggregates, deep soil)	CL (first emerg.) / incubation	SOM (occluded fraction)	Months-years
Emission				
Biotic respiration	Plant-derived C, SOM	CL (first emerg.) / MICE, incubation	Soil CO_2 efflux (partitioning)	Days-months
Acidification	Inorganic C	-	Inorganic C	Months-years
Emission of CH_4 and VOCs	Plant-derived C, SOM	CL (first emerg.) / MICE, incubation	Soil CH_4 and VOC efflux	Days-months

Pulse labelling is appropriate to study short-term responses of plant C cycling based on assimilation and allocation of fresh assimilates, such as the speed of phloem transport measured by the C transfer time from leaves to the root respiratory fluxes. But pulse labelling is not suitable to study processes in large C stocks with slow turnover time or processes that involve the C cycling of other OM compounds than fresh assimilates. For those processes continuous labelling is more suitable, since it labels OM for longer durations and thus more homogeneously (e.g. labelling of all types of rhizodeposits).

The continuous labelling of plants can be applied to estimate the change in C allocation (biosynthesis), the C residence time in plant-soil compartments (e.g. of microbial C) or the mid-term response of plant C cycling (e.g. adaptation of photosynthesis). For all other processes that are influenced by the quantity and quality of plant-derived C inputs, a continuous and homogeneous labelling from first emergence of leaves is the ideal labelling technique. Within the MICE facility the short to mid-term C dynamics of belowground C cycling (e.g. rhizodeposition, biotic respiration) can be studied, while long-term dynamics (e.g. stabilisation processes) have to be assessed by the incubation of labelled OM (produced in the MICE facility) in the laboratory or the field.

In this project we also tested a (continuous) multi-isotope labelling approach using ^{18}O and ^{2}H in combination with the ^{13}C labelling (section 4.1.3). OM in the leaves was successfully labelled with the three stable isotopes and the labels could be traced within the plant. The multi-isotope labelling has the potential to make changes in the biosynthesis of different OM compounds visible based on bulk analysis and to elucidate OM transformations during degradation or stabilisation processes. In a first step the method could be applied to investigate O and H exchange and fractionation processes during OM cycling.

5.3 Plant-soil interactions are functional

The first experiment in the MICE facility that was targeted on studying plant-soil interactions revealed that C cycling processes are not only causal linked, but functional driven by biota. On the one hand, the release of plant-derived C belowground was not a steady proportion of what was assimilated aboveground. The plants increased the fraction of net assimilated C released belowground in response to their nutrient limitation during initial plant development (section 4.3.1). On the other hand, the observed positive rhizosphere priming effect was not positively correlated with the amount, but rather with the increase in the relative plant-C release (section 4.3.2). Thus the accelerated SOM decomposition seemed to be induced by the plant activity, i.e. the release of compounds with the function to increase the nutrient acquisition through increase in SOM mineralisation and not by the regular and passive plant-C release.

These results indicate that living organisms have the capability to actively respond to the limiting conditions in their environment and thus illustrate nicely the answer to the initial question, what the difference is between a living and a dead organism: Living organisms can (re)act to its environment and improve its living conditions by functional driven changes in their C cycling (assimilation, allocation, deposition, degradation) with further effects on soil C dynamics (stabilisation, emission).

6 Perspectives

The initial experiments conducted in the MICE facility were dedicated to test the methodology. We used one type of plant-soil systems and steady environmental conditions. Thus we paved the way, but have only started to explore the response of plant-soil C cycling to environmental changes with a holistic approach. As highlighted with this PhD thesis, I think that future research on C cycle feedback to climate should be focused on atmosphere-biota-soil interactions and their relevance for ecosystem C exchange. Below I describe how we could improve our mechanistic understanding of climate feedbacks with the MICE facility by increasing stepwise the level of complexity.

6.1 Short-term response to climate change

Multi-factorial changes of climate conditions affect the physiology of plants and soil biota driving plant-soil C cycling. The MICE facility can be applied to study the changes in plant-soil C cycling processes, their interactions and the net C exchange with manipulative experiments simulating multi-factorial changes (temperature, humidity, CO_2 concentration) of the air and soil conditions. The measurement of the C stock and flux dynamics (e.g. thermal acclimation), abiotic environment (e.g. nutrient availability, aggregation) and biological activity (e.g. extracellular enzymes) over time will help to elucidate the mechanisms behind the response of plant-soil C cycling.

For example the mechanisms driving rhizodeposition and its effect on C cycling are still poorly understood. The experimental results of this project indicated that the rhizodeposition might be an active response of plants to their nutrient limitation with large impacts on the SOM degradation and C emission. It is plausible, but it is not known if a similar mechanism could be induced by climate change (e.g. due to increased nutrient competition) and drive C cycle feedbacks.

6.2 Lagged effects induced by climate change

The change in plant-soil systems due to the short-term response to climate change can induce lagged effects in C cycling. These can be studied with long-term experiments in laboratory or field environments based on plant-soil systems grown and labelled in the MICE facility. Such experiments will help to identify mechanisms that are relevant for long-term feedbacks to climate change.

For example there is evidence that root-derived C is preferentially stabilised in the SOM. Analogous to the increased allocation into C assimilating tissues (shoots) under light limitation observed in the experiments in this project, an increased allocation to water

assimilating tissues (roots) is expected during drought. This change in the quality of SOM input might offset the change in the input quantity in the long-term, due to the preferential stabilisation of root-derived C. If this is the case and which mechanisms are behind the preferential stabilisation could be studied with a long-term decomposition experiment.

6.3 Variability in ecosystem responses

The short-term responses and lagged effects will differ in ecosystems that vary in their above- and belowground communities and soil types. The MICE facility can be used to explore the similarity and divergence in the responses of C cycling to climate change of different plant species, soil types (with their natural microbial communities) and their combinations. This will help to identify mechanisms that are species or soil type specific (e.g. related to mutualistic symbiosis, plant functional type or soil mineralogy), to evaluate the relevance of mechanisms for different ecosystem types (e.g. grassland vs. forest) and to estimate the importance of competition and biodiversity for C cycling.

The MICE facility is a versatile tool to explore plant-soil interactions at the interface between controlled laboratory and natural ecosystem environments. Thus it will contribute to improve our mechanistic understanding of terrestrial C cycle feedbacks to climate change as input to global climate models.

References

Amelung W, Brodowski S, Sandhage-Hofmann A, Bol R. 2008. Combining biomarker with stable isotope analyses for assessing the transformation and turnover of soil organic matter. *Advances in Agronomy* 100: 155–250.

Arneth A, Harrison SP, Zaehle S, Tsigaridis K, Menon S, Bartlein PJ, Feichter J, Korhola A, Kulmala M, O'Donnell D, et al. 2010. Terrestrial biogeochemical feedbacks in the climate system. *Nature Geoscience* 3: 525–532.

Bahn M, Schmitt M, Siegwolf RTW, Richter A, Brüggemann N. 2009. Does photosynthesis affect grassland soil-respired CO_2 and its carbon isotope composition on a diurnal timescale? *New Phytologist* 182: 451–460.

Bardgett RD. 2011. Plant-soil interactions in a changing world. *F1000 Biology Reports* 3: 1–6.

Bardgett RD, Freeman C, Ostle NJ. 2008. Microbial contributions to climate change through carbon cycle feedbacks. *The ISME Journal* 2: 805–814.

Bardgett RD, Manning P, Morriën E, De Vries FT. 2013. Hierarchical responses of plant-soil interactions to climate change: consequences for the global carbon cycle. *Journal of Ecology* 101: 334–343.

Behie SW, Bidochka MJ. 2014. Nutrient transfer in plant-fungal symbioses. *Trends in Plant Science* 19: 734–740.

Berg G, Smalla K. 2009. Plant species and soil type cooperatively shape the structure and function of microbial communities in the rhizosphere. *FEMS Microbiology Ecology* 68: 1–13.

Billings SA, Ballantyne IV F. 2013. How interactions between microbial resource demands, soil organic matter stoichiometry, and substrate reactivity determine the direction and magnitude of soil respiratory responses to warming. *Global Change Biology* 19: 90–102.

Blagodatskaya E, Kuzyakov Y. 2008. Mechanisms of real and apparent priming effects and their dependence on soil microbial biomass and community structure: critical review. *Biology and Fertility of Soils* 45: 115–131.

Blanco-Canqui H, Lal R. 2004. Mechanisms of carbon sequestration in soil aggregates. *Critical Reviews in Plant Sciences* 23: 481–504.

Bradford MA. 2013. Thermal adaptation of decomposer communities in warming soils. *Frontiers in Microbiology* 4: 1-16.

Brand WA, Coplen TB. 2012. Stable isotope deltas: tiny, yet robust signatures in nature. *Isotopes in Environmental and Health Studies* 48: 393–409.

Bronick C. 2005. Soil structure and management: a review. *Geoderma* 124: 3–22.

Bugmann H, Bigler C. 2011. Will the CO_2 fertilization effect in forests be offset by reduced tree longevity? *Oecologia* 165: 533–544.

Carrillo Y, Dijkstra FA, Pendall E, LeCain D, Tucker C. 2014. Plant rhizosphere influence on microbial C metabolism: the role of elevated CO_2, N availability and root stoichiometry. *Biochemistry* 117: 229–240.

Carvalhais N, Forkel M, Khomik M, Bellarby J, Jung M, Migliavacca M, Mu M, Saatchi S, Santoro M, Thurner M, et al. 2014. Global covariation of carbon turnover times with climate in terrestrial ecosystems. *Nature* 514: 213–217.

Chapin III FS, Matson PA, Vitousek PM. 2012a. Changes in the earth system. Principles of Terrestrial Ecosystem Ecology. New York Dordrecht Heidelberg London: Springer, 401–422.

Chapin III FS, Matson PA, Vitousek PM. 2012b. *Principles of terrestrial ecosystem ecology* (FSI Chapin, PA Matson, and PM Vitousek, Eds.). New York Dordrecht Heidelberg London: Springer.

Chapin III FS, McFarland J, McGuire AD, Euskirchen ES, Ruess RW, Kielland K. 2009. The changing global carbon cycle: linking plant-soil carbon dynamics to global consequences. *Journal of Ecology* 97: 840–850.

Chapin III FS, Randerson JT, McGuire AD, Foley JA, Field CB. 2008. Changing feedbacks in the climate–biosphere system. *Frontiers in Ecology and the Environment* 6: 313–320.

Chapin III FS, Sturm M, Serreze MC, McFadden JP, Key JR, Lloyd AH, Mcguire AD, Rupp TS, Lynch AH, Schimel JP, et al. 2005. Role of Land-Surface Changes in Arctic Summer Warming. *Science* 310: 657–660.

Chen R, Senbayram M, Blagodatsky S, Myachina O, Dittert K, Lin X, Blagodatskaya E, Kuzyakov Y. 2014. Soil C and N availability determine the priming effect: microbial N mining and stoichiometric decomposition theories. *Global Change Biology* 20: 2356–2367.

Cheng W, Parton WJ, Gonzalez-Meler MA, Phillips R, Asao S, McNickle GG, Brzostek E, Jastrow JD. 2014. Synthesis and modeling perspectives of rhizosphere priming. *New Phytologist* 201: 31–44.

Churchland C, Grayston SJ. 2014. Specificity of plant-microbe interactions in the tree mycorrhizosphere biome and consequences for soil C cycling. *Frontiers in Microbiology* 5: 1–20.

Conant RT, Ryan MG, Ågren GI, Birge HE, Davidson EA, Eliasson PE, Evans SE, Frey SD, Giardina CP, Hopkins FM, et al. 2011. Temperature and soil organic matter decomposition rates - synthesis of current knowledge and a way forward. *Global Change Biology* 17: 3392–3404.

Coplen TB. 2011. Guidelines and recommended terms for expression of stable-isotope-ratio and gas-ratio measurement results. *Rapid Communications in Mass Spectrometry* 25: 2538–2560.

Davidson EA, Janssens IA. 2006. Temperature sensitivity of soil carbon decomposition and feedbacks to climate change. *Nature* 440: 165–173.

Dawson TE, Mambelli S, Plamboeck AH, Templer PH, Tu KP. 2002. Stable isotopes in plant ecology. *Annual Review of Ecology and Systematics* 33: 507–559.

De Deyn GB, Cornelissen JHC, Bardgett RD. 2008. Plant functional traits and soil carbon sequestration in contrasting biomes. *Ecology Letters* 11: 516–531.

Dieleman WIJ, Janssens IA. 2011. Can publication bias affect ecological research? A case study on soil respiration under elevated CO_2. *New Phytologist* 190: 517–521.

Dijkstra FA, Carrillo Y, Pendall E, Morgan JA. 2013. Rhizosphere priming: a nutrient perspective. *Frontiers in Microbiology* 4: 1–8.

Drigo B, Kowalchuk GA, van Veen JA. 2008. Climate change goes underground: effects of elevated atmospheric CO_2 on microbial community structure and activities in the rhizosphere. *Biology and Fertility of Soils* 44: 667–679.

Dungait JAJ, Hopkins DW, Gregory AS, Whitmore AP. 2012. Soil organic matter turnover is governed by accessibility not recalcitrance. *Global Change Biology* 18: 1781–1796.

Epron D, Bahn M, Derrien D, Lattanzi FA, Pumpanen JS, Gessler A, Högberg P, Maillard P, Dannoura M, Gérant D, et al. 2012. Pulse-labelling trees to study carbon allocation dynamics: a review of methods, current knowledge and future prospects. *Tree Physiology* 32: 776–798.

Farquhar GD, Ehleringer JR, Hubick KT. 1989. Carbon isotope discrimination and photosynthesis. *Annual Review of Plant Physiology and Plant Molecular Biology* 40: 503–537.

Farquhar GD, Sharkey TD. 1982. Stomatal conductance and photosynthesis. *Annual Review of Plant Physiology* 33: 317–345.

Fatichi S, Leuzinger S, Körner C. 2013. Moving beyond photosynthesis: from carbon source to sink-driven vegetation modeling. *New Phytologist* 201: 1086–1095.

Field CB, Lobell DB, Peters HA, Chiariello NR. 2007. Feedbacks of terrestrial ecosystems to climate change. *Annual Review of Environment and Resources* 32: 1–29.

Franks PJ, Adams MA, Amthor JS, Barbour MM, Berry JA, Ellsworth DS, Farquhar GD, Ghannoum O, Lloyd J, McDowell NG, et al. 2013. Sensitivity of plants to changing atmospheric CO_2 concentration: from the geological past to the next century. *New Phytologist* 197: 1077–1094.

Fransson P. 2012. Elevated CO_2 impacts ectomycorrhiza-mediated forest soil carbon flow: fungal biomass production, respiration and exudation. *Fungal Ecology* 5: 85–98.

Friedlingstein P, Prentice IC. 2010. Carbon–climate feedbacks: a review of model and observation based estimates. *Current Opinion in Environmental Sustainability* 2: 251–257.

Gärdenäs AI, Ågren GI, Bird JA, Clarholm M, Hallin S, Ineson P, Kätterer T, Knicker H, Nilsson SI, Näsholm T, et al. 2011. Knowledge gaps in soil carbon and nitrogen interactions – from molecular to global scale. *Soil Biology and Biochemistry* 43: 702–717.

Giardina CP, Litton CM, Crow SE, Asner GP. 2014. Warming-related increases in soil CO_2 efflux are explained by increased below-ground carbon flux. *Nature Climate Change*: 1–6.

Gornish ES, Tylianakis JM. 2013. Community shifts under climate change: mechanisms at multiple scales. *American Journal of Botany* 100: 1422–1434.

Gregory PJ. 2006. Roots, rhizosphere and soil: the route to a better understanding of soil science? *European Journal of Soil Science* 57: 2–12.

Hartmann A, Schmid M, Tuinen D Van, Berg G. 2008. Plant-driven selection of microbes. *Plant and Soil* 321: 235–257.

Heimann M, Reichstein M. 2008. Terrestrial ecosystem carbon dynamics and climate feedbacks. *Nature* 451: 289–292.

Hinsinger P, Bengough AG, Vetterlein D, Young IM. 2009. Rhizosphere: biophysics, biogeochemistry and ecological relevance. *Plant and Soil* 321: 117–152.

Hinsinger P, Gobran GR, Gregory PJ, Wenzel WW. 2005. Rhizosphere geometry and heterogeneity arising from root-mediated physical and chemical processes. *New Phytologist* 168: 293–303.

Hodge A, Fitter AH. 2013. Microbial mediation of plant competition and community structure. *Functional Ecology* 27: 865–875.

Högberg P, Högberg MN, Göttlicher SG, Betson NR, Keel SG, Metcalfe DB, Campbell C, Schindlbacher A, Hurry V, Lundmark T, et al. 2008. High temporal resolution tracing of photosynthate carbon from the tree canopy to forest soil microorganisms. *New Phytologist* 177: 220–228.

Högberg P, Read DJ. 2006. Towards a more plant physiological perspective on soil ecology. *Trends in Ecology and Evolution* 21: 548–554.

Holtum JAM, Winter K. 2010. Elevated [CO_2] and forest vegetation: more a water issue than a carbon issue? *Functional Plant Biology* 37: 694–702.

Houghton RA. 2007. Balancing the global carbon budget. *Annual Review of Earth and Planetary Sciences* 35: 313–347.

IPCC. 2013a. Summary for policymakers. In: Stocker TF, Qin D, Plattner G-K, Tignor M, Alen SK, Boschung J, Nauels A, Xia Y, Bex V, Midgley PM, eds. Climate Change 2013: The Physical Science Basis. Contribution of Working Group I to the Fifth Assessment Report of the Intergovernmental Panel of Cimate Change. Cambridge, United Kingdom and New York, NY, USA: Cambridge University Press, 1535 pp.

IPCC. 2013b. *Climate change 2013: The physical science basis. Contribution of working group I to the fifth assessment report of the intergovernmental panel on climate change* (TF Stocker, D Qin, G-K Plattner, M Tignor, SK Allen, J Boschung, A Nauels, Y Xia, V Bex, and PM Midgley, Eds.). Cambridge, United Kingdom and New York, NY, USA: Cambridge University Press.

Iversen CM. 2010. Digging deeper: fine-root responses to rising atmospheric CO_2 concentration in forested ecosystems. *New Phytologist* 186: 346–357.

Joergensen R. 1996. The fumigation-extraction method to estimate soil microbial biomass: Calibration of the k_{EC} value. *Soil Biology and Biochemistry* 28: 25–31.

Jones DL, Hodge A, Kuzyakov Y. 2004. Plant and mycorrhizal regulation of rhizodeposition. *New Phytologist* 163: 459–480.

Jones DL, Nguyen C, Finlay RD. 2009. Carbon flow in the rhizosphere: carbon trading at the soil–root interface. *Plant and Soil* 321: 5–33.

Keeling CD. 1958. The concentration and isotopic abundances of atmospheric carbon dioxide in rural areas. *Geochimica et Cosmochimica Acta* 13: 322–334.

Kim S, Kramer RW, Hatcher PG. 2003. Graphical method for analysis of ultrahigh-resolution broadband mass spectra of natural organic matter, the van Krevelen diagram. *Analytical Chemistry* 75: 5336–5344.

Kim D-G, Vargas R, Bond-Lamberty B, Turetsky MR. 2012. Effects of soil rewetting and thawing on soil gas fluxes: a review of current literature and suggestions for future research. *Biogeosciences* 9: 2459–2483.

Kirschbaum M. 2006. The temperature dependence of organic-matter decomposition—still a topic of debate. *Soil Biology and Biochemistry* 38: 2510–2518.

Körner C. 2006. Plant CO_2 responses: an issue of definition, time and resource supply. *New Phytologist* 172: 393–411.

Körner C. 2011. The grand challenges in functional plant ecology. *Frontiers in Plant Science* 2: 1–3.

Kreyling J, Jentsch A, Beier C. 2014. Beyond realism in climate change experiments: gradient approaches identify thresholds and tipping points. *Ecology Letters* 17: 125.

Kulmatiski A, Beard KH, Stevens JR, Cobbold SM. 2008. Plant-soil feedbacks: a meta-analytical review. *Ecology Letters* 11: 980–992.

Kuzyakov Y. 2010. Priming effects: Interactions between living and dead organic matter. *Soil Biology and Biochemistry* 42: 1363–1371.

Kuzyakov Y. 2011. Prime time for microbes. *Nature Climate Change* 1: 295–297.

Kuzyakov Y, Domanski G. 2000. Carbon input by plants into the soil. Review. *Journal of Plant Nutrition and Soil Science* 163: 421–431.

Kuzyakov Y, Xu X. 2013. Competition between roots and microorganisms for nitrogen: mechanisms and ecological relevance. *New Phytologist* 198: 656–669.

Lambers H, Mougel C, Jaillard B, Hinsinger P. 2009. Plant-microbe-soil interactions in the rhizosphere: an evolutionary perspective. *Plant and Soil* 321: 83–115.

LeBauer DS, Reseder KK. 2008. Nitrogen limitation of net primary productivity in terrestrial ecosystems is globally distributed. *Ecology* 89: 371–379.

Lenton TM, Held H, Kriegler E, Hall JW, Lucht W, Rahmstorf S, Joachim H. 2008. Tipping elements in the Earth's climate system. *Proceedings of the National Academy of Sciences* 105: 1786–1793.

Leuzinger S, Hättenschwiler S. 2013. Beyond global change: lessons from 25 years of CO_2 research. *Oecologia* 171: 639–651.

Leuzinger S, Luo Y, Beier C, Dieleman W, Vicca S, Körner C. 2011. Do global change experiments overestimate impacts on terrestrial ecosystems? *Trends in Ecology and Evolution* 26: 236–241.

Liu L, Greaver TL. 2009. A review of nitrogen enrichment effects on three biogenic GHGs: the CO_2 sink may be largely offset by stimulated N_2O and CH_4 emission. *Ecology Letters* 12: 1103–1117.

Liu L, Greaver TL. 2010. A global perspective on belowground carbon dynamics under nitrogen enrichment. *Ecology Letters* 13: 819–828.

Looijen RC. 1998. Holism and reductionism in biology and ecology. The mutual dependence of higher and lower level research programmes. : 269.

Lu M, Zhou X, Luo Y, Yang Y, Fang C, Chen J, Li B. 2011. Minor stimulation of soil carbon storage by nitrogen addition: A meta-analysis. *Agriculture, Ecosystems and Environment* 140: 234–244.

Lu M, Zhou X, Yang Q, Li H, Luo Y, Fang C, Chen J, Yang X, Li B. 2013. Responses of ecosystem carbon cycle to experimental warming: a meta-analysis. *Ecology* 94: 726–738.

Luo Y. 2007. Terrestrial Carbon–Cycle Feedback to Climate Warming. *Annual Review of Ecology, Evolution, and Systematics* 38: 683–712.

Luo Y, Melillo J, Niu S, Beier C, Clark JS, Classen AT, Davidson EA, Dukes JS, Evans RD, Field CB, et al. 2011. Coordinated approaches to quantify long-term ecosystem dynamics in response to global change. *Global Change Biology* 17: 843–854.

Luo Y, Weng E. 2011. Dynamic disequilibrium of the terrestrial carbon cycle under global change. *Trends in Ecology and Evolution* 26: 96–104.

Von Lützow M, Kögel-Knabner I. 2009. Temperature sensitivity of soil organic matter decomposition—what do we know? *Biology and Fertility of Soils* 46: 1–15.

Maestrini B, Nannipieri P, Abiven S. 2014. A meta-analysis on pyrogenic organic matter induced priming effect. *Global Change Biology Bioenergy*: n/a–n/a.

Matamala R, Stover DB. 2013. Introduction to a Virtual Special Issue: modeling the hidden half – the root of our problem. *New Phytologist* 200: 939–942.

Matyssek R, Agerer R, Ernst D, Munch J-C, Osswald W, Pretzsch H, Priesack E, Schnyder H, Treutter D. 2005. The plant's capacity in regulating resource demand. *Plant Biology* 7: 560–580.

McCarthy HR, Oren R, Johnsen KH, Gallet-Budynek A, Pritchard SG, Cook CW, Ladeau SL, Jackson RB, Finzi AC. 2010. Re-assessment of plant carbon dynamics at the Duke free-air CO_2 enrichment site: interactions of atmospheric [CO_2] with nitrogen and water availability over stand development. *New Phytologist* 185: 514–528.

McDowell NG, Pockman WT, Allen CD, Breshears DD, Cobb N, Kolb T, Plaut J, Sperry J, West A, Williams DG, et al. 2008. Mechanisms of plant survival and mortality during drought: why do some plants survive while others succumb plants drought? *New Phytologist* 178: 719–739.

Meharg AA. 1994. A critical review of labelling techniques used to quantify rhizosphere carbon-flow. *Plant and Soil* 166: 55–62.

Meir P, Cox P, Grace J. 2006. The influence of terrestrial ecosystems on climate. *Trends in Ecology and Evolution* 21: 254–260.

Metcalfe DB, Fisher RA, Wardle DA. 2011. Plant communities as drivers of soil respiration: pathways, mechanisms, and significance for global change. *Biogeosciences* 8: 2047–2061.

Moorcroft PR. 2006. How close are we to a predictive science of the biosphere? *Trends in Ecology and Evolution* 21: 400–407.

Morgan JA, Pataki DE, Körner C, Clark H, Grosso SJ Del, Grünzweig JM, Knapp AK, Mosier AR, Newton PCD, Niklaus PA, et al. 2004. Water relations in grassland and desert ecosystems exposed to elevated atmospheric CO_2. *Oecologia* 140: 11–25.

Murage E, Voroney P. 2007. Modification of the original chloroform fumigation extraction technique to allow measurement of $\delta^{13}C$ of soil microbial biomass carbon. *Soil Biology and Biochemistry* 39: 1724–1729.

Norby RJ, Jackson RB. 2000. Root dynamics and global change: seeking an ecosystem perspective. *New Phytologist* 147: 3–12.

Norby RJ, Zak DR. 2011. Ecological lessons from free-air CO_2 enrichment (FACE) experiments. *Annual Review of Ecology, Evolution, and Systematics* 42: 181–203.

Oades JM. 1993. The role of biology in the formation, stabilization and degradation of soil structure. *Geoderma* 56: 377–400.

Ohno T, He Z, Sleighter RL, Honeycutt CW, Hatcher PG. 2010. Ultrahigh resolution mass spectrometry and indicator species analysis to identify marker components of soil- and plant biomass- derived organic matter fractions. *Environmental Science and Technology* 44: 8594–8600.

Ostle NJ, Smith P, Fisher R, Woodward FI, Fisher JB, Smith JU, Galbraith D, Levy P, Meir P, McNamara NP, et al. 2009. Integrating plant-soil interactions into global carbon cycle models. *Journal of Ecology* 97: 851–863.

Parkhurst DF. 1994. Tansley review no. 65. Diffusion of CO_2 and other gases inside leaves. *New Phytologist* 126: 449–479.

Pataki DE. 2003. The application and interpretation of Keeling plots in terrestrial carbon cycle research. *Global Biogeochemical Cycles* 17.

Paterson E, Midwood AJ, Millard P. 2009. Through the eye of the needle: a review of isotope approaches to quantify microbial processes mediating soil carbon balance. *New Phytologist* 184: 19–33.

Paterson E, Sim A. 2013. Soil-specific response functions of organic matter mineralization to the availability of labile carbon. *Global Change Biology* 19: 1562–1571.

Pendall E, Bridgham S, Hanson PJ, Hungate B, Kicklighter DW, Johnson DW, Law BE, Luo Y, Megonigal JP, Olsrud M, et al. 2004. Below-ground process responses to elevated CO_2 and temperature: a discussion of observations, measurement methods, and models. *New Phytologist* 162: 311–322.

Phillips RP. 2007. Towards a rhizo-centric view of plant-microbial feedbacks under elevated atmospheric CO_2. *New Phytologist* 173: 664–667.

Poorter H, Fiorani F, Stitt M, Schurr U, Fink A, Gibon Y, Usadel B, Munns R, Atkin OK, Tardieu F, et al. 2012. The art of growing plants for experimental purposes: a practical guide for the plant biologist. *Functional Plant Biology* 39: 821–838.

Poorter H, Niklas KJ, Reich PB, Oleksyn J, Poot P, Mommer L. 2012. Biomass allocation to leaves, stems and roots: meta-analyses of interspecific variation and environmental control. *New Phytologist* 193: 30–50.

Post WM, Emanuel WR, Zinke PJ, Stangenberger AG. 1982. Soil carbon pools and world life zones. *Nature* 298: 156–159.

Prentice IC, Cramer W, Harrison SP, Leemans R, Robert A, Solomon AM, Vallgatan O. 1992. A global biome model based on plant physiology and dominance , soil properties and climate. *Journal of Biogeography* 19: 117–134.

Preston CM, Schmidt MWI. 2006. Black (pyrogenic) carbon: a synthesis of current knowledge and uncertainties with special consideration of boreal regions. *Biogeosciences* 3: 397–420.

Van der Putten WH, Bardgett RD, Bever JD, Bezemer TM, Casper BB, Fukami T, Kardol P, Klironomos JN, Kulmatiski A, Schweitzer JA, et al. 2013. Plant-soil feedbacks: the past, the present and future challenges. *Journal of Ecology* 101: 265–276.

Raich JW, Schlesinger WH. 1992. The global carbon dioxide flux in soil respiration and its relationship to vegetation and climate. *Tellus* 44B: 81–99.

Reich PB, Hungate BA, Luo Y. 2006. Carbon-Nitrogen interactions in terrestrial ecosystems in response to rising atmospheric carbon dioxide. *Annual Review of Ecology, Evolution, and Systematics* 37: 611–636.

Reichstein M, Bahn M, Ciais P, Frank D, Mahecha MD, Seneviratne SI, Zscheischler J, Beer C, Buchmann N, Frank DC, et al. 2013. Climate extremes and the carbon cycle. *Nature* 500: 287–295.

Richardson AE, Barea J-M, McNeill AM, Prigent-Combaret C. 2009. Acquisition of phosphorus and nitrogen in the rhizosphere and plant growth promotion by microorganisms. *Plant and Soil* 321: 305–339.

Schmidt MWI, Torn MS, Abiven S, Dittmar T, Guggenberger G, Janssens IA, Kleber M, Kögel-Knabner I, Lehmann J, Manning DAC, et al. 2011. Persistence of soil organic matter as an ecosystem property. *Nature* 478: 49–56.

Schulze E-D. 2006. Biological control of the terrestrial carbon sink. *Biogeosciences* 3: 147–166.

Seneviratne SI, Corti T, Davin EL, Hirschi M, Jaeger EB, Lehner I, Orlowsky B, Teuling AJ. 2010. Investigating soil moisture–climate interactions in a changing climate: a review. *Earth-Science Reviews* 99: 125–161.

Sierra CA. 2011. Temperature sensitivity of organic matter decomposition in the Arrhenius equation: some theoretical considerations. *Biogeochemistry* 108: 1–15.

Singh N, Abiven S, Torn MS, Schmidt MWI. 2012. Fire-derived organic carbon in soil turns over on a centennial scale. *Biogeosciences* 9: 2847–2857.

Singh BK, Bardgett RD, Smith P, Reay DS. 2010. Microorganisms and climate change: terrestrial feedbacks and mitigation options. *Nature reviews. Microbiology* 8: 779–790.

Six JS, Bossuyt H, Degryze S, Denef K. 2004. A history of research on the link between (micro)aggregates, soil biota, and soil organic matter dynamics. *Soil and Tillage Research* 79: 7–31.

Sleighter RL, Hatcher PG. 2007. The application of electrospray ionization coupled to ultrahigh resolution mass spectrometry for the molecular characterization of natural organic matter. *Journal of Massspectrometry* 42: 559–574.

Smith NG, Dukes JS. 2013. Plant respiration and photosynthesis in global-scale models: incorporating acclimation to temperature and CO_2. *Global Change Biology* 19: 45–63.

Subke J-A, Bahn M. 2010. On the "temperature sensitivity" of soil respiration: Can we use the immeasurable to predict the unknown? *Soil Biology and Biochemistry* 42: 1653–1656.

Sutherland WJ, Freckleton RP, Godfray HCJ, Beissinger SR, Benton T, Cameron DD, Carmel Y, Coomes DA, Coulson T, Emmerson MC, et al. 2013. Identification of 100 fundamental ecological questions. *Journal of Ecology* 101: 58–67.

Thornton B, Paterson E, Midwood AJ, Sim A, Pratt SM. 2004. Contribution of current carbon assimilation in supplying root exudates of Lolium perenne measured using steady-state C labelling. *Physiologia Plantarum* 120: 434–441.

Treseder K. 2004. A meta-analysis of mycorhizal responses to nitrogen, phosphorus, and atmospheric CO_2 in field studies. *New Phytologist* 164: 347–355.

Walther G-R, Post E, Convey P, Menzel A, Parmesan C, Beebee TJC, Fromentin J-M, Hoegh-Guldberg O, Bairlein F. 2002. Ecological responses to recent climate change. *Nature* 202: 389–395.

Wang X, Liu L, Piao S, Janssens IA, Tang J, Liu W, Chi Y, Wang J, Xu S. 2014. Soil respiration under climate warming: differential response of heterotrophic and autotrophic respiration. *Global Change Biology* 20: 3229–3237.

Wardle DA, Bardgett RD, Klironomos JN, Setälä H, van der Putten WH, Wall DH. 2004. Ecological linkages between aboveground and belowground biota. *Science* 304: 1629–1633.

Warembourg FR, Estelrich HD. 2000. Towards a better understanding of carbon flow in the rhizosphere: a time-dependent approach using carbon-14. *Biology and Fertility of Soils* 30: 528–534.

Werner RA, Brand WA. 2001. Referencing strategies and techniques in stable isotope ratio analysis. *Rapid Communications in Mass Spectrometry* 15: 501–519.

Werner C, Schnyder H, Cuntz M, Keitel C, Zeeman MJ, Dawson TE, Badeck F-W, Brugnoli E, Ghashghaie J, Grams TEE, et al. 2012. Progress and challenges in using stable isotopes to trace plant carbon and water relations across scales. *Biogeosciences* 9: 3083–3111.

Zak DR, Pregitzer KS, King JS, Holmes WE. 2000. Elevated atmospheric CO_2, fine roots and the response of soil microorganisms: a review and hypothesis. *New Phytologist* 147: 201–222.

Zhu B, Gutknecht JLM, Herman DJ, Keck DC, Firestone MK, Cheng W. 2014. Rhizosphere priming effects on soil carbon and nitrogen mineralization. *Soil Biology and Biochemistry* 76: 183–192.

Part B: Manuscripts

Manuscript I 'The MICE facility'

Submission planed as

Studer, M. S., Maier, R., Schmidt, M. W. I., Siegwolf, R. T. W., Woodhatch, I., Abiven, S. The MICE facility: Multi-isotope labelling in a Controlled Environment to trace organic matter dynamics in the plant-soil system with a holistic approach. Methods in Ecology and Evolution. 2015.

Abstract

Feedbacks of terrestrial carbon (C) cycle to climate change are the result of complex interactions between C cycling processes. To improve our mechanistic understanding of the response of plant-soil systems to environmental change we need new tools that are able to distinguish different C fluxes and stocks, processes and their interactions.

We developed a laboratory facility to study C cycling dynamics based on stable isotope techniques in near-natural plant-soil systems grown in controlled environments. The hermetical separation of the aboveground (shoots) and belowground compartments (roots, soil) allows distinct above- and belowground manipulation of environmental conditions, stable isotope labelling and monitoring of plant-soil C stocks and fluxes.

Here we demonstrate the efficiency of the facility to regulate the air temperature, humidity and CO_2 concentrations and to monitor net photosynthesis, dark respiration and soil respiratory rates to assess net C exchanges of the plant-soil system with the atmosphere. Further we highlight the potential of the facility to separate fluxes or stocks with stable isotope labelling and tracing on the example of ^{13}C-CO_2 labelling and soil respiratory flux partitioning.

The facility provides an example of a new generation of laboratory facilities to study the plant-soil C cycling with a holistic approach. It can be applied to conduct manipulative experiments under various environmental and soil conditions (e.g. elevated CO_2, drought, nutrient limitation) to study the response of plant-soil interactions of above- and belowground C cycling processes. Thus the facility is a new tool to improve our mechanistic understanding of potential plant-soil C cycle feedback to climate change.

1 Introduction

The global change has and will have large impacts on human and natural systems (Walther et al. 2002; Lenton et al. 2008). Adaptation and mitigation to these changes require confident projection of future climate (and its impacts) and thus deep

understanding of feedback mechanisms. Biogeochemical feedbacks of terrestrial ecosystems (e.g. changes in CO_2 emissions) could be as large as physical feedbacks (e.g. changes in albedo), but their magnitudes are still largely unknown (Arneth et al. 2010). The research on carbon (C) cycle feedbacks was directed by the fundamental assumption, that the aboveground assimilation driven by plant photosynthesis and the belowground emission driven by heterotrophic respiration of soil organic matter (SOM) can be conceptually isolated and analysed separately (Heimann & Reichstein 2008). However, the research in the last decades made it evident that the interactions between plant and soil are crucial for C cycling (e.g. as discussed in Metcalfe et al., 2011; Bardgett et al., 2008; De Deyn et al., 2008). This lead to a change in paradigm in plant and soil research (Högberg & Read 2006; Körner 2011; Schmidt et al. 2011) and highlighted the need to study plant-soil C dynamics with a holistic approach, combining the knowledge from different disciplines.

The main challenge in the research of C cycle feedbacks of terrestrial ecosystems to climate change is, that the feedbacks occur at spatial (global) and temporal scales (decades to centuries) we cannot experimentally explore. Thus we can only formulate hypothesis about "potential feedback mechanisms" and incorporate them into complex global climate models to predict future changes in climate and C cycling (Moorcroft 2006). These models are based on our mechanistic understanding of processes and interactions in the C cycle (Moorcroft 2006; Ostle et al. 2009; Friedlingstein & Prentice 2010).

Plant-soil feedback mechanisms are the result of a cascade of interactions in terrestrial C cycle processes. The level of complexity increases with scale, what impairs the mechanistic understanding of the observations at large scales (Leuzinger et al. 2011). The way to improve our knowledge is to stepwise explore and formulate potential feedback hypothesis under controlled environments (at small scales) and test their applicability at larger scales with field-scale and long-term experiments (Luo et al. 2011; Kreyling et al. 2014).

A major challenge in studying C cycling is the measurement of distinct C fluxes or changes in C stocks in an environment that is dominated by C and highly sensitive to disturbances. Stable isotope techniques are a powerful tool to trace C (Dawson et al. 2002; Amelung et al. 2008). Stable isotopes differ in their mass, but behave very similar in the environment. Thus the artificial addition of the less abundant ^{13}C to the plant's atmosphere as ^{13}C-CO_2 is applied to label the assimilated C, which can then be traced in the plant-soil system that consists mainly of ^{12}C. The application of other isotopes in combination with ^{13}C, as for example ^{18}O and ^{2}H (Studer et al. 2014b) or ^{15}N (e.g.

Wichern et al., 2007; Bird and Torn, 2006) can be used to study C cycling in combination with other biogeochemical cycles.

We developed a new laboratory facility, the MICE (Multi-Isotope labelling In a Controlled Environment) facility, to study the C cycling mechanisms in entire plant-soil systems grown under controlled but manipulable environmental conditions with stable isotope techniques. We describe the unique configuration of the facility in the materials and method section, which provides a common atmosphere for the aboveground compartments of the plant-soil systems (shoots), but a hermetical separation to the individual belowground compartments (roots, rhizosphere, soil). Then we demonstrate with a series of experiments the efficiency of the system to regulate the environmental conditions and monitor plant-soil C fluxes and discuss the potential application of the facility.

2 Materials and methods

2.1 Chamber configuration

The MICE facility consists of two labelling chambers with separate air circulation and a combined gas sampling system for the belowground (soil pots) components. Each chamber contains 15 plants arranged in five rows that share a common atmosphere (upper system) but root in individual soil pots (lower system). This setup allows for separate labelling and tracing of above- and belowground C fluxes and stocks described below.

2.1.1 The upper system

The upper system is a polycarbonate (Makrolon, Bayer AG) cuboid (1.27 m width x 0.74 m depth x 1.24 m height) that encloses the plant shoots and different instruments to regulate its environmental conditions (described below). The front plate can be removed and the bottom plate holds five slots to insert the plants. The slots are closed with small polycarbonate pieces and Kapton tape and the upper system is hermetically sealed from the lower system by a malleable sealant (Terostat-IX, Henkel AG & Co.) wrapped around the stems before closing. The front plate holds five windows (diameter 18 cm) to sample the plant-soil systems during an experiment with minor disturbance to the (labelled) atmosphere.

2.1.2 The lower system

The lower system consists of 15 individual pots (23.5 cm diameter x 25 cm height) per chamber containing the belowground plant components of the plant-soil system (roots,

rhizosphere, bulk soil) connected to a valve system to monitor the CO_2 fluxes (described below). The top edge of the pots has a rubber gasket pressed up against the bottom plate of the upper system cuboid to hermetically seal them from the laboratory atmosphere. The pots are aerated with outdoor air through gas in- and outlets to prevent anaerobic conditions. Further the pots have separate water in- and outlets that allow for individual watering and sampling of the soil water solution.

The pots are typically filled with 3 cm coarse quartz sand to embed the water outlet and 17 cm soil leaving an air collar of 5 cm at the top (soil volume 6.3 dm^3, air volume of 1.9 dm^3). In addition the soil can be separated into inner rhizosphere and outer root-free soil by a mesh-cylinder (15 cm diameter x 17 cm height, volume of 4.0 dm^3) made of stainless steel and covered with a 30 µm mesh (PETEX, Sefar AG).

2.2 Automatic regulation and monitoring

The GDU-28 software developed by DMP Ltd (Fehraltorf, Switzerland) controls the instruments and sensors for the automatic regulation and monitoring of the environmental parameters within the MICE facility. The software is based on LabVIEW 2011 (National Instruments Corp.) and is interfaced to the hardware via a set of relays switching the instruments on/off and (analogue and digital) data connections to log the sensor measurements.

2.2.1 Light availability (upper system) - Day and night cycles

The light is on-off controlled by an external software developed by Lumartix SA (Aubonne, Switzerland) for the plasma light engines (Lumixo-S, Lumartix SA). In the software the day-night cycles and light intensity levels (800 - 1200 W m^{-2}) can be selected.

Two light engines are installed above each chamber. A reflector encloses the plasma light bulbs and the Makrolon walls are covered with a reflecting foil (Avery T-7505, Avery Dennison Corp.) in order to distribute the light homogeneously. Three axial fans cool the Makrolon chamber surface and a pipe system powered by a larger fan removes the hot air from the reflector and the light engines out of the laboratory.

A quantum sensor (LI-190, LI-COR Inc.) installed in the middle of the cuboid detects the day-night cycles to regulate the other environmental parameters accordingly. The light intensity at canopy height is on average 350 µmol mol^{-1} s^{-1} (at 1200 W m^{-2}) and reflects the solar spectrum.

2.2.2 CO_2 concentrations (upper system) - Shoot CO_2 gas exchange

Two infrared gas analyzers (IRGA, LI-840A, LI-COR Inc.) monitor the atmospheric CO_2 concentration (in µmol mol^{-1}) in the upper chamber systems. The CO_2 concentration level is frequently adjusted based on an upper and lower CO_2 concentration threshold with two-point controllers (DMP 2014). The CO_2 scrubber, a Plexiglas tube filled with Soda lime (Drägersorb 800 Plus, Dräger Medical AG & Co.), is activated to lower the concentration and CO_2 is injected from a gas cylinder to increase the concentration level. The automatic CO_2 control can be regularly paused in order to monitor the shoot photosynthesis and respiration based on the CO_2 concentration changes ("monitoring time") and to measure the IRGA zero line with a CO_2 and H_2O absorber, a Plexiglas tube filled with Soda lime and Magnesium-perchlorate (Sigma-Aldrich Co.).

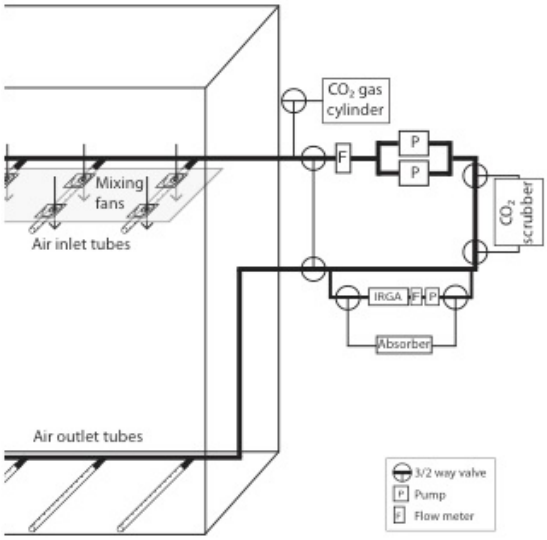

Figure 1. The upper system. The figure illustrates the configuration of one upper system of the MICE facility with its main gas circuit that holds an infrared gas analyzer (IRGA) to monitor the CO_2 and H_2O concentrations and equipment to regulate the CO_2 concentration (CO_2 absorption by the scrubber and injection from the gas cylinder) and calibrate the IRGA (CO_2 and H_2O absorption).

The instruments to regulate the CO_2 concentration are installed in a gas circuit made of Teflon tubing attached to the upper chamber cuboid (Figure 1). Two membrane pumps (N815 KNE, KNF Neuberger AG) circulate the air from and to the chamber through perforated Plexiglas tubes, installed between the plant rows at the bottom (outlet) and the top (inlet) of the chamber (flow 16 l min^{-1}). Eight axial fans placed above the air inlet tubes provide a well-mixed atmosphere. A bypass to the main gas circuit powered by a small pump (NMP 09 L, KNF Neuberger AG) feeds the air through the IRGA (flow 0.4 l min^{-1}). The scrubber and the CO_2 gas cylinder are attached to the main gas circuit by 3/2 way solenoid valves (SMC Pneumatics AG).

2.2.3 Temperature and humidity (upper system) - Relative humidity

The regulation of the air humidity is intrinsically tied to the regulation of the air temperature due to the condensation of water during cooling. Two resistance thermometers (Pt-100, TAI-PK, Wisag AG) and the two IRGAs monitor the temperature (in °C) and absolute air humidity (in mmol H_2O mol^{-1} air) in the upper chamber systems (used for the relative humidity calculation). The temperature and absolute humidity is regulated based on individual set points for the day- and night-time with PID or two-point controllers (DMP 2014). The chamber air is cooled and dried with an air-conditioning system and heated and humidified by resistors ("heater") and ultrasonic vaporizers ("humidifiers"), respectively (Figure 2).

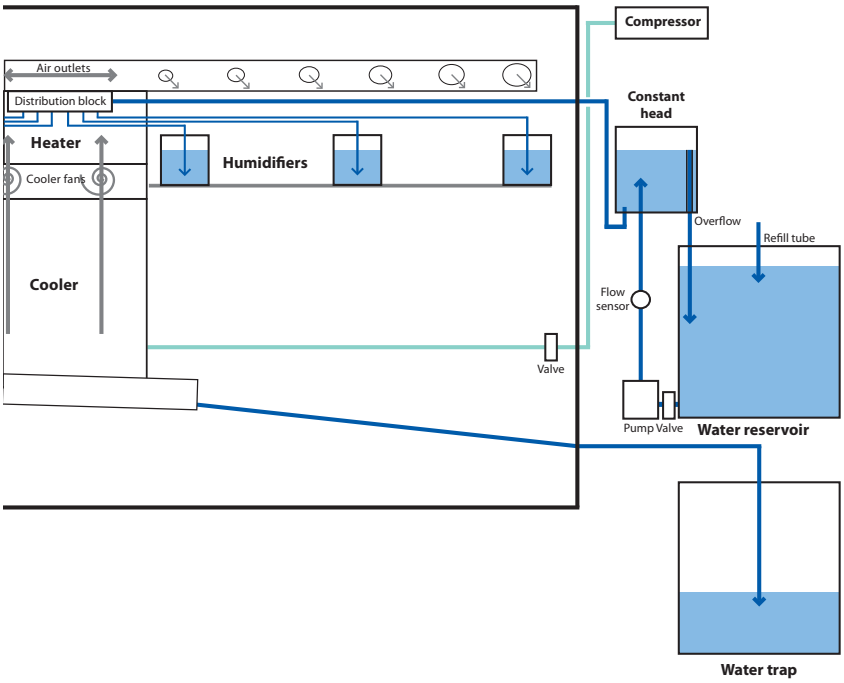

Figure 2. Air conditioning, humidifier and heater system. The figure illustrates the equipment used to regulate the temperature and humidity in the upper system of the MICE facility. The lines indicate the cooling liquid circuit (light blue) and the direction of the water (dark blue) and the air flow (grey).

The air-conditioning system consists of the cooler unit - a finned radiator installed at the back wall within the upper chamber - that is connected to the main compressor outside the chamber (Optyma SC12/12 GXT2, Danfoss A/S). A valve regulates the circulation of the cooled liquid (- 5 °C) between the compressor and the cooler unit (Figure 2). The GDU-28 software activates or deactivates the cooler unit via a digital input on the controller (EKC 202, Danfoss A/S) of the air-conditioning system. Fans above the cooler blow the chamber air through the radiator from the bottom to the top. The radiator is

frequently defrosted and the condensed water is collected in a water trap outside the chamber (everything hermetically sealed).

The heater - a finned aluminum block heated by four resistances (68 Ω, 200 W) screwed onto it - is installed above the cooler unit and forms with it one airtight unit (Figure 2). Thus the cooler fans blow the (cooled) air through the heater and back into the chamber through a perforated Plexiglas tube at the top of the chamber. The temperature of the heater is monitored by another resistance thermometer and controlled by a PID or two-point controller (DMP, 2014).

The humidifiers - six ultrasonic vaporizers (AOS 7146, AIR-O-SWISS) per chamber - are installed in front of the cooler/heater air outlet (Figure 2). The humidifiers are connected with water filled tubing to a constant head for automatic refilling. A water pump connected to a water reservoir continuously refills the constant head. A flow sensor (water wheel with a photo sensor) monitors the water flow and a blocking valve prevents the emptying of the constant head when the water pump is off.

2.2.4 CO_2 concentrations (lower system) - Soil CO_2 efflux

A third IRGA (LI-840A, LI-COR Inc.) measures the CO_2 concentration in the air of up to twenty pots in the lower system based on a complex valve system with 3/2 way solenoid valves (6012 and 6014, Bürkert AG). A sequencer in the GDU-28 software connects the pot in- and outlets repeatedly to the IRGA to monitor the soil CO_2 efflux rates (scan mode). Further the in- and outlet of a single pot can be looped with the IRGA to manually sample the CO_2 efflux through a septum (loop mode). Outside the measuring times a pot is simply aerated like the rest of the pots (aeration mode).

In the scan mode the CO_2 concentration of the pot inlet (background) air is measured before each outlet measurement. The amount of activated pots, the duration of the in- and outlet monitoring and the waiting time between the measurements can be chosen according to the experimental design and determines the measurement frequency of the soil CO_2 efflux of the activated pots. The septum mode is manually activated in the GDU-28 software. The tubing of the septum loop is flushed with background air between the measurements of the individual pots. The pots are aerated in the aeration mode with three membrane pumps (N815 KNE, KNF Neuberger AG). Throttle valves and flow meters installed before each pot adjust the flow rate (typically 1.3 l min^{-1}). As in the upper system the zeroline of the IRGA is monitored regularly.

2.3 Isotope labelling and tracing

In the MICE facility stable isotope labels can be above- (e.g. in the gaseous form) or belowground (e.g. dissolved in water) and traced in either plant-soil compartments. Here we describe the ^{13}C-CO_2 label application.

2.3.1 ^{13}C-CO_2 labelling

The ^{13}C label can be added in a pulse or continuously, whereby both techniques can be used to asses the C transfer, partitioning and residence time (Studer et al. 2014a). The label is injected via the CO_2 cylinder attached to the upper system (Figure 1). At the beginning of a labelling experiment the CO_2 in the chamber is scrubbed to a low level (e.g. 200 µmol mol^{-1}) and replenished with labelled gas by manual control to minimize the dilution of the label added. In a continuous labelling experiment, the labelled gas is automatically injected thereafter when the CO_2 level drops below the selected threshold. In a pulse experiment the cylinder is exchanged with CO_2 with near ambient isotopic signature (from mineral sources).

2.3.2 ^{13}C tracing

The isotopic composition of unlabelled material (background) and the maximum label strength of fresh assimilates has to be assessed to trace the ^{13}C label in plant-soil C stocks and fluxes. The background ^{13}C content is measured either by sampling plant-soil material before labelling or in an unlabelled control experiment. The maximum label strength is assessed by the isotopic composition of the chamber air (sampled via a septum in the main gas circuit), taking into account the isotopic fractionation during photosynthesis (Farquhar et al. 1989).

The hermetical separation of the upper and lower system prevents artefacts in the ^{13}C tracing in the soil CO_2 efflux due to (back-)diffusion of ^{13}C dissolved in soil water during the labelling (e.g. as in Högberg et al., 2008; Bahn et al., 2009). In the MICE facility the ^{13}C can only be transported through the plant, i.e. ^{13}C detected in belowground stocks and fluxes has to be plant-derived.

The isotopic composition of the soil CO_2 efflux is estimated with the Keeling plot approach (Keeling 1958; Pataki 2003). The air sampled within the septum loop witch increasing CO_2 concentrations represents a mixture between background air used to aerate the pots and the CO_2 emitted from the soil. Three gas samples are taken for isotopic analysis: the background air and two air samples with a difference of 100 µmol CO_2 mol^{-1} (measured by the IRGA). The isotopic signature of the CO_2 efflux is determined

by the intercept of the linear regression line of the isotopic signature (expressed in atom excess fraction) plotted against the inverse of the CO_2 concentration.
To trace the label in the plant-soil stocks, the sampling windows in the front plate of the chamber cuboid can be opened. Thus sub-samples or whole plant-soil systems can be harvested with minor disturbance to the labelled atmosphere.

2.4 Calculations

2.4.1 Data extraction

The GDU-28 software logs every five seconds the time and the data of all sensors and instruments. Separate columns indicate the activation of relays, the measurement modes (e.g. zeroing, scan mode) and the pot number of the current measurement in the lower system. The data is analysed with the open source software R statistics (R Core Team, 2014).

2.4.2 Relative humidity

The relative humidity is calculated according to Equation 1-3 based on the absolute H2O concentration and the air temperature measured in the upper systems and the pressure detected in the IRGA of lower system (which is not influenced by the large membrane pumps as in the upper system).

$$rH(\%) = \frac{e}{e_{sat}} \cdot 100 \qquad \text{(Eqn 1)}$$

, where rH is the relative air humidity (in %), e is the partial pressure of water vapour (Eqn 2) and e_{sat} is the saturation vapour pressure (Eqn 3).

$$e\ (kPa) = \frac{aH}{1000} \cdot p_{lab} \qquad \text{(Eqn 2)}$$

, where aH is the absolute humidity given as the mole fraction of water vapour (mmol mol^{-1}) and p_{lab} is the atmospheric pressure (in kPa).

$$e_{sat}(kPa) = 0.61365 \cdot e^{\frac{17.502 \cdot T_{ch}}{240.97 + T_{ch}}} \qquad \text{(Eqn 3)}$$

, where T_{ch} is the chamber air temperature (in °C).

2.4.3 Molar volume

The molar air volume (V_m) is calculated according to Equation 4, based on the current temperature (upper system) and pressure (lower system) conditions.

$$V_m(dm^3 mol^{-1}) = \frac{R \cdot T_{ch}}{p_{lab}} \qquad \text{(Eqn 4)}$$

, where p_{lab} is the atmospheric pressure (in Pa) in the laboratory, R is the universal gas constant (= 8.3144621 J K^{-1} mol^{-1}) and T_{ch} is the air temperature (in K).

2.4.4 Shoot CO_2 fluxes - photosynthesis and dark respiration

The changes of the atmospheric CO_2 concentration due to shoot photosynthesis and respiration are measured by the IRGA and assessed by the slope of the linear regression during the monitoring time (function "lm(x ~ y)", R Core Team 2014). The daily mean net photosynthetic (p_{net}) and dark respiration (r_{dark}) rates are calculated according to Equation 5 and 6.

$$p_{net,t=x}(\mu mol\ m^{-2}s^{-1}) = \frac{\sum\left(\frac{\Delta[CO_2]}{\Delta t}\cdot\frac{V_{ch}}{V_m\cdot LA_{tot}}\right)_{ch(daytime),t=x}}{n_{daytime,t=x}} \quad \text{(Eqn 5)}$$

$$r_{dark,t=x}(\mu mol\ m^{-2}s^{-1}) = \frac{\sum\left(\frac{\Delta[CO_2]}{\Delta t}\cdot\frac{V_{ch}}{V_m\cdot LA_{tot}}\right)_{ch(nighttime),t=x}}{n_{nighttime,t=x}} \quad \text{(Eqn 6)}$$

, where $\Delta[CO_2]/\Delta t$ is the CO_2 concentration change in the upper chamber system (in µmol mol^{-1} s^{-1}), V_{ch} is the chamber air volume (= 1.165 m^3), V_m is the molar volume (Eqn 4) and LA_{tot} is the total leaf area at the sampling date t = x, and $n_{daytime,t=x}$ and $n_{nighttime,t=x}$ is the number of $\Delta[CO_2]/\Delta t$ measurements made in the day- and at night-time, respectively.

The total amount of net assimilated C ($A_{net,t=x}$) is calculated for each plant individual based on its leaf area (Equation 7).

$$A_{net,t=x}(mg\ plant^{-1}day^{-1}) = \left(p_{net,t=x}\cdot f_{day} + r_{dark,t=x}\cdot f_{night}\right)\cdot LA_{t=x}\cdot M(C) \quad \text{(Eqn 7)}$$

, where $p_{net,t=x}$ and $r_{dark,t=x}$ are the daily photosynthetic or dark respiratory rates (Eqn 5 and 6, transformed in µmol C m^{-2} day^{-1}), f_{day} and f_{night} is the fraction of light and dark hours per day, respectively, $LA_{t=x}$ is the leaf area (in m^2) of the plant individual and M(C) is the molar weight of C (12.011 x 10^{-3} mg $µmol^{-1}$).

2.4.5 Total soil CO_2 efflux

The soil CO_2 efflux rate ($r_{soil,t=x}$) of the individual pots is assessed based on the CO_2 concentration difference ($\Delta[CO_2]_{in,out}$) in µmol mol^{-1}) between the pot in- and outlet measured by the IRGA in the lower system (Equation 8). $\Delta[CO_2]_{in,out}$ is calculated by subtracting the average of the background air CO_2 concentrations measured before and after ($[CO_2]_{in}$) each pot measurement from the average concentration of the pot outlet measurements ($[CO_2]_{out}$).

$$r_{soil,t=x}(\mu mol\ m^{-2}s^{-1}) = \frac{\sum\left(\frac{\Delta[CO_2]_{in,out}\cdot F_{pot}}{V_m\cdot PA}\right)_{t=x}}{n_{t=x}} \qquad \text{(Eqn 8)}$$

, where ($\Delta[CO_2]_{in,out}$) is the CO_2 concentration difference between the in- and outlet (in µmol mol^{-1}), F_{pot} is the pot aeration rate, V_m is the molar volume (Eqn 4), $n_{t=x}$ is the amount of CO_2 concentration change measurements on day t = x and PA is the pot area (= 0.0328 m^2).

The daily amount of C released as CO_2 belowground per pot ($R_{soil,t=x}$ in mg pot^{-1} day^{-1}), is calculated by multiplying the daily respiration rates $r_{soil,t=x}$ with the pot area and the molar C weight.

2.4.6 Partitioning of soil CO_2 efflux

The plant-derived and the SOM-derived CO_2 efflux can be partitioned in experiments with continuous ^{13}C-CO_2 labelling from first emergence of leaves (Kuzyakov & Domanski 2000). The estimation of the plant-derived respiration rate ($R_{pd,t=x}$) is based on the fraction of plant-derived on the total respiration ($f_{Rpd,t=x}$) assessed by a two end-members mixing model (Equation 9). The isotopic signature of the CO_2 efflux measured ($R_{soil,t=x}$) represents a mixture of the isotopic signatures of the two end-members: the SOM-derived ($R_{soil,ctrl}$) and the plant-derived soil CO_2 efflux ($R_{pd,t=x}$).

$$R_{pd,t=x}(mg\ pot^{-1}day^{-1}) = R_{soil,t=x}\cdot f_{pd,t=x} = R_{soil,t=x}\cdot \frac{x(^{13}C)_{R_{soil,\,t=x}} - x(^{13}C)_{R_{soil,\,ctrl}}}{x(^{13}C)_{R_{pd,\,t=x}} - x(^{13}C)_{R_{soil,\,ctrl}}} \qquad \text{(Eqn 9)}$$

, where $R_{soil,t=x}$, is the daily amount of respired C (in mg pot^{-1} day^{-1}) and $x(^{13}C)$ is the ^{13}C atom fraction (calculated according to Coplen 2011) of the soil efflux sampled during the experiment ($x(^{13}C)_{Rsoil,t=x}$), in before labelling or in the unlabelled control ($x(^{13}C)_{Rsoil,ctrl}$) and of the plant-derived efflux ($x(^{13}C)_{Rpd,t=x}$) estimated by the net C assimilation rates (Eqn 7) and the maximum label strength.

2.5 Experimental settings

We show the data of four experiments to demonstrate the capacity of the MICE facility to regulate the environmental conditions (Experiments 1) and to monitor C fluxes (Experiments 2). First we conducted two short-term experiments to test the efficiency of the upper (Exp. 1a) and lower system (Exp. 2a) without the presence of plants. Then we applied the facility in two long-term experiments with plants to demonstrate its efficiency to regulate the environmental conditions (Exp. 1b) and to monitor C dynamics (Exp. 2b).

2.5.1 Exp. 1a: Capacity of the instruments to modify environmental conditions

The chambers were empty and hermetically sealed to measure the capacity of the different instruments to modify the air temperature, humidity and CO_2 concentration. First we tested the efficiency of the CO_2 regulation. We injected CO_2 and estimated the scrubber capacity (in µmol mol^{-1} h^{-1}) in the range of 500 to 350 µmol mol^{-1}. Then we tested the effect of the light engines, the air-conditioning, humidifiers and heaters on the air temperature and humidity. We switched the instruments in the following sequence, awaiting the equilibration time in each step: light engines on (overnight) -> air-conditioner on (5 h) -> humidifiers on (2 h) -> humidifiers off (overnight) -> single humidifiers on (4 h) -> humidifiers off, light engines off (3 h) -> heater on (overnight) -> heater off (3 h) -> air-conditioner off (overnight). We estimated the heating/cooling capacity (in °C h^{-1}) and the humidifying/drying capacity (in mmol mol^{-1} h^{-1}) within the first hour after the activation of the instruments.

2.5.2 Exp. 1b: Efficiency of the regulation to produce a controlled environment

The upper chamber was filled with plant-soil systems (wheat in columns filled with agricultural soil), hermetically sealed and the environmental conditions were automatically regulated. Here we show the environmental data to demonstrate the efficiency of the MICE facility to reproduce steady climatic conditions, but the experiment was aimed to produce labelled material for a follow up study (Friedli et al., unpublished). The light engines were on 14 hours per day and we selected equal day/night thresholds for the temperature (23 °C, PID controlled) and humidity (19 mmol mol^{-1}, two-point controlled). The CO_2 concentration thresholds were 420 ± 1 µmol mol^{-1} (scrubber) and 380 ± 1 µmol mol^{-1} (CO_2 injection).

2.5.3 Exp. 2a: Estimation of soil CO_2 efflux rates

Ten pots were installed in the lower chamber system to test the validity of the soil CO_2 efflux calculation based on temporal distinct measurements of the pot in- and outlet air. This was necessary due to the anthropogenic variation in the outdoor air used to aerate the pots (pot inlet air). We left five pots empty as control and filled the other five pots with different amounts of soil: three with 4.7 kg (4.3 kg dry weight equivalent), one with 4.2 and one with 3.7 kg (3.8 and 3.3 kg dry weight equivalent, respectively) slightly moist soil from Experiment 1b. The pot in- and outlet air was measured by the scan mode for five minutes with two minutes waiting time between the measurements. Thus

the soil CO_2 efflux was measured for each pot every two hours and the average daily efflux rates were calculated as in Equation 8.

2.5.4 Exp. 2b: Above- and belowground (^{13}C-)CO_2 fluxes

The above- and belowground C fluxes were monitored for 70 days to demonstrate the efficiency of the MICE facility to assess plant and soil C dynamics. We grew poplar plants (*Populus deltoides x nigra*) in pots filled with cambisol soil and hermetically sealed them around the cuttings. We continuously labelled the shoots with ^{13}C (with 6 atom% ^{13}C-CO_2) from first emergence of leaves and traced the ^{13}C in soil respiratory CO_2 effluxes. Here we present and discuss the validity of the CO_2 flux measurements. All other data is discussed in Studer et al. 2015 (in preparation).

We conducted first an unlabelled (control) then labelled experiment. In the second experiment the plants were limited in their growth due to reduced reserves in the stem cuttings after storage. They produced only a third of the biomass and leaf area compared to the plants in the first experiment (optimal growth). The light availability was generally low (80 µmol photons m^{-2} s^{-1}), because the experiments were conducted in an earlier version of MICE facility (Xenon light sources). The 12 hours day-night length provided the plants with 3.5 mol photons m^{-2} day^{-1} corresponding to a shady place in nature (Poorter et al. 2012). The atmospheric CO_2 concentration (520 µmol mol^{-1}), the humidity (72 % relative air humidity, soil moisture close to field capacity) and temperature (30 °C) were non-limiting for photosynthesis.

The aboveground CO_2 gas exchange (of 15 plants) was monitored during five minutes every 30 minutes. The leaf area was measured at the last sampling date and was assumed to increase linearly over time (starting at day 3), as documented for *Populus deltoides x nigra* by others (Marron et al. 2003, 2005, 2008; Monclus et al. 2005). We monitored the soil CO_2 efflux in six individual pots, whereby each pot was scanned once per hour (five min in-/outlet measurement including two minutes waiting time). Further we repeatedly sampled the air in the upper and lower chamber system (twice a week till day 35 and once a week thereafter) and measured the isotopic composition by isotopic ratio mass spectrometry.

3 Results and discussion

3.1 Automatic regulation for a controlled environment

3.1.1 Temperature and humidity

The testing of the instruments to regulate the air temperature and humidity proofed that they have similar drying/humidifying and cooling/heating capacities (Table 1). The light engines have the largest effect on the temperature (Table 1a). They heat up the chamber by 10 °C within 3-6 hours to a level of 36 °C, making a cooling during daytime indispensable. The cooling effect of the air-conditioning (- 8 °C) and the humidifiers (- 4 °C) can compensate for the warming of the light engines, given that both instruments are very efficient in cooling (5 - 6 °C h^{-1}). A re-heating might be necessary, especially when the light engines are off (night-time) and the air-conditioning is on (temperature level of around 17 °C). The heater has a similar capacity (+ 8 °C, 6 °C h^{-1}) and response time as the air-conditioning and is thus capable to re-heat the air. The light engines have also an effect on the humidity (+ 5 mmol mol^{-1} h^{-1}) by increased evaporation of the water within the humidifiers. However, this effect is negligible compared to the drying effect of the air-conditioning (- 36 mmol mol^{-1} h^{-1}), and the capacity of the humidifiers (+ 41 mmol mol^{-1} h^{-1}, Table 1b). The test with single humidifiers showed that four out of six humidifiers are sufficient to maintain a constant humidity level (of 80 % relative humidity) when the air-conditioning is on.

Table 1. Capacity of instruments to regulate the air temperature and humidity in the MICE facility. The heating/cooling (a) and humidifying/drying (b) capacity is characterized by the total change and the speed of change (time till equilibrium, change rate). The level at equilibrium reflects the conditions achieved in the chamber when the instruments are permanently on/off. The table is ordered according to the sequence of instrument activation: light engines on -> air-conditioning (AC) on -> humidifiers on -> humidifiers and light engines off -> heater on.

	Light engines	Air-conditioning	Humidifiers	Heater
a) Temperature				
Total change (°C)	9.9	- 7.7	-3.8	8.1
Time till equilibrium (h)	3-6	2	<1	2
Change rate* (°C h^{-1})	4.8	- 5.2	- 6.1	+ 6.5
Equilibrium level (°C)	35.6	27.9	24.1	25.9
b) Humidity				
Total change (mmol mol^{-1})	33	- 37	17	
Time till equilibrium (h)	9	1	< 1	
Change rate* (mmol mol^{-1} h^{-1})	5	- 36	41	
Equilibrium level (mmol mol^{-1} / %)	42 / 68	5 / 12	26 / 83	

*estimated in the first hour after activation

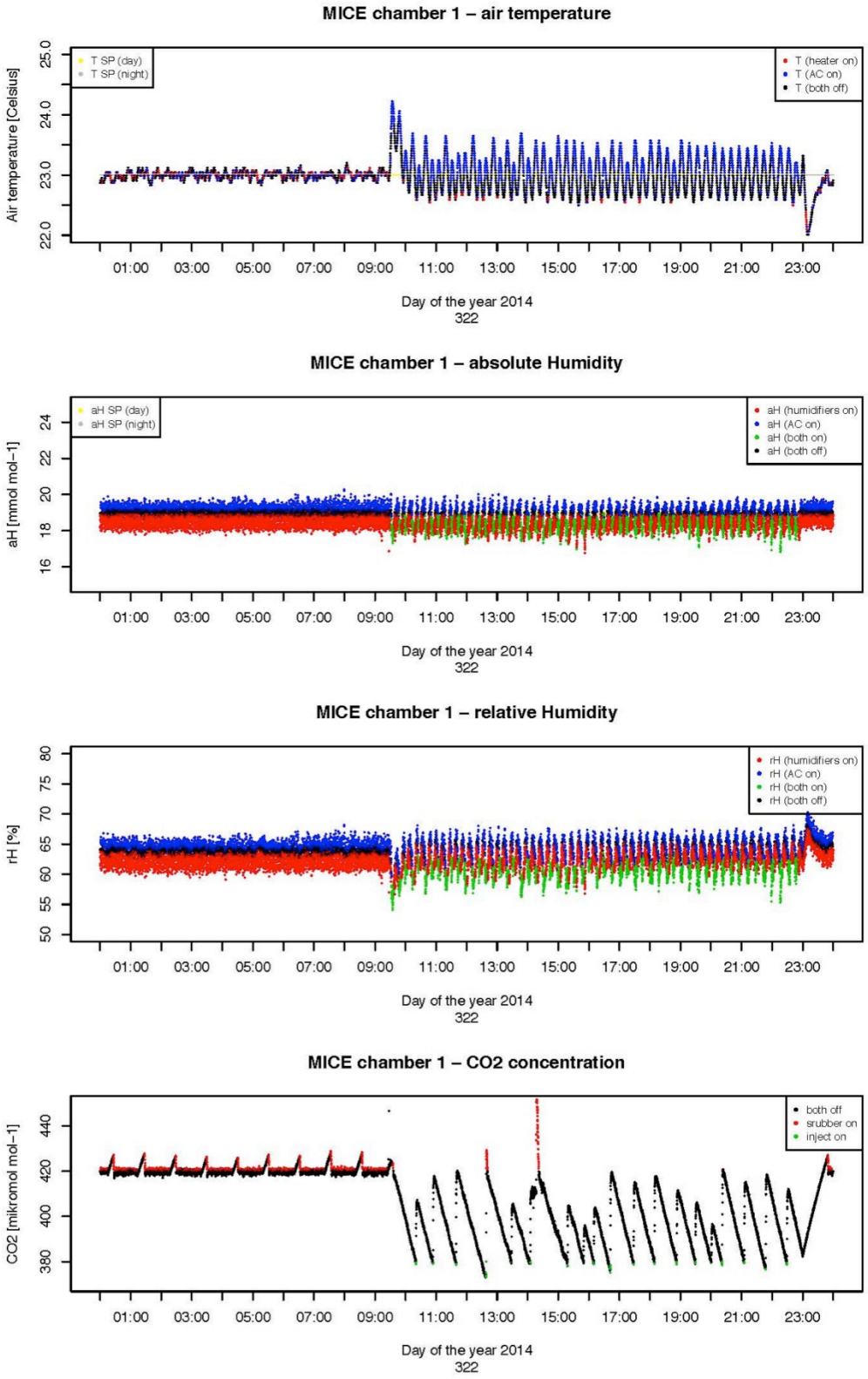

Figure 3. Environmental conditions. Example of the air temperature (in °C), the absolute and relative air humidity (in mmol mol^{-1} and %, respectively) and CO_2 concentration (in µmol mol^{-1}) monitored in the upper system during one day. The temperature is regulated by the air-conditioning (AC) and heaters, the humidity by the AC and humidifiers (Figure 2) and the CO_2 concentration by the scrubber and the injection (Figure 1) based on set points (SP). The light was on 9:15-23:00 and the CO_2 dynamics were monitored hourly (CO_2 control switched off).

The first test of the automatic regulation in the presence of plant-soil systems confirmed the efficiency of the instruments to regulate the environmental conditions (Figure 4). The temperature and absolute humidity varied by ± 0.3 °C and ± 0.5 mmol mol^{-1} in the daytime and ± 0.1 °C and ± 0.4 mmol mol^{-1} at night-time, respectively. This resulted in a variability of ± 2.2 % relative humidity in the daytime and ± 1.6 % at night-time. Thus the regulation efficiency is comparable to other laboratory facilities (e.g. Soong et al., 2014; Lukac et al., 2011).

3.1.2 CO_2 concentration

The tests with empty chambers showed that the injection of pure CO_2 increases the CO_2 concentration within seconds to the desired level and that the CO_2 scrubbing was more efficient at higher CO_2 levels (8 - 9 µmol mol^{-1} min^{-1} between 550 - 450 µmol mol^{-1}), than at lower levels (6 - 7 µmol mol^{-1} min^{-1} between 450 - 350 µmol mol^{-1}).

The automatic regulation of the CO_2 concentration in presence of plants (Figure 3) demonstrated that the concentration at night-time is constant at the level of the threshold chosen for the scrubber, while at daytime the concentration varies between the thresholds of the scrubber and the CO_2 injection.

3.2 Monitoring of C fluxes

3.2.1 Shoot CO_2 fluxes

The dynamics in the aboveground CO_2 fluxes monitored during initial plant development were as expected for *Populus deltoides* species, which need 2 - 3 weeks till full leaf expansion (Dickmann 1971; Reich 1983; Marron et al. 2008). In the first two weeks the dark respiration rates were high due intense catabolic activity and the photosynthetic capacity gradually increased (Figure 4) until it reached a steady level after 2 - 3 weeks. The net photosynthetic rate was 1.56 ± 0.02 and 1.49 ± 0.04 µmol CO_2 m^{-2} s^{-1} and the dark respiratory rate 0.30 ± 0.01 and 0.49 ± 0.03 µmol CO_2 m^{-2} s^{-1} in the optimal and limited plant-soil systems, respectively. Thus the photosynthetic rates were slightly reduced and the respiratory rates clearly enhanced in the growth-limited plants. The variability in the daily aboveground fluxes decreases with time due to larger and faster CO_2 concentration changes and thus more precise estimation of the photosynthetic and respiratory rates.

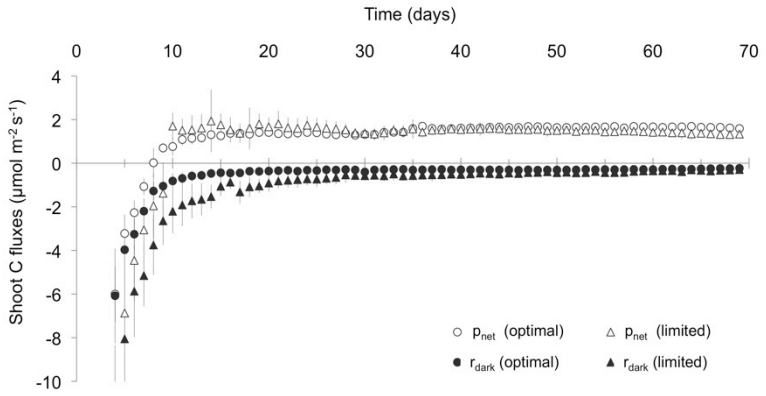

Figure 4. Shoot CO_2 fluxes during initial plant development. Example of daily net photosynthetic (p_{net}) and dark respiratory (e_{dark}) fluxes (in µmol m^{-2} leaf area s^{-1}) measured in the upper system of the MICE facility (containing 15 plant shoots). The poplars were limited in their growth due diminished reserves in the cuttings after storage. Indicated are daily average values ± one standard deviation of 24 measurements per day- and night-time.

The detected flux rates are generally very low compared to 7 - 20 µmol CO_2 m^{-2} s^{-1} maximum photosynthetic capacity and 1 - 4 µmol CO_2 m^{-2} s^{-1} dark respiration reported by others for *Populus deltoides x nigra* (Marron et al. 2008; Ow et al. 2008; Woo 2010). The reduced aboveground fluxes can be ascribed mainly to the low light availability in the current experiment (e.g. as demonstrated for *Populus* species by Landhäusser and Lieffers, 2001; Wertin and Teskey, 2008). However, a comparison of the results with leaf-level CO_2 gas exchange measurements on the same species at similar light conditions shows that our shoot estimates are at its lower end (Larson & Gordon 1969). This reflects the difference between whole-tree and leaf-level gas exchange measurements (e.g. as demonstrated for *Populus* plant-soil systems by Horwath et al., 1994). In whole-tree estimates the CO_2 exchange of branches and stems which are less or not photosynthetically active are included. Furthermore, the whole-tree estimates are done at the given conditions and do not estimate the maximum photosynthetic capacity under saturated conditions as in leaf-level gas-exchange chambers. Thus whole-tree measurements as performed by the MICE facility generally yield lower photosynthetic rates than leaf-level measurements, but they are more suitable to estimate the C budget of entire plant-soil systems (Horwath et al. 1994; Leuzinger & Hättenschwiler 2013).

3.2.2 Soil CO_2 fluxes

The validity test of the soil CO_2 efflux estimates demonstrated that the measurement principle in the MICE facility based on the difference between the pot in- and outlet is robust and can cope with the CO_2 concentration fluctuations of the background (pot inlet) air. The maximum error introduced for a single measurement was 0.1 µmol CO_2

m^{-2} s^{-1} (Figure 5). The soil CO_2 efflux rates were lower in pots with lower amounts of soil. However, the variability in the daily rates was in the same range in pots with different or equal soil amounts (Table 2) and generally accounted for 4 - 7 % of the average efflux rate. This indicates that the natural variability in the CO_2 effluxes of (inhomogeneous) soil is larger than the variability due to different amounts of soil filled into the pots.

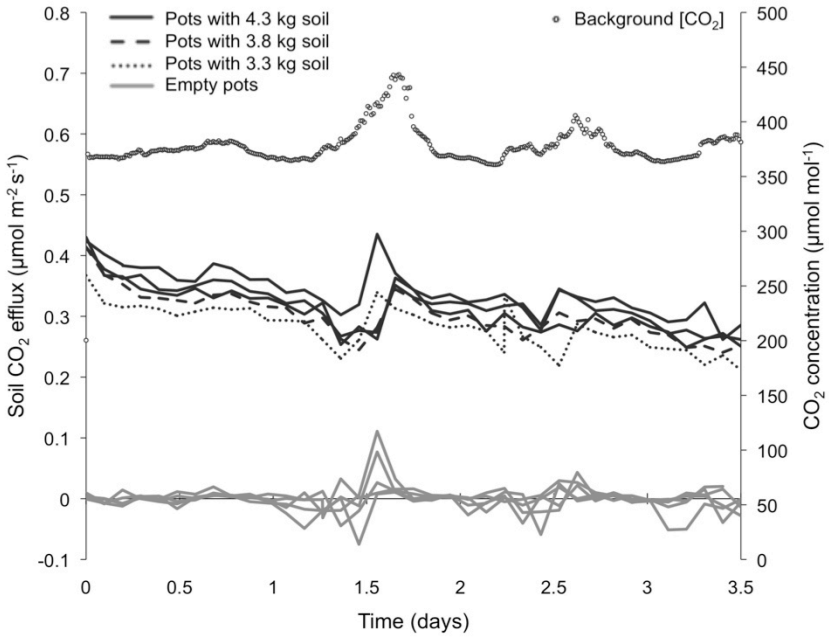

Figure 5. Soil CO_2 efflux estimations in relation to the variability in the background air CO_2 concentrations. The soil CO_2 efflux (left axis) from different pots in the MICE facility is estimated based on the CO_2 concentration difference of the pot out- and inlet air (background air, right axis). Fast changes in the background air CO_2 concentration (white circles) reduce the precision in the soil CO_2 efflux estimations (black lines) as indicated by the flux estimations in empty pots (grey lines).

Table 2. Variability in daily soil CO_2 efflux rates estimated in pots filled with different amounts of soil. The values represented are the average ± one standard deviation of average daily respiratory fluxes estimated for the three pots filled with equal amount of soil (4.3 kg dry weight equivalent) or estimated for the three pots with equal amounts of soil and the two pots with 0.5 kg less soil. In brackets the standard deviation in relation to the average rate is indicated (in %).

	Daily soil CO_2 efflux rates (µmol m^{-2} s^{-1})	
Day	**Pots with equal soil weights**	**Pots with different soil weights**
1	0.363 ± 0.015 (4.1 %)	0.340 ± 0.024 (7.0 %)
2	0.320 ± 0.021 (6.6 %)	0.301 ± 0.017 (5.8 %)
3	0.309 ± 0.017 (5.6 %)	0.289 ± 0.020 (6.8 %)

The long-term monitoring of the soil CO_2 effluxes demonstrated that the MICE facility successfully detects changes in belowground C dynamics due to plant activity. In the first experiment with optimal growth no change in the soil efflux rate was observed,

expect for some small fluctuation, which were correlated with the watering events (Figure 6a). The variability between the single pots was in the range of 7 - 18 % of the average soil CO_2 efflux rate and thus higher than in pots without root activity (Table 2). In the second experiment, where the plants were limited in their cutting reserves, we observed large peaks in the total soil CO_2 efflux rate after 3 - 4 weeks of plant growth (Figure 6b). The peaks could be indentified as the result of positive rhizosphere priming of the SOM decomposition by increased plant-C release as a response to the nutrient limitation (discussed in Studer et al., in preparation).

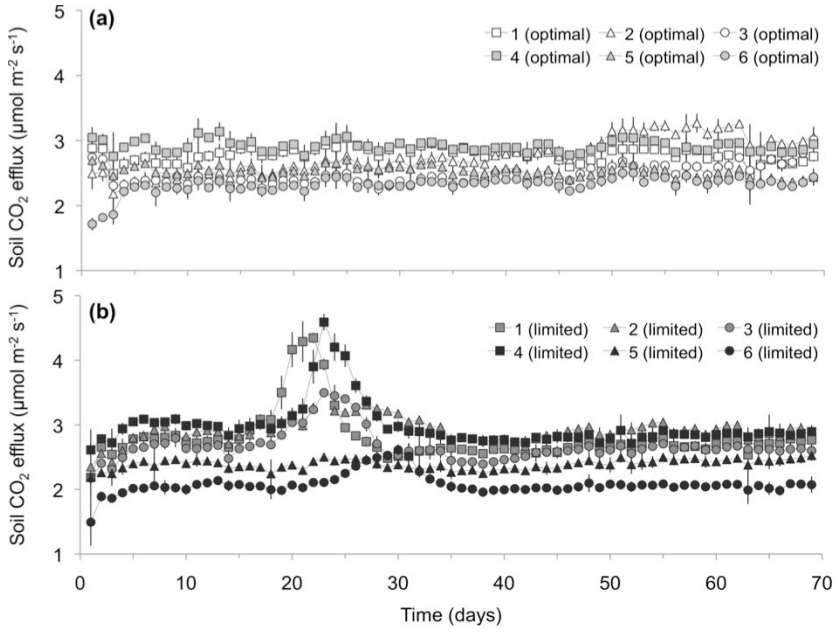

Figure 6. Soil CO_2 effluxes during initial plant development. Example of soil respiratory fluxes (in µmol m^{-2} ground area s^{-1}) measured in plant-soil systems with optimal (a) and limited (b) plant growth (Figure 4). Indicated are the daily average values ± one standard deviation of 24 measurements per day monitored in six individual pots.

The total soil efflux rate was on average 2.6 ± 0.3 µmol CO_2 m^{-2} s^{-1} in the two experiments (peaks excluded). Thus the efflux rates are comparable, but at the lower end of fluxes measured in the field on temperate forest cambisol soil surfaces (e.g. as in Rodeghiero & Cescatti, 2005; Ishizuka et al., 2006; Ruehr & Buchmann, 2010; Kutsch et al., 2010). The smaller soil depths and the less intense rooting in the pots explain the lower soil respiration rates measured in the laboratory compared to the field.

3.3 ^{13}C labelling and tracing

The ^{13}C label added to the upper chamber system (6 atom% ^{13}C-CO_2 or 4709 ‰ $\delta^{13}C$) is strongly diluted by respired ^{12}C (Figure 7a). The atmospheric CO_2 remained significantly labelled as soon as the aboveground net C balance was positive (after 10 days). The label

strength increased with time, due to the higher ^{13}C-CO_2 injection frequency (CO_2 assimilation) and the diminishing fraction of ^{12}C respired (due to the labelling of the plant material). Nevertheless, seventy days were needed to approach the maximum label strength. Thus the label strength of the chamber atmosphere has to be taken into account for the estimation of the plant-derived fraction of the soil CO_2 efflux (e.g. as in Studer et al. in preparation) and cannot be derived from the signature of the label added.

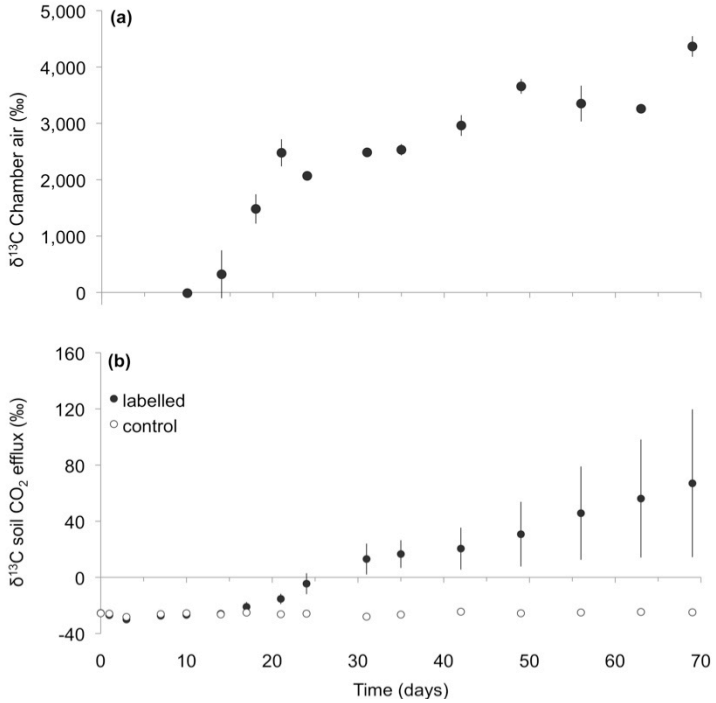

Figure 7. ^{13}C-CO_2 labelling and tracing. $\delta^{13}C$ signature of the atmosphere in the upper system (a) and estimated for the soil CO_2 efflux in lower system (b) during a continuous labelling experiment (6 atom% ^{13}C-CO_2) from first emergence of leaves (black circles) and in the unlabelled control experiment (white circles) conducted in one chamber of the MICE facility. The error bars indicate the standard deviation of three replicate measurements (a) or six pot individuals (b). The error bars in the control experiment in (b) are smaller than the symbols.

In the soil CO_2 efflux the first ^{13}C signal is detected one week after aboveground atmosphere was labelled (Figure 7b). This proves that the ^{13}C-CO_2 did not diffuse from the upper- to the lower chamber system and that thus the ^{13}C signal detected in the soil CO_2 efflux was plant-derived (e.g. root or rhizomicrobial respiration of plant-derived C). The amount of respired ^{13}C and its variability between the plant-soil systems increased as expected with plant root development, whereby the variability was related to the difference in plant C assimilation (details in Studer et al. in preparation).

4 Conclusions

The unique configuration makes the MICE facility very versatile in its application to study C cycling:

- The hermetical separation of the upper and lower system allows for distinct monitoring of above- and belowground C stocks and fluxes and the application of diverse isotope labelling techniques to trace compounds and study interactions with other biogeochemical cycles (e.g. water, nutrients).
- The two independently and automatically controlled upper chamber systems can be used to simulate different (multifactor) climate scenarios.
- The individual pots in the lower system provide the opportunity to study the effect of soil conditions (e.g. soil moisture, nutrient availability) on plant-soil C cycling.
- The frequent of CO_2 gas exchange (assimilation, respiration) and the harvesting windows enables the detection of C dynamics in fluxes and stock over time.

Here we demonstrated with a series of experiments that

- the instruments and the automatic control efficiently regulate the CO_2 concentration, air temperature and humidity in the MICE facility.
- the MICE facility can be used to detect changes in C cycling in plant-soil systems grown at different conditions (e.g. reserve limitation in cuttings).
- the net photosynthetic rate assessed in the MICE facility reflects the net C assimilation of the entire aboveground system (including stems) and is thus more suitable to detect changes in the plant-soil C cycling budget than leaf-level approaches.
- the soil respiratory rates assessed in the MICE facility are comparable to field measurements, whereat the contribution of the plant-derived respiration is low in pots with single plants compared to natural ecosystems.
- the continuous application of stable isotopes (^{13}C-CO_2) to the upper system can be used to partition plant-derived and SOM-derived soil CO_2 effluxes in the MICE facility.

The MICE facility is a new tool to separately but simultaneously measure the plant and soil driven C dynamics and thus to study plant-soil C cycling with a holistic approach to improve our knowledge of the underlying mechanisms. In the near future we will use the MICE facility to study the response of plant-soil systems to climate change, with special focus on the belowground C cycle. For example it is still largely unknown how environmental conditions (e.g. elevated CO_2 concentrations, drought) affect the belowground plant C input in plant-soil systems and to what extend this process will alter other soil C cycle processes (e.g. microbial decomposition of SOM) and thus lead to

a positive or negative feedback to climate change via changes in the soil CO_2 efflux (Drigo et al. 2008; Bardgett 2011; Cheng et al. 2014). The MICE facility has also great potential to study the response of plant-soil C cycling in manipulative experiments to changes in atmospheric CO_2 concentration (e.g. elevated CO_2), air and soil moisture (e.g. drought), air temperature (e.g. warming), light availability (e.g. shading), nutrient cycling (e.g. increased N deposition), pollution (e.g. heavy metal contamination), soil structure (e.g. aggregation), biological activity (e.g. mycorrhization) or plant community (e.g. competition).

Author contributions

S.A. and M.W.I.S. acquired the funding of the facility and the projects related to it. R.M., I.W. and M.S.S. designed, built and developed the facility hardware, M.S.S. designed and conducted the experiments and wrote the manuscript. S.A. and R.T.W.S. gave intellectual inputs on the design and development of the facility, the design of the experiments and on the manuscript.

Acknowledgements

We would like to thank the funding agencies of the MICE facility. The facility was initially funded by the chair of Soil Science and Biogeochemistry (Prof. M. W. I. Schmidt), Department of Geography, University of Zurich and further developed based on the R'Equip funding (Nr. 144982) of the Swiss National Science Foundation (SNSF) with support of the Faculty of Science and the Department of Geography, University of Zurich. Further contributors were the SNSF project nr. 135233 and the University of Zurich Research Priority Program "Global change and biodiversity".

Further we would like to thank all people involved in the construction and development of the facility with special acknowledgment to R. Künzli (DMP Ltd) for the development of the GDU-28 software, and C. Friedli to provide experimental data.

References

Amelung, W., Brodowski, S., Sandhage-Hofmann, A. & Bol, R. (2008). Combining biomarker with stable isotope analyses for assessing the transformation and turnover of soil organic matter. Advances in Agronomy, 100, 155–250.

Arneth, A., Harrison, S.P., Zaehle, S., Tsigaridis, K., Menon, S., Bartlein, P.J., Feichter, J., Korhola, A., Kulmala, M., O'Donnell, D., Schurgers, G., Sorvari, S. et al.(2010). Terrestrial biogeochemical feedbacks in the climate system. Nature Geoscience, 3, 525–532.

Bahn, M., Schmitt, M., Siegwolf, R.T.W., Richter, A. & Brüggemann, N. (2009). Does photosynthesis affect grassland soil-respired CO_2 and its carbon isotope composition on a diurnal timescale? New Phytologist, 182, 451–60.

Bardgett, R.D. (2011). Plant-soil interactions in a changing world. F1000 Biology Reports, 3, 1–6.

Bardgett, R.D., Freeman, C. & Ostle, N.J. (2008). Microbial contributions to climate change through carbon cycle feedbacks. The ISME journal, 2, 805–814.

Bird, J.A. & Torn, M.S. (2006). Fine roots vs. needles: a comparison of ^{13}C and ^{15}N dynamics in a ponderosa pine forest soil. Biogeochemistry, 79, 361–382.

Cheng, W., Parton, W.J., Gonzalez-Meler, M.A., Phillips, R., Asao, S., McNickle, G.G., Brzostek, E. & Jastrow, J.D. (2014). Synthesis and modeling perspectives of rhizosphere priming. New Phytologist, 201, 31–44.

Coplen, T.B. (2011). Guidelines and recommended terms for expression of stable-isotope-ratio and gas-ratio measurement results. Rapid Communications in Mass Spectrometry, 25, 2538–2560.

Dawson, T.E., Mambelli, S., Plamboeck, A.H., Templer, P.H. & Tu, K.P. (2002). Stable isotopes in plant ecology. Annual Review of Ecology and Systematics, 33, 507–559.

De Deyn, G.B., Cornelissen, J.H.C. & Bardgett, R.D. (2008). Plant functional traits and soil carbon sequestration in contrasting biomes. Ecology letters, 11, 516–531.

Dickmann, D.I. (1971). Photosynthesis and respiration by developing leaves of cottonwood (*Populus deltoides* Bartr.). Botanical Gazette, 132, 253–259.

DMP (2014). MICE V2.0 Software Handbook. DMP Ltd, Fehraltdorf, Switzerland.

Drigo, B., Kowalchuk, G. a. & van Veen, J. A. (2008). Climate change goes underground: effects of elevated atmospheric CO_2 on microbial community structure and activities in the rhizosphere. Biology and Fertility of Soils, 44, 667–679.

Farquhar, G.D., Ehleringer, J.R. & Hubick, K.T. (1989). Discrimination and photosynthesis. Annual Review of Plant Physiology and Plant Molecular Biology, 40, 503–537.

Friedlingstein, P. & Prentice, I. (2010). Carbon–climate feedbacks: a review of model and observation based estimates. Current Opinion in Environmental Sustainability, 2, 251–257.

Heimann, M. & Reichstein, M. (2008). Terrestrial ecosystem carbon dynamics and climate feedbacks. Nature, 451, 289–292.

Högberg, P., Högberg, M.N., Göttlicher, S.G., Betson, N.R., Keel, S.G., Metcalfe, D.B., Campbell, C., Schindlbacher, A., Hurry, V., Lundmark, T., Linder, S. & Näsholm, T. (2008). High temporal resolution tracing of photosynthate carbon from the tree canopy to forest soil microorganisms. New Phytologist, 177, 220–228.

Högberg, P. & Read, D.J. (2006). Towards a more plant physiological perspective on soil ecology. Trends in Ecology and Evolution, 21, 548–554.

Horwath, W.R., Pregitzer, K.S. & Paul, E.A. (1994). ^{14}C allocation in tree-soil systems. Tree Physiology, 14, 1163–1176.

Ishizuka, S., Sakata, T., Sawata, S., Ikeda, S., Takenaka, C., Tamai, N., Sakai, H., Shimizu, T., Kan-Na, K., Onodera, S., Tanaka, N. & Takahashi, M. (2006). High potential for increase in CO_2 flux from forest soil surface due to global warming in cooler areas of Japan. Annals of Forest Science, 63, 537–546.

Keeling, C.D. (1958). The concentration and isotopic abundances of atmospheric carbon dioxide in rural areas. Geochimica et Cosmochimica Acta, 13, 322–334.

Körner, C. (2011). The grand challenges in functional plant ecology. Frontiers in Plant Science, 2, 1–3.

Kreyling, J., Jentsch, A. & Beier, C. (2014). Beyond realism in climate change experiments: gradient approaches identify thresholds and tipping points. Ecology letters, 17, 125–e1.

Kutsch, W.L., Persson, T., Schrumpf, M., Moyano, F.E., Mund, M., Andersson, S. & Schulze, E.-D. (2010). Heterotrophic soil respiration and soil carbon dynamics in the deciduous Hainich forest obtained by three approaches. Biogeochemistry, 100, 167–183.

Kuzyakov, Y. & Domanski, G. (2000). Carbon input by plants into the soil. Review. Journal of Plant Nutrition and Soil Science, 163, 421–431.

Landhäusser, S.M. & Lieffers, V.J. (2001). Photosynthesis and carbon allocation of six boreal tree species grown in understory and open conditions. Tree Physiology, 21, 243–250.

Larson, P.R. & Gordon, J.C. (1969). Leaf development, photosynthesis and C^{14} distribution in *Populus deltoides* seedlings. American Journal of Botany, 56, 1058–1066.

Lenton, T.M., Held, H., Kriegler, E., Hall, J.W., Lucht, W., Rahmstorf, S. & Joachim, H. (2008). Tipping elements in the Earth's climate system. Proceedings of the National Academy of Sciences, 105, 1786–1793.

Leuzinger, S. & Hättenschwiler, S. (2013). Beyond global change: lessons from 25 years of CO_2 research. Oecologia, 171, 639–651.

Leuzinger, S., Luo, Y., Beier, C., Dieleman, W., Vicca, S. & Körner, C. (2011). Do global change experiments overestimate impacts on terrestrial ecosystems? Trends in Ecology and Evolution, 26, 236–241.

Lukac, M., Milcu, A., Wildman, D., Anderson, R., Sloan, T. & Ineson, P. (2011). Non-intrusive monitoring of atmospheric CO_2 in analogue models of terrestrial carbon cycle. Methods in Ecology and Evolution, 2, 103–109.

Luo, Y., Melillo, J., Niu, S., Beier, C., Clark, J.S., Classen, A.T., Davidson, E., Dukes, J.S., Evans, R.D., Field, C.B., Czimczik, C.I., Keller, M., et al. (2011). Coordinated approaches to quantify long-term ecosystem dynamics in response to global change. Global Change Biology, 17, 843–854.

Marron, N., Brignolas, F., Delmotte, F.M. & Dreyer, E. (2008). Modulation of leaf physiology by age and in response to abiotic constraints in young cuttings of two *Populus deltoides × P . nigra* genotypes. Annals of forest science, 65, 404.

Marron, N., Dreyer, E., Boudouresque, E., Delay, D., Petit, J.-M., Delmotte, F.M. & Brignolas, F. (2003). Impact of successive drought and re-watering cycles on growth and specific leaf area of two *Populus x canadensis* (Moench) clones, "Dorskamp" and "Luisa_Avanzo."Tree Physiology, 23, 1225–1235.

Marron, N., Villar, M., Dreyer, E., Delay, D., Boudouresque, E., Petit, J.-M., Delmotte, F.M., Guehl, J.-M. & Brignolas, F. (2005). Diversity of leaf traits related to productivity in 31 *Populus deltoides x Populus nigra* clones. Tree Physiology, 25, 425–35.

Metcalfe, D.B., Fisher, R.A. & Wardle, D.A. (2011). Plant communities as drivers of soil respiration: pathways, mechanisms, and significance for global change. Biogeosciences, 8, 2047–2061.

Monclus, R., Dreyer, E., Delmotte, F.M., Villar, M., Delay, D., Boudouresque, E., Petit, J.-M., Marron, N., Bréchet, C. & Brignolas, F. (2005). Productivity, leaf traits and carbon isotope discrimination in 29 *Populus deltoides x P. nigra clones*. New Phytologist, 167, 53–62.

Moorcroft, P.R. (2006). How close are we to a predictive science of the biosphere? Trends in Ecology and Evolution, 21, 400–407.

Ostle, N.J., Smith, P., Fisher, R., Ian Woodward, F., Fisher, J.B., Smith, J.U., Galbraith, D., Levy, P., Meir, P., McNamara, N.P. & Bardgett, R.D. (2009). Integrating plant-soil interactions into global carbon cycle models. Journal of Ecology, 97, 851–863.

Ow, L.F., Griffin, K.L., Whitehead, D., Walcroft, A.S. & Turnbull, M.H. (2008). Thermal acclimation of leaf respiration but not photosynthesis in *Populus deltoides x nigra*. New Phytologist, 178, 123–134.

Pataki, D.E. (2003). The application and interpretation of Keeling plots in terrestrial carbon cycle research. Global Biogeochemical Cycles, 17.

Poorter, H., Fiorani, F., Stitt, M., Schurr, U., Fink, A., Gibon, Y., Usadel, B., Munns, R., Atkin, O.K., Tardieu, F. & Pons, T.L. (2012). The art of growing plants for experimental purposes: a practical guide for the plant biologist. Functional Plant Biology, 39, 821–838.

R Core Team (2014). R: A Language and Environment for Statistical Computing. R Foundation for Statistical Computing. Retrieved from http://www.r-project.org

Reich, P.B. (1983). Effects of low concentrations of O_3 on net photosynthesis, dark respiration, and chlorophyll contents in aging hybrid poplar leaves. Plant Physiology, 73, 291–296.

Rodeghiero, M. & Cescatti, A. (2005). Main determinants of forest soil respiration along an elevation/temperature gradient in the Italian Alps. Global Change Biology, 11, 1024–1041.

Ruehr, N.K. & Buchmann, N. (2010). Soil respiration fluxes in a temperate mixed forest: seasonality and temperature sensitivities differ among microbial and root-rhizosphere respiration. Tree Physiology, 30, 165–176.

Schmidt, M.W.I., Torn, M.S., Abiven, S., Dittmar, T., Guggenberger, G., Janssens, I.A., Kleber, M., Kögel-Knabner, I., Lehmann, J., Manning, D.A.C., Nannipieri, P., Rasse, D.P., et al. (2011). Persistence of soil organic matter as an ecosystem property. Nature, 478, 49–56.

Soong, J.L., Reuss, D., Pinney, C., Boyack, T., Haddix, M.L., Stewart, C.E. & Cotrufo, M.F. (2014). Design and operation of a continuous ^{13}C and ^{15}N labeling chamber for uniform or differential, metabolic and structural, plant isotope labeling. Journal of Visualized Experiments : JoVE, e51117.

Studer, M.S., Siegwolf, R.T.W. & Abiven, S. (2014a). Carbon transfer, partitioning and residence time in the plant-soil system: a comparison of two $^{13}CO_2$ labelling techniques. Biogeosciences, 11, 1637–1648.

Studer, M.S., Siegwolf, R.T.W., Leuenberger, M. & Abiven, S. (2014b). Multi-isotope labelling (^{13}C, ^{18}O, ^{2}H) of fresh assimilates to trace organic matter dynamics in the plant-soil system. Biogeosciences Discussions, 11, 1–33.

Studer, M.S., Siegwolf, R.T.W., Schmidt, M.W.I. & Abiven, S. (2015): Increased plant-derived soil respiration vs. assimilation induces massive rhizosphere priming in resource limited plant-soil systems. In preparation.

Walther, G., Post, E., Convey, P., Menzel, A., Parmesan, C., Beebee, T.J.C., Fromentin, J., I, O.H. & Bairlein, F. (2002). Ecological responses to recent climate change. Nature, 202, 389–395.

Wertin, T.M. & Teskey, R.O. (2008). Close coupling of whole-plant respiration to net photosynthesis and carbohydrates. Tree Physiology, 28, 1831–1840.

Wichern, F., Mayer, J., Joergensen, R.G. & Müller, T. (2007). Rhizodeposition of C and N in peas and oats after ^{13}C–^{15}N double labelling under field conditions. Soil Biology and Biochemistry, 39, 2527–2537.

Woo, S.Y. (2010). Epidermal leaf characteristics and seasonal changes of net photosynthesis of five *Populus*. African Journal of Biotechnology, 9, 1455–1458.

Manuscript II '^{13}C labelling techniques'

Published as

Studer, M. S., Siegwolf, R. T. W. and Abiven, S.: Carbon transfer, partitioning and residence time in the plant-soil system: a comparison of two $^{13}CO_2$ labelling techniques, Biogeosciences, 11(6), 1637–1648, doi:10.5194/bg-11-1637-2014, 2014.

Abstract

Various $^{13}CO_2$ labelling approaches exist to trace carbon (C) dynamics in plant-soil systems. However, it is not clear if the different approaches yield the same results. Moreover, there is no consistent way of data analysis to date. In this study we compare with the same experimental setup the two main techniques: pulse and continuous labelling. We evaluate how these techniques perform to estimate the C transfer time, the C partitioning along time and the C residence time in different plant-soil compartments.

We used identical plant-soil systems (*Populus deltoides x nigra*, Cambisol soil) to compare the pulse labelling approach (exposure to 99 atom% $^{13}CO_2$ for three hours, traced for eight days) with a continuous labelling (exposure to 10 atom% $^{13}CO_2$, traced for 14 days). The experiments were conducted in climate chambers under controlled environmental conditions. Before label addition and at four successive sampling dates, the plant-soil systems were destructively harvested, separated into leaves, petioles, stems, cuttings, roots and soil and soil microbial biomass was extracted. The soil CO_2 efflux was sampled throughout the experiment. To model the C dynamics we used an exponential function to describe the ^{13}C signal decline after pulse labelling. For the evaluation of the ^{13}C distribution during the continuous labelling we applied a logistic function.

Pulse labelling is best suited to assess the minimum C transfer time from the leaves to other compartments, while continuous labelling can be used to estimate the mean transfer time through a compartment, including short-term storage pools. The C partitioning between the plant-soil compartments obtained was similar for both techniques, but the time of sampling had a large effect: Shortly after labelling the allocation into leaves was overestimated and the soil $^{13}CO_2$ efflux underestimated. The results of belowground C partitioning were consistent for the two techniques only after eight days of labelling, when the ^{13}C import and export was at equilibrium. The C mean residence times estimated by the rate constant of the exponential and logistic function

were not valid here (non-steady state). However, the duration of the accumulation phase (continuous labelling) could be used to estimate the C residence time.
Pulse and continuous labelling techniques are both well suited to assess C cycling. With pulse labelling, the dynamics of fresh assimilates can be traced, whereas the continuous labelling gives a more integrated result of C cycling, due to the homogeneous labelling of C pools and fluxes. The logistic model applied here, has the potential to assess different parameters of C cycling independent on the sampling date and with no disputable assumptions.

1 Introduction

Carbon (C) cycling within terrestrial ecosystems has been extensively studied in the last decades, still many processes and plant-soil-atmosphere C fluxes are not well understood. How single plants or whole ecosystems will respond to changes in climate (temperature, water availability and atmospheric CO_2 concentration) is still a matter of intense research. Of special interest is the speed of C cycling, the C allocation patterns and the C residence time within different compartments of the plant-soil system, in order to better understand the interactions between different processes and predict the changes in terrestrial C fluxes induced by climate change.
Stable isotope tracing is a powerful tool to study the C fluxes and pools within the plants and the soil with minor disturbance (Brüggemann et al., 2011; Dawson et al., 2002; Werner et al., 2012). The use of natural labelling approaches (based on isotopic fractionation occurring during biochemical reactions in plant and soil) is valuable in many cases, but is inappropriate if more than two sources are involved or if the difference in the isotopic composition of the sources is too small (Bowling et al., 2008; Werth and Kuzyakov, 2010). Artificial labelling techniques (using stable or radioactive isotopes) can overcome these difficulties (Amelung et al., 2008; Epron et al., 2012; Glaser, 2005).
In the last decades, various labelling approaches have been used. These approaches differ in the duration of label exposure, the applied label strength and the sampling intervals. Two main techniques can be distinguished to label organic matter by exposure of the plant to labelled CO_2: pulse and continuous labelling (field of applications reviewed in Meharg, 1994; Kuzyakov & Domanski, 2000). In a pulse labelling (PL) experiment, highly ^{13}C enriched CO_2 (usually 99 atom% $^{13}CO_2$) is added in a pulse, i.e. over a short period of time (a few hours) and the label is traced in the plant-soil system in the following days (Epron et al., 2012; Leake et al., 2006). In continuous labelling (CL)

experiments, the plant is continuously exposed to less strongly labelled CO_2 (generally <10 atom% $^{13}CO_2$) or ^{13}C - depleted CO_2 over the whole experimental period and samples are taken during and/or at the end of the labelling (e.g. in Esperschütz et al., 2009; Yevdokimov et al., 2006). With continuous labelling, C dynamics can be studied over larger time periods, as for example in Free Air CO_2 Enrichment (FACE) experiments, where whole ecosystem areas are exposed to elevated CO_2 (^{13}C - depleted) for several years (e.g. in Grams et al., 2010; Keel et al., 2006). However, the continuous labelling technique has also been applied at the same time scales as the pulse labelling technique (days-weeks), but it is not clear if these approaches yield the same results regarding C cycling within plant-soil systems and how we can interpret them. While there are generally accepted approaches to analyse the ^{13}C dynamics in plants after pulse labelling (exponential model), no consistent approach exists for the continuous labelling technique.

To make best use of the two $^{13}CO_2$ labelling techniques and their results, a proper evaluation of the techniques is essential. A comparison based on literature is difficult, since they have been applied to numerous plant species and soil types and under a variety of environmental conditions. Studies based on identical plant-soil systems grown under controlled environmental conditions are needed in order to elucidate the potential of these labelling techniques to assess C dynamics and to evaluate how one can compare them. To our knowledge, only one study has made such a direct comparison so far, in which the focus lay on the effect of labelling duration on belowground C partitioning (Warembourg and Estelrich, 2000).

In this study we compare the results for above- and belowground plant-soil compartments, obtained by pulse and (short-term) continuous labelling and discuss their potential to estimate the C transfer time, C partitioning and C residence time. We suggest a new approach to assess the C dynamics based on the ^{13}C dynamics during continuous labelling, test if the results regarding C cycling are comparable for both techniques and if the time point of sampling matters.

2 Material and methods

2.1 Plants and soil

Poplar trees (*Populus deltoides x nigra*, Dorskamp clone) were grown in a cambisol soil, sampled from the upper 15 cm in a beech forest (8°33'E, 47°23'N, 500 m elevation). The soil had a clay loam texture (20 % sand, 45 % silt, 35 % clay), with a pH of 4.8 and an organic C and N content of 2.2 % and 0.2 %, respectively. The soil was sieved by hand

through a square sieve (2.5 x 3.5 cm) leaving the soil structure largely intact, while large pieces of organic material and coarse gravel were removed. The plant pots were filled with 7.5 dm^3 moist soil (average dry weight of 2642 ± 402 g).

The poplar trees, 15 per experiment, were grown indoors under artificial light by sprouting from stem cuttings for five weeks and were then transferred into the labelling chambers (described below), where they were left for one week to acclimatize prior to labelling. One day before labelling the dry weight of newly produced biomass (plant biomass without the cutting) was 4.0 ± 1.2 g and the total leaf area 692 ± 113 cm^2 per plant. During the PL and CL experiment the plant biomass increased by 28 % and 65 % and the leaf area by 42 % and 111 %, respectively.

2.2 Labelling chamber and procedure

2.2.1 The MICE facility

The experiments were conducted in the "Multi-Isotope labelling in a Controlled Environment" (MICE) facility at the University of Zurich. The upper parts of the plant-soil system (shoots) are hermetically separated from the lower parts (roots, soil). The upper part of the chamber has a volume of 1.2 m^3 (area 0.94 m^2, 1.24 m height) and is made of transparent polycarbonate plates. To facilitate sampling with minor disturbances to the labelling atmosphere, small sampling windows are installed in the front plate of the chamber. The lower part of the chamber consists of 15 individual plant pots.

The front plate of the chamber can be removed and the bottom plate has five open gaps with a width of 2 cm, where the plants can be slid in. The gaps are closed with polycarbonate pieces and malleable sealant (Terostat IX, Henkel AG & Co.) wrapped around the cuttings, to prevent the diffusion of the labelled gas from the plants' atmosphere into the soil. The plant roots are in individual soil pots, which are also hermetically separated from the room atmosphere. The pots are aerated individually, with ambient air (flow rate = 0.8 L min^{-1}), to prevent anaerobic conditions. Further, each pot has a separate in- and outlet for watering.

The environmental conditions in the chamber (CO_2 concentration, air humidity and light) are automatically regulated (valve system programmed with LabVIEW, National Instruments Switzerland Corp.). The $^{12}CO_2$ and H_2O concentrations in the chamber atmosphere and of the pot in- and outlets are monitored online with infrared gas analyzers (LI-840A, LI-COR Inc.). In addition, gas samples can be taken manually from up to nine individual pots for further analysis of the soil $^{13}CO_2$ efflux.

2.2.2 Labelling procedure

To label the plants we added CO_2 enriched in ^{13}C to the shoots (upper chamber system). In the pulse labelling (PL) experiment, the CO_2 concentration in the chamber was reduced first, after the lights switched on, to 250 ppm within 0.5 hours. Then 99 atom% $^{13}CO_2$ (Cambridge Isotope Laboratories, Inc.) was injected up to a concentration of 1000 ppm CO_2 and kept on this concentration level (CO_2 saturation) for 2.5 hours. After flushing the chamber with ambient air, the plant shoots were exposed to CO_2 with isotopic signatures close to ambient air ($\delta^{13}C$ = -3 ‰) from a CO_2 gas cylinder till the end of the experiment (8 days). In the continuous labelling (CL) experiment, 10 atom% $^{13}CO_2$ (Cambridge Isotope Laboratories, Inc.) was added continuously to the upper chamber system (for 14 days).

Due to technical restrictions the light intensity within the labelling chambers was low (79 ± 25 µmol m^{-2} s^{-1}) and the temperature high (31 ± 3 °C). Day-night cycles of twelve hours assured a positive C balance. To ensure optimal C assimilation at the given light availability, the CO_2 concentration was held on a high level (495-540 ppm), the soil was kept moist (close to 100 % field capacity) and the plants were grown in a humid environment (65-74 % relative air humidity) throughout both experiments.

2.3 Sample collection

2.3.1 Destructive harvests

The plant-soil systems were destructively harvested at five sampling dates with three replicates each. The first sampling was done one day before the labelling experiment started and represents the natural isotopic background signature (thereafter referred to as sampling date t = 0). Subsequently, plant-soil systems were sampled 0.1 (2 hours), 1, 2 and 8 days after the pulse labelling and after 1, 2, 8 and 14 days during the continuous labelling experiment. The sampled bulk materials were dried in the oven (24 hours at 60 °C) for later $\delta^{13}C$ analysis.

At each sampling date, the total leaf area was measured with a handheld area meter (CID-203 Laser leaf area meter, CID Inc.) and the plant-soil systems were separated into leaves, petioles, stems, cuttings, roots (washed with deionised water and carefully dabbed with tissue) and bulk soil (visible roots were removed with tweezers). The soil microbial biomass was extracted from fresh soil by chloroform fumigation extraction (CFE). The extraction was performed according to Murage & Voroney (2007), but we used 1 M KCl and did not remove excess salts. Subsamples of the CFE extracts were stored in a freezer for later elemental analysis. The remaining CFE extracts were freeze-dried for $\delta^{13}C$ analysis.

2.3.2 Soil respiration

Soil CO_2 efflux samples were collected one day before the beginning of the labelling, five times during the first day (2, 4, 6, 8, 21 hours) and after 1, 2, 3, 4, 5 and 8 days in both experiments. During the CL, additional samples were collected after 11 and 14 days. The gas samples were taken from three pots corresponding to the last sampling date. To analyse the soil $^{13}CO_2$ efflux, each pot was connected to a closed loop. A pump circulated the air (flow rate of 0.8 L min^{-1}) from the pot to a T-piece, equipped with a septum for manual gas sampling, through the gas analyzer (LI-840A, LI-COR Inc.) and back to the same pot. At each sampling date, three gas samples per pot were taken for $\delta^{13}C$ analyses. First, the air used to aerate the pots was sampled (atmospheric background). Then the pot was cut off from the aeration and linked to the loop. Two samples with a span of 100 ppm CO_2 were taken in order to assure a high precision in the estimation of the isotopic signature of the soil respiration (Pataki, 2003). The soil respiration rate was assessed by the slope of the linear regression line of the increase in the CO_2 concentration measured between the two sampling times.

The isotopic signature of the soil respiration was then estimated by the Keeling plot approach (Keeling, 1958; Pataki, 2003). The approach is based on a two end-member mixing model (assuming preservation of mass), where the two end-members are the atmospheric background and the soil $^{13}CO_2$ efflux. The isotopic signature of the sampled CO_2 (in the pot) shows a linear relationship to the inverse of its concentration. The intercept of the linear regression line yields the isotopic signature of one end-member (soil $^{13}CO_2$ efflux). In a recent publication, Brand & Coplen (2012) have demonstrated the non-linearity of the δ notation and that δ values should consequently not be used to assess mass balances when the differences in the δ values are large (as it is usually the case in labelling experiments). Therefore we used ^{13}C atom fraction, instead of the δ values, to calculate the signature of the soil respiration based on the Keeling plot approach.

2.4 Isotopic and elemental analysis

2.4.1 Procedure

The dried plant and soil samples were milled to a fine power with a steel ball mill and weighed into tin capsules. The elemental C content of the solid samples was analysed in an elemental analyzer (CHN-900, Leco Corp). The elemental C analysis of the liquid CFE extracts was performed by a TOC-500 analyzer (Shimadzu Corp.).

The isotopic analyses were done by isotope ratio mass spectrometry (IRMS). To estimate the isotope ratios, the solid samples were combusted in an elemental analyser (EA 1110, Carlo Erba) and the resulting CO_2 was transferred in a helium stream via a variable open-split interface (ConFlo II, Finnigan MAT) to the mass spectrometer (Delta S, Thermo Finnigan; Werner et al., 1999). The precision of the $\delta^{13}C$ solids analyses was ± 0.12 ‰ (CL) and ± 0.09 ‰ (PL). The gaseous soil CO_2 efflux samples were transferred in a helium stream directly from the gasbench (Gasbench II, Thermo Finnigan) to the mass spectrometer (Delta Plus XL, Thermo Finnigan). The precision of the gaseous $\delta^{13}C$ analyses was ± 0.44 ‰ (CL) and ± 0.51 ‰ (PL). The precisions indicated here are the standard deviations of working standards (leaf biomass, commercially available CO_2) measured frequently along with the experimental samples.

2.4.2 Calculations

The isotopic ratios measured were expressed in the delta (δ) notation relative to the international standard Vienna Pee Dee Belemnite (V-PDB, $^{13}C/^{12}C$ = 0.0111802). The significance of the ^{13}C enrichment was tested by t-tests (unpaired, two-sided, R statistics) at the individual sampling dates (t = x), compared to the natural isotopic background measured before labelling (t = 0). The excess atom fraction $x^E(^{13}C)_{P/reference}$ within a plant-soil compartment, was calculated according to Coplen (2011) in order to assess mass balances (reference is t = 0). The total mass of label recovered in excess $m^E(^{13}C)$ (in mg ^{13}C) within the plant tissues, the soil, the microbial biomass and the soil respiration was then calculated by multiplying the excess atom fraction with the C pool size or C flux present and taking into account the change in molar C weight due to the ^{13}C tracer addition (Eq. 1-3), as suggested by Brand and Coplen (2012).

$$m^E(^{13}C)_{PT,S}[mg] = \frac{x^E(^{13}C)_{PT,S} \cdot m(C)_{PT,S} \cdot M(^{13}C)}{x(^{12}C)_{PT,S} \cdot M(^{12}C) + x(^{13}C)_{PT,S} \cdot M(^{13}C)} \quad (1)$$

, where $m(C)_{PT,S}$ is the mass (in mg) of C present in a plant tissue (PT) or in the soil organic matter (S), $x(^{12}C)_{PT,S}$ and $x(^{13}C)_{PT,S}$ is its ^{12}C and ^{13}C atom fraction, respectively, and $M(^{12}C)$ and $M(^{13}C)$ the molar weight (mg mol^{-1}) of ^{12}C and ^{13}C.

$$m^E(^{13}C)_{MB}[mg] = \frac{x^E(^{13}C)_{MB} \cdot m_S \cdot c(C)_{MB} \cdot M(^{13}C)}{x(^{12}C)_{MB} \cdot M(^{12}C) + x(^{13}C)_{MB} \cdot M(^{13}C)} \quad (2)$$

, where m_S is the mass of soil (in mg dry weight) and $c(C)_{MB}$ is the microbial biomass (MB) C concentration (fraction of total soil dry weight). The latter was assessed by elemental analysis of the fumigated vs. non-fumigated CFE extracts, applying a conversion factor of 0.45, as suggested by Joergensen (1996).

$$m^E(^{13}C)_{SR}[mg \cdot day^{-1}] = \frac{x^E(^{13}C)_{SR} \cdot F(C)_{SR} \cdot M(^{13}C)}{x(^{12}C)_{SR} \cdot M(^{12}C) + x(^{13}C)_{SR} \cdot M(^{13}C)} \quad (3)$$

, where $F(C)_{SR}$ is the soil respiration (SR) rate (in mg C day^{-1}) extrapolated to 24 hours.

The cumulative loss of ^{13}C by soil respiration (in mg) was estimated by the integral of the curve fits, for the three measured pots separately. To fit the curve in the PL experiment, we used the model proposed by Warembourg & Estelrich (2000). The increase at the beginning was described by a logarithmic function and the decline of the signal after the label peak with an exponential function. In the CL experiment we used a logistic function to fit the curve, as described below.

2.5 Tracing ^{13}C to assess C dynamics

2.5.1 Description of the ^{13}C distribution

The dynamics of ^{13}C recovered after PL in the plant-soil compartments are characterized by three phases (Fig. 1a). An initial lag phase (no detectable signal), a phase dominated by the import of ^{13}C from other compartments, until a maximum label strength is reached (peak) and a phase of net ^{13}C export (exponential decay), controlled by ^{13}C transfer to other compartments and respiratory losses. Thus the import versus export of ^{13}C determines the shape of the signal peak (as discussed in Epron et al., 2012).

There is no consistent approach to describe the ^{13}C dynamics in the plant-soil system during CL (of pre-existing plants). Warembourg and Estelrich (2000) used a logarithmic function to describe the tracer dynamics in experiments with different labelling durations. However, when plants were exposed continuously to the label, they observed sigmoidal-shaped curves. We tested the logistic and the logarithmic curve fit on our ^{13}C mass excess data. In all plant-soil compartments the logistic model yielded a better fit than the logarithmic model and it proved to be quite robust (Supplement). Therefore we applied a logistic function to describe the tracer dynamics within plant-soil compartments during CL experiments.

Logistic growth functions have their origin in ecology (population growth), but they have also been used to describe the accumulation of specific compounds and nutrients in plant tissues (e.g in Bonvehi et al., 1997; Moustakas & Ntzanis, 2005; Iwahashi et al., 2012; Gutierrez-Gonzalez et al., 2013). As after pulse labelling, three phases can be distinguished (Fig. 1b), which represent the development towards homogeneously labelled C pools. The initial lag phase reflects the ^{13}C transfer time, i.e. the time needed for the ^{13}C to be transported from the chloroplast to the particular plant-soil compartment, analogous to the lag phase in the PL. A phase of exponential (net) ^{13}C

accumulation follows thereafter, which slows down after the inflection point, due to increased labelling of the C export (respiratory losses, transfer to other compartments). In the final stage (stationary phase) the C import and export are homogeneously labelled, i.e. the ^{13}C, which is introduced into the compartment, is in equilibrium with the ^{13}C exported. If the system is in a non-steady state, the stationary phase would only be temporary. E.g. during plant growth, the amount of ^{13}C would steadily increase after the steady state (second accumulation phase, Fig. 1b).

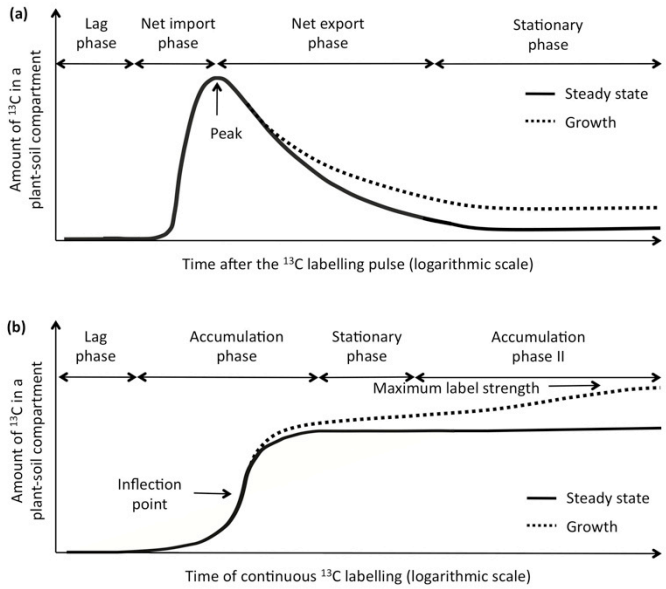

Fig. 1. Visualisation of the ^{13}C dynamics expected in plant-soil compartments after pulse labelling (a) or during continuous labelling (b) given for a system at steady state or at growth (change in pool size). The short-term dynamics can be described by three phases: (1) lag phase (time needed for C transfer), (2) phase dominated by ^{13}C import or net accumulation and (3) phase dominated by ^{13}C export or stationary phase (equilibrium between ^{13}C import and export). On the long-term a forth phase can be identified, which is characterized by stationary (pulse labelling) or increasing (continuous labelling) ^{13}C contents.

2.5.2 C transfer time and C partitioning

The speed of C transfer is usually assessed by the first significant ^{13}C signal detection ("lag time"), but the period to the maximum has also been used as indicator for the C transfer time in PL studies (Kuzyakov and Gavrichkova, 2010). We used the lag time to assess the minimum transfer time of fresh assimilates from the leaves to other plant-soil compartments. The mean transfer times of C within the plant-soil compartments were estimated by the time of the signal peak (PL) or the time of inflection (CL) minus the lag phase (which was negligible in this study with small tree seedlings). The mean C transfer time reflects the time needed until the majority of the labelled compounds are transferred into a plant or soil compartment and the export of the labelled compounds gains importance.

The C partitioning was assessed with both techniques by the relative ^{13}C distribution within the different plant-soil compartments at each sampling date. The fraction of ^{13}C within the leaf, petiole, stem, cutting, root and microbial biomass (in %) was calculated as total amount of ^{13}C in the compartment, relative to the sum of ^{13}C in all compartments. The belowground C partitioning was estimated analogously, for roots, microbial biomass and cumulative respiratory C loss. The bulk soil was excluded due to the lack of significant signal detection. The effect of sampling date and labelling technique on the estimation of C partitioning was tested with a two-way ANOVA (R statistics, R Core Team, 2013). Thus the C partitioning reflects the amount of C from fresh assimilates remaining in a plant-soil compartment relative to the amount within the other compartments (and does not refer to a proportion of net C assimilation allocated into a plant tissue or soil compartment). As an alternative to assessing C partitioning, we tested the use of the ^{13}C peak amount (PL) and the amount of ^{13}C at the stationary level (CL) for the calculation of the relative ^{13}C distribution between the single plant-soil compartments.

2.5.3 C residence time

The mean C residence time (MRT) is the time that a carbon atom remains on average in a compartment and is defined as the ratio of the holding capacity (pool size) and the (net) C flux through the pool. The MRT is assessed in tracer studies by measuring the changes in the label strength in a pool over time and deducing C fluxes by mathematical models fitted to the data points. We used R statistics (R Core Team, 2013) to fit the models by nonlinear least squares (function "nls"). The MRT was calculated as the inverse of the rate constant (MRT = 1/k) of the exponential model (Eq. 4) and the logistic model (Eq. 5) in the PL and CL, respectively. Thus, the rate constant in the PL is based only on the ^{13}C efflux, while in CL it is based on the net ^{13}C flux, making the latter more reasonable to estimate the C residence time as defined above. However, both models are only valid to describe one kinetic pool, with constant pool size (steady state) and proportional fluxes (first order kinetics).

$$y = a \cdot e^{-k(t-b)} \tag{4}$$

where a is the amount of ^{13}C at the peak measured, k is the rate constant of the tracer loss after the label peak (Fig. 1a, export phase), t is the time after labelling and b is time when the peak was detected.

$$y = \frac{a}{1 + e^{-k(t-b)}} \tag{5}$$

where a is the amount of ^{13}C at the stationary level (Fig. 1b), k is the rate constant of the ^{13}C accumulation, t is the time of labelling and b is the time at the inflection point.

In addition we used the duration of the accumulation phase (CL) as an indicator for the C residence time. It is the time needed (after the time lag) to reach equilibrium between the ^{13}C import and export (Fig. 1b). The length of the accumulation phase was assessed by the time the derivative of the logistic curve (mg ^{13}C day^{-1}) was less than 1 % of the stationary level.

3 Results and discussion

3.1 ^{13}C detection and distribution

Table 1. $\delta^{13}C$ signal detection in the plant-soil compartments. $\delta^{13}C$ values ± one standard deviation (in ‰) of the plant tissues, microbial biomass, soil organic matter (SOM) and the soil respiration are indicated for the five sampling dates (in days after the pulse or during the continuous labelling). * indicates a significant enrichment in ^{13}C (t-test, $P < 0.05$) compared to the natural isotopic background (sampling date 0 days).

Plant-soil compartment	Pulse labelling sampling dates [days]				
	0	0.1	1	2	8
Leaves	-29.8 (±0.8)	926.4* (±161.4)	548.0* (±76.4)	419.4* (±60.3)	276.2* (±41.0)
Petioles	-31.0 (±0.5)	408.2* (±85.2)	405.5* (±46.9)	371.9* (±61.0)	275.3* (±40.4)
Stems	-30.8 (±0.1)	418.8* (±90.5)	461.3* (±54.0)	480.3* (±58.1)	331.0* (±66.0)
Cuttings	-30.2 (±0.5)	-26.7* (±1.5)	-22.5* (±2.0)	-22.9* (±2.8)	-25.5 (±3.3)
Roots	-30.5 (±1.6)	-21.2 (±5.2)	210.3* (±79.3)	232.4* (±25.7)	142.4* (±53.6)
Microbial biomass	-24.6 (±0.2)	-24.4 (±0.3)	-23.4 (±0.9)	-23.7* (±0.4)	-24.3 (±0.3)
SOM	-27.5 (±0.0)	-27.7 (±0.0)	-27.6* (±0.0)	-27.6 (±0.1)	-27.5 (±0.2)
Soil respiration	-27.8 (±1.3)	-11.2 (±9.2)	556.7 (±283.1)	326.9* (±104.3)	21.6* (±16.1)
Plant-soil compartment	**Continuous labelling sampling dates [days]**				
	0	**1**	**2**	**8**	**14**
Leaves	-30.6 (±0.1)	263.0* (±38.3)	283.6* (±77.4)	984.5* (±228.4)	1122.6* (±140.6)
Petioles	-32.8 (±0.2)	163.9* (±56.2)	212.8* (±75.2)	908.5* (±277.3)	941.9* (±292.7)
Stems	-31.4 (±0.6)	209.6* (±84.2)	281.3* (±87.6)	1093.7* (±402.2)	1119.9* (±367.6)
Cuttings	-31.2 (±0.3)	-27.0* (±1.6)	-26.9 (±1.9)	-14.6 (±15.8)	-14.5* (±2.1)
Roots	-30.8 (±0.7)	98.1* (±12.5)	90.8 (±62.9)	646.5 (±335.1)	618.0 (±310.9)
Microbial biomass	-24.7 (±0.1)	-24.1 (±0.4)	-24.0 (±0.4)	-21.1 (±4.1)	-22.4 (±1.5)
SOM	-28.0 (±0.1)	-27.9 (±0.0)	-27.8 (±0.2)	-27.5 (±0.5)	-27.5* (±0.2)
Soil respiration	-27.5 (±0.8)	96.0 (±71.7)	148.4 (±71.6)	504.5 (±280.6)	491.5* (±160.2)

The fresh plant tissues (leaves, petioles, stems, roots) were enriched in ^{13}C by hundreds of per mil $\delta^{13}C$ in both experiments (Table 1), indicating a substantial assimilation and incorporation of ^{13}C. The variability of total ^{13}C assimilated was quite high between the plant replicates, reducing the significance of the isotopic enrichments measured. In the compartments with a large C pool (cuttings, microbial biomass, soil organic matter), the increase in $\delta^{13}C$ signal was only a few per mil and it was mostly not statistically significant. The signal strength of the labelled assimilates was diluted by mixing with the present carbon pool, and in case of the PL, additionally by new unlabelled assimilates

transferred to the plant-soil compartment, resulting in isotopic enrichments close to the IRMS detection limit in large C pools.

The expression of mass excess ^{13}C (Fig. 2) takes into account the present pool size and demonstrates the total amount of ^{13}C distributed in the plant-soil system. After pulse labelling, the leaves showed the highest peak in ^{13}C (13.7 ± 2.1 mg), followed by the stems (3.2 ± 0.9 mg), the cuttings (0.9 ± 0.2 mg), the petioles (0.7 ± 0.2 mg) and the roots (0.4 ± 0.1 mg). Even in the microbial biomass a small label peak could be observed (0.02 ± 0.01 mg) in parallel to the peak in the soil $^{13}CO_2$ efflux (0.39 ± 0.22 mg day^{-1}). The same distribution pattern was detected in the continuous labelling experiment. After 14 days of labelling 19.6 ± 5.8 mg ^{13}C was recovered in the leaves, 7.7 ± 3.5 mg in the stems, 2.0 + 0.7 mg in the petioles, 1.5 + 0.5 mg in the cuttings, 0.8 ± 0.5 mg in the roots, 0.05 ± 0.03 in the microbial biomass and 0.32 ± 0.11 mg ^{13}C day^{-1} was respired belowground.

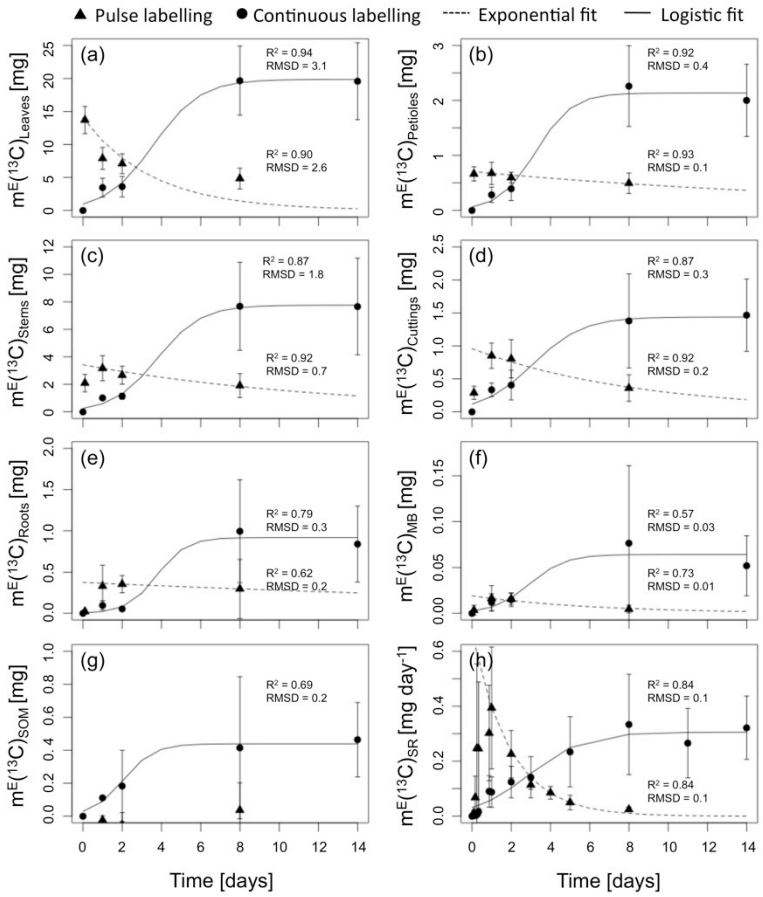

Fig. 2. Dynamics in the ^{13}C distribution. ^{13}C label recovered after the pulse and during the continuous exposure of the plants to $^{13}CO_2$ in leaves (a), petioles (b), stems (c), cuttings (d), roots (e), microbial biomass MB (f), soil organic matter SOM (g) and in the soil respiration SR (h) expressed as mass of ^{13}C in excess m^E [mg ^{13}C and mg ^{13}C day^{-1}]. Error bars indicate ± one standard deviation of the three plant individuals. The best fits (nonlinear least squares) are given for the exponential function after pulse labelling and for the logistic increase during continuous labelling. The coefficient of determination (R^2) and the root-mean-square-deviation (RMSD) were calculated with the individual measurement points. A sensitivity analysis of the logistic model fit can be found in the Supplement.

3.2 C transfer time

The soil respiration was significantly enriched in ^{13}C within five hours after pulse labelling and nine hours after the continuous labelling started. Such a fast minimum C transfer time from the leaves to the soil has already been reported for young poplars (Horwath et al., 1994) and other tree seedlings (Barthel et al., 2011; Pumpanen et al., 2008). The individual plant-soil compartments were enriched in ^{13}C already on the first sampling date. Hence we missed the lag time to the specific compartments due to the low sampling frequency of the destructive harvests. The delay in the signal detection in the CL compared to the PL is due to the weaker label strength of the fresh assimilates (10 atom% vs. 99 atom% ^{13}C in the PL). The same amount of labelled assimilates transferred into a compartment yields a lower signal in the CL than in the PL and as a result more time is needed until the lower detection limit is reached. The minimum C transfer times measured by the PL and CL technique are therefore not directly comparable.

Table 2. Parameters (a, b, k) of the exponential and the logistic model used to describe the ^{13}C dynamics in the pulse (PL) and continuous (CL) labelling, respectively. Parameter a is the total amount of ^{13}C [mg] at the signal peak (PL) or at the stationary level (CL), parameter b marks the time of the signal peak (PL) or the time of inflection (CL) and parameter k is the rate constant describing the decrease (PL) and increase (CL) of the ^{13}C abundance in a compartment, which is the basis for the mean residence time (MRT) calculation.

	Pulse labelling, exponential model				**Continuous labelling, logistic model**				
Plant-soil compartment	Peak, amount [mg ^{13}C (fraction of total)] **(a)**	Peak, time [days] **(b)**	Rate constant **(k)**	MRT [days] **(1/k)**	Stationary level, amount [mg ^{13}C (fraction of total)] **(a)**	Inflection, time [days] **(b)**	Rate constant **(k)**	MRT [days] **(1/k)**	Stationary level, time [days]
Leaves	13.70 (73 %)	0.1	0.286	3.5	19.85 (62 %)	3.6	0.83	1.2	7.2
Petioles	0.68 (4 %)	1	0.047	21.1	2.14 (7 %)	3.3	1.08	0.9	6.5
Stems	3.17 (17 %)	1	0.077	13.0	7.76 (24 %)	3.8	0.89	1.1	7.6
Cuttings	0.85 (5 %)	1	0.118	8.5	1.44 (4 %)	3.1	0.78	1.3	6.2
Roots	0.35 (2 %)	2	0.029	34.0	0.92 (3 %)	3.8	1.33	0.8	7.6
Microbial biomass	0.02 (0 %)	1	0.179	5.6	0.06 (0 %)	2.9	1.10	0.9	5.9
SOM					0.44	2.1	1.29	0.8	4.2
Soil respiration	0.39	1	0.520	1.9	0.31	2.9	0.73	1.4	5.9

The mean transfer times (Table 2, parameter b) were two days shorter in the PL (0-2 days) than in the CL experiment (2-4 days). In the PL experiment, the mean transfer time increased with the distance to the assimilating leaves, e.g. it was one day in the aboveground plant tissues and two days in the roots. Thus the mean transfer time assessed by the label peak in PL reflects mainly the minimum transfer time of the labelled assimilates from the leaves to the other plant-soil compartments, due to a preferential labelling of labile compounds with PL (Meharg, 1994). By contrast, the mean transfer times assessed by CL are the shortest in the belowground soil

compartments (SOM, microbial biomass) and the longest in the stems, roots and leaves, which are the plant organs known to store most C (Barbaroux et al., 2003). This indicates that continuous labelling leads to a more homogeneous labelling, including transient C storage pools, extending the mean transfer time by two days compared to the observation in the PL experiment. Thus the mean transfer time assessed by the inflection point in the CL experiment is rather an indicator for the C transfer through the compartment (short-term C cycling) than into the compartment (C transfer from other tissues).

3.3 C partitioning

The patterns of the relative ^{13}C distribution within the plant-soil compartments obtained by the two labelling techniques were similar throughout and equivalent at the end of the experiments (Table 3). The differences in the proportion of C allocated into the plant-soil compartments at the specific sampling dates were up to 6.6 % between the two labelling techniques (Table 3), as for example in the leaves and stems at sampling date one. However, the only significant difference observed was a slightly higher allocation to the petioles (+0.2-1.7 %) and to the microbial biomass (+0.1 %) with CL compared to PL. The results of the last destructive sampling reveal that most of the assimilated C remained in the leaves (62.5 ± 0.5 %), followed by the stems (23.4 ± 0.1 %), petioles (6.3 ± 0.1 %), cuttings (4.7 ± 0.1 %), roots (2.9 ± 0.6 %) and microbial biomass (0.1 ± 0.1 %). Thus the bigger part (> 90 %) of net assimilated C was recovered in the aboveground plant tissues. We assume that the dominant allocation into leaf biomass was promoted by the low light availability in the climate chambers, which was limiting for C assimilation, and by the high soil water and nutrient availability in the pots, reducing the need for root production. Increased shoot vs. root allocation has been observed in poplar trees grown under high N and water availability (Coleman et al., 2004; Pregitzer et al., 1990) or under light limitation in the understory (Landhäusser and Lieffers, 2001) before.

The time of sampling had, like the labelling approach, a minor effect on the results of the C partitioning in the plant-soil compartments (Table 3). Between the sampling on the first day and day eight, a significant difference was observed in the petioles (+1.4 %) and the cuttings (-2.3 %), but the changes in all other plant-soil compartments were not significant. In contrast, the C partitioning observed directly after PL (0.1 days) was largely different. The allocation into the leaves was overestimated by approximately 20 % compared to the following sampling dates. Similarly, a trend of increased C allocation into the leaves (by 5 %) at the early sampling dates can be observed in the CL

experiment. The overestimation of the C allocation to leaves within the first days of labelling or directly after pulse labelling is due to the time lag in tracer distribution. As shown in the previous section, the mean ^{13}C transfer time from leaves to roots was two days in the PL, and the data from the CL indicates, that a steady state between tracer import and export in the plant compartments was reached approximately after six days (discussed in the next section).

Table 3. Estimation of C partitioning between plant and soil compartments indicated by the relative ^{13}C distribution (in %) and for the different sampling dates after pulse and during continuous labelling (± one standard deviation is indicated in brackets). The effects of labelling technique ("labelling") and sampling date ("sampling") were tested for the sampling dates in common (1, 2 and 8 days) by two-way analysis of variance (ANOVA). No significant interaction effect was detected between the independent variables. The significance levels indicated are $P < 0.05$ (*) and $P < 0.01$ (**).

Plant-soil compartment	Pulse labelling, sampling dates [days]				Continuous labelling, sampling dates [days]				Significance level P (Sampling date 1, 2, 8)	
	0	1	2	8	1	2	8	14	Labelling	Sampling
Leaves	81.9 (±2.0)	61.2 (±3.1)	61.6 (±1.9)	62.2 (±4.2)	67.8 (±4.3)	65.4 (±3.7)	62.3 (±4.6)	62.9 (±3.9)	0.053	0.317
Petioles	4.0 (±0.4)	5.2 (±0.7)	5.2 (±0.5)	6.3 (±0.1)	5.4 (±0.8)	6.9 (±0.5)	7.1 (±0.1)	6.4 (±0.5)	0.014 (*)	0.006 (**)
Stems	12.3 (±1.8)	24.4 (±4.1)	23.2 (±2.5)	23.5 (±3.8)	17.8 (±5.8)	19.0 (±4.8)	23.4 (±2.9)	23.4 (±3.7)	0.064	0.253
Cuttings	1.7 (±0.3)	6.6 (±0.3)	6.8 (±1.2)	4.6 (±1.7)	6.9 (±1.5)	7.3 (±2.1)	4.2 (±1.0)	4.7 (±0.9)	0.875	0.003 (**)
Roots	0.1 (±0.1)	2.4 (±1.4)	3.0 (±0.3)	3.4 (±3.1)	1.9 (±0.8)	1.1 (±0.6)	2.8 (±1.2)	2.5 (±0.8)	0.184	0.215
Microbial biomass	0.0 (±0.0)	0.1 (±0.1)	0.1 (±0.0)	0.1 (±0.0)	0.2 (±0.1)	0.3 (±0.2)	0.2 (±0.2)	0.2 (±0.1)	0.032 (*)	0.438

To assess the belowground C partitioning, the time of sampling is of much greater importance (Table 4). At the end of the experiments, 13.3 ± 1.3 % of the ^{13}C recovered was detected belowground. Most of it was released as CO_2 (81.2 ± 0.9 %), and a small amount remained in the root (18.0 ± 0.3 %) and microbial biomass (0.7 ± 0.6 %). The results obtained at a specific sampling date are similar for the two labelling techniques, except for the generally higher proportion of ^{13}C detected in the microbial biomass with CL. However, the results at the different sampling dates were very distinct. At the early sampling dates, the estimated C allocation to roots was more expressed or even dominating (43-75 % in the PL and 31-65 % in the CL). This might be due a time lag in the tracer distribution at the plant-soil interface. As discussed above, the first labelled assimilates were detected belowground within a few hours. However, much more time (6-8 days) was needed to reach an equilibrium (stationary state) in the belowground C fluxes (Table 2). This is in line with the one week allocation time proposed by Warembourg & Estelrich (2000) and the time delay of 5-6 days in the steady labelling of root exudation observed by Thornton et al. (2004). Accordingly, a time lag between the

label strength in the roots and the rhizomicrobial respiration might have caused the underestimation of the proportion of respired C to total belowground C at the beginning of the experiment.

Table 4. Estimation of belowground C partitioning indicated by the relative ^{13}C distribution (in %) between belowground pools and fluxes measured at different sampling dates after pulse and during continuous labelling (± one standard deviation is indicated in brackets). The effects of labelling technique ("labelling") and sampling date ("sampling") were tested for the sampling dates in common (1, 2 and 8 days) by two-way analysis of variance (ANOVA). No significant interaction effect was detected between the independent variables. The significance levels indicated are $P < 0.05$ (*) and $P < 0.01$ (**).

Belowground C pool / flux	Pulse labelling, sampling dates [days]				Continuous labelling, sampling dates [days]				Significance level P (Sampling date 1, 2, 8)	
	0	1	2	8	1	2	8	14	Labelling	Sampling
Roots	74.8 (±21.5)	57.2 (±1.7)	42.5 (±9.9)	17.8 (±11.9)	64.7 (±13.5)	31.0 (±9.2)	35.0 (±10.4)	18.2 (±5.4)	0.523	0.004 (**)
Microbial biomass	15.0 (±22.4)	2.7 (±0.5)	1.9 (±0.9)	0.3 (±0.2)	7.2 (±3.7)	8.6 (±5.7)	2.4 (±11.0)	1.2 (±5.2)	0.005(**)	0.019 (*)
Soil respiration	10.2 (±13.5)	40.1 (±2.2)	55.6 (±10.8)	81.9 (±12.0)	28.1 (±12.7)	60.4 (±11.5)	62.6 (±11.0)	80.6 (±5.2)	0.208	0.001 (**)

Another way to estimate the C partitioning between the plant-soil compartments independent of the sampling time, is the use of the amount of ^{13}C at the label peak or the stationary level, i.e. by the parameter "a" of the exponential and logistic model, respectively (Table 2). The estimation in the CL matches the above-mentioned average values of C partitioning. The differences are less than 1 % in the compartments. But the results of the relative amount at the label peaks in PL overestimate the allocation to the leaves (73.0 %) and underestimate the allocation to petioles (3.6 %) and stems (16.9 %). This might be due to a lack in label peak detection. The leaves were sampled directly after labelling, while the next sampling date was one day later. The peak in the petioles and stems might have occurred in between and thus the peak amount could have been underestimated.

3.4 C residence time

The estimates of the mean residence time (MRT) assessed by the rate constant (k) of the exponential and logistic function (Fig. 2) of the PL experiment are higher than the one of the CL experiment (Table 2). In the PL experiment, the longest MRT was detected in roots (34 days), then the MRT decreased in the order of petioles (21 days), stems (13 days), cuttings (9 days), microbial biomass (6 days) and leaves (3 days). These residence times are in the range of values reported in literature. For example, mean residence times of 16-41 days have been reported for fine roots (Keel et al., 2012), 3.2 days for the total microbial biomass (Yevdokimov et al., 2007) and 2.4 days for leaves of beech

seedling (Ruehr et al., 2009). In the CL experiment, the MRTs were around one day in all plant-soil compartments. The cuttings, leaves and stems had the highest MRT (1.1-1.3 days), followed by the petioles and microbial biomass (0.9 days) and the lowest MRTs were detected in the roots and SOM (0.8 days).

The large differences in the MRTs obtained by the two labelling techniques are probably due to the strong assumptions of the simple exponential and logistic models applied, which do not match reality. The mathematical models applied describe the dynamics in a single pool, whereas plant tissues and the soil organic matter consist of several C pools (e.g. labile and structural). Investigating the C allocation and turnover in specific plant or soil C pools requires a more complex modelling (e.g. as in Kuzyakov et al., 1999; Street et al., 2011; Streit et al., 2012).

One assumption of the simple exponential decay and logistic growth model is constant pool size (steady state). In this study, as in many other labelling studies with young plants, the plant-soil system was not at a steady state, but characterized by plant growth. Under such conditions the accumulation of ^{13}C in the structural pool is enlarged and the ^{13}C export (detected by the decay model in PL studies) is reduced (Figure 1a). This leads to an underestimation of the decline rates and thus to an overestimation of the MRTs assessed by the PL technique (results of a model including a non-zero asymptote to account for growth are given in the Supplement). The logistic model of the CL technique is more robust regarding the steady state assumption, since the whole transition and not only the export phase is analysed. However, if the system is not at steady state, the rate constant tends to be overestimated and consequently the MRT underestimated (Supplement).

Another assumption of the exponential decay model of the PL technique is that the dynamics are governed by ^{13}C efflux, but it has been shown that remobilisation of stored ^{13}C is leading to ^{13}C influx even after the signal peak (Barthel et al., 2011; Endrulat et al., 2010; Epron et al., 2011). This is particularly relevant for compartments, which are farther away from the assimilating leaves and are characterized by a broad label peak (e.g. in roots, microbial biomass). The prolonged import of ^{13}C even after the signal peak leads to the underestimation of the decline rate. Therefore we can assume that especially the MRTs of the belowground compartments are overestimated with the PL technique.

As an alternative to the rate constant (k), the length of the accumulation phase (in the CL) can be used to estimate the mean C residence time (Fig. 1b). It reflects the time between first label appearance and steady state of the ^{13}C import and export of a compartment. In the present study this residence time was 4-8 days in the different

plant-soil compartments (Table 2). The longest residence time was estimated for the roots and stems (7.6 days), followed by the leaves (7.2 days), petioles (6.5 days), cuttings (6.2 days), microbial biomass and soil respiration (5.9 days) and in the SOM (4.2 days). We think that this estimation of the C residence time is the most reasonable, since it is not based on the assumptions described above. However, we would expect a longer residence time in the SOM than in the microbial biomass. The poor estimation of the SOM MRT is caused by the low enrichment detected, which was close to the detection limit and therefore not significant.

3.5 Comparisons of techniques

The pulse labelling technique is most suitable to detect the minimum C transfer time from the leaves to the roots. The complete labelling of the fresh assimilates facilitates a fast signal detection in the plant compartments. However, the amount of assimilates labelled during the relatively short labelling period is not sufficient to achieve a detectable signal in large C pools, such as the soil organic matter. Consequently the investigation of C partitioning and C residence time is restricted to those pools, which allow a clear signal detection (e.g. at least twice the magnitude of the background noise). A further disadvantage of the pulse labelling technique is, that the key parameter to consider is the decline of the ^{13}C signal. Thus the estimation of C allocation is based on what remains in a compartment (and not on what is allocated to it). The calculation of the mean residence time by simple exponential or logistic models are based on the assumption that the system is at steady state, but such conditions hardly exist in nature. Thus the calculation of the mean residence time based on the rate constant of the exponential model provides at best an approximation (as it is the case for the logistic model in continuous labelling experiments).

Continuous labelling labels the compounds not as strongly, but for longer durations and more homogeneously. Therefore this technique has the potential to detect ^{13}C dynamics (allocation priorities) in all plant-soil compartments, and can be applied to determine even large C pools. The parameters of the logistic model used to describe the tracer dynamics lead to more specific information on C cycling. The time lag is an indicator for the minimum transfer time, however its assessment is poorer than with the PL technique. The time of inflection (minus the lag time) marks the mean C transfer time through a compartment and thus illustrates the short-term C cycling including transient storage pools. The length of the accumulation phase is an indicator for the mean C residence time in a compartment and the level of the steady state reflects the amount of C allocated into it.

4 Conclusions

The C transfer time, C partitioning and C residence time can be assessed with both labelling techniques. The results of the C transfer time of fresh assimilates from the leaves, through the plant and to the belowground compartments are not comparable for the two techniques. Pulse labelling is better suited to assess the minimum transfer time. However, PL is restricted to small C pools, due to the dilution of the tracer signal in large C pools.

The plant-soil C partitioning pattern obtained by the PL and CL technique are comparable, but the time of sampling is crucial. One has to account for the time lag in C transfer from the leaves to other compartments and for the residence time of the C within them. In the current study on young poplar trees, 4-8 days were required for the homogeneous labelling of the ^{13}C import and export in order to obtain consistent results of C partitioning.

The simple exponential and logistic models used to assess the C mean residence times are based on assumptions of constant pool size and proportional fluxes. These assumptions are, as in this study, often not appropriate. The logistic model (accumulation phase) is better suited to obtain estimates of the mean residence time in systems at non-steady state (e.g. during plant growth). The application of the logistic model to describe the distribution of the ^{13}C in continuous labelling studies would have to be further evaluated in new experiments and in existing data sets.

Acknowledgements

This study was funded by the Swiss National Science Foundation (project number 135233). We thank the members of the Soil Science and Biogeochemistry (University of Zurich, UZH) and of the Ecosystem Fluxes (Paul Scherrer Institute, PSI) research group for valuable discussions. Especially we thank I. Lötscher (PSI), I. Woodhatch (UZH), R. Maier (UZH) and R. Künzli (DMP Ltd) for technical assistance.

References

Amelung, W., Brodowski, S., Sandhage-Hofmann, A. and Bol, R.: Combining biomarker with stable isotope analyses for assessing the transformation and turnover of soil organic matter, Adv. Agron., 100, 155–250, 2008.

Barbaroux, C., Bréda, N. and Dufrêne, E.: Distribution of above-ground and below-ground carbohydrate reserves in adult trees of two contrasting broad-leaved species (*Quercus petraea* and *Fagus sylvatica*), New Phytol., 157, 605–615, 2003.

Barthel, M., Hammerle, A., Sturm, P., Baur, T., Gentsch, L. and Knohl, A.: The diel imprint of leaf metabolism on the $\delta^{13}C$ signal of soil respiration under control and drought conditions, New Phytol., 192, 925–938, 2011.

Bonvehi, J. S., Jorda, R. E. and Jaen, J. A.: The ripening process of kiwifruits (*Actinidia deliciosa*) grown in Catalonia, Spain, J. Food Quality, 20, 371–380, 1997.

Bowling, D. R., Pataki, D. E. and Randerson, J. T.: Carbon isotopes in terrestrial ecosystem pools and CO_2 fluxes, New Phytol., 178, 24–40, 2008.

Brand, W. A. and Coplen, T. B.: Stable isotope deltas: tiny, yet robust signatures in nature, Isot. Environ. Healt. S., 48, 393–409, 2012.

Brüggemann, N., Gessler, A., Kayler, Z. E., Keel, S. G., Badeck, F.-W., Barthel, M., Boeckx, P., Buchmann, N., Brugnoli, E., Esperschütz, J., Gavrichkova, O., Ghashghaie, J., Gomez-Casanovas, N., Keitel, C., Knohl, A., Kuptz, D., Palacio, S., Salmon, Y., Uchida, Y. and Bahn, M.: Carbon allocation and carbon isotope fluxes in the plant-soil-atmosphere continuum: a review. Biogeosciences 2011, 8, 3457–3489.

Coleman, M. D., Friend, A. L. and Kern, C. C.: Carbon allocation and nitrogen acquisition in a developing *Populus deltoides* plantation, Tree Physiol., 24, 1347–1357, 2004.

Coplen, T. B.: Guidelines and recommended terms for expression of stable-isotope-ratio and gas-ratio measurement results, Rapid Commun. Mass Sp., 25, 2538–2560, 2011.

Dawson, T. E., Mambelli, S., Plamboeck, A. H., Templer, P. H. and Tu, K. P.: Stable isotopes in plant ecology, Annu. Rev. Ecol. and Syst., 33, 507–559, 2002.

Endrulat, T., Saurer, M., Buchmann, N. and Brunner, I.: Incorporation and remobilization of ^{13}C within the fine-root systems of individual *Abies alba* trees in a temperate coniferous stand, Tree Physiol., 30, 1515–1527, 2010.

Epron, D., Bahn, M., Derrien, D., Lattanzi, F. A., Pumpanen, J. S., Gessler, A., Högberg, P., Maillard, P., Dannoura, M., Gérant, D. and Buchmann, N.: Pulse-labelling trees to study carbon allocation dynamics: a review of methods, current knowledge and future prospects, Tree Physiol., 32, 776–798, 2012.

Epron, D., Ngao, J., Dannoura, M., Bakker, M. R., Zeller, B., Bazot, S., Bosc, A., Plain, C., Lata, J. C., Priault, P., Barthes, L. and Loustau, D.: Seasonal variations of belowground carbon transfer assessed by in situ $^{13}CO_2$ pulse labelling of trees, Biogeosciences, 8, 1153–1168, 2011.

Esperschütz, J., Gattinger, A., Buegger, F., Lang, H., Munch, J. C., Schloter, M. and Winkler, J. B.: A continuous labelling approach to recover photosynthetically fixed carbon in plant tissue and rhizosphere organisms of young beech trees (*Fagus sylvatica* L.) using ^{13}C depleted CO_2, Plant Soil, 323, 21–29, 2009.

Glaser, B.: Compound-specific stable-isotope ($\delta^{13}C$) analysis in soil science, J. Plant Nutr. Soil Sc., 168, 633–648, 2005.

Grams, T. E. E., Werner, H., Kuptz, D., Ritter, W., Fleischmann, F., Andersen, C. P. and Matyssek, R.: A free-air system for long-term stable carbon isotope labeling of adult forest trees, Trees, 25, 187–198, 2010.

Gutierrez-Gonzalez, J. J., Wise, M. L. and Garvin, D. F.: A developmental profile of tocol accumulation in oat seeds, J. Cereal Sc., 57, 79–83, 2013.

Horwath, W. R., Pregitzer, K. S. and Paul, E. A.: ^{14}C allocation in tree-soil systems, Tree Physiol., 14, 1163–1176, 1994.

Iwahashi, M., Tachibana, Y. and Ohta, Y.: Accumulation of calcium, magnesium, potassium and sodium with growth of individual leaves, petioles and stems of cucumber plants, Soil Sci. Plant Nutr., 28, 441–449, 1982.

Joergensen, R.: The fumigation-extraction method to estimate soil microbial biomass: Calibration of the k^{EC} value, Soil Biol. Biochem., 28, 25–31, 1996.

Keel, S. G., Campbell, C. D., Högberg, M. N., Richter, A., Wild, B., Zhou, X., Hurry, V., Linder, S., Näsholm, T. and Högberg, P.: Allocation of carbon to fine root compounds and their residence times in a boreal forest depend on root size class and season, New Phytol., 194, 972–981, 2012.

Keel, S. G., Siegwolf, R. T. W. and Körner, C.: Canopy CO_2 enrichment permits tracing the fate of recently assimilated carbon in a mature deciduous forest, New Phytol., 172, 319–329, 2006.

Keeling, C. D.: The concentration and isotopic abundances of atmospheric carbon dioxide in rural areas, Geochim. Cosmochim. Ac., 13, 322–334, 1958.

Kuzyakov, Y. and Domanski, G.: Carbon input by plants into the soil. Review, J. Plant Nutr. Soil Sc., 163, 421–431, 2000.

Kuzyakov, Y. and Gavrichkova, O.: Time lag between photosynthesis and carbon dioxide efflux from soil: a review of mechanisms and controls, Glob. Change Biol., 16, 3386–3406, 2010.

Kuzyakov, Y., Kretzschmar, A. and Stahr, K.: Contribution of Lolium perenne rhizodeposition to carbon turnover of pasture soil, Plant Soil, 213, 127–136, 1999.

Landhäusser, S. M. and Lieffers, V. J.: Photosynthesis and carbon allocation of six boreal tree species grown in understory and open conditions, Tree Physiol., 21, 243–250, 2001.

Leake, J., Ostle, N., Rangelcastro, J. and Johnson, D.: Carbon fluxes from plants through soil organisms determined by field $^{13}CO_2$ pulse-labelling in an upland grassland, Appl. Soil Ecol., 33, 152–175, 2006.

Meharg, A. A.: A critical review of labelling techniques used to quantify rhizosphere carbon-flow, Plant Soil, 166, 55–62, 1994.

Moustakas, N. K. and Ntzanis, H.: Dry matter accumulation and nutrient uptake in flue-cured tobacco (*Nicotiana tabacum* L.), Field Crop Res., 94, 1–13, 2005.

Murage, E. and Voroney, P.: Modification of the original chloroform fumigation extraction technique to allow measurement of $\delta^{13}C$ of soil microbial biomass carbon, Soil Biol. Biochem., 39, 1724–1729, 2007.

Pataki, D. E.: The application and interpretation of Keeling plots in terrestrial carbon cycle research, Global Biogeochem. Cy., 17, 2003.

Pregitzer, K. S., Dickmann, D. I., Hendrick, R. and Nguyen, P. V: Whole-tree carbon and nitrogen partitioning in young hybrid poplars, Tree Physiol., 7, 79–93, 1990.

Pumpanen, J. S., Heinonsalo, J., Rasilo, T., Hurme, K.-R. and Ilvesniemi, H.: Carbon balance and allocation of assimilated CO_2 in Scots pine, Norway spruce, and Silver birch seedlings determined with gas exchange measurements and ^{14}C pulse labelling, Trees, 23, 611–621, 2008.

R Core Team: R: A Language and Environment for Statistical Computing, R Foundation for Statistical Computing [online] Available from: http://www.r-project.org, 2013.

Ruehr, N. K., Offermann, C. A., Gessler, A., Winkler, J. B., Ferrio, J. P., Buchmann, N. and Barnard, R. L.: Drought effects on allocation of recent carbon: from beech leaves to soil CO_2 efflux, New Phytol., 184, 950–961, 2009.

Street, L. E., Subke, J. A., Sommerkorn, M., Heinemeyer, A. and Williams, M.: Turnover of recently assimilated carbon in arctic bryophytes., Oecologia, 167, 325–37, 2011.

Streit, K., Rinne, K. T., Hagedorn, F., Dawes M.A., Saurer, M., Hoch, G., Werner, R. A., Buchmann, N. and Siegwolf, R. T. W.: Tracing fresh assimilates through *Larix decidua* exposed to elevated CO_2 and soil warming at the alpine treeline using compound-specific stable isotope analysis. New Phytol., 197, 838–849, 2012.

Thornton, B., Paterson, E., Midwood, A. J., Sim, A. and Pratt, S. M.: Contribution of current carbon assimilation in supplying root exudates of *Lolium perenne* measured using steady-state C labelling, Physiol. Plantarum, 120, 434–441, 2004.

Warembourg, F. R. and Estelrich, H. D.: Towards a better understanding of carbon flow in the rhizosphere: a time-dependent approach using carbon-14, Biol. Fert. Soils, 30, 528–534, 2000.

Werner, C., Schnyder, H., Cuntz, M., Keitel, C., Zeeman, M. J., Dawson, T. E., Badeck, F.-W., Brugnoli, E., Ghashghaie, J., Grams, T. E. E., Kayler, Z. E., Lakatos, M., Lee, X., Máguas, C., Ogée, J., Rascher, K. G., Siegwolf, R. T. W., Unger, S., Welker, J., Wingate, L. and Gessler, A.: Progress and challenges in using stable isotopes to trace plant carbon and water relations across scales, Biogeosciences, 9, 3083–3111, 2012.

Werner, R. A., Bruch, B. A. and Brand, W. A.: ConFlo III - an interface for high precision delta(13)C and delta(15)N analysis with an extended dynamic range, Rapid Commun. Mass Spec., 13, 1237–1241, 1999.

Werth, M. and Kuzyakov, Y.: ^{13}C fractionation at the root–microorganisms–soil interface: A review and outlook for partitioning studies, Soil Biol. Biochem., 42, 1372–1384, 2010.

Yevdokimov, I., Ruser, R., Buegger, F., Marx, M. and Munch, J.: Microbial immobilisation of ^{13}C rhizodeposits in rhizosphere and root-free soil under continuous ^{13}C labelling of oats, Soil Biol. Biochem., 38, 1202–1211, 2006.

Yevdokimov, I. V, Ruser, R., Buegger, F., Marx, M. and Munch, J. C.: Interaction between rhizosphere microorganisms and plant roots: ^{13}C fluxes in the rhizosphere after pulse labeling, Eurasian Soil Sci., 40, 766–774, 2007.

Supplementary material

A) Comparison of curve fits to describe the ^{13}C dynamics in the continuous labelling experiment

Table 1. Logarithmic versus logistic curve fit of the ^{13}C dynamics. Coefficients of determination (R^2) and root-mean-square-deviation (RMSD) of the logarithmic and logistic curve fit (non linear least squares) on the ^{13}C mass excess data assessed for the plant-soil compartments during the continuous labelling experiment.

Plant-soil compartment	Logarithmic fit		Logistic fit	
	R^2	RMSD	R^2	RMSD
Leaves	0.91	4.08	0.94	3.08
Petioles	0.88	0.52	0.92	0.39
Stems	0.84	2.20	0.87	1.79
Cuttings	0.85	0.40	0.87	0.35
Roots	0.73	0.36	0.79	0.29
MB	0.53	0.04	0.57	0.03
SOM	0.68	0.21	0.69	0.19
SR	0.67	0.12	0.70	0.11

B) Comparison two formulas to calculate the rate constant for the mean residence time estimation

Simple functions (steady state assumption):

$$y = a \cdot e^{-k(t-b)} \quad (1a)$$

where a is the amount of ^{13}C at the peak measured, k is the rate constant of the tracer loss after the label peak (Fig. 1a, export phase), t is the time after labelling and b is time when the peak was detected.

$$y = \frac{a}{1 + e^{-k(t-b)}} \quad (1b)$$

where a is the amount of ^{13}C at the stationary level (Fig. 1b), k is the rate constant of the ^{13}C accumulation, t is the time of labelling and b is the time at the inflection point.

Functions extended for non-steady state:

$$y = (a - c) \cdot e^{-k(t-b)} + c \qquad (2a)$$

where c is the non-zero asymptote

$$y = \frac{a + c \cdot t}{1 + e^{-k(t-b)}} \qquad (2b)$$

where c is the accumulation factor of the accumulation phase II (Manuscript Fig. 1b).

Table 2. Mean residence times [MRT] estimated by the exponential decay (pulse labelling) or logistic growth (continuous labelling) model under the assumption of steady state (simple exponential/logistic functions, Eq. 1a/b) or non-steady state (non-zero asymptote / accumulation phase II, Eq. 2a/b). As indicators of the model accuracy the coefficients of determination (R^2) and root-mean-square-deviation (RMSD) are given.

	MRT [days]		R^2		RMSD [mg]	
	Steady state	Non-steady state	Steady state	Non-steady state	Steady state	Non-steady state
a) Pulse labelling						
Leaves	3.5	1.0	0.90	0.97	2.6	1.5
Petioles	21.1	1.8	0.93	0.94	0.1	0.1
Stems	13.0	0.5	0.92	0.93	0.7	0.7
Cuttings	8.5		0.92		0.2	
Roots	34.0		0.62		0.2	
MB	5.6		0.73		0.01	
SOM						
SR	1.9	1.7	0.84	0.84	0.1	0.1
a) Continuous labelling						
Leaves	1.2	1.4	0.94	0.94	3.1	3.1
Petioles	0.9	1.2	0.92	0.93	0.4	0.4
Stems	1.1	1.4	0.87	0.88	1.8	1.8
Cuttings	1.3	1.1	0.87	0.87	0.3	0.3
Roots	0.8		0.79		0.3	
MB	0.9	1.2	0.57	0.60	0.03	0.03
SOM	0.8	0.7	0.69	0.69	0.2	0.2
SR	1.4	1.4	0.84	0.84	0.1	0.1

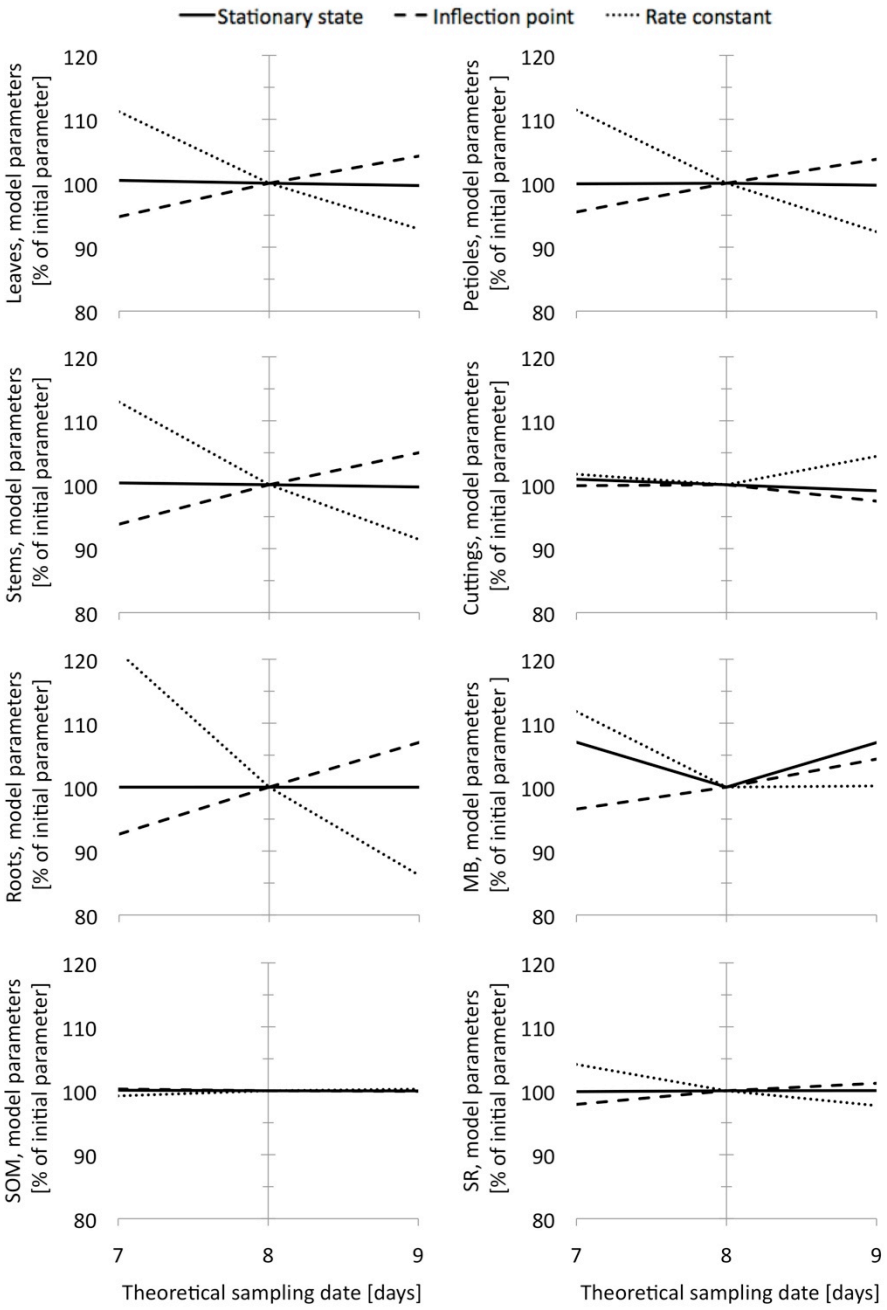

Fig. 1. Sensitivity analysis of the logistic model. The change in the model parameters stationary state, inflection point and rate constant are illustrated relative to the initial parameter at sampling date eight (given in %). The sensitivity analysis is based on the shift of the data point at day eight (see Figure 2) to day seven or nine and recalibration of the model.

Manuscript III 'Multi-isotope labelling'

Published as

Studer, M. S., Siegwolf, R. T. W., Leuenberger, M. and Abiven, S.: Multi-isotope labelling of organic matter by diffusion of $^{2}H/^{18}O$-H_2O vapour and ^{13}C-CO_2 into the leaves and its distribution in the plant, Biogeosciences, 12, 1865-1879, doi:10.5194/bgd-12-1865-2015, 2015.

Abstract

Isotope labelling is a powerful tool to study elemental cycling within terrestrial ecosystems. Here we describe a new multi-isotope technique to label organic matter (OM).

We exposed poplars (*Populus deltoids x nigra*) for 14 days to an atmosphere enriched in $^{13}CO_2$ and depleted in $^{2}H^{18}_2O$. After 1 week, the water-soluble leaf OM $\delta^{13}C$ = 1346 ± 162 ‰) and the leaf water were strongly labelled ($\delta^{18}O$ = - 63 ± 8 ‰, $\delta^{2}H$= - 156 ± 15 ‰). The leaf water isotopic composition was between the atmospheric and stem water, indicating a considerable back-diffusion of vapour into the leaves (58–69 %) in the opposite direction to the net transpiration flow. The atomic ratios of the labels recovered ($^{18}O/^{13}C$, $^{2}H/^{13}C$) were 2–4 times higher in leaves than in the stems and roots. This could be an indication of the synthesis of more condensed compounds in roots and stems (e.g. lignin vs. cellulose) or might be the result of O and H exchange and fractionation processes during phloem transport and biosynthesis.

We demonstrate that the three major OM elements (C, O, H) can be labelled and traced simultaneously within the plant. This approach could be of interdisciplinary interest in the fields of plant physiology, palaeoclimatic reconstruction or soil science.

1 Introduction

Artificial labelling with stable isotopes facilitates the observation of bio(geo)chemical cycling of elements or compounds with minor disturbance to the plant–soil systems. It has provided many insights into plant carbon allocation patterns (e.g. Simard et al., 1997; Keel et al., 2006; Högberg et al., 2008), water dynamics (e.g. Plamboeck et al., 2007; Kulmatiski et al., 2010) and soil OM processes (e.g. Bird and Torn, 2006; Girardin et al., 2009) in terrestrial ecosystems. Only a few studies have used labelling approaches with more than one stable isotope, for example, to study the interactions between the

carbon and nitrogen cycle (e.g. Bird and Torn, 2006; Schenck zu Schweinsberg-Mickan et al., 2010). However, to our knowledge, isotopic labelling of organic matter (OM) with its three major elements, carbon (C), oxygen (O) and hydrogen (H), has never been done in ecosystem studies before, even though combined ^{13}C, ^{18}O and ^{2}H analyses have been widely used to study plant physiological processes and to reconstruct past climatic conditions (Hangartner et al., 2012; Roden and Farquhar, 2012; Scheidegger et al., 2000; Werner et al., 2012). Similarly, artificial labelling with those isotopes would be useful not only to clarify basic mechanisms related to the plant water-use efficiency or the oxygen and hydrogen signals in tree rings but also to study other OM dynamics in the plant–soil system such as OM decomposition in the soil.

The C, O and H contents of OM have been applied to distinguish major groups of compounds by plotting the atomic ratios O/C and H/C in a van Krevelen diagram (Kim et al., 2003; Ohno et al., 2010; Sleighter and Hatcher, 2007). This approach is based on the distinct molecular composition of organic compounds. For example, the glucose molecule ($C_6H_{12}O_6$) is characterized by high O/C (= 1) and H/C (= 2) ratios and is the precursor of other compounds, such as cellulose $(C_6H_{10}O_5)_{[n]}$ O/C = 0.8, H/C = 1.7, Fig. 3a). Condensation or reduction reactions during biosynthesis lead to other compound groups with lower atomic ratios (e.g. lignin) or similar H/C but lower O/C ratios (e.g. lipids, proteins) compared to glucose. Following the logic of the van Krevelen diagram, we wanted to test whether we can use the isotopic ratios $^{18}O/^{13}C$ and $^{2}H/^{13}C$ of the labels recovered in plant–soil bulk materials after labelling the fresh assimilates with those stable isotopes in order to detect the utilization of the labelled assimilates for the synthesis of different OM compounds. With this multi-labelling approach we would gain information about the characteristics of the OM formed by simple isotopic analysis of bulk material. This has several advantages compared to compound-specific analysis, such as being much less laborious and less expensive and yielding integrated information on the bulk OM sampled.

In this study we added the ^{13}C, ^{18}O and ^{2}H labels via the gaseous phase in the plants' atmosphere (CO_2, water vapour). Pre-grown plants were exposed to the labelled atmosphere continuously for 14 days under laboratory conditions, and the labels added were traced in different plant compartments (leaves, petioles, new stems, stem cuttings, roots) and soil OM at different points in time. We applied a simple isotope mixing model to estimate the fraction of ^{18}O and ^{2}H that entered the leaf by diffusion from the atmosphere into the leaf intercellular cavities and plotted the atomic and isotopic ratios of the OM formed in van Krevelen diagrams to test whether the multi-isotope labelling approach can be used to detect changes in the OM characteristics.

2 Material and Methods

2.1 Plants and soil

The soil, a Cambisol, was sampled from the upper 15 cm in a beech forest (8° 33' E, 47° 23' N, 500 m elevation), coarse sieved (2.5 x 3.5 cm), and large pieces of hardly decomposed organic material were removed. The soil had a clay-loam texture, a pH of 4.8, an organic C content of 2.8% and a C/N ratio of 11. The plant pots (volume = 8.2 dm^3) were filled with 3018 ± 177 g soil (dry weight equivalent). Fifteen poplar seedlings (*Populus deltoids x nigra*, Dorskamp clone) were grown indoors from 20 cm long stem cuttings for 5 weeks before they were transferred into labelling chambers (described below). They were kept in the chamber for acclimatization for 1 week prior to labelling. At the beginning of the labelling experiments, the average dry weight of fresh plant biomass (without the original stem cutting) was 3.3 ± 0.1 g and the average total leaf area was 641 ± 6 cm^2 per plant. At the end of the experiment (last sampling) the dry weight was 5.4 ± 1.1 g and the total leaf area was 1354 ± 161 cm^2. The leaf area was measured with a handheld area meter (CID-203 laser leaf area meter, CID Inc.).

2.2 Labelling chamber, procedure and environmental conditions

The labelling chambers (MICE – Multi-Isotope labelling in a Controlled Environment – facility) provide a hermetical separation of the shoots (leaves, petioles and new stems) from the roots, rhizosphere and the soil. The plant shoots are enclosed by one large polycarbonate cuboid (volume 1.2 m^3) with a removable front plate and five 2 cm wide gaps in the bottom plate to slide in three plants in each row. Small polycarbonate pieces, Kapton tape and a malleable sealant (Terostat IX, Henkel AG & Co.) wrapped around the stem cuttings were used to seal off the upper from the lower chamber. The belowground compartments (soil and roots) are in 15 individual pots, which are hermetically sealed from the laboratory and aerated with outdoor air. This setup ensures that all plants receive the same labelling treatment and prevents the diffusion of labelled atmospheric gases into the soil.

The environmental conditions in the MICE facility are automatically controlled and monitored by a software programme (based on LabVIEW, National Instruments Switzerland Corp.), The software switches the light sources (xenon lamps, HELLA KGaA Hueck & Co) and different valves (3/2 way, Bürkert-Contromatic AG) on/off. The valves include or exclude instruments in a gas circuit attached to the upper chamber to

regulate the CO_2 and H_2O concentration, which is measured by an infrared gas analyser (LI-840, LICOR Inc.). The chamber air is fed by a vacuum pump (N 815, KNF Neuberger AG) through perforated glass tubes within a water reservoir to humidify the air or through a Peltier-cooled water condenser to dry the air (Appendix Fig. A1). Further, the chamber air can be fed through a Plexiglas tube filled with soda lime to absorb the CO_2, or CO_2 is injected from a gas cylinder.

The isotope labels (^{13}C, ^{18}O and ^{2}H) were added continuously for 14 days via gaseous phase to the plant shoots. We used CO_2 enriched in ^{13}C (10 at.% ^{13}C-CO_2, Cambridge Isotope Laboratories Inc.) as well as water vapour depleted in ^{18}O and ^{2}H ($\delta^{18}O$ = - 370 ‰ and $\delta^{2}H$ = - 813 ‰, waste product from enrichment columns at the Paul Scherrer Institute). Thus the labelled gases added were enriched by 8.90 at.% ^{13}C and depleted by 0.07 at.% ^{18}O and 0.01 at.% ^{2}H relative to the ambient air.

The soil moisture was maintained at 100% field capacity and the relative air humidity was 74% in order to promote the back-diffusion of water into the leaves. The light intensity was low (80 ± 25 µmol m^{-2} s^{-1} photosynthetic active radiation), and the CO_2 concentration was kept at 508 ± 22 ppm in order to maintain a high atmospheric carbon supply. The day–night cycles were 12 h and the temperature within the labelling chamber was 31 ± 3 °C throughout the experiments.

2.3 Sample collection

The plant–soil systems were destructively harvested at five sampling dates (three replicates each) to detect the dynamics of the labelling over time. The first sampling was done 1 day before the labelling experiment started (unlabelled control, referred to as t = 0). Subsequently, plant–soil systems were sampled after 1, 2, 8 and 14 days of continuous labelling.

At each sampling date the plant–soil systems were separated into leaves, petioles, stems, cuttings, roots (washed with deionized water and carefully dabbed with tissue) and bulk soil (visible roots were removed with tweezers). A subsample of six leaves was sampled all along the stem (homogeneously distributed). The uppermost leaves, that were newly formed and completely labelled during the experiment, were excluded, since we wanted to study the tracer uptake and translocation dynamics in already existing leaves prior to the treatment. In one out of the three plant replicates we took two leaf sub-samples from distinct positions along the shoot. We sampled six leaves from the upper half of the shoot and six leaves from the lower half hereafter referred to as “top” and “bottom”, respectively vials in a water bath. Leaves, stems, roots and bulk soil were collected in

airtight glass vials and frozen immediately at -20 °C for later cryogenic vacuum extraction of the tissue water. Cuttings and petioles were dried for 24 h at 60 °C.

The tissue water was extracted with cryogenic vacuum extraction by heating the frozen samples within the sampling vials in a water bath at 80 °C under a vacuum (10^{-3} mbar) for 2 h. The evaporating water was collected in U vials submersed in a liquid nitrogen cold trap. After thawing (within the closed U vials), the water samples were transferred into vials and stored frozen at -20° C for later $\delta^{18}O$ and $\delta^{2}H$ analysis. To study the water dynamics, additional water vapour samples from the chamber air were collected by Peltier-cooled water condensers in external air circuit connected to the plant labelling chamber and analysed for $\delta^{18}O$ and $\delta^{2}H$.

The dried plant residues of the cryogenic vacuum extraction were used for isotopic bulk analyses as described below. The water-soluble OM was extracted from the leaves by hot water extraction. Sixty milligrams of milled leaf material was dissolved in 1.5 mL of deionized water and heated in a water bath (80 °C) for 30 min. After cooling and centrifugation (10000 g, 2 min), the supernatant was freeze-dried and analysed for $\delta^{13}C$. $\delta^{2}H$ analyses were not possible on the hot water extracts, that represent mainly sugars, due to incomplete equilibration with ambient water vapour (Filot, 2010).

2.4 Isotopic and elemental analyses

All samples were milled to a fine powder with a steel ball mill and weighed into tin ($\delta^{13}C$ analyses) or silver ($\delta^{18}O$ and $\delta^{2}H$ analyses) capsules and measured by isotope-ratio mass spectrometers (IRMS). The $\delta^{13}C$ samples were combusted at 1700 °C in an elemental analyser (EA 1110, Carlo Erba) and the resulting CO_2 was transferred in a helium stream via a variable open-split interface (ConFlo II, Finnigan MAT) to the IRMS (Delta S, Thermo Finnigan; see Werner et al., 1999). The samples for $\delta^{18}O$ analyses were pyrolysed at 1040 °C in an elemental analyser (EA 1108, Carlo Erba) and transferred via ConFlo III interface (Thermo Finnigan) to the IRMS (Delta plus XL, Thermo Finnigan). The samples for $\delta^{2}H$ analyses were equilibrated with water vapour of known signature prior to the IRMS measurements in order to determine the isotopic signature of the non-exchangeable hydrogen (as described in Filot et al., 2006; Hangartner et al., 2012). After equilibration the samples were pyrolysed in a thermochemical elemental analyser (TC/EA, Thermo-Finnigan) at a temperature of 1425 °C and the gaseous products were carried by a helium stream via a ConFlow II open split interface (Thermo Finnigan) into the IRMS (Isoprime, Cheadle). The amount of exchangeable hydrogen (25–27%) and oxygen (2–3%) was measured for the leaf, stem and root tissue using depleted water vapour to equilibrate the samples. The measurement precisions of the solid sample

analyses were 0.12 ‰ $\delta^{13}C$, 0.54 ‰ $\delta^{18}O$ and 1 ‰ $\delta^{2}H$, and were assessed by working standards measured frequently along with the experimental samples. The precisions were lower than reported for measurements of natural abundance, since highly labelled sample material was analysed.

Elemental C, H and N content of solid samples was analysed in an elemental analyser (CHN-900, Leco Corp.), as was the elemental O content (RO-478, Leco Corp.).

The liquid samples from the cryogenic vacuum extraction (tissue water) were pyrolysed in an elemental analyser (TC/EA, Thermo Finnigan) and the evolving CO and H_2 gases were transferred via the ConFlo III interface (Thermo Finnigan) to an IRMS (Delta plus XL, Thermo Finnigan) for oxygen and hydrogen isotope ratio analysis (Gehre et al., 2004). The precision of the liquid sample measurement was ± 0.75 ‰ $\delta^{18}O$ and ± 1.59 ‰ $\delta^{2}H$.

2.5 Calculations

Isotopic ratios were expressed in delta (δ) notation as the deviation (in ‰) from the international standards Vienna Pee Dee Belemnite (V-PDB, $^{13}C/^{12}C = 1.11802 \times 10^{-2}$) and Vienna Standard Mean Ocean Water (V-SMOW, $^{18}O/^{16}O = 2.0052 \times 10^{-3}$ and $^{2}H/^{1}H = 1.5575 \times 10^{-4}$). The significance of changes in isotopic signature between the sampling dates and the unlabelled control (t = 0) were statistically tested via t tests performed by R software (R Core Team, 2014).

In the following paragraphs we describe first the calculations for the leaf water source partitioning (Eqn 1–4). These equations are given for the oxygen isotope (^{18}O), but they also apply for hydrogen (^{2}H). Then we describe the calculations for the relative recovery of the isotopes ($^{18}O/^{13}C$ and $^{2}H/^{13}C$) in the bulk OM (Eqn 5–7).

The leaf water isotopic signature (at steady state) can be described by a model of Dongmann et al. (1974) to calculate leaf water $H_2{}^{18}O$ enrichment, a derivative of Craig and Gordon (1965) (Eqn 1). According to this model, the isotopic signature of the leaf water (L) is the result of kinetic (ε^k) and equilibrium (ε^*) fractionation processes during evaporation of the source water (S) within the leaves and the backdiffusion of atmospheric water vapour (V) into the leaves as affected by relative air humidity (h).

$$\delta^{18}O_L = \delta^{18}O_S + \varepsilon^k + \varepsilon^* + \left(\delta^{18}O_V - \delta^{18}O_S - \varepsilon^k\right) \cdot h \qquad \text{Eqn 1}$$

We used a two-source isotope mixing model (Eqn 2, principles described in Dawson et al., 2002) to assess the contribution of the two main water pools (soil and atmospheric water) to the leaf water based on its isotopic signatures. An overview on the input data for the mixing model is given in Appendix A (Fig. A1).

$$f_{source,2} = \frac{\delta^{18}O_{leaf,water} - \delta^{18}O_{source,1}}{\delta^{18}O_{source,2} - \delta^{18}O_{source,1}}$$ Eqn 2

, where $\delta^{18}O_{leaf,water}$ is the isotopic signature (in ‰) of water extracted from the leaves at a specific sampling date and $\delta^{18}O_{source,1}$ and $\delta^{18}O_{source,2}$ are the theoretical isotopic signatures of the leaf water if all of the water were to originate from either the soil (source 1) or the atmospheric (source 2) water pool.

The first source, hereafter referred to as "evaporating source", represents the water taken up from the soil by the roots, which is transported via the xylem to the leaf, where it evaporates. The isotopic signature of the evaporating source (Eqn 3) is estimated by the maximum leaf water enrichment that would occur at 0% relative air humidity, i.e. by the first part of the Dongmann approach (solving Eqn 1 with h = 0).

$$\delta^{18}O_{source,1} = \delta^{18}O_{stem,water} + \varepsilon^{k} + \varepsilon^{*}_{atm}$$ Eqn 3

, where $\delta^{18}O_{stem,water}$ is the isotopic signature (in ‰) of the water extracted from the stem tissue (approximating the xylem water) and and ε^{k} and ε^{*}_{atm} are the kinetic and equilibrium fractionation terms, respectively, at the specific sampling date.

The second source, hereafter named "condensation source", refers to the water vapour that diffuses from the atmosphere into the leaves and condenses on the cell walls. The contribution of this source would be maximal at 100% relative humidity, which results in Eqn 4 when solving Eqn 1 with h = 1.

$$\delta^{18}O_{source,2} = \delta^{18}O_{atm,vap} + \varepsilon^{*}_{atm} = \delta^{18}O_{atm,cond} - \varepsilon^{*}_{pelt} + \varepsilon^{*}_{atm}$$ Eqn 4

, where $\delta^{18}O_{atm,vap}$ is the isotopic signature of the water vapour of the chamber atmosphere and ε^{*}_{atm} is the equilibrium fractionation inside the chamber at the specific sampling date. The signature of the atmospheric water vapour was measured on its condensate ($\delta^{18}O_{atm,cond}$) collected in the Peltier water trap, which was therefore corrected with the equilibrium fractionation during condensation inside the Peltier-cooled water condenser (ε^{*}_{pelt}).

The kinetic fractionation due to the difference in molecular diffusivity of the water molecule species (ε^{k} = 20.7 ‰ $\delta^{18}O$ and 10.8 ‰ $\delta^{2}H$) was estimated according to Cappa et al. (2003) for a laminar boundary layer (Schmidt number q = 2/3; Dongmann et al., 1974). The equilibrium fractionation due to the phase change during evaporation and condensation at different temperatures was calculated as in Majoube (1971) with the conditions present at the specific day. The condensation (dew point) temperature inside the Peltier-cooled water condenser ($T_{pelt,DP}$) was determined based on the remaining

humidity and the air pressure of the air leaving the condenser (details on the calculation are given in Appendix B). The equilibrium fractionation factors during the labelling experiment were on ε^*_{atm} = 8.9 ± 0.2 ‰ for $\delta^{18}O$ and 72.7 ± 2.7 ‰ for $\delta^{2}H$ at T = 31.3 ± 2.7 °C inside the labelling chamber and ε^*_{pelt} = 11.1 ± 0.2 ‰ for $\delta^{18}O$ and 103.3 ± 3.3 ‰ for $\delta^{2}H$ at $T_{pelt,DP}$ = 6.0 ± 2.5 °C inside the water condenser.

We compared the distribution of the assimilated labels (^{13}C, ^{18}O, ^{2}H) in the leaf, stem and root tissue by its isotopic ratios. Therefore we converted the δ-notation to atom fraction (Eqn 5) according to Coplen (2011).

$$x(^{13}C)_{t=x} = \frac{1}{1 + \frac{1}{(\delta^{13}C_{t=x}/1000 + 1) \cdot R_{V-PDB}}} \qquad \text{Eqn 5}$$

, where $\delta^{13}C_{t=x}$ is the isotopic signature (in ‰) of the bulk tissue at sampling date x and R is the ratio of the heavier to the lighter isotope ($^{13}C/^{12}C$) of the international standard V-PDB. The atom fraction of ^{18}O and ^{2}H was calculated accordingly but using RV-SMOW as a reference and neglecting the ^{17}O isotope amount.

For the van Krevelen approach we calculated the elemental ratios. The relative label distribution within the plant organic matter (tissue, OM), hereafter referred to as $^{18}O/^{13}C$ and $^{2}H/^{13}C$ ratio, was calculated based on the excess atom fraction measured in each tissue (Eqn 6).

$$\frac{x^E\left(^{18}O_{tissue,OM}\right)_{t=x/t=0}}{x^E\left(^{13}C_{tissue,OM}\right)_{t=x/t=0}} = \frac{x\left(^{18}O_{tissue,OM}\right)_{t=x} - x\left(^{18}O_{tissue,OM}\right)_{t=0}}{x\left(^{13}C_{tissue,OM}\right)_{t=x} - x\left(^{13}C_{tissue,OM}\right)_{t=0}} \qquad \text{Eqn 6}$$

, where $x^E(^{18}O)_{t=x/t=0}$ and $x^E(^{13}C)_{t=x/t=0}$ are the excess atom fractions of the labels detected at a specific sampling date (t = x), relative to the unlabelled control (t = 0). Equations 6 and 7 were analogously calculated for the $^{2}H/^{13}C$ ratio.

In a second step we corrected the isotopic ratios ($^{18}O/^{13}C$ and $^{2}H/^{13}C$) with the maximum label strength of the precursor of the plant OM, i.e. the maximum label strength of fresh assimilates (Eqn 7). The maximum label strength was approximated by the excess atom fraction relative to the unlabelled control (x^E) measured in the leaf water-soluble organic matter (wsOM) and the leaf water for the ^{13}C and the ^{18}O and ^{2}H label strength, respectively. The leaf water is the direct source of hydrogen in assimilates and the indirect source of oxygen via the atmospheric CO_2 dissolved in water (Schmidt et al., 2001, 2003). The oxygen isotope composition of dissolved CO_2 equilibrates immediately with the leaf water signature, whereby carbonic anhydrase catalyses this process and induces a temperature-dependent kinetic ^{18}O fractionation

(Gillon and Yakir, 2000; Uchikawa and Zeebe, 2012). The fractionation was assumed to be constant in this experiment with controlled temperature and was thus omitted by the calculation of the excess atom fraction.

$$\frac{x^E_{norm}\left({}^{18}O_{tissue,OM}\right)_{t=x\,/\,t=0}}{x^E_{norm}\left({}^{13}C_{tissue,OM}\right)_{t=x\,/\,t=0}} = \frac{x^E\left({}^{18}O_{tissue,OM}\right)_{t=x\,/\,t=0}}{x^E\left({}^{13}C_{tissue,OM}\right)_{t=x\,/\,t=0}} \cdot \frac{x^E\left({}^{13}C_{leaf,wsOM}\right)_{t=x\,/\,t=0}}{x^E\left({}^{18}O_{leaf,water}\right)_{t=x\,/\,t=0}} \qquad \text{Eqn 7}$$

3 Results

3.1 Labelling of the leaf water and water-soluble OM

The ^{18}O and ^{2}H label added as water vapour to the chamber atmosphere ($\delta^{18}O$ = - 370 ‰, $\delta^{2}H$ = - 813 ‰) was mixed with transpired water, which was isotopically enriched compared to the added label (Fig. 1). The isotopic signature of the water vapour within the chamber air stabilized after 4 days at a level of - 112 ± 4 ‰ $\delta^{18}O$ and - 355 ± 7 ‰ $\delta^{2}H$. Thus the atmospheric water vapour signature was depleted in ^{18}O by 94 ± 4 ‰ and in ^{2}H by 183 ± 7 ‰ compared to the unlabelled atmosphere.

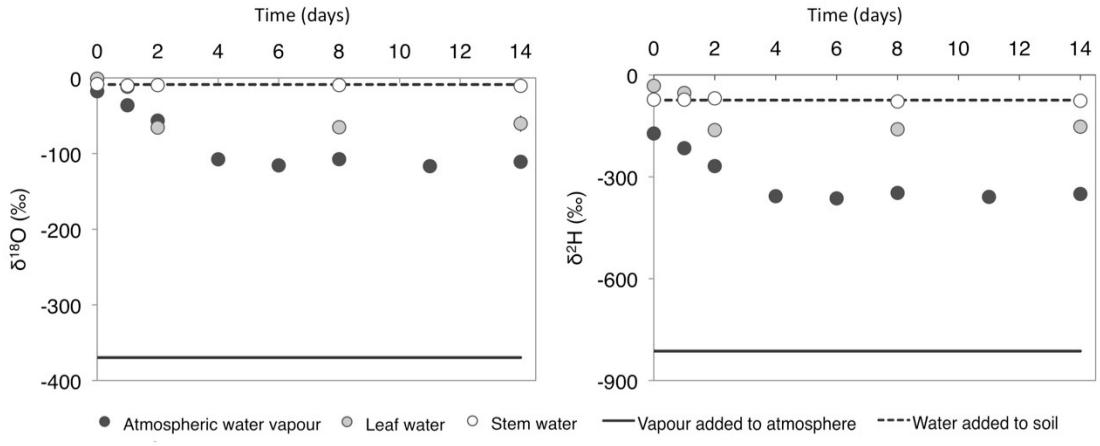

Figure 1. Temporal dynamics in the water isotopic signatures of the plant–soil–atmosphere system during continuous $^{2}H_2{}^{18}O$ labelling (a) $\delta^{18}O$ and (b) $\delta^{2}H$ signature (in ‰) of the depleted water label added as water vapour to the atmosphere (solid line), the water added to the soil (dashed line), the resulting water vapour in the chamber atmosphere (black circles) and the extracted leaf (grey circles) and stem water (white circles). Error bars on the leaf water indicate ± 1 standard deviation of three plant replicates.

The leaf water was strongly depleted and its isotopic signature was stable at a level of 64 ± 7 ‰ for $\delta^{18}O$ and - 158 ± 13 ‰ for $\delta^{2}H$ after 2 days of labelling with the depleted water vapour (Fig. 1). The leaf water was thus on average depleted by 63 ± 7 ‰ for $\delta^{18}O$ and 126 ± 14 ‰ for $\delta^{2}H$ compared to the unlabelled leaf water signature and was between the signature of the atmospheric water vapour and the water added to the soil

$\delta^{18}O$ = - 9 ± 0 ‰, $\delta^{2}H$ = - 74 ± 2 ‰). This indicates that a substantial amount of the leaf water originated from the atmospheric water pool, suggesting that it entered the leaf via diffusion through the stomata. The depletion of the water within a leaf was dependent on its position on the shoot (Fig. 2c, e). The leaf water of the leaves sampled in the upper half of the shoot was 7 ± 2 ‰ and 18 ± 8 ‰ less depleted in $\delta^{18}O$ and $\delta^{2}H$ than the leaves sampled at the lower half. The isotopic signature of the stem water ($\delta^{18}O$ = - 10 ± 0 ‰ and $\delta^{2}H$ = - 74 ± 4 ‰), as well as the root ($\delta^{18}O$ = - 6 ± 1 ‰ and $\delta^{2}H$ = - 58 ± 4 ‰) and the soil water ($\delta^{18}O$ = - 6 ± 1 ‰ and $\delta^{2}H$ = - 63 ± 3 ‰), was not significantly depleted and reflected the signature of the water added to the soil (Fig. 1).

Table 1. Diffusion of atmospheric water vapour into the leaf water. $\delta^{18}O$ and $\delta^{2}H$ signatures of leaf water and its two sources: (i) the evaporating source (Eqn 3), estimated by the stem water signature plus kinetic and equilibrium leaf water enrichment (assuming full evaporation without back-diffusion), and (ii) the condensation source (Eqn 4), assessed by the atmospheric water vapour signature plus equilibrium fractionation to account for the gas–liquid phase change. The contribution of the second source (diffusion and condensation of atmospheric water vapour) to the leaf water ($f_{source,2/leaf,water}$) was estimated by a two-source isotope mixing model for ^{18}O and ^{2}H separately (Eqn 2). Presented are the average values of three plant replicates for each sampling date ± 1 standard deviation.

Sampling date (days)	Leaf water[1]		Source 1: Evaporating source[2]		Source 2: Condensation source[2]		$f_{source,2/leaf,water}$[2]	
	$\delta^{18}O$ (‰)	$\delta^{2}H$ (‰)	$\delta^{18}O$ (‰)	$\delta^{2}H$ (‰)	$\delta^{18}O$ (‰)	$\delta^{2}H$ (‰)	^{18}O (%)	^{2}H (%)
0	-1.0 (±0.5)	-32.0 (±1.8)	21.3 (±0.4)	10.9 (±2.6)	-8.8	-99.7	74.2 (±1.2)	38.8 (±0.3)
1	-11.7 (±1.8)	-53.0 (±5.9)	19.5 (±0.3)	10.3 (±3.2)	-27.3	-143.3	66.6 (±3.9)	41.2 (±3.2)
2	-65.6 (±6.5)	-162.3 (±8.6)	20.0 (±0.6)	14.4 (±2.1)	-47.6	-196.0	126.6 (±9.8)	84.0 (±4.1)
8	-65.2 (±2.0)	-159.9 (±3.8)	20.0 (±0.7)	5.3 (±3.9)	-98.6	-274.8	71.8 (±1.5)	59.0 (±0.8)
14	-60.4 (±10.7)	-152.3 (±21.2)	19.3 (±0.4)	9.5 (±5.1)	-101.8	-275.8	65.8 (±8.7)	56.8 (±6.8)

[1] directly measured

[2] calculated

At the second sampling date, the leaf water seemed to be more depleted than the water vapour within the chamber air (Fig. 1). This is the result of different sampling procedures. The leaf sampling was performed at one point in time (3 h after the light switched on), while the atmospheric water vapour collected by condensation represents an average for the previous 24 h. Therefore the depletion of the water vapour is underestimated before the equilibrium of the isotopic signature in the atmosphere was reached. In the following the average values of signatures detected after the equilibrium was reached are given (t = 8 and t = 14). We estimated the contribution of the

atmospheric water vapour that enters the leaf by diffusion to the leaf water isotopic signature with a two-source mixing model (Table 1). The results were obtained for the two water isotopes ^{18}O and ^{2}H separately. Both indicated a substantial contribution of the atmospheric water vapour to the leaf water isotopic signature, whereby the estimates based on the oxygen isotope yielded a higher contribution (69 ± 7 %) than the hydrogen estimates (58 ± 4 %). The estimates for the leaves sampled at different position on the shoot varied by 5 %, whereas the contribution of atmospheric water to the leaf water was higher in the leaves sampled at the bottom (71 ± 4 % based on ^{18}O and 60 ± 2 % based on ^{2}H) than in the leaves at the top (66 ± 2 % and 55 ± 0 %, respectively) of the shoots.

The ^{13}C-CO_2 added (8938 ‰ $\delta^{13}C$) was presumably also strongly diluted by respired ^{12}C-CO_2, but we did not measure the isotopic signature of the CO_2 within the chamber air. The leaf water-soluble OM was significantly enriched as early as 1 day after labelling and levelled off towards the end of the experiment. On the last two sampling dates its isotopic signature was on average 1346 ± 162 ‰ $\delta^{13}C$.

3.2 Labelling of the bulk OM

All three applied labels could be detected in the plant bulk material (Table 2). We measured the isotopic signature of the non-exchangeable hydrogen, which was estimated to be 74 ± 1 % of the total OM. After 14 days of continuous labelling, the leaves, petioles, stems and roots were enriched by 650-1150 ‰ in $\delta^{13}C$, depleted by 4-17 ‰ in $\delta^{18}O$ and 6-31 ‰ in $\delta^{2}H$. Thus the plant biomass was significantly labelled even under the extreme environmental conditions (high temperature and low light availability) that were critical for net C assimilation (increasing tissue respiration and reducing photosynthesis, respectively). However, the labelling was not strong enough to trace the OM within the large OM pools of the cuttings and soil OM, in which the change in isotopic signature was close to the detection limit or could not be detected. The measured depletion in ^{18}O of the bulk soil can be accounted for natural variability, since the same effect has been observed in non-treated soil (data not shown here).

Table 2. Multi-isotope labelling of bulk OM. $\delta^{13}C$, $\delta^{18}O$ and $\delta^{2}H$ signatures (in ‰) of the plant–soil compartments (three replicates ± 1 standard deviation) measured before and after 1, 2, 8 and 14 days of continuous labelling. A significant enrichment ($\delta^{13}C$) and depletion ($\delta^{18}O$, $\delta^{2}H$) compared to the unlabelled control (t = 0) is highlighted with * (t test, P < 0:05). The degree of labelling is indicated by the change in the isotopic signature of the last sampling date (t = 14) compared to the control (t = 0).

	Sampling date (days)					
$\delta^{13}C$ (‰)	0	1	2	8	14	14 - 0 [(1)]
Leaves	-30.8 (±0.4)	161.5* (±37.4)	189.7 (±128.7)	570.7* (±81.0)	812.5* (±235.0)	843.3 ±235.0)
Petioles	-32.8 (±0.2)	163.9* (±56.2)	212.8* (±75.2)	908.5* (±277.3)	941.9* (±292.7)	974.7 (±292.7)
Stems	-31.4 (±0.6)	209.6* (±84.2)	281.3* (±87.6)	1093.7* (±402.2)	1119.9* (±367.6)	1151.3 (±367.6)
Cuttings	-31.2 (±0.3)	-27.0* (±1.6)	-26.9 (±1.9)	-14.6 (±15.8)	-14.5* (±2.1)	16.8 (±2.1)
Roots	-30.8 (±0.7)	98.1* (±12.5)	90.8 (±62.9)	646.5 (±335.1)	618.0* (±310.9)	648.8 (±310.9)
Bulk soil	-28.0 (±0.1)	-27.9 (±0.0)	-27.8 (±0.2)	-27.5 (±0.5)	-27.5 (±0.2)	0.5 (±0.3)
$\delta^{18}O$ (‰)	0	1	2	8	14	14 - 0 [(1)]
Leaves	25.9 (±0.8)	25.2 (±0.8)	21.9 (±2.0)	15.0* (±0.4)	9.0* (±3.0)	-16.9 (±3.2)
Petioles	21.0 (±0.2)	20.4 (±0.4)	19.5* (±0.4)	14.3* (±1.6)	12.8* (±2.3)	-8.2 (±2.3)
Stems	22.4 (±0.4)	22.2 (±0.1)	20.6* (±0.8)	14.7* (±2.4)	13.3* (±2.8)	-9.1 (±2.8)
Cuttings	21.3 (±1.5)	21.9 (±0.1)	21.8 (±0.4)	21.5 (±0.3)	21.5 (±0.4)	0.2 (±1.5)
Roots	21.2 (±0.6)	20.6 (±0.6)	20.9 (±0.4)	18.2 (±1.5)	17.5* (±1.7)	-3.7 (±1.8)
Bulk soil	14.8 (±0.4)	14.0 (±0.3)	13.8* (±0.4)	13.0* (±0.1)	13.5 (±0.8)	-1.3 (±0.9)
$\delta^{2}H$ (‰)	0	1	2	8	14	14 - 0 [(1)]
Leaves	-146.6 (±2.5)		-158.1 (±7.8)	-169.2* (±5.5)	-178.0* (±9.4)	-31.3 (±9.7)
Petioles	-138.3 (±1.8)				-150.9 (±6.7)	-12.6 (±7.3)
Stems	-129.2 (±4.2)		-136.3 (±4.7)	-153.3 (±14.8)	-152.9* (±9.4)	-23.7 (±10.3)
Cuttings	-167.3 (±2.8)				-172.8 (±6.3)	-5.5 (±6.9)
Roots	-129.7 (±6.4)		-134.0 (±12.5)	-137.0 (±6.8)	-135.9 (±7.7)	-6.2 (±10.0)
Bulk soil	-101.5 (±1.1)				-101.9 (±1.3)	0.4 (±1.7)

[(1)] Isotopic difference for the entire labelling experiment

The labelling of the leaf bulk OM occurred in parallel to the labelling of the leaf water and water-soluble OM (Fig. 2). The leaf OM was enriched in ^{13}C after 1 day (Fig. 2b) and depleted in ^{18}O and ^{2}H after 2 days (Fig. 2d, f). The incorporation of the label into the leaf OM was, like the labelling of the leaf water, dependent on the position on the shoot. The biomass of the leaves at the top was more enriched in ^{13}C (by up to 673 ‰) than the biomass of the leaves at the bottom of the shoots and, in contrast to the leaf water, more depleted in ^{18}O and ^{2}H (by up to 9 and 21 ‰, respectively) at the top than at the bottom. This indicates a higher overall assimilation in the leaves at the top of the shoot.

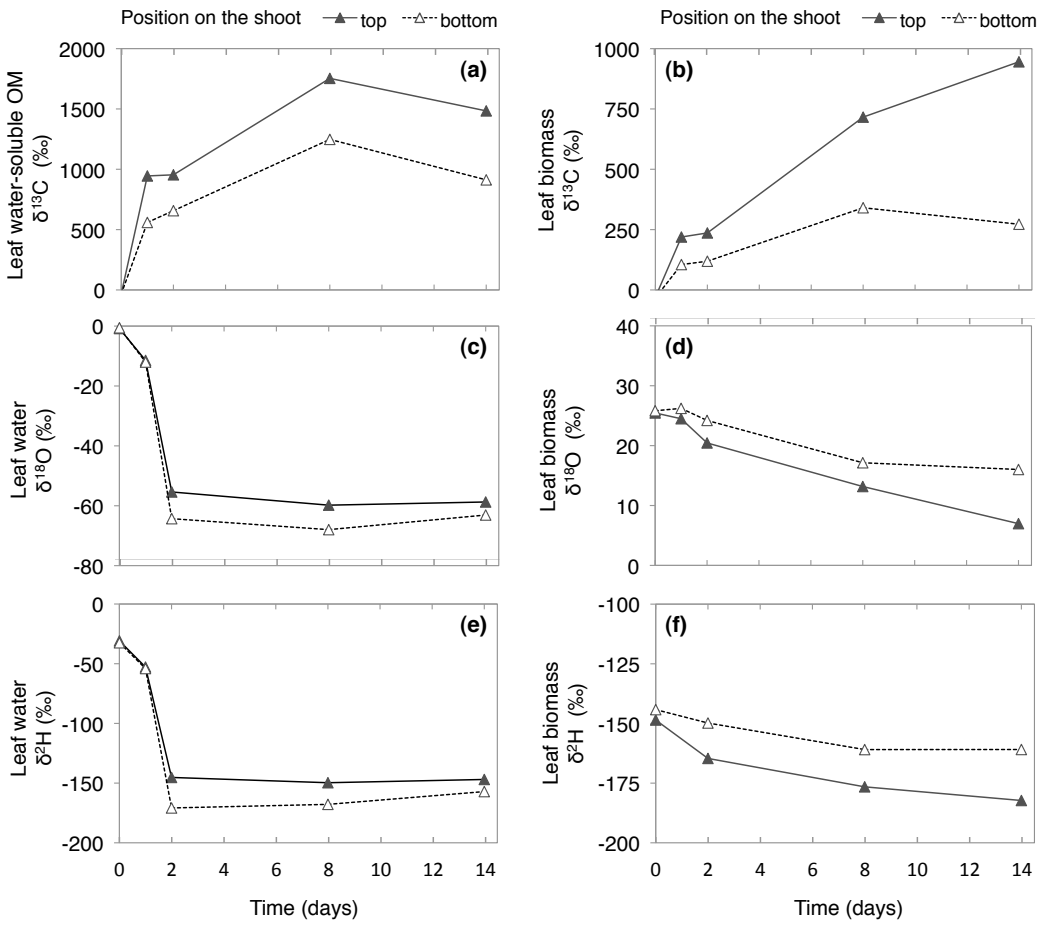

Figure 2. Incorporation of the gaseous labels (enriched $^{13}CO_2$, depleted $^{2}H_2{}^{18}O$) into the plant matter. (a, b) $\delta^{13}C$, (c, d) $\delta^{18}O$ and (e, f) $\delta^{2}H$ signature (in ‰) within leaves sampled at the top (solid line, black triangles), or at the bottom (dashed line, white triangles) of the shoot. Illustrated are the signatures of (a) the leaf water-soluble OM, (b, e, f) leaf biomass and (c, e) leaf water

3.3 Atomic and isotopic ratios to characterize OM

The atomic ratios of the plant bulk OM were in the range of 13.7–115.4 C/N, 0.70–0.83 O/C and 1.56–1.72 H/C (Table 3). The leaf OM was characterized by the lowest C/N and O/C ratios and concurrently by highest H/C ratios (Fig. 3a). The other plant tissues indicated a linear trend in decreasing O/C and H/C and increasing C/N ratios in the order of stems, petioles, roots and cuttings.

Table 3. Atomic and isotopic ratios of the labelled bulk OM. C/N, O/C and H/C atomic ratios and $^{18}O/^{13}C$ and $^{2}H/^{13}C$ isotopic ratios (of the excess atom fraction) measured in different plant compartments after the equilibrium in the atmospheric labelling was reached. Indicated are average values of two sampling dates (t = 8 and 14) with three plant replicates each (± 1 standard deviation).

Compartment	C/N	O/C	H/C	$^{18}O/^{13}C$[1]	$^{2}H/^{13}C$[1]
Leaves	13.7 (±0.4)	0.70 (±0.01)	1.72 (± 0.04)	0.43 (±0.07)	0.41 (±0.06)
Petioles	35.4 (±1.3)	0.77 (±0.01)	1.64 (±0.01)	0.18 (±0.03)	0.14 (±0.03)[2]
Stems	32.0 (±4.0)	0.83 (±0.01)	1.71 (±0.02)	0.17 (±0.03)	0.23 (±0.06)
Cuttings	115.4 (±7.2)	0.72 (±0.01)	1.56 (±0.02)	n.m.[3]	n.m.[3]
Roots	29.9 (±2.0)	0.73 (±0.02)	1.61 (±0.02)	0.12 (±0.03)	0.07 (±0.11)

[1] Ratio of excess atom fraction normalized by the maximum label strength (Eqn 7)
[2] Only the last sampling date was measured (t = 14)
[3] Not measured

The recovery of the three isotopes varied between the leaf, stem and root tissue, while they were similar between the sampling dates (Fig. 3b). The isotopic ratios of the excess atom fractions were 3.5 ± 0.4 x 10^{-3} $^{18}O/^{13}C$ and 5.3 ± 0.5 x 10^{-4} $^{2}H/^{13}C$ in the leaves, 1.4 ± 0.1 x 10^{-3} $^{18}O/^{13}C$ and 2.9 ± 0.6 x 10^{-4} $^{2}H/^{13}C$ in the stems and 1.0 ± 0.2 x 10^{-3} $^{18}O/^{13}C$ and 1.0 ± 1.4 x 10^{-4} $^{2}H/^{13}C$ in the roots after the equilibrium in the leaf water and watersoluble OM labelling was reached. Thus the $^{18}O/^{13}C$ ratios were on average 2.6 (± 0.2) times lower in the stems and 3.8 (± 0.7) times lower in the roots than in the leaves (Table 3) and the $^{2}H/^{13}C$ ratios were 1.9 (± 0.2) and 3.1 (± 0.6) times lower in the stems and roots, respectively, than in the leaves.

The isotopic ratios were in the range of 0.17–0.43 $^{18}O/^{13}C$ and 0.14–0.23 $^{2}H/^{13}C$ after the correction for the maximum label strength, approximated by the ^{18}O, ^{2}H and ^{13}C excess atom fraction within the leaf water and the water-soluble OM, respectively. The normalized isotopic ratios were thus in the order of magnitude of the atomic ratios reported for OM compounds (Table 3, Fig. 3c) but they were in the range characteristic for condensed hydrocarbons and thus lower than expected for fresh OM.

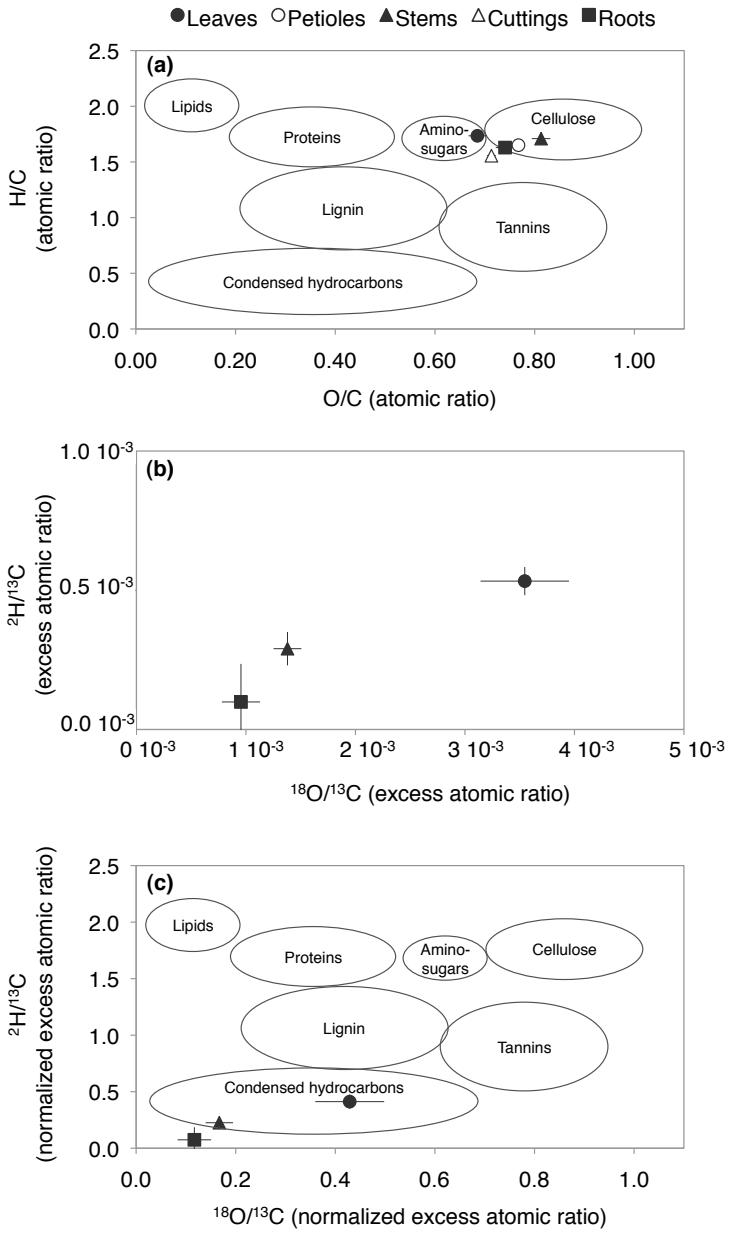

Figure 3. Atomic and isotopic ratios to illustrate change in OM characteristics. (a) Atomic and (b, c) isotopic ratios of oxygen and hydrogen to carbon within the leaves (black circles), petioles (white circles), stems (black triangles), stem cutting (white triangles) and roots (black squares). The circles overlain on the plots in (a) and (c) indicate atomic ratios characteristic for different compound classes (adapted from Sleighter and Hatcher, 2007). Panel (a) illustrates the atomic ratio of all tissues measured (15 replicates ± 1 standard deviation, panel (b) the isotopic ratios of the ^{13}C, ^{18}O and ^{2}H excess atom fraction (relative to the unlabelled tissues) measured after equilibrium in the labelling (see Fig. 1 and 2) was reached (t = 8 and 14, six replicates ± 1 standard deviation) and panel (c) shows the isotopic ratios after normalization with the maximum label strength detected in the leaf water (^{18}O, ^{2}H) and water-soluble OM (^{13}C).

4 Discussion

4.1 Diffusion of atmospheric water vapour into the leaf

The strong depletion in $\delta^{18}O$ and $\delta^{2}H$ observed in the leaf water indicates a high back-diffusion of labelled water vapour from the atmosphere into the leaf. The diffusion is dependent on the gradient between atmospheric and leaf water vapour pressure and the stomatal conductance (Parkhurst, 1994). The higher the atmospheric water vapour pressure (the smaller the gradient), the more water molecules diffuse back into the leaf. The latter is further enhanced the larger the stomatal conductance is (Reynolds Henne, 2007). Here we maintained the atmospheric vapour pressure constant at a high level, ensuring a high back-diffusion at a given stomatal conductance. In our experiment the leaf water $\delta^{18}O$ and $\delta^{2}H$ signature is determined by (i) the signature and the amount of labelled (depleted) water vapour diffusing into the leaf intercellular cavities; (ii) by the enrichment due to transpiration (kinetic and equilibrium fractionation); and (iii) by the influx of xylem water, which is isotopically enriched relative to the labelled water vapour. The latter is proportionally enhanced by increasing transpiration rates as a result of the diffusion convection process of H_2O (Péclet effect; Farquhar and Lloyd 1993).

The distinct label signal in the water sampled in leaves at different positions on the shoot indicates differences in the transpiration rate. Meinzer et al. (1997) demonstrated in large poplar trees that shading or lower irradiance leads to lower stomatal conductance and transpiration rates. Thus the back-diffusion in the leaves on the bottom might have been reduced due to lower stomatal conductance. However, the increased transpiration in the leaves at the top led to an even stronger dilution of the isotopic signal in the leaf water due to (i) increased evaporative leaf water enrichment and (ii) the Péclet effect (enhanced influx of xylem water, which was enriched compared to the labelled atmospheric water vapour).

The amount of leaf water that entered the leaf by backdiffusion was estimated to be 58–69%. This result is in contradiction to the common perception that most of the leaf water is taken up from the soil via roots. However it is in line with the observations made by Farquhar and Cernusak (2005), who modelled the leaf water isotopic composition in the non-steady state and estimated the contribution of atmospheric water to the leaf water to be approximately two-thirds of the total water supply. Although, our estimates are based on a modelling approach that does not take into account the Péclet effect or daily fluctuations in the isotopic signatures as described below, our estimates correspond very well to the findings of Farquhar and Cernusak (2005).

The model used to estimate the quantitative contribution of the two water sources is based on the measured signature of the leaf water ($\delta^{18}O_{leaf,water}$) and the estimated signatures of the water at the evaporating and condensation ($\delta^{18}O_{source,1}$ and $\delta^{18}O_{source,2}$, respectively). The "dilution" of the (laminar) leaf water with the relatively enriched xylem water through the Péclet effect is included in the $\delta^{18}O_{leaf,water}$. This explains the lower contribution of atmospheric water (-5%) estimated in the leaves sampled at the top (due to the Péclet effect resulting from higher transpiration rates) compared to the leaves sampled at the bottom of the shoot.

Some inaccuracy in the two-source mixing model estimates might have been introduced by daily fluctuations in the environmental and labelling conditions. The mixture ($\delta^{18}O_{leaf,water}$) was sampled after 3 h of light, whereas the estimation of the two sources ($\delta^{18}O_{source,1}$ and $\delta^{18}O_{source,2}$) is based on daily average values of environmental parameters and the atmospheric water vapour ($\delta^{18}O_{atm,vap}$) label strength. In our experiment, fluctuations in $\delta^{18}O_{atm,vap}$ were caused by adding the labelled vapour mainly during nighttime, when transpiration was low. Thus the atmospheric label strength was presumably highest before the lights were switched on and gradually diluted during the day by transpired water vapour. Hence the actual $\delta^{18}O_{atm,vap}$ at the time of plant sampling was probably more depleted than the measured average signature. Therefore $\delta^{18}O_{source,2}$ and its contribution to the leaf water was slightly overestimated. The effect of the temperature fluctuations (± 3 °C) via changes in the equilibrium fractionation was minor for the outcome of the mixing model <1 %.

Nonetheless, the strong depletion of the leaf water in ^{2}H and ^{18}O proves that back-diffusion of atmospheric water vapour into the leaf is an important mechanisms for leaf water uptake. This supports the hypothesis that atmospheric water vapour diffusion might be as important as the flux of water from the xylem into the leaf (at least under humid conditions) and be an important mechanisms for the reversed water flow observed in the tropics (Goldsmith, 2013). Furthermore, these results demonstrate that the leaf water isotopic composition is strongly affected by the atmospheric signature at humid conditions and that thus the applicability of the dual-isotope approach (Scheidegger et al., 2000), e.g. to reconstruct past climate conditions by tree ring analysis, is only valid if the source water and atmospheric vapour $\delta^{18}O$ are similar. The backdiffusion of atmospheric vapour at high humidity could be another factor in addition to the evaporative enrichment (as demonstrated by Roden and Farquhar, 2012) to overshadow the effects of stomatal conductance on the leaf $\delta^{18}O$ signature.

4.2 Tracing OM

The O/C and H/C ratio of the plant bulk material was close to the signature of cellulose (Fig. 3a). The leaves had a lower O/C ratio with a constant high H/C ratio, indicating that its OM contains more reduced compounds such as amino sugars or proteins, which is also supported by its low C/N ratio. The trend of decreasing O/C and H/C ratios observed in the other tissues is in the direction of condensation reactions. This trend most likely indicates the increasing lignification of OM from shoots, to roots, to cuttings.

The same trend has been observed in the ratios of the labels added from the leaf, to the stem, to the root OM (Fig. 3b, c). The lower isotopic O/C and H/C ratios in the root and stem tissue compared to the leaf tissue could indicate the utilization of the labelled assimilates for the synthesis of more condensed compounds (e.g. lignin) in those tissues. However, other factors affecting the isotopic ratios of the OM are the maximum label strength, the exchange of hydrogen and oxygen with xylem water during transport and biosynthesis, and the isotopic fractionation during metabolism.

The isotopic ratios (Fig. 3b) were around three orders of magnitudes smaller than the expected atomic ratios of OM (Sleighter and Hatcher, 2007). This is mainly due to the different maximum label strength, which was highest for the ^{13}C and lowest for the ^{2}H. After correction for this factor, the isotopic ratios were in the range of the atomic ratios characteristic for condensed hydrocarbons (Fig. 3c). The isotopic ratios might be lower than expected due to inaccurate approximation of the maximum label strength of fresh assimilates (by the leaf water and water-soluble OM) or be the result of ^{18}O and ^{2}H label losses during transport and biosynthesis.

One reason for the label loss might be the use of other (more enriched) sources during biosynthesis. For example, O_2 (enriched by 23‰ $\delta^{18}O$) has been identified as a further source of aromatic compounds, such as phenols and sterols (Schmidt et al., 2001). However, for hydrogen, water is the only known source (Schmidt et al., 2003) and therefore the use of other O or H sources during biosynthesis cannot explain the (major) loss of the ^{18}O and ^{2}H label.

Another potential reason could be the kinetic fractionation during biosynthesis that leads to distinct isotopic signatures of different OM compounds (described in Schmidt et al., 2001, 2003; Badeck et al., 2005; Bowling et al., 2008). However, assuming constant isotopic fractionation during the experiment with constant environmental conditions, the isotopic ratios would not be affected, since they are based on the excess atom fraction relative to the unlabelled OM.

A third reason for the loss of the ^{18}O and ^{2}H label could be the exchange of hydrogen and oxygen atoms with water. O and H exchanges with tissue water during transport and the synthesis of new compounds (as recently discussed for oxygen in phloem sugars and cellulose in Offermann et al., 2011, and Gessler et al., 2013). O of carbonyl groups (Barbour, 2007; Sternberg et al., 1986) and H in nucleophilic OH and NH groups or H adjacent to carbonyl groups (Augusti et al., 2006; Garcia-Martin et al., 2001) exchange with water. Thus biochemical reactions lead to different isotopomers of organic compounds (Augusti and Schleucher, 2007). The proportion of O and H exchanged can be considerable; for example, during cellulose synthesis, around 40% of O and H is exchanged with the tissue water (Roden and Ehleringer, 1999; Yakir and DeNiro, 1990). The exchange with water explains to some extent the stronger relative ^{18}O and ^{2}H signal in the leaf OM compared to the stem and root OM, since the leaf water was labelled, while the stem and root water was not. The $^{18}O/^{13}C$ isotopic ratios in particular were increased in the leaf OM compared to the relations observed in the atomic ratios (Fig. 3a). The leaf OM had the lowest O/C atomic ratios but the highest $^{18}O/^{13}C$ isotopic ratios of all plant compartments (Table 3). This effect is less expressed for the $^{2}H/^{13}C$ ratios, since only the fraction of hydrogen that does not exchange with ambient water vapour was measured. The non-exchangeable fraction (74%) is hydrogen bound to carbon (Filot et al., 2006), which is hardly exchanged with xylem water.

5 Conclusions

We present a new technique to label OM at its place of formation by the application of labels through the gaseous phase ($^{13}CO_2$ and $^{2}H_2{}^{18}O$). In this study we were able to show that, in a humid atmosphere, the atmospheric water vapour isotopic signature dominates the leaf water signature due to a strong back-diffusion of water vapour into the leaf. Further, we detected differences in the relative distribution of ^{13}C, ^{18}O and ^{2}H in the leaves, stems and roots. This could indicate the synthesis of different compounds in the particular tissues and thus a change in OM characteristics, but it could also be the result of exchange and fractionation processes during transport and biosynthesis. To further test these two possibilities, a better estimation of the maximum label strength by compound-specific sugar analysis would be needed, which has been further developed for $\delta^{13}C$ (Rinne et al., 2012) and for $\delta^{18}O$ (Zech et al., 2013) recently but does not yet exist for $\delta^{2}H$ analysis

The multi-isotope labelling technique can be used to assess the amount of vapour diffusing into the leaves and to trace the dynamics of the labelled OM. It could be applied

in soil sciences, as for example to track the decomposition pathways of soil OM inputs or in the field of plant physiology and palaeoclimatic reconstruction, for example to further investigate the O and H exchange and fractionation processes during transport and metabolic processes or the importance of the ambient air humidity besides its isotopic composition for the climate signal stored in tree-ring cellulose. Furthermore, the multi-isotope labelling technique has the potential to make changes in OM characteristics visible (e.g. C allocation into the non-structural vs. structural pool), for example after a change in climatic conditions, and to trace the labelled OM during its decomposition within the soil.

Acknowledgements

This study was funded by the Swiss National Science Foundation (SNSF), project no. 135233. We would like to thank M.W. I. Schmidt for his support; M. Saurer for his comments on the manuscript; R. Künzli, I. Lötscher, R. Maier, P. Nyfeler and I. Woodhatch for technical assistance; and the soil science and biogeochemistry (University of Zurich) and ecosystem fluxes (Paul Scherrer Institute) research groups for valuable discussions.

References

Augusti, A., Betson, T. R. and Schleucher, J.: Hydrogen exchange during cellulose synthesis distinguishes climatic and biochemical isotope fractionations in tree rings, New Phytol., 172, 490–499, doi:10.1111/j.1469-8137.2006.01843.x, 2006.

Augusti, A. and Schleucher, J.: The ins and outs of stable isotopes in plants, New Phytol., 174, 473–475, doi:10.1111/j.1469-8137.2007.02075.x, 2007.

Badeck, F.-W., Tcherkez, G., Nogués, S., Piel, C. and Ghashghaie, J.: Post-photosynthetic fractionation of stable carbon isotopes between plant organs - a widespread phenomenon, Rapid Commun. Mass Spectrom., 19, 1381–1391, doi:10.1002/rcm.1912, 2005.

Barbour, M. M.: Stable oxygen isotope composition of plant tissue: a review, Funct. Plant Biol., 34, 83–94, doi:10.1071/FP06228, 2007.

Bird, J. A. and Torn, M. S.: Fine roots vs. needles: a comparison of ^{13}C and ^{15}N dynamics in a ponderosa pine forest soil, Biogeochemistry, 79, 361–382, doi:10.1007/s10533-005-5632-y, 2006.

Bowling, D. R., Pataki, D. E. and Randerson, J. T.: Carbon isotopes in terrestrial ecosystem pools and CO_2 fluxes, New Phytol., 178, 24–40, doi:10.1111/j.1469-8137.2007.02342.x, 2008.

Cappa, C. D., Hendricks, M. B., Depaolo, D. J. and Cohen, R. C.: Isotopic fractionation of water during evaporation, J. Geophys. Res., 108, 4525, doi:10.1029/2003JD003597, 2003.

Coplen, T. B.: Guidelines and recommended terms for expression of stable-isotope-ratio and gas-ratio measurement results, Rapid Commun. Mass Spectrom., 25, 2538–2560, doi:10.1002/rcm.5129, 2011.

Craig, H. and Gordon, L. I.: Deuterium and oxygen 18 variations in the ocean and the marine atmosphere, in Stable isotopes in oceanographic studies and paleo-temperatures, edited by E. Tongiorgi, pp. 9–130, Spoleto, Pisa, Italy., 1965.

Dawson, T. E., Mambelli, S., Plamboeck, A. H., Templer, P. H. and Tu, K. P.: Stable isotopes in plant ecology, Annu. Rev. Ecol. Syst., 33, 507–559, doi:10.1146/annurev.ecolsys. 33.020602.095451, 2002.

Dongmann, G., Nürnberg, H. W., Förstel, H. and Wagener, K.: On the enrichment of $H_2{}^{18}O$ in the leaves of transpiring plants, Radiat. Environ. Biophys., 11, 41–52, doi:10.1007/ BF01323099, 1974.

Farquhar, G. D. and Cernusak, L. A.: On the isotopic composition of leaf water in the non-steady state, Funct. Plant Biol., 32, 293–303, doi:10.1071/FP04232, 2005.

Farquhar, G. D. and Lloyd, J.: Carbon and oxygen isotope effects in the exchange of CO_2 between terrestrial plants and the atmosphere, in Stable isotopes and plant carbon-water relations, edited by J. R. Ehleringer, A. E. Hall, and G. D. Farquhar, pp. 47–70, Academic Press, Waltham., 1993.

Filot, M.: Isotopes in tree-rings: Development and application of a rapid preparative online equilibration method for the determination of D / H ratios of nonexchangeable hydrogen in tree-ring cellulose, 106 pp., Bern., 2010.

Filot, M. S., Leuenberger, M., Pazdur, A. and Boettger, T.: Rapid online equilibration method to determine the D/H ratios of non-exchangeable hydrogen in cellulose, Rapid Commun. Mass Spectrom., 20, 3337–3344, doi:10.1002/rcm, 2006.

Garcia-Martin, M. L., Ballesteros, P. and Cerda, S.: The metabolism of water in cells and tissues as detected by NMR methods, Prog. Nucl. Magn. Reson. Spectrosc., 39, 41–77, doi:10.1016/S0079-6565(01)00031-0, 2001.

Gehre, M., Geilmann, H., Richter, J., Werner, R. A. and Brand, W. A.: Continuous flow $^{2}H/^{1}H$ and $^{18}O/^{16}O$ analysis of water samples with dual inlet precision, Rapid Commun. Mass Spectrom., 18, 2650–2660, doi:10.1002/rcm.1672, 2004.

Gessler, A., Brandes, E., Keitel, C., Boda, S., Kayler, Z. E., Granier, A., Barbour, M., Farquhar, G. D. and Treydte, K.: The oxygen isotope enrichment of leaf-exported assimilates - does it always reflect lamina leaf water enrichment?, New Phytol., 200, 144–157, doi:10.1111/nph.12359, 2013.

Girardin, C., Rasse, D. P., Biron, P., Ghashghaie, J. and Chenu, C.: A method for ^{13}C-labeling of metabolic carbohydrates within French bean leaves (*Phaseolus vulgaris* L.) for decomposition studies in soils, Rapid Commun. Mass Spectrom., 23, 1792–1800, doi:10.1002/rcm, 2009.

Goldsmith, G. R.: Changing directions : the atmosphere-plant–soil continuum, New Phytol., 199, 4–6, 2013.

Hangartner, S., Kress, A., Saurer, M., Frank, D. and Leuenberger, M.: Methods to merge overlapping tree-ring isotope series to generate multi-centennial chronologies, Chem. Geol., 294, 127–134, doi:10.1016/j.chemgeo.2011.11.032, 2012.

Högberg, P., Högberg, M. N., Göttlicher, S. G., Betson, N. R., Keel, S. G., Metcalfe, D. B., Campbell, C., Schindlbacher, A., Hurry, V., Lundmark, T., Linder, S. and Näsholm, T.: High temporal resolution tracing of photosynthate carbon from the tree canopy to forest soil microorganisms, New Phytol., 177, 220–228, doi:10.1111/j.1469-8137. 2007.02238.x, 2008.

Keel, S. G., Siegwolf, R. T. W. and Körner, C.: Canopy CO_2 enrichment permits tracing the fate of recently assimilated carbon in a mature deciduous forest, New Phytol., 172, 319–329, doi:10.1111/j.1469-8137.2006.01831.x, 2006.

Kim, S., Kramer, R. W. and Hatcher, P. G.: Graphical method for analysis of ultrahigh-resolution broadband mass spectra of natural organic matter, the van Krevelen diagram, Anal. Chem., 75, 5336–5344, doi:10.1021/ac034415p, 2003.

Kulmatiski, A., Beard, K. H., Verweij, R. J. T. and February, E. C.: A depth-controlled tracer technique measures vertical, horizontal and temporal patterns of water use by trees and grasses in a subtropical savanna, New Phytol., 188, 199–209, doi:10.1111/j.1469-8137.2010.03338.x, 2010.

Majoube, M.: Fractionnement en oxygène 18 et en deutérium entre l'eau et sa vapeur, J. Chim. Phys. physico-chimie Biol., 68, 1423–1435, 1971.

Meinzer, F. C., Hinckley, T. M. and Ceulemans, R.: Apparent responses of stomata to transpiration and humidity in a hybrid poplar canopy, Plant, Cell Environ., 20, 1301–1308, doi:10.1046/j.1365-3040.1997.d01-18.x, 1997.

Offermann, C., Ferrio, J. P., Holst, J., Grote, R., Siegwolf, R. T. W., Kayler, Z. E. and Gessler, A.: The long way down-are carbon and oxygen isotope signals in the tree ring uncoupled from canopy physiological processes?, Tree Physiol., 31, 1088–1102, doi:10.1093/treephys/tpr093, 2011.

Ohno, T., He, Z., Sleighter, R. L., Honeycutt, C. W. and Hatcher, P. G.: Ultrahigh resolution mass spectrometry and indicator species analysis to identify marker components of soil- and plant biomass- derived organic matter fractions, Environ. Sci. Technol., 44, 8594–8600, doi:10.1021/es101089t, 2010.

Parkhurst, D. F.: Tansley review no. 65. Diffusion of CO_2 and other gases inside leaves, New Phytol., 126, 449–479, doi:10.1111/j.1469-8137.1994.tb04244.x, 1994.

Plamboeck, A. H., Dawson, T. E., Egerton-Warburton, L. M., North, M., Bruns, T. D. and Querejeta, J. I.: Water transfer via ectomycorrhizal fungal hyphae to conifer seedlings, Mycorrhiza, 17, 439–447, doi:10.1007/s00572-007-0119-4, 2007.

Reynolds Henne, C. E.: A study of leaf water $\delta^{18}O$ composition using isotopically-depleted $H_2{}^{18}O$-vapour, in Climate-isotope relationships in trees under non-limiting climatic conditions from seasonal to century scales, pp. 77–92, University of Bern., 2007.

Rinne, K. T., Saurer, M., Streit, K. and Siegwolf, R. T. W.: Evaluation of a liquid chromatography method for compound-specific $\delta^{13}C$ analysis of plant carbohydrates in alkaline media, Rapid Commun. Mass Spectrom., 26, 2173–85, doi:10.1002/rcm.6334, 2012.

Roden, J. S. and Ehleringer, J. R.: Hydrogen and oxygen isotope ratios of tree-ring cellulose for riparian trees grown long-term under hydroponically controlled environments, Oecologia, 121, 467–477, doi:10.1007/s004420050953, 1999.

Roden, J. S. and Farquhar, G. D.: A controlled test of the dual-isotope approach for the interpretation of stable carbon and oxygen isotope ratio variation in tree rings, Tree Physiol., 32, 1–14, doi:10.1093/treephys/tps019, 2012.

Scheidegger, Y., Saurer, M., Bahn, M. and Siegwolf, R. T. W.: Linking stable oxygen and carbon isotopes with stomatal conductance and photosynthetic capacity: A conceptual model, Oecologia, 125, 350–357, doi:10.1007/S004420000466, 2000.

Schenck zu Schweinsberg-Mickan, M., Joergensen, R. G. and Müller, T.: Fate of ^{13}C- and ^{15}N-labelled rhizodeposition of *Lolium perenne* as function of the distance to the root surface, Soil Biol. Biochem., 42, 910–918, doi:10.1016/j.soilbio.2010.02.007, 2010.

Schmidt, H.-L., Werner, R. A. and Eisenreich, W.: Systematics of ^{2}H patterns in natural compounds and its importance for the elucidation of biosynthetic pathways, Phytochem. Rev., 2, 61–85, doi:10.1023/B:PHYT.0000004185.92648.ae, 2003.

Schmidt, H.-L., Werner, R. A. and Rossmann, A.: O-18 pattern and biosynthesis of natural plant products, Phytochemistry, 58, 9–32, doi:10.1016/S0031-9422(01)00017-6, 2001.

Simard, S. W., Durall, D. M. and Jones, M. D.: Carbon allocation and carbon transfer between *Betula papyrifera* and *Pseudotsuga menziesii* seedlings using a ^{13}C pulse-labeling method, Plant Soil, 191, 41–55, doi:10.1023/A:1004205727882, 1997.

Sleighter, R. L. and Hatcher, P. G.: The application of electrospray ionization coupled to ultrahigh resolution mass spectrometry for the molecular characterization of natural organic matter, J. Massspectrometry, 42, 559–574, doi:10.1002/jms, 2007.

Steinmann, K., Siegwolf, R. T. W., Saurer, M. and Körner, C.: Carbon fluxes to the soil in a mature temperate forest assessed by ^{13}C isotope tracing, Oecologia, 141, 489–501, doi:10.1007/s00442-004-, 2004.

Sternberg, L. D. S. L. O., DeNiro, M. J. D. and Savidge, R. A.: Oxygen isotope exchange between metabolites and water during biochemical reactions leading to cellulose synthesis, Plant Physiol., 82, 423–427, doi:10.1104/pp.82.2.423, 1986.

Studer, M. S., Siegwolf, R. T. W. and Abiven, S.: Carbon transfer, partitioning and residence time in the plant-soil system: a comparison of two $^{13}CO_2$ labelling techniques, Biogeosciences, 11, 1637–1648, doi:10.5194/bg-11-1637-2014, 2014.

Uchikawa, J. and Zeebe, R. E.: The effect of carbonic anhydrase on the kinetics and equilibrium of the oxygen isotope exchange in the CO_2–H_2O system: Implications for $\delta^{18}O$ vital effects in biogenic carbonates, Geochim. Cosmochim. Acta, 95, 15–34, doi:10.1016/j.gca.2012.07.022, 2012.

Werner, C., Schnyder, H., Cuntz, M., Keitel, C., Zeeman, M. J., Dawson, T. E., Badeck, F.-W., Brugnoli, E., Ghashghaie, J., Grams, T. E. E., Kayler, Z. E., Lakatos, M., Lee, X., Máguas, C., Ogée, J., Rascher, K. G., Siegwolf, R. T. W., Unger, S., Welker, J., Wingate, L. and Gessler, A.: Progress and challenges in using stable isotopes to trace plant carbon and water relations across scales, Biogeosciences, 9, 3083–3111, doi:10.5194/bg-9-3083-2012, 2012.

Yakir, D. and DeNiro, M. J. D.: Oxygen and hydrogen isotope fractionation during cellulose metabolism in *Lemna gibba* L., Plant Physiol., 93, 325–332, doi:10.1104/pp.93.1.325, 1990.

Zech, M., Saurer, M., Tuthorn, M., Rinne, K., Werner, R. a, Siegwolf, R., Glaser, B. and Juchelka, D.: A novel methodological approach for δ(18)O analysis of sugars using gas chromatography-pyrolysis-isotope ratio mass spectrometry., Isotopes Environ. Health Stud., 49, 492–502, doi:10.1080/10256016.2013.824875, 2013.

Appendix A

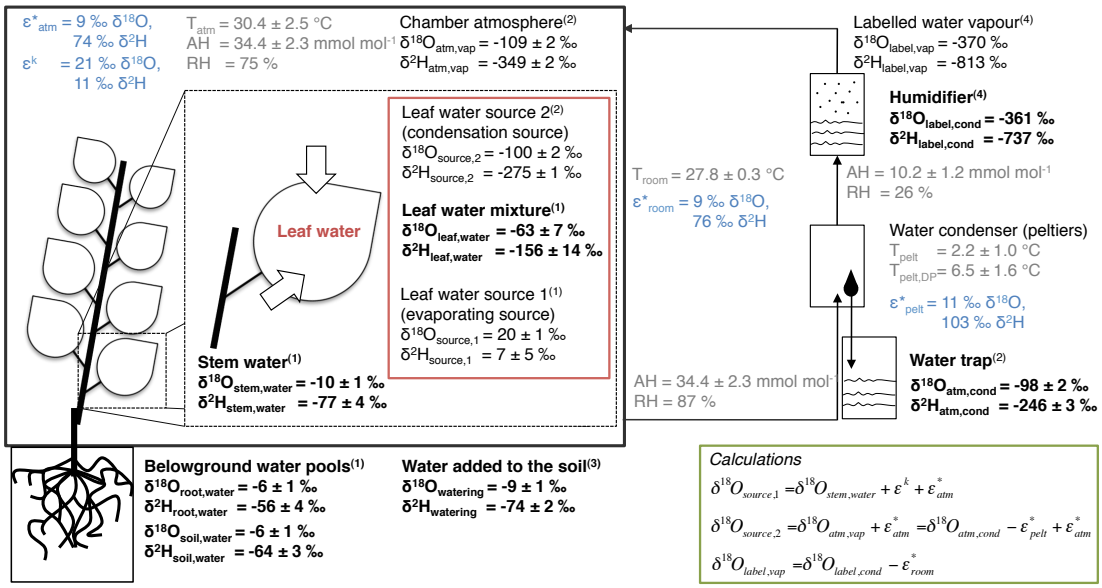

(1) Sampled after 3/12 hours daylight; errors represent variability between plant individuals (three plant replicates each sampling date).
(2) Integrated value over 2-3 days (water trap analysed at day 6, 8, 11 and 14), errors represent variability between sampling date 8 and 14.
(3) Average of all watering dates (day 0, 2, 6, 8, 11); errors represent variability between sampling dates.
(4) Measured at the beginning of the experiment

Figure A1. Overview of the input data of the two-source isotope mixing model. $\delta^{18}O$ and $\delta^{2}H$ signatures of the water pools of the chamber system are presented as average values after equilibrium in the labelling was reached (t = 8 and 14 days). The monitored environmental conditions (T = temperature, AH = absolute humidity and RH = relative humidity) are shown in grey. The equilibrium and kinetic fractionation factors, highlighted in blue, were calculated according to Majoube (1971) and Cappa et al. (2003), respectively. The fractionation factors were used for the calculations (green box) of the signatures in the non-directly measured pools and the isotopic signatures of the evaporating and condensation source of the leaf water (red box). The equations are given for $\delta^{18}O$, but apply for $\delta^{2}H$ analogously. Please note that the data reported here are average values of the last two sampling dates, while in the results section we present the data of single sampling dates or average values of the whole labelling experiment (environmental conditions, equilibrium fractionation factors).

Appendix B

Calculation of the relative air humidity and the dew-point temperature

The dew-point temperature, i.e. the temperature at which the water condensed inside the Peltier-cooled water condenser ($T_{pelt,DP}$) was calculated by solving Eqn B1 with the humidity measured in the air after the condenser 10 ± 1 mmol mol^{-1} AH, 26% RH).

$$RH(T) = \frac{e}{e(T)} \cdot 100 \tag{B1}$$

, where RH is the relative air humidity (in %), e is the partial pressure of water vapour (calculated according to Eqn B2) and e(T) is the saturation vapour pressure (in kPa, calculated according to Eqn B3).

$$e = \frac{AH}{1000} \cdot p \tag{B2}$$

, where AH is the absolute humidity given as the mole fraction of water vapour (mmol mol^{-1}) and p is the atmospheric pressure (in kPa).

$$e(T) = 0.61365 \cdot e^{\frac{17.502 \cdot T}{240.97 + T}} \tag{B3}$$

, where T is the room air temperature (in °C).

Manuscript IV 'Rhizosphere priming'

Submission planed as

Studer, M. S., Siegwolf, R. T. W., Schmidt, M. W. I., Abiven, S. Increased plant-derived soil respiration vs. assimilation induces massive rhizosphere priming in resource limited plant-soil systems. Frontiers in Plant Science. 2015.

Abstract

Plants are major contributors to the soil respiration and the plant activity in the rhizosphere can alter the decomposition of native soil organic matter (SOM), which is called priming effect. However the mechanisms behind the rhizosphere priming and to what extent the plant actively controls it is unclear. One potential mechanism could be the increase in specific rhizodeposits to enhance the nutrient availability through stimulation of SOM decomposition.

We grew poplar plants in natural soil for ten weeks in climate chambers at low light availability and applied a continuous ^{13}C-CO_2 labelling from first emergence of leaves to separate the plant-derived C from other C stocks and fluxes. The above- and belowground CO_2 fluxes (photosynthesis, respiration) were monitored with high frequency, sampled regularly to trace the ^{13}C and the plant-soil systems were destructively harvested after 70 days.

The net C assimilation rates were low due to light limitation. The plants grown from the 7.5 months stored cuttings were strongly limited in their growth and in nutrients (chlorotic leaves), presumably caused by low cutting reserves and retarded root development. The variability in the leaf area (339 ± 204 cm^2) and thus in the overall assimilation was large between the plant individuals, however the C allocation patterns were generally consistent: the more assimilated aboveground the more ^{13}C was detected in the belowground stocks and fluxes. The dynamics of the soil respiration revealed a large priming effect in the growth-limited plants (5 - 59 mg C day^{-1} at peak time). The increase in soil respiration was more than one magnitude larger than the plant-derived respiration (1 - 2 mg C day^{-1}) and the amount of primed C and plant-derived C was not correlated in the plant-soil individuals. But the amount of C released by the plants belowground as CO_2 was increased during the priming to 29 - 90 % of net assimilated C compared to the basal rate of 18 ± 3 %, whereby the increase was largest in the most growth-limited plant.

The results suggest that the plants increased their belowground C release as response to nutrient limitation and that this enhanced the mineralisation of SOM. This indicates that plants can actively change the SOM dynamics to improve their living conditions.

1 Introduction

Soil respiration is the second largest flux of terrestrial organic carbon (C) after plant photosynthesis (Schlesinger and Andrews, 2000). Plant-derived respiration (root and rhizomicrobial respiration) contributes 48 % to the total soil respiration, ranging from 10-90 % depending on season and vegetation type (Hanson et al., 2000). Furthermore, plants interact with the surrounding soil by the release of organic compounds from living roots (rhizodeposition) and thus affect also microbial decomposition of soil organic matter (SOM). This effect is called rhizosphere priming and represents another plant-induced contribution to the total soil respiration next to the plant-derived (root and rhizomicrobial) respiration, which can be considerable. In the presence of plants, the SOM decomposition rates increased up to 380 % compared to unplanted soil and rhizosphere priming has been suggested to be one of the main processes determining the response of terrestrial C cycling to climate change (Heimann and Reichstein, 2008; Cheng et al., 2014). However, the mechanisms behind the rhizosphere priming are not yet clear, i.e. how rhizodeposition quantity or quality and the priming are related and to what extent the plants exert control over it.

Many observed a positive correlation between the amount of C input and the magnitude of the priming effect after labile organic C amendment to the soil (Paterson and Sim, 2013; Mary et al., 1993) or in plant-soil systems (Dijkstra and Cheng, 2007; Dijkstra et al., 2006; Zhu et al., 2014; Bengtson et al., 2012), while a few studies indentified the organic matter input quality as crucial factor determining the rhizosphere priming (Zhu and Cheng, 2012; Drake et al., 2013).

Plants are considered to have little direct control over the amount of rhizodeposition, i.e. that most rhizodeposits are lost as a result of passive diffusion and thus related to the root solute concentration (Jones et al., 2004). However, plants can increase the exudation of compounds with specific functions in response to environmental stimuli (Nguyen, 2003). One important function is the improvement of nutrient acquisition, for example by initiating and maintaining symbiotic interactions with microorganisms (exudation of chemoattractants, supply of substrate) or by directly increasing the nutrient solubility and mobility through extracellular plant enzymes, complexation with

exuded organic compounds or change in rhizosphere pH (reviewed by Dakora & Phillips, 2002; Paterson, 2003; Jones et al., 2004; Richardson et al., 2009).

Studies with hydroponic or sand cultures demonstrated that the plants increase the amount of belowground C release in response to limited N availability (e.g. Aitkenhead-Peterson & Kalbitz, 2005; Allard et al., 2006; Phillips et al., 2009) and change its composition depending on the type of the deficient nutrient (e.g. Carvalhais et al., 2011). Thus there is evidence from the field of plant sciences, that plants actively change the quantity and quality of rhizodeposits released in response to environmental constraints (e.g. nutrient deficiency), but the link to SOM dynamics is missing. There are only few studies on intact plant-soil systems that investigated the change in belowground plant C input and the SOM respiration (basal and primed C) together, as either a plant response to environmental constraints, such as defoliation, shading or competition (Hamilton III and Frank, 2001; Kuzyakov and Cheng, 2001; Pausch et al., 2013), or as a result of diurnal or phenological changes (Kuzyakov and Cheng, 2001; Zhu et al., 2014; Dijkstra and Cheng, 2007; Cheng et al., 2003; Bader and Cheng, 2007).

In this study, we grew plants under resource limitation (low light intensities, low storage reserves in the cutting) and studied the temporal dynamics in the main C fluxes during initial shoot and root development. The experimental setup (in growth chambers) allowed us to separately measure the above- and belowground fluxes (net photosynthesis, soil respiration) and apply a continuous ^{13}C labelling to distinguish the SOM present before root emergence and new plant-derived C (and its respiratory fluxes). We investigated two aspects of plant-soil C cycling and addressed following questions: i) The relation between above- and belowground C fluxes: are there consistent patterns between aboveground assimilation and plant-derived (root and rhizomicrobial) and plant-induced (primed) soil respiration? and ii) the temporal dynamics in the respiratory C fluxes during initial plant development: does the plant-derived respiration and the rhizosphere priming gradually increase with plant root and rhizosphere development (priming related to the quantity of rhizodeposits) or are there distinct temporal dynamics (priming related to the quality, i.e. the function of rhizodeposits)?

2 Material and Methods

2.1 Plants and soil

As model plant-soil system we used poplar trees (*Populus deltoides x nigra*, Dorskamp clone) grown from stem cuttings in natural forest soil (Cambisol, upper 10 cm, 8°33'E,

47°23'N, 500 m elevation). The stem cuttings were cut during winter and stored for 4 and 7.5 months at 0 - 4 °C until planting. Before planting, all except the uppermost bud were removed from the cutting.

The soil was collected one month before planting, sieved to 35 mm and stored moist until usage. The soil has a clay loam texture (38 % clay, 40 % silt, 22 %), is rich in C and N (5.3 % total C, 3.4 % organic C, 0.3 % N) and has a pH of 6.9. The pots (volume = 11 l) were filled with sand and soil one week before planting and were transferred into the labelling chambers for acclimatisation. At the bottom of the pots a 30 mm thick layer of quartz sand (grain size 2.0 - 3.2 mm) embedded the drainage tube (water outlet). On top of the sand layer we filled the soil in two compartments: The rhizosphere soil, inside a stainless steel cylinder covered with a fine mesh (30 µm PETEX, Sefar AG, Switzerland) that prevents the roots (but not the fungal hyphen) from growing through (1.8 kg dry weight) and the root-free soil around the cylinder (1.4 kg dry weight).

2.2 Experimental setup

A total of 15 poplar plants were grown from stem cuttings for 70 days in climate chambers under controlled environmental conditions. The climate chambers are hermetically separated in an upper (containing the shoots) and a lower system (containing the roots and the soil). This setup enables the sampling of soil respired CO_2 without contamination of ^{13}C-CO_2 (added to the shoots) diffusing into the soil. The upper system consists of a polycarbonate cuboid (volume of 1.2 m^3), enclosing the poplar shoots. It is connected to a gas circuit for automatic regulation of the CO_2 and H_2O concentrations, which are measured by an infrared gas analyser (IRGA, LI-840, Licor Ltd.). The lower system consists of 15 individual pots enclosing the root-soil compartments and valves that connect the pots to another IRGA and a septum for manual gas sampling. All pots are hermetically sealed from the laboratory atmosphere and are aerated with outdoor air. The climate chambers are described in more detail in Studer et al., 2014.

We conducted the experiment twice, first unlabelled (control, 4 months old cuttings) and then with a ^{13}C labelling treatment (7.5 months old cuttings). The environmental conditions were identical in the two experiments. The light intensity was 80 µmol photons m^{-2} s^{-1} and the day and night lengths were 12 hours. Thus each plant received 3.5 mol photons day^{-1}, what corresponds to a shady place in nature (Poorter et al., 2012). In order to ensure an optimal C assimilation we kept the CO_2 concentration under the given light intensity at saturation (518 +/- 7 ppm CO_2, corrected for undetected

excess ^{13}C-CO_2) and the humidity at a high level (74 ± 5 % relative air humidity, soil moisture content close to field capacity). The air temperature was 30 ± 1 °C.

2.3 Labelling procedure

We applied a continuous ^{13}C labelling from first emergence of leaves, since there are many drawbacks related to pulse labelling to trace the total plant C input into the soil (Rasmussen, 2011; Kuzyakov and Domanski, 2000). We sealed the poplars with a malleable sealant (Terostat-IX, Henkel AG & Co.) around the stem cuttings to separate the above- and belowground compartments. After closing the chamber we first removed the CO_2 via a CO_2-scrubber filled with Soda lime (Drägersorb 800 Plus, Dräger Medical AG & Co.) to a concentration of 245 ppm and then injected 10 atom% ^{13}C-CO_2 to a level of 500 ppm. Thereafter 6 atom% ^{13}C-CO_2 was automatically injected, when the CO_2 level in the chamber dropped below 480 ppm.

The isotopic composition of the chamber atmosphere was not constant at 6 atom% ^{13}C, but showed a logarithmic increase over time (supplementary material, Fig. S1). These dynamics were caused by less frequent label injection at the beginning of the experiment, when the net shoot C assimilation was low (slow decline of the CO_2 concentration in the chamber air). Furthermore the ^{13}C-CO_2 added was more diluted with respired ^{12}C at the beginning than at the end of the experiment.

2.4 Sampling procedure

We took manual gas samples of the soil CO_2 efflux in six pots every 3 - 4 days during the first 24 days and weekly thereafter. The isotopic signature of the respired CO_2 was assessed by the Keeling plot approach (details in Studer et al., 2014) and was used to estimate the plant-derived fraction of the total soil CO_2 efflux.

After 70 days of growth, five plant-soil systems were destructively harvested and separated into leaves, stems (newly developed stem, inclusive petioles), cuttings, roots, rhizosphere soil and root-free soil. The other ten plants were used for a root decomposition study, therefore only its aboveground parts were analysed. The leaf area was measured with a handheld area meter (CID-203 Laser leaf area meter, CID Inc.) directly after opening the chambers. The aboveground plant tissues were sampled and immediately transferred in the oven and dried at 60 °C for 24 hours. The rhizosphere soil (inside the mesh-cylinder) was separated from the root-free soil, whereby fresh samples of both soil compartments were taken for subsequent chloroform fumigation extraction of the microbial biomass. The roots were removed from the rhizosphere soil

with tweezers, washed with deionised water and dried in the oven (60 °C, 24 h). All dried residues were milled with a ball mill to a fine powder for later elemental and isotopic $\delta^{13}C$ analysis.

The fresh soil samples were sieved to 5 mm and visible roots and quartz sand grains were removed with tweezers. Six subsamples of 13 g dry weight equivalent were taken. Half of the subsamples were immediately extracted with 1M KCl solution and half were fumigated for 24 hours with chloroform prior to extraction (details on the extraction procedure are given in Murage & Voroney, 2007). Extract subsamples were frozen for later total dissolved organic carbon measurement or freeze-dried for $\delta^{13}C$ analysis. The isotopic signature and the quantity of the microbial biomass C in the rhizosphere soil (MB_{rhiz}) and the root free soil (MB_{rf}) was estimated by the difference between the fumigated and non-fumigated treatment and applying a conversion factor of 0.45 (Murage and Voroney, 2007; Joergensen, 1996).

2.5 Elemental and isotopic analyses

The elemental C content of the solid samples and the chloroform fumigation extracts were measured with a CHN-900 (Leco Corp) and TOC-500 (Shimadzu Corp.) elemental analyser, respectively. The isotopic $\delta^{13}C$ analyses of the solid and gaseous samples were done by isotope ratio mass spectrometry coupled to a gasbench or to an elemental analyzer via an open-split interface (details in Studer et al., 2014 and Werner et al., 1999). The isotopic composition of the samples were expressed as atom fraction (Equation 1) for further mass balance calculations.

$$x(^{13}C) = \frac{1}{1 + \frac{1}{(\delta^{13}C / 1000 + 1) \cdot R_{V-PDB}}} \quad (1)$$

, where $R_{V\text{-}PDB}$ is isotopic ratio of the heavy to the light carbon isotope of the international standard Vienna Pee Dee Belemnite (V_{PDB}, $^{13}C/^{12}C = 0.0111802$).

The isotopic label strength in the different plant-soil compartments were expressed as the total mass of label recovered at the last sampling date (t = 70) per plant in excess ($m^E(^{13}C)_{compartment,t=70}$). $m^E(^{13}C)$ was calculated according to the guidlines given by Coplen (2011) and Brand & Coplen (2012), i.e. by multiplying the excess atom fraction with the C pool size or C flux present and accounting for the change in molar C weight due to the ^{13}C tracer addition (as in Studer et al., 2014). As reference for the excess atom fraction estimation, we used the isotopic signature of unlabelled material measured in a previous experiment (Studer et al., 2014).

Table 1: Description of the variables used, of their measurement principle and units.

Variable	Explanation	Measurement	Units
A_{net}	Daily amount of net assimilated C per plant	Average of p_{net} (n = 24) and r_{dark} (n=24) measured in one day and conversion to mass per plant (based on LA)	mg C $plant^{-1}$ day^{-1}
LA	Leaf area	Assessed by a leaf area meter for each plant individual at t = 70 and estimated for each date (t=x) based on the assumption of linear increase after first leaf emergence (at t = 3)	cm^2
MB	Microbial biomass	Difference between chloroform fumigated and non-fumigated extracts and application of a conversion factor of 0.45	mg
$m^E(^{13}C)$	Mass of ^{13}C recovered in excess in plant-soil compartments	$x^E(^{13}C)$ and C pool size of plant-soil compartments and fluxes multiplied with its C stock or flux size	mg $plant^{-1}$
p_{net}	Net photosynthetic rate of shoots (per leaf area)	Average of rates measured in the daytime based on CO_2 concentration changes in the upper chamber system (containing all plants) assessed every 30 min	µmol m^{-2} s^{-1}
r_{dark}	Dark respiration rate of shoots (per leaf area)	Average of rates measured at night-time based on CO_2 concentration changes in the upper chamber system (containing all plants) assessed every 30 min	µmol m^{-2} s^{-1}
r_{pd}	Plant-derived soil respiration rate (per ground area)	r_{soil} multiplied with the fraction of plant-derived respiration estimated by a two-endmembers mixing model (based on $x(^{13}C)r_{soil}$ in the unlabelled control and the assimilated C from the chamber CO_2)	µmol m^{-2} s^{-1}
R_{pd}	Daily amount of plant-derived C respired per pot	Average of $r_{pd,t=x}$ measured in one day (n = 24) and conversion to mass per pot (based on pot area)	mg C pot^{-1} day^{-1}
R_{primed}	Daily amount of additional (primed) C respired per pot	Difference between the measured daily respiration rate and the basal rate of soil respiration before and after the peak (Fig 1b), conversed to mass per pot.	mg C pot^{-1} day^{-1}
r_{soil}	Total soil respiration rate (per ground area)	Average of rates measured every 60 min in each pot based on CO_2 concentration change between pot in- and outlets (and the aeration flux of each pot)	µmol m^{-2} s^{-1}
R_{soil}	Daily amount of C respired per pot	Average of $r_{soil,t=x}$ measured in one day (n = 24) and conversion to mass per pot (based on pot area)	mg C pot^{-1} day^{-1}
t=x	Sampling date	t = 1 - 70	day
$x(^{13}C)$	Atom fraction of ^{13}C on total C	Isotope ratio mass spectrometry, calculation pathway see Coplen (2011)	
$x^E(^{13}C)$	Excess atom fraction of ^{13}C on total C	$x(^{13}C)_{sample} - x(^{13}C)_{control}$	

2.6 C flux monitoring and partitioning

2.6.1 Photosynthesis, dark respiration and total soil respiration

The aboveground (net photosynthesis, dark respiration, net assimilation) and belowground C fluxes (soil respiration) were calculated based on the CO_2 concentration changes measured in the upper and lower chamber system. The CO_2 fluxes were monitored every half an hour aboveground and hourly belowground. The net photosynthetic (p), respiratory (r) and assimilation (a) fluxes were expressed in two ways i) in the commonly used units µmol CO_2 m^{-2} (leaf area) s^{-1} (aboveground fluxes) and µmol CO_2 m^{-2} (ground area) s^{-1} (belowground fluxes), referred to in the following with small letters (p, r) and ii) as amount of carbon (in mg) assimilated or released by a plant or pot in one day in order to compare the above- and belowground C fluxes, referred to in the text with capital letters (R, A). A description of variables and its definitions are listed in Table 1. Details on the calculation pathways are given in supplementary material.

2.6.2 Plant-derived soil respiration

The continuous labelling from first emergence of leaves labelled all plant-derived C with ^{13}C. This allowed us to partition the amount of plant-derived respiration C (R_{pd}) from the total respiration in each pot based on a two end-members mixing model (Equation 2).

$$R_{pd,t=x}(mg\ pot^{-1}day^{-1}) = R_{soil,t=x} \cdot f_{pd,t=x} = R_{soil,t=x} \cdot \frac{x(^{13}C)_{R_{soil,t=x}} - x(^{13}C)_{R_{soil,ctrl}}}{x(^{13}C)_{R_{pd,t=x}} - x(^{13}C)_{R_{soil,ctrl}}} \quad (2)$$

, where $R_{soil,t=x}$ is the daily amount of respired C (in mg pot^{-1} day^{-1}), $f_{Rpd,t=x}$ is the fraction of plant-derived on the total respiration and $x(^{13}C)$ is the ^{13}C atom fraction of the soil CO_2 efflux measured in a pot during the labelling experiment ($x(^{13}C)_{Rsoil,t=x}$), monitored in the unlabelled control experiment ($x(^{13}C)_{Rsoil,ctrl}$, n = 75), or estimated for the plant-derived efflux ($x(^{13}C)_{Rpd,t=x}$) on day t = x.

We assumed that the plant-derived respiration ($x(^{13}C)_{Rpd,t=x}$) bears the same isotopic signature as the plant organic matter. The plant organic matter was analysed just after 70 days, therefore we estimated its isotopic composition during the labelling experiment by the cumulative isotopic signature of the previously assimilated C (Equation 3).

$$x(^{13}C)_{R_{pd,t=x}} = \frac{\sum_{t=1}^{t=x}\left(x(^{13}C)_{C_{ass,t=x}} \cdot A_{net,t=x}\right)}{\sum_{t=1}^{t=x}\left(x(^{13}C)_{C_{ass,t=x}} \cdot A_{net,t=x}\right) + \sum_{t=1}^{t=x}\left(x(^{12}C)_{C_{ass,t=x}} \cdot A_{net,t=x}\right)} \quad (3)$$

, where $x(^{13}C)_{Cass,t=x}$ is the ^{13}C atom fraction of assimilated C, estimated by the isotopic composition of the CO_2 in the chamber atmosphere (Fig. S1) with an offset of 27 ‰ $\delta^{13}C$ (= 0.000295 $x(^{13}C)$) due to the ^{13}C discrimination (Farquhar et al., 1989), $x(^{12}C)_{Cass,t=x}$ and ^{12}C atom fraction of assimilated C, calculated ad 1 - $x(^{13}C)_{Cass,t=x}$ and $A_{net,t=x}$ is the daily assimilation rate (in mg C $plant^{-1}$, Fig. 3a) on day t = x.

The total amount of C respired by the roots and the rhizomicrobial community by the end of the experiment ($R_{pd,t=70}$) was estimated by cumulating the daily amounts of plant-derived C respired ($R_{pd,t=x}$).

2.6.3 Primed soil respiration

We calculated the primed C as the increase of the total soil respiration above its basal rate. The basal soil respiration rate was calculated as the average of the daily respiration rates before and after the peak in total soil respiration (Fig. 1b). The amount of primed C per day (R_{primed}) was then calculated by the difference between the current and the basal soil respiration rate (and converted to amount per pot).

3 Results and discussion

3.1 C assimilation limited by low light availability

The dynamics in the aboveground CO_2 fluxes reflect the gradual increase of photosynthetic capacity during initial leaf development. In the first days after planting, the fluxes were dominated by respiration (Fig. 1a), indicating the intense catabolic activity during the early stage of leaf growth. Thereafter the proportion between respiratory CO_2 loss and photosynthetic CO_2 uptake shifts in the favour of photosynthesis until full leaf expansion, which was about two weeks after leaf emergence. After ten days of growth, a positive net photosynthetic C uptake occurred in the daytime and on day 14 a positive daily net C balance was reached (Fig. 1a, 2a). These dynamics are in line with previous observations on poplar leaf development (Dickmann, 1971; Marron et al., 2008; Reich, 1983).

After full development of the initial leaves, the photosynthetic (p_{net}) and dark respiration rate (r_{dark}) remained on a level of 1.52 ± 0.14 µmol CO_2 m^{-2} s^{-1} and 0.55 ± 0.23 µmol CO_2 m^{-2} s^{-1} (Fig. 1a) respectively. The aboveground CO_2 fluxes were low compared to other studies on the same species that reported maximum photosynthetic capacity of 7 - 20 µmol CO_2 m^{-2} s^{-1} and dark respiration rates of 1 - 4 µmol CO_2 m^{-2} s^{-1} (Marron et al., 2008; Ow et al., 2008; Woo, 2010), but they were comparable to the results of Larson & Gordon (1969) obtained with poplar grown under similar light conditions. Thus the low

photosynthetic rates measured confirm that the plants were limited in their C supply under the low light conditions.

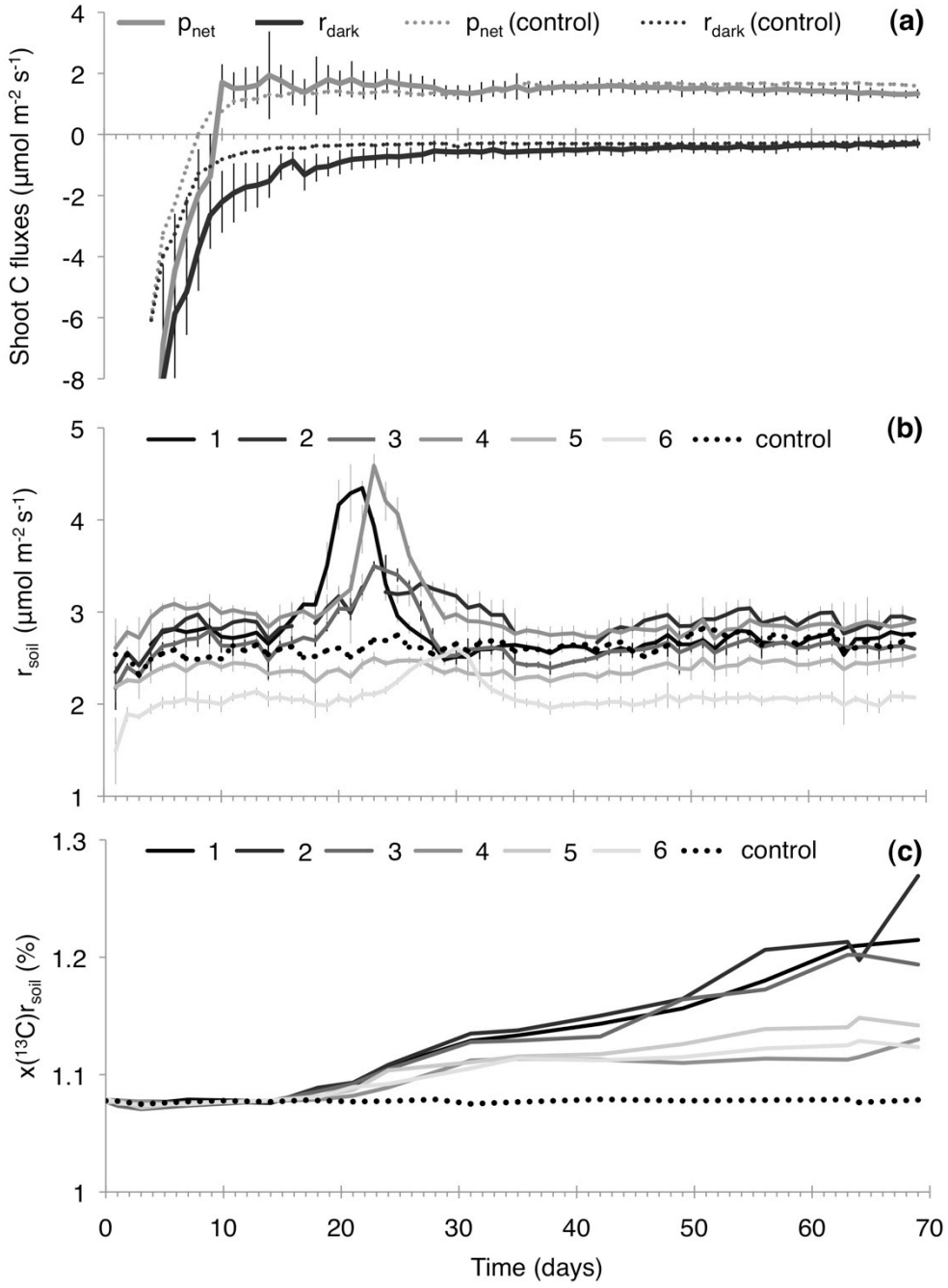

Figure 1: Dynamics of the (a) daily mean net photosynthetic (p_{net}) and dark respiration (r_{dark}) rates (in µmol CO_2 m^{-2} leaf area s^{-1}) of the poplar shoots, (b) soil respiration rates (in µmol CO_2 m^{-2} ground area s^{-1}) measured in six individual pots and (c) of the plant-derived isotope label detected in the soil respiration, expressed as ^{13}C atom fraction (in %). The error bars indicate +/- one standard deviation of the fluxes measured on day t=x (n = 24). The control is the average value of all six pots measured in the unlabelled experiment.

3.2 Nutrient deficiency limits plant growth

After 70 days of growth the poplar shoots were 17 ± 6 cm long and carried 16 ± 2 leaves with a total leaf area of 339 ± 204 cm^2 and a total biomass of 1.1 ± 0.8 g in the labelled experiment. The plants were half as tall and developed approximately one third of the biomass and the leaf area compared to the control experiment (Tab. 2). Furthermore the leaf development was delayed by 1 - 2 days (Fig. 1a) and we observed intervenial chlorosis on the oldest leaves in the labelled experiment (supplementary material, Fig. S2), which is a sign for magnesium (Mg) or iron (Fe) deficiency.

Table 2: Plant characteristics after 70 days of growth in the unlabelled control experiment (with 4 months old cuttings) and in the main experiment (with 7.5 months old cuttings) with isotope label application. Average values (± one standard deviation) are indicated. Significance of the difference is tested by two-sided t-test.

Plant traits	Control experiment (4 month storage)	Labelled experiment (7.5 month storage)	P ≤ 0.05
Leaf biomass* (mg)	1884 (± 660)	799 (± 496)	yes
Petioles+Stems* (mg)	1163 (± 575)	330 (± 263)	yes
Cuttings* (mg)	3775 (± 1002)	3447 (± 636)	no
Root biomass** (mg)	180 (± 85)	48 (± 32)	yes
Root/shoot**	0.06 (± 0.02)	0.04 (± 0.02)	no
Leaf area* (cm^2)	881 (± 309)	339 (± 204)	yes
Shoot length* (cm)	37 (± 10)	17 (± 6)	yes
Number of leaves*	21 (± 3)	16 (± 2)	yes

* n=15, **n=5

The environmental conditions and the plant and soil material used in the two experiments were the same, except that the stem cuttings have been stored longer (7.5 months vs. 4 months in the control experiment). Cold storage (at 4 °C) slows down metabolic processes, but respiration is not completely prevented, thus carbohydrate concentrations (especially starch) in the cuttings slowly decrease over time (Druege, 2000). The initial sugar availability in the stem cuttings is predominantly determining growth and adventitious root formation in high-light adapted plants grown under low light conditions (Druege et al., 2004). The plants in the later experiment with the older cuttings were limited in their C reserves, explaining the delay in the leaf development compared to the control.

The chlorosis was not expected, since poplar are generally rapid accumulators of nutrients (Stettler et al., 1996), but it assumedly indicates that the nutrient reserves in the cuttings were limited as well and that the root development and thus the nutrient acquisition capacity were retarded. It is reasonable that the plant needs to establish the photosynthetic tissue sufficiently before other organs (e.g. roots) can be further

developed under these conditions. The diminished capacity of nutrient uptake by the scarce root biomass will lead to a nutrient deficiency in the plants with all its other phenomena and consequences. A recent study has demonstrated that Mg (and potassium K) is the first among other macronutrients to shows visual symptoms of deficiency (Viégas et al., 2011). Thus it is plausible that the observed chlorosis was due to Mg deficiency, but that the plants were limited in other nutrients as well.

These findings suggest that the C (and nutrient) reserves in the cuttings after 7.5 months of cold storage were not sufficient to provide enough resources for optimal leaf and root development. The limited reserves in the cuttings highly affected their growth performance and most likely caused the large variability observed between the plant individuals.

3.3 Consistent allocation patterns with low belowground C allocation

The root biomass (0.05 ± 0.03 g) and the root/shoot ratios (0.04 ± 0.02) were very low compared to other studies on the same species, that reported ratios of 0.27-1.79 (Pregitzer et al., 1990; Barigah et al., 1994; Horwath et al., 1994). This result is in line with the decrease in belowground C allocation observed in poplars grown at high N and water availability (Coleman et al., 2004; Pregitzer et al., 1990) or under low light availability (Landhäusser and Lieffers, 2001). The higher allocation into photosynthetic active tissue under the low light conditions matches the functional equilibrium theory, which says that plants increase their C allocation to shoots, when aboveground resources (light, CO_2) are restricted, whereas they invest more into roots, when belowground resources (water, nutrients) are limited (Poorter and Nagel, 2000). However, the plants suffered nutrient deficiencies, as mentioned above. The still low allocation into roots, was probably caused by the impaired phloem loading and transport due to the Mg (and K) deficiencies (Cakmak et al., 1994; Cakmak and Kirkby, 2008). This would explain the lower root/shoot ratios observed in the smaller plant individuals (Fig. 2a), which were presumably more limited in their nutrient reserves and growth.

The allocation patterns of total C allocated belowground were consistent for the six plant individuals harvested, that differed largely in their leaf area (Fig. 2). The larger the leaf area, and consequently the amount of labelled C assimilated aboveground, the higher was the amount of ^{13}C recovered in the root biomass (Fig. 2b), rhizosphere microbial biomass (Fig. 2c) and the (plant-derived) soil respiration (Fig. 2d). We found

no label in the microbial biomass of the root-free soil, confirming that this part of the soil was not affected by the plants activity.

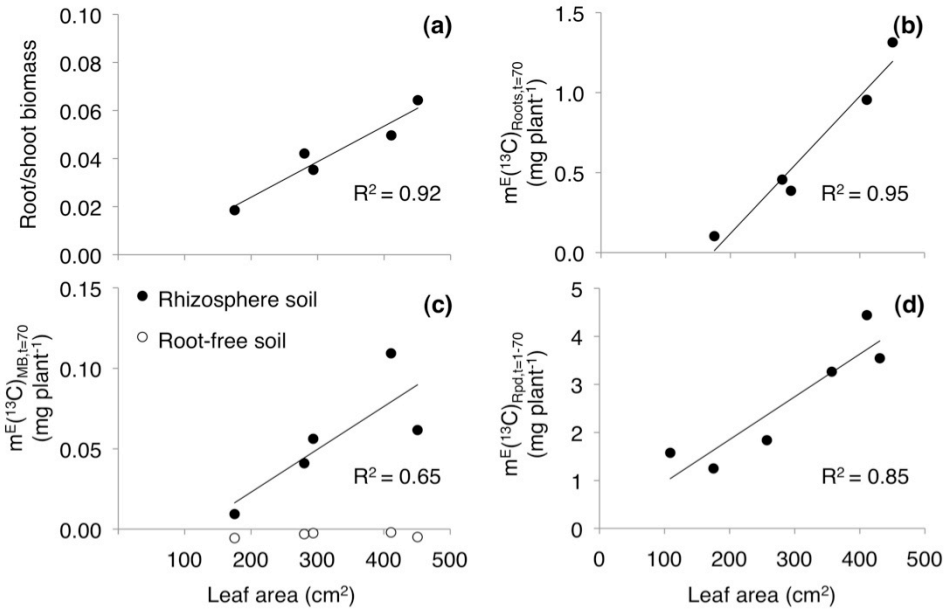

Figure 2: Correlation between the aboveground leaf area, which is a proxy for the overall assimilation and the growth performance (reserve limitation) of the different plant individuals, and (a) the root/shoot biomass ratio and (b,c,d) the amounts of label recovered in excess (in mg ^{13}C plant^{-1}) after 70 days of labeling (b) in the root biomass, (c) in the microbial biomass (MB) within the rhizosphere and root-free soil and (d) in the plant-derived soil respiration (R_{pd}).

The comparison of two plant-soil systems with different leaf area (indicator for growth limitation) indicated that both plants allocated the same amount of net assimilated C belowground (16 %). The larger plant allocated 19 % of the belowground C into the root biomass and 2 % into the microbial biomass, whereat the rest was respired. This allocation pattern is comparable to the observations made by Högberg et al. (2002), that suggest an incorporation of 25 % into the root biomass. However in the strongly limited smaller plant the belowground C loss as CO_2 seemed to be massively enlarged, only 8 % of belowground C remained in the root biomass, while 92 % was respired.

These results confirm the general proportional relationship between aboveground C assimilation and the amount of C belowground allocation to roots, rhizosphere microorganisms and plant-derived (root and rhizomicrobial) respiration. However, the differences between the plant individuals already indicate slightly different allocation patterns in response to the constraining conditions (nutrient limitation).

3.4 Low plant-derived respiration flux, but high rhizosphere priming of SOM

The soil respiration rate (r_{soil}) was on average 2.6 ± 0.2 µmol CO_2 m^{-2} s^{-1} and thus at the lower end of fluxes measured in the field on temperate forest cambisol soil surfaces (e.g. Rodeghiero & Cescatti, 2005; Ishizuka et al., 2006; Ruehr & Buchmann, 2010; Kutsch et al., 2010). This is expected in pot experiments with smaller soil depth and less intense rooting than in natural ecosystems. That, and the fact that we studied small tree seedlings resulted in a low contribution of plant-derived CO_2 release to the total soil respiration (estimated in the labelled experiment), which was less than 6 % compared to around 50 % measured in field studies (Ruehr & Buchmann, 2010; Kutsch et al., 2010). The total plant-derived respiration (R_{pd}) was 2.7 ± 1.7 mg $plant^{-1}$ day^{-1} after 70 days of plant growth. The applied stable isotope technique does not allow the partitioning of the root and rhizomicrobial respiration. But the comparison with the autotrophic respiration rate of the shoot tissue let us assume that the rhizomicrobial respiration was the larger contributor to the plant-derived respiration than the root respiration. Under the rough assumption that the respiration rate per g root biomass equals the shoot respiration rate (7.5 mg C g(biomass C)$^{-1}$ day^{-1}), the root respiration would be 0.2 mg C $plant^{-1}$ day^{-1} and would thus contribute less than 7 % to the plant-derived respiration.

The temporal dynamics in the soil respiration differed for two experiments. In the labelled experiment we observed a large increase in the soil respiration between the third and fifth week after planting, while in the control experiment only small fluctuation related to watering events occurred (Fig. 1b). This increase was not significant in each plant-soil systems, and the peaks appeared at different points in time (after 22 - 30 days). At peak time, the respiration rates were enlarged by 6 - 63 % above the basal rate before and thereafter.

The total soil respiration rate started to rise shortly after the initial leaves were fully developed and a positive aboveground net C balance was reached on day 14 (Fig. 1a) and a first ^{13}C signal was detected in the efflux on day 18 (Fig. 1c), linking the event to plant C dynamics. However, the increase in the amount of the total soil respiration was more than one magnitude larger than the amount of plant-derived respiration (Fig. 3b, Fig. 4), indicating that the increase in soil respiration was not directly plant-derived. But the parallel occurrence with the plant-derived respiration (mainly rhizomicrobial mineralization of root-derived C) strongly suggests that the increase in total CO_2 efflux was plant-induced (rhizosphere priming).

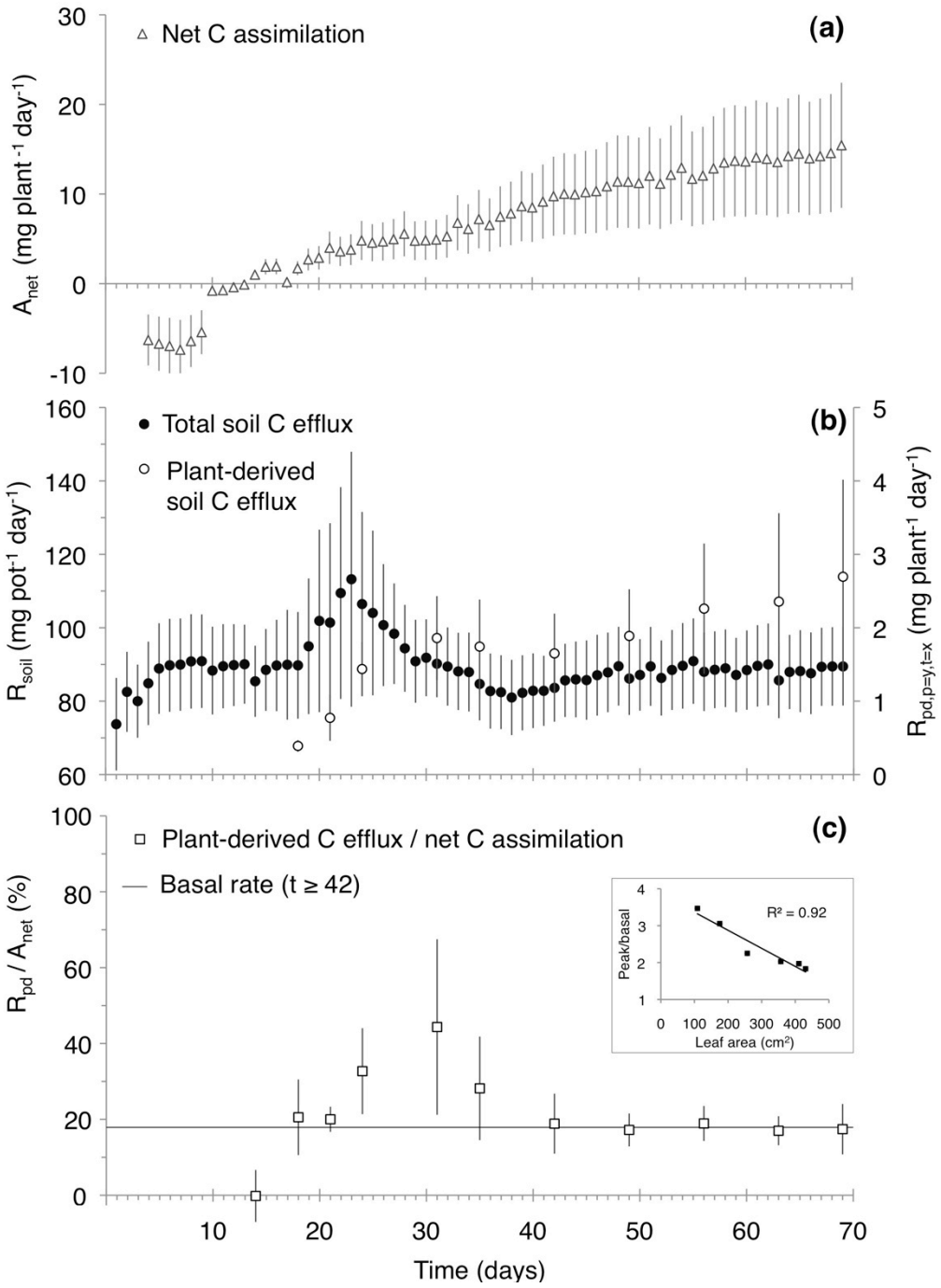

Figure 3: Dynamics of (a) the net aboveground C assimilation (A_{net} in mg C plant^{-1} day^{-1}), (b) the belowground respiratory C effluxes (in mg C pot^{-1} day^{-1}) given as total soil respiration (R_{soil}) and plant-derived respiration (R_{pd}) and (c) of the ratio (in %) between plant-derived respiration and assimilation (R_{pd}/A_{net}). The basal rate of belowground C release relative to the assimilation is indicated in (c) with a black line and was calculated as the average of the last five data points (t ≥ 42). The small figure in (c) shows the correlation between the leaf area and the magnitude of the increase in R_{pd}/A_{net}, given as the ratio between the peak height and the basal rate of belowground C release. The error bars indicate +/- one standard deviation of the fluxes measured in the plant pots (n = 6), i.e. are indicating the variability between the plant individuals.

The priming effect lasted for approximately 10 days. A total amount of 18 - 310 mg C was primed in the individual pots with rates of 5 - 59 mg day^{-1} at peak time (corresponding to 3 - 33 mg C kg^{-1} rhizosphere soil), while 1 to 2 mg C day^{-1} of the total respiration was plant-derived during this period (Fig. 4). At peak time the amount of primed SOM-C was up to 90 times the amount of mineralized plant-derived C, but there was no (positive) correlation between the amount of plant-derived C and the priming effect. This, and the fact that we did not observe any priming effect in the control treatment (with larger root biomass) or an increase in the priming effect over time indicates, that the quantity of belowground C release was not responsible for the rhizosphere priming effect observed here.

The quantity-related rhizosphere priming might have been too small to detect in this study. The amount of roots (< 0.1 g $plant^{-1}$) and plant-derived respiration (< 6 mg C $plant^{-1}$ day^{-1}) were low, therefore we can expect a low plant C input into the soil. Other studies, that detected a quantitative effect of plant C input on soil priming (Dijkstra et al., 2006; Zhu et al., 2014), were performed on plant-soil systems with 1 - 2 magnitudes larger plant root biomasses (1 - 3 g and 1 - 11 g), while they detected priming effects in the range of 0 - 15 mg C pot^{-1} day^{-1} and 2 - 10 mg C kg^{-1} day^{-1}, respectively. Assuming that the amount of plant C release is associated with the root biomass of a plant, we could expect in our study a quantity related efflux in the range of 0 - 5 mg primed C pot^{-1} day^{-1}, which is minor compared to the average respiration rate of 90 ± 6 mg C pot^{-1} day^{-1}.

3.5 Rhizosphere priming accompanied by increased plant-derived respiration vs. assimilation

The daily amount of assimilation (A_{net}) and the plant-derived respiration (R_{pd}) tend to increase linearly with time (Fig. 3 a,b), except for the period between sampling day 21 and 42, when the plant-derived respiration was slightly enlarged. During the linear phase (t ≥ 42 days, basal rate), 18 ± 3 % of the net assimilated C was released belowground as CO_2 (Fig. 3c), which is in line with other estimates (Uren, 2007; Kuzyakov and Domanski, 2000). Before that, the relative belowground C release (R_{pd}/A_{net}) peaked around day 31. At this time the amount respired was 45 ± 23 % of net assimilated C. The variability between the plant individuals was high, ranging from 29 to 90 % release of assimilated C as plant-derived respiration at peak time. The increase (peak height) relative to the basal rate (Fig. 3c) was correlated with the leaf area in each individual plant-soil system (small graph in Fig. 3c): the smaller the leaf area (and thus the overall assimilation) the higher was the increase in the belowground C release (relative to the aboveground assimilation). This suggests that the plants increased their

belowground C release into the soil, irrespective of the constrained C assimilation, as response to the growth limitation induced by the nutrient deficiency. Thus it is plausible, that the nutrient limited plants increased the release of specific compounds with the function to increase the nutrient acquisition into the soil. However, there was no correlation between primed C and the increase in belowground C release relative to the assimilation, indicating that other factors determined the effect of these compounds on the SOM degradation.

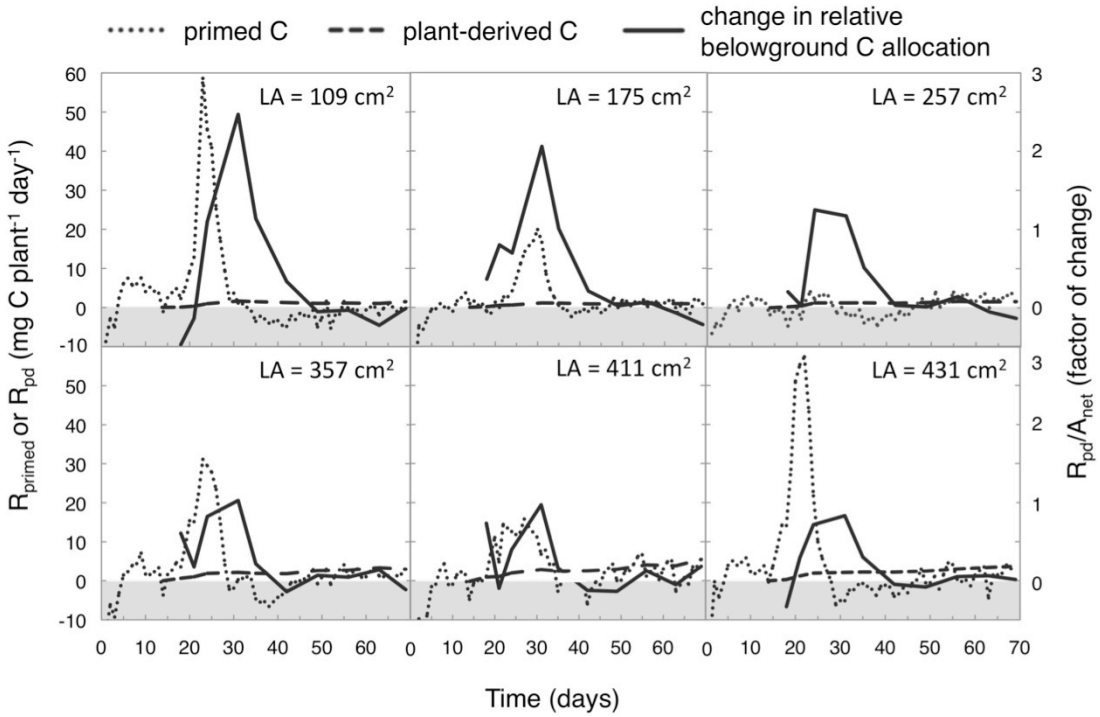

Figure 4: Dynamics in the daily amount of primed C (R_{primed}), estimated by the increase of the soil respiration above the basal rate after the observed peak (Fig. 3b), the daily amount plant-derived C respiration (R_{pd}) and the change in the relative belowground C release expressed as factor of increase/decrease relative to the basal rate of assimilated C released belowground (R_{pd}/A_{net}, Fig. 3c) of six individual plant-soil systems characterized by different leaf areas (LA). The plant-derived C respiration is an indicator for the quantity of rhizodeposition, the increase in the relative belowground C release is considered to be associated with the release of compounds with a specific function for the plant nutrient acquisition and the leaf area is a indicator for the development stage of the plant individual (measured after 70 days of growth), which is most probably related to the nutrient deficiency in the individuals. Negative values are marked with a grey bar.

The comparison of the dynamics in the amount of primed C with the amount of plant-derived C (indicator for rhizodeposition quantity, Fig. 3b) and the change in the relative belowground C release compared to the basal rate (indicator for the rhizodeposition quality, Fig. 3c) reveals that the peak in the relative belowground C release occurs after the peak in priming (Fig. 4). The delay in the peak of respiration/assimilation (R_{pd}/A_{net})

could be the result of time lags between the three processes assimilation, rhizodeposition and mineralisation. In a previous experiment with the same species and similar environmental conditions, we measured a minimum C transfer time from the leaves to the CO_2 efflux of 5 hours and a mean residence time of 4 - 6 days for plant C inputs in the soil C pools (Studer et al., 2014). Thus we can assume that the time lag between the assimilation and rhizodeposition is short, while the residence time causes a shift of a few days between the actual rhizodeposition and the signal detected in the plant-derived respiration. However, as discussed above, the phloem loading and transport is most likely impaired by Mg (or K) deficiencies, which can cause an accumulation of carbohydrates in the leaves (Cakmak et al., 1994). The transport of the temporarily stored assimilates to roots after recovery from acute Mg deficiency, caused by the retarded root development, and its release to the rhizosphere would explain the extremely high belowground respiratory C loss (90 % of net assimilated C) observed in the smallest plant (which suffered most of nutrient limitation) and in belowground C release after priming (i.e. nutrient release).

We hypothesise that there were two processes occurring in succession. First, a release of rhizodeposits with the target to increase nutrient availability and second, a release of temporarily stored carbohydrates after the nutrient deficiency was resolved. In response to the nutrient deficiencies, the plants actively increased the release of specific compounds to increase the root nutrient acquisition (reviewed by Dakora & Phillips, 2002; Paterson, 2003; Jones et al., 2004; Richardson et al., 2009). This could be compounds that i) increase the mobility/solubility of the nutrients (e.g. organic acids), ii) enhance the decomposition of SOM (e.g. extracellular enzymes), iii) are energy supply for symbionts and rhizosphere microorganisms (e.g. mycorrhiza, growth promoting rhizobacteria). However, if the compounds also enhance SOM decomposition is known to depend on soil related factors, such as soil nutrient status and competition with microorganisms (Chen et al., 2014; Dijkstra et al., 2013; Craine et al., 2007) or the accessibility of SOM and the environmental conditions for microbial decomposition (Dungait et al., 2012; Schmidt et al., 2011). Thus the small volume of soil explored by the plant during the initial root growth in this experiment might have caused a physical (spatial) disconnection of rhizodeposits, microorganisms and SOM and thus hampered the rhizosphere priming (Dungait et al., 2012).

4 Conclusions

In this study we observed the dynamics in C cycling during initial plant development in plant-soil systems, which were limited in the C supply (low C-assimilation due to low light intensities) and in the C reserves (7.5 months cutting storage). The plants that were most limited showed the lowest plant growth (and assimilation), but against our expectations, they had the highest belowground C release (relative to the C assimilation). We hypothesize that this release had the function of improving plant nutrient acquisition, because a massive increase in the SOM decomposition (rhizosphere priming) has been observed in parallel.

This study confirmed the general allocation patterns between the amount of aboveground assimilation and belowground C input (C allocation to roots, microbial biomass and plant-derived respiration). However it also highlights that plant-soil systems are not permanently in a steady state. C allocation patterns can change massively when the plant is exposed to stress conditions and the change in the belowground C allocation can affect other terrestrial C cycle fluxes, such as the decomposition of SOM. If the observed mechanisms can be confirmed in natural ecosystems, this would suggest that C cycling at the plant-soil interface (root, rhizosphere) is important for ecosystem C budgets and for the ecosystem response to climate change or extreme events. Future research should focus on the change in rhizodeposition quantity and quality at different stress conditions (e.g. water limitation during drought) and its effect on the C cycling of the whole plant-soil system (respiratory fluxes, feedback through the nutrient cycles).

Acknowledgements

We would like to thank the Swiss National Science Foundation for funding of the project (project nr. 135233). Furthermore we thank I. Woodhatch, R. Künzli, C. Schreiner, N. Singh, B. Maestrini, C. Lötscher, S. Meier, J. Siegrist, A. Tella and M. Hilf for their contributions to the technical and experimental work.

Author contributions

M. S. S., S. A. and R. T. W. designed the experiment; M. S. S. acquired, analyzed and interpreted the data and drafted the manuscript. All co-authors contributed intellectually to the data interpretation and revised the manuscript.

The authors declare that the research was conducted in the absence of any commercial or financial relationships that could be construed as a potential conflict of interest.

References

Aitkenhead-Peterson, J. A., and Kalbitz, K. (2005). Short-term response on the quantity and quality of rhizo-deposited carbon from Norway spruce exposed to low and high N inputs. *J. Plant Nutr. Soil Sci.* 168, 687–693. doi:10.1002/jpln. 200420468.

Allard, V., Robin, C., Newton, P. C. D., Lieffering, M., and Soussana, J. F. (2006). Short and long-term effects of elevated CO_2 on Lolium perenne rhizodeposition and its consequences on soil organic matter turnover and plant N yield. *Soil Biol. Biochem.* 38, 1178–1187. doi:10.1016/j.soilbio.2005.10.002.

Bader, N. E., and Cheng, W. (2007). Rhizosphere priming effect of Populus fremontii obscures the temperature sensitivity of soil organic carbon respiration. *Soil Biol. Biochem.* 39, 600–606. doi:10.1016/j.soilbio.2006.09.009.

Barigah, T. S., Saugier, B., Mousseau, M., Guittet, J., and Ceulemans, R. (1994). Photosynthesis, leaf area and productivity of 5 poplar clones during their establishment year. *Ann. For. Sci.* 51, 631–625. doi:10.1051/forest:19940607.

Bengtson, P., Barker, J., and Grayston, S. J. (2012). Evidence of a strong coupling between root exudation, C and N availability, and stimulated SOM decomposition caused by rhizosphere priming effects. *Ecol. Evol.* 2, 1843–1852. doi:10.1002/ ece3.311.

Brand, W. A., and Coplen, T. B. (2012). Stable isotope deltas: tiny, yet robust signatures in nature. *Isotopes Environ. Health Stud.* 48, 393–409. doi:10.1080/ 10256016.2012.666977.

Cakmak, I., Hengeler, C., and Horst, M. (1994). Partitioning of shoot and root dry matter and carbohydrates in bean plants suffering from phosphorus, potassium and magnesium deficiency. J. *Exp. Bot.* 45, 1245–1250. doi:10.1093/jxb/45.9.1245.

Cakmak, I., and Kirkby, E. a. (2008). Role of magnesium in carbon partitioning and alleviating photooxidative damage. *Physiol. Plant.* 133, 692–704. doi:10.1111/ j.1399-3054.2007.01042.x.

Carvalhais, L. C., Dennis, P. G., Fedoseyenko, D., Hajirezaei, M.-R., Borriss, R., and von Wirén, N. (2011). Root exudation of sugars, amino acids, and organic acids by maize as affected by nitrogen, phosphorus, potassium, and iron deficiency. *J. Plant Nutr. Soil Sci.* 174, 3–11. doi:10.1002/jpln.201000085.

Chen, R., Senbayram, M., Blagodatsky, S., Myachina, O., Dittert, K., Lin, X., Blagodatskaya, E., and Kuzyakov, Y. (2014). Soil C and N availability determine the priming effect: microbial N mining and stoichiometric decomposition theories. *Glob. Chang. Biol.* 20, 2356–2367. doi:10.1111/gcb.12475.

Cheng, W., Johnson, D. W., and Fu, S. (2003). Rhizosphere effects on decomposition: controls of plant species, phenology, and fertilization. *Soil Sci. Soc. Am. J.* 67, 1418–1427.

Cheng, W., Parton, W. J., Gonzalez-Meler, M. A., Phillips, R., Asao, S., McNickle, G. G., Brzostek, E., and Jastrow, J. D. (2014). Synthesis and modeling perspectives of rhizosphere priming. *New Phytol.* 201, 31–44. doi:0.1111/nph.12440.

Coleman, M. D., Friend, A. L., and Kern, C. C. (2004). Carbon allocation and nitrogen acquisition in a developing Populus deltoides plantation. *Tree Physiol.* 24, 1347–1357.

Coplen, T. B. (2011). Guidelines and recommended terms for expression of stable-isotope-ratio and gas-ratio measurement results. *Rapid Commun. Mass Spectrom.* 25, 2538–2560. doi:10.1002/rcm.5129.

Craine, J. M., Morrow, C., and Fierer, N. (2007). Microbial nitrogen limitation increases decomposition. *Ecology* 88, 2105–2113. doi:10.1890/06-1847.1.

Dakora, F. D., and Phillips, D. A. (2002). Root exudates as mediators of mineral acquisition in low-nutrient environments. *Plant Soil* 245, 35–47. doi:10.1023/A:1020809400075.

Dickmann, D. I. (1971). Photosynthesis and respiration by developing leaves of cottonwood (Populus deltoides Bartr.). *Bot. Gaz.* 132, 253–259. doi:10.1086/ 336588.

Dijkstra, F. A., Carrillo, Y., Pendall, E., and Morgan, J. A. (2013). Rhizosphere priming: a nutrient perspective. *Front. Microbiol.* 4, 1–8. doi:10.3389/fmicb. 2013.00216.

Dijkstra, F. A., and Cheng, W. (2007). Interactions between soil and tree roots accelerate long-term soil carbon decomposition. *Ecol. Lett.* 10, 1046–1053. doi:10.1111/j.1461-0248.2007.01095.x.

Dijkstra, F. A., Cheng, W., and Johnson, D. (2006). Plant biomass influences rhizosphere priming effects on soil organic matter decomposition in two differently managed soils. *Soil Biol. Biochem.* 38, 2519–2526. doi:10.1016/j.soilbio.2006.02. 020.

Drake, J. E., Darby, B. A., Giasson, M.-A., Kramer, M. A., Phillips, R. P., and Finzi, A. C. (2013). Stoichiometry constrains microbial response to root exudation- insights from a model and a field experiment in a temperate forest. *Biogeosciences* 10, 821–838. doi:10.5194/bg-10-821-2013.

Druege, U. (2000). Relation between nitrogen status, carbohydrate distribution and subsequent rooting of Chrysanthemum cuttings as affected by pre-harvest nitrogen supply and cold-storage. *Ann. Bot.* 85, 687–701. doi:10.1006/anbo.2000.1132.

Druege, U., Zerche, S., and Kadner, R. (2004). Nitrogen- and storage-affected carbohydrate partitioning in high-light-adapted Pelargonium cuttings in relation to survival and adventitious root formation under low light. *Ann. Bot.* 94, 831–842. doi:10.1093/aob/mch210.

Dungait, J. A. J., Hopkins, D. W., Gregory, A. S., and Whitmore, A. P. (2012). Soil organic matter turnover is governed by accessibility not recalcitrance. *Glob. Chang. Biol.* 18, 1781–1796. doi:10.1111/j.1365-2486.2012.02665.x.

Farquhar, G. D., Ehleringer, J. R., and Hubick, K. T. (1989). Carbon isotope discrimination and photosynthesis. Annu. Rev. Plant Physiol. *Plant Mol. Biol.* 40, 503–537. doi:10.1146/annurev.arplant.40.1.503.

Hamilton III, E. W., and Frank, D. A. (2001). Can plants stimulate soil microbes and their own nutrient supply? Evidence from a grazing tolerant grass. *Ecology* 82, 2397–2402. doi:10.1890/0012-9658(2001)082[2397:CPSSMA]2.0.CO;2.

Hanson, P. J., Edwards, N. T., Garten, C. T., and Andrews, J. A. (2000). Separating root and soil microbial contributions to soil respiration: a review of methods and observations. *Biogeochemistry* 48, 115–146. doi:10.1023/A:1006244819642.

Heimann, M., and Reichstein, M. (2008). Terrestrial ecosystem carbon dynamics and climate feedbacks. *Nature* 451, 289–292. doi:10.1038/nature06591.

Högberg, P., Nordgren, A., and Agren, G. I. (2002). Carbon allocation between tree root growth and root respiration in boreal pine forest. *Oecologia* 132, 579–581. doi:10.1007/s00442-002-0983-8.

Horwath, W. R., Pregitzer, K. S., and Paul, E. A. (1994). ^{14}C allocation in tree-soil systems. *Tree Physiol.* 14, 1163–1176.

Ishizuka, S., Sakata, T., Sawata, S., Ikeda, S., Takenaka, C., Tamai, N., Sakai, H., Shimizu, T., Kan-Na, K., Onodera, S., et al. (2006). High potential for increase in CO_2 flux from forest soil surface due to global warming in cooler areas of Japan. *Ann. For. Sci.* 63, 537–546. doi:10.1051/forest.

Joergensen, R. (1996). The fumigation-extraction method to estimate soil microbial biomass: Calibration of the k_{EC} value. *Soil Biol. Biochem.* 28, 25–31. doi:10.1016/ 0038-0717(95)00102-6.

Jones, D. L., Hodge, A., and Kuzyakov, Y. (2004). Plant and mycorrhizal regulation of rhizodeposition. *New Phytol.* 163, 459–480. doi:10.1111/j.1469-8137.2004. 01130.x.

Kutsch, W. L., Persson, T., Schrumpf, M., Moyano, F. E., Mund, M., Andersson, S., and Schulze, E.-D. (2010). Heterotrophic soil respiration and soil carbon dynamics in the deciduous Hainich forest obtained by three approaches. *Biogeochemistry* 100, 167–183. doi:10.1007/s10533-010-9414-9.

Kuzyakov, Y., and Cheng, W. (2001). Photosynthesis controls of rhizosphere respiration and organic matter decomposition. *Soil Biol. Biochem.* 33, 1915–1925. doi:10.1016/S0038-0717(01)00117-1.

Kuzyakov, Y., and Domanski, G. (2000). Carbon input by plants into the soil. Review. *J. Plant Nutr. Soil Sci.* 163, 421–431. doi:10.1002/1522-2624(200008) 163:4<421::AID-JPLN421>3.0.CO;2-R.

Landhäusser, S. M., and Lieffers, V. J. (2001). Photosynthesis and carbon allocation of six boreal tree species grown in understory and open conditions. *Tree Physiol.* 21, 243–250.

Larson, P. R., and Gordon, J. C. (1969). Leaf development, photosynthesis and C^{14} distribution in Populus deltoides seedlings. *Am. J. Bot.* 56, 1058–1066. doi:10.2307/2440930.

Marron, N., Brignolas, F., Delmotte, F. M., and Dreyer, E. (2008). Modulation of leaf physiology by age and in response to abiotic constraints in young cuttings of two Populus deltoides × P . nigra genotypes. *Ann. For.* Sci. 65, 404. doi:10.1051/forest.

Mary, B., Fresneau, C., Morel, J. L., and Mariotti, A. (1993). C and N cycling during decomposition of root mucilage, roots and glucose in soil. *Soil Biol. Biochem.* 25, 1005–1014. doi:10.1016/0038-0717(93)90147-4.

Murage, E., and Voroney, P. (2007). Modification of the original chloroform fumigation extraction technique to allow measurement of $\delta^{13}C$ of soil microbial biomass carbon. *Soil Biol. Biochem.* 39, 1724–1729. doi:10.1016/j.soilbio.2007. 01.026.

Nguyen, C. (2003). Rhizodeposition of organic C by plant: mechanisms and controls. *Agronomie* 23, 375–396. doi:10.1051/agro.

Ow, L. F., Griffin, K. L., Whitehead, D., Walcroft, A. S., and Turnbull, M. H. (2008). Thermal acclimation of leaf respiration but not photosynthesis in Populus deltoides x nigra. *New Phytol.* 178, 123–134. doi:10.1111/j.1469-8137.2007.02357.x.

Paterson, E. (2003). Importance of rhizodeposition in the coupling of plant and microbial productivity. *Eur. J. Soil Sci.* 54, 741–750. doi:10.1046/j.1365-2389. 2003.00557.x.

Paterson, E., and Sim, A. (2013). Soil-specific response functions of organic matter mineralization to the availability of labile carbon. *Glob. Chang. Biol.* 19, 1562–1571. doi:10.1111/gcb.12140.

Pausch, J., Zhu, B., Kuzyakov, Y., and Cheng, W. (2013). Plant inter-species effects on rhizosphere priming of soil organic matter decomposition. *Soil Biol. Biochem.* 57, 91–99. doi:10.1016/j.soilbio.2012.08.029.

Phillips, R. P., Bernhardt, E. S., and Schlesinger, W. H. (2009). Elevated CO_2 increases root exudation from loblolly pine (Pinus taeda) seedlings as an N-mediated response. *Tree Physiol.* 29, 1513–1523. doi:10.1093/treephys/tpp083.

Poorter, H., Fiorani, F., Stitt, M., Schurr, U., Fink, A., Gibon, Y., Usadel, B., Munns, R., Atkin, O. K., Tardieu, F., et al. (2012). The art of growing plants for experimental purposes: a practical guide for the plant biologist. *Funct. Plant Biol.* 39, 821–838. doi:10.1071/FP12028.

Poorter, H., and Nagel, O. (2000). The role of biomass allocation in the growth response of plants to different levels of light, CO_2, nutrients and water: a quantitative review. *Aust. J. Plant Physiol.* 27, 595–607.

Pregitzer, K. S., Dickmann, D. I., Hendrick, R., and Nguyen, P. V (1990). Whole-tree carbon and nitrogen partitioning in young hybrid poplars. *Tree Physiol.* 7, 79–93.

Rasmussen, J. (2011). Why we need to restrict the use of “rhizodeposition” and the Janzen and Bruinsma equation. *Soil Biol. Biochem.* 43, 2213–2214. doi:10.1016/ j.soilbio.2011.05.023.

Reich, P. B. (1983). Effects of low concentrations of O_3 on net photosynthesis, dark respiration, and chlorophyll contents in aging hybrid poplar leaves. *Plant Physiol.* 73, 291–296. doi:10.1104/pp.73.2.291.

Richardson, A. E., Barea, J.-M., McNeill, A. M., and Prigent-Combaret, C. (2009). Acquisition of phosphorus and nitrogen in the rhizosphere and plant growth promotion by microorganisms. *Plant Soil* 321, 305–339. doi:10.1007/s11104-009-9895-2.

Rodeghiero, M., and Cescatti, A. (2005). Main determinants of forest soil respiration along an elevation/temperature gradient in the Italian Alps. *Glob. Chang. Biol.* 11, 1024–1041. doi:10.1111/j.1365-2486.2005.00963.x.

Ruehr, N. K., and Buchmann, N. (2010). Soil respiration fluxes in a temperate mixed forest: seasonality and temperature sensitivities differ among microbial and root-rhizosphere respiration. *Tree Physiol.* 30, 165–176. doi:10.1093/treephys/tpp106.

Schlesinger, W. H., and Andrews, J. A. (2000). Soil respiration and the global carbon cycle. *Biogeochemistry* 48, 7–20. doi:10.1023/A:1006247623877.

Schmidt, M. W. I., Torn, M. S., Abiven, S., Dittmar, T., Guggenberger, G., Janssens, I. A., Kleber, M., Kögel-Knabner, I., Lehmann, J., Manning, D. A. C., et al. (2011). Persistence of soil organic matter as an ecosystem property. *Nature* 478, 49–56. doi:10.1038/nature10386.

Stettler, R. F., Breadshaw, H. D. J., Heilman, P. E., and Hinckley, T. M. (1996). *Biology of Populus and its Implications for Management and Conservation*. NRC Research Press.

Studer, M. S., Siegwolf, R. T. W., and Abiven, S. (2014). Carbon transfer, partitioning and residence time in the plant-soil system: a comparison of two $^{13}CO_2$ labelling techniques. *Biogeosciences* 11, 1637–1648. doi:10.5194/bg-11-1637-2014.

Uren, N. C. (2007). "Functions of Compounds Released into the Rhizosphere by Soil-Grown Plants," in *The Rhizosphere*, eds. R. Pinton, Z. Varanini, and P. Nannipieri (CRC Press, Taylor & Francis Group), 1–21.

Viégas, I. D. J. M., Naif, A. P. M., da Conceicao, H. E. O., Lobato, A. K. da S., Frazão, D. A. C., Neto, C. F. de O., and Cordeiro, R. A. M. (2011). Visual symptoms, growth and nutrients of Alpinia purpurata plants exposed to N , P , K , Ca , Mg and S deficiencies. *J. Food, Agric. Environ.* 9, 3–6.

Werner, R. A., Bruch, B. A., and Brand, W. A. (1999). ConFlo III - an interface for high precision delta(13)C and delta(15)N analysis with an extended dynamic range. *Rapid Commun. Mass Spectrom.* 13, 1237–1241. doi:10.1002/(SICI)1097-0231(19990715)13:13<1237::AID-RCM633>3.0.CO;2-C.

Woo, S. Y. (2010). Epidermal leaf characteristics and seasonal changes of net photosynthesis of five Populus. *African J. Biotechnol.* 9, 1455–1458. doi:10.5897/AJB09.1656.

Zhu, B., and Cheng, W. (2012). Nodulated soybean enhances rhizosphere priming effects on soil organic matter decomposition more than non-nodulated soybean. *Soil Biol. Biochem.* 51, 56–65. doi:10.1016/j.soilbio.2012.04.016.

Zhu, B., Gutknecht, J. L. M., Herman, D. J., Keck, D. C., Firestone, M. K., and Cheng, W. (2014). Rhizosphere priming effects on soil carbon and nitrogen mineralization. *Soil Biol. Biochem.* 76, 183–192. doi:10.1016/j.soilbio.2014. 04.033.

Supplementary material

Calculation S.1 Molar volume

The molar air volume is calculated according to Equation S1, based on monitored temperature and pressure conditions.

$$V_m(dm^3 mol^{-1}) = \frac{R \cdot T_{ch}}{p_{lab}} \quad \text{(S1)}$$

, where p_{lab} is the atmospheric pressure (in Pa) in the laboratory, R is the universal gas constant (= 8.3144621 J K^{-1} mol^{-1}) and T_{ch} is the air temperature (in K).

Calculation S.2 Aboveground C fluxes

The daily mean net photosynthetic (p_{net}) and dark respiration (r_{dark}) rates were calculated based on the change in CO_2 concentration in the upper chamber system containing the 15 plant shoots (Equation S2 and S3).

$$p_{net,t=x}(\mu mol\ m^{-2}s^{-1}) = \frac{\sum\left(\frac{\Delta[CO_2]}{\Delta t} \cdot \frac{V_{ch}}{V_m \cdot LA_{tot}}\right)_{ch(daytime),t=x}}{n_{daytime,t=x}} \quad \text{(S2)}$$

$$r_{dark,t=x}(\mu mol\ m^{-2}s^{-1}) = \frac{\sum\left(\frac{\Delta[CO_2]}{\Delta t} \cdot \frac{V_{ch}}{V_m \cdot LA_{tot}}\right)_{ch(nighttime),t=x}}{n_{nighttime,t=x}} \quad \text{(S3)}$$

, where $\Delta[CO_2]/\Delta t$ is the CO_2 concentration change in the upper chamber system (in µmol mol^{-1} s^{-1}), V_{ch} is the chamber air volume (= 1.228 m^3), V_m is the molar volume (S1), and LA_{tot} is the total leaf area at the sampling date t = x and $n_{daytime,t=x}$ and $n_{nighttime,t=x}$ is the number of $\Delta[CO_2]/\Delta t$ measurements made in the day- and at night-time, respectively.

The total amount of net assimilated C ($A_{net,t=x}$) is calculated for each plant individual based on its leaf area (Equation S4).

$$A_{net,t=x}(mg\ plant^{-1}day^{-1}) = \left(p_{net,t=x} \cdot f_{day} + r_{dark,t=x} \cdot f_{night}\right) \cdot LA_{t=x} \cdot M(C) \quad \text{(S4)}$$

, where $p_{net,t=x}$ and $r_{dark,t=x}$ are the daily photosynthetic or dark respiratory rates (S2 and S3, transformed in µmol C m^{-2} day^{-1}), $f_{day/night}$ is the fraction of light and dark hours per day (0.5 day day^{-1}), respectively, $LA_{t=x}$ is the leaf area (in m^2) of the plant individual and M(C) is the molar weight of C (12.011 x 10^{-3} mg μmol^{-1}).

Since the leaf area was measured only at the last sampling date (t = 70 days), we assumed linear growth of the leaf area over time (starting at day 3, when the first leaf tips were developed). This assumption is based on the experience of previous

experiments and has been reported for *Populus deltoides x nigra* leaves by others (Marron et al., 2008, 2005; Monclus et al., 2005; Marron et al., 2003).

Calculation S.3 Belowground C fluxes

The soil CO_2 efflux rate of the individual pots is assessed based on the CO_2 concentration difference ($\Delta[CO_2]_{in,out}$ in µmol mol^{-1}) between the pot in- and outlet measured by the IRGA in the lower system. $\Delta[CO_2]_{in,out}$ is calculated by subtracting the average of the background air CO_2 concentrations measured before and after each pot measurement from the average concentration of the pot outlet measurements. The daily mean soil respiration rate ($r_{soil,t=x}$) was then calculated as the average of the respiration rates measured during the course of the day (Equation S5).

$$r_{soil,t=x}(\mu mol\ m^{-2}s^{-1}) = \frac{\sum\left(\frac{\Delta[CO_2]_{in,out}\cdot F_{pot}}{V_m \cdot PA}\right)_{t=x}}{n_{t=x}} \qquad \text{(S5)}$$

, where ($\Delta[CO_2]_{in,out}$) is the CO_2 concentration difference between the in- and outlet (in µmol mol^{-1}), F_{pot} is the pot aeration rate (1.3 l min^{-1}), V_m is the molar volume (Equation S1), $n_{t=x}$ is the number of respiration flux measurements on day t = x and PA is the pot area (= 0.0328 m^2).

The daily amount of C released as CO_2 belowground per pot ($R_{soil,t=x}$ in mg pot^{-1} day^{-1}), is calculated by multiplying the daily respiration rates $r_{soil,t=x}$ with the pot area and the molar C weight.

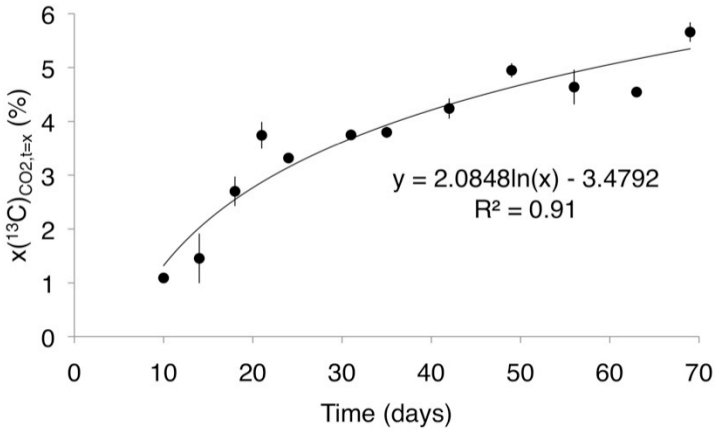

Fig. S1: Maximum atmospheric label strength. The isotopic signature of the CO_2 (given in excess atom fraction and expressed in %) within the chamber air was increasing over time. It was lower than the 6 atom% ^{13}C-CO_2 injected, due to the dilution with respired ^{12}C. The formula of the best logarithmic curve fit (black line) was used to estimate the signature of the fresh assimilates.

Fig. S2: Leaf chlorosis observed in the oldest leaves. Deficiency symptoms were detected in all plants on the lowest leaves.

Part C: Appendix

Poster presentations

Studer M. S., Siegwolf R. T. W., Schmidt M. W. I., Abiven S. (2014): Carbon transfer, partitioning and residence time in the plant-soil system:a comparison of two ^{13}C-CO_2 labelling techniques. EGU (European Geoscience Union) General Assembly, 2. May 2014, Vienna, Austria

Studer M.S., Abiven S., Siegwolf R.T.W., Schmidt M.W.I. (2012): Tracing organic matter dynamics within the plant-soil system by continuous multi-isotope labelling (^{13}C, ^{18}O and ^{2}H). SOM-5 Workshop, 7.-11. October 2012, Ascona, Switzerland.

Studer M.S., Abiven S., Schmidt M.W.I., Siegwolf R.T.W. (2012): Dual isotope labelling (^{13}C and ^{18}O) for studying organic matter dynamics within the plant-soil system. Poster. ISOECOL, 20.-24. August 2012, Brest, France.

Studer M., Abiven S., Siegwolf R.T.W., Schmidt M.W.I. (2012): How to trace organic matter input by living plants into and within the soil? EGU (European Geoscience Union) General Assembly, 23.-27. April 2012, Vienna, Austria.

Studer M., Abiven S., Schmidt M.W.I., Siegwolf R.T.W. (2011): Pulse vs. continuous multi-isotope labelling of plant-soil systems. GASIR (German Association of Stable Isotope Research) Meeting, 10.-13. October 2011, PSI Villigen, Switzerland.

Studer M., Abiven S., Siegwolf R.T.W., Schmidt M.W.I. (2011): Multi-Isotope labelling (^{13}C, ^{18}O, ^{2}H) in a Controlled Environment (MICE): A new tool for studying the allocation of organic molecules within the plant-soil system? EGU (European Geoscience Union) General Assembly, 4.-8. April 2011, Vienna, Austria.

Studer M., Schneider M.P.W., Moreno J. M., Resco V., Abiven, S. (2009): A tool to estimate fire intensity and chemical structure of black carbon inputs into soil. Poster. Swiss Geoscience Meeting, 20.-21. November 2009, Neuchâtel, Switzerland.

Acknowledgements

The MICE development would not have been successful without the extraordinary contributions of colleagues and collaborators (sorted according to the hours spent with me in the MICE-cellar) and I would like to thank all of you very much for the time (and nerves) you spent on this project and the advices you gave me:

- Ivan Woodhatch (2B, UZH): initial design, technical development and support
- Samuel Abiven (2B, UZH): scientific input, initial design and fundraising
- Roland Künzli (DMP Ltd): software development, documentation and support
- Reto Maier & team (Physical Workshop, UZH): initial design and physical construction
- Rolf Siegwolf (PSI): scientific input, initial design
- Michael Schmidt (UZH): initial funding

Further I would like to thank everyone that helped me to keep a good work-life balance..

.. at work: Thanks to Samuel and his group members for private invitations and good team spirit; to my room mates Max, Nimisha, Bea and guests for the nice atmosphere in the office; to Ivan and Dagmar an the whole 2B team for many conversations and valuable exchange of ideas; to Anett for interesting discussions about teaching (among other things); to Rolf, the SIRG team and especially Ineke for private invitations and the good atmosphere at PSI.

.. at home: Special thanks go to my family, Berti, Urs, Tobias, Rahel, Sibylle, Marc and Christoph, and to all my friends for their support, the good times we spend together and for giving me balance in life.

I would also like to thank all the technical staff helping me with the analyses at PSI, ETH, UZH, WSL and UniBE: Daniel Christen, Nourreddine Hajjar, Michael Hilf, René Husi, Bruno Kägi, Ineke Lötscher, Peter Nyffeler, Lola Schmid, Michael Schneider, Claudia Schreiner and Theres Zwimpfer.

I thank Bettina Weibel and Berti Studer for cross-reading this thesis and Anett Hofmann for the comments on the German summary.

And at last but not least I thank my supervisors Samuel and Rolf to guide me through my time as PhD student and for all their support.